University of Alberta

Formation, identification, and repair of γ-radiation-induced DNA-protein crosslinks in mammalian cells

by

SHARON LUCILLE BARKER ©

A thesis submitted to the Faculty of Graduate Studies and Research in partial fulfillment of the requirements for the degree of Doctor of Philosophy

Department of Oncology

Edmonton, Alberta

Fall 2005

Library and Archives Canada
Published Heritage Branch
395 Wellington Street
Ottawa ON K1A 0N4
Canada

Bibliothèque et Archives Canada
Direction du Patrimoine de l'édition
395, rue Wellington
Ottawa ON K1A 0N4
Canada

0-494-08612-2

Your file *Votre référence*
ISBN:
Our file *Notre retèrence*
ISBN:

NOTICE:
The author has granted a non-exclusive license allowing Library and Archives Canada to reproduce, publish, archive, preserve, conserve, communicate to the public by telecommunication or on the Internet, loan, distribute and sell theses worldwide, for commercial or non-commercial purposes, in microform, paper, electronic and/or any other formats.

The author retains copyright ownership and moral rights in this thesis. Neither the thesis nor substantial extracts from it may be printed or otherwise reproduced without the author's permission.

AVIS:
L'auteur a accordé une licence non exclusive permettant à la Bibliothèque et Archives Canada de reproduire, publier, archiver, sauvegarder, conserver, transmettre au public par télécommunication ou par l'Internet, prêter, distribuer et vendre des thèses partout dans le monde, à des fins commerciales ou autres, sur support microforme, papier, électronique et/ou autres formats.

L'auteur conserve la propriété du droit d'auteur et des droits moraux qui protège cette thèse. Ni la thèse ni des extraits substantiels de celle-ci ne doivent être imprimés ou autrement reproduits sans son autorisation.

In compliance with the Canadian Privacy Act some supporting forms may have been removed from this thesis.

While these forms may be included in the document page count, their removal does not represent any loss of content from the thesis.

Conformément à la loi canadienne sur la protection de la vie privée, quelques formulaires secondaires ont été enlevés de cette thèse.

Bien que ces formulaires aient inclus dans la pagination, il n'y aura aucun contenu manquant.

Canada

"I must say a word about fear. It is life's only true opponent. … if your fear becomes a wordless darkness that you avoid, perhaps even manage to forget, you open yourself to further attacks of fear because you never truly fought the opponent who defeated you."

Adapted from "Life of Pi" by Yann Martel

Abstract

DNA-protein crosslinks (DPCs) are induced by a variety of commonly encountered agents, including metals, aldehydes and radiation, as well as chemotherapeutic drugs. There is tremendous variability in the literature with respect to our understanding of the induction, stability, and proposed repair pathways for DPCs induced by various agents. Different crosslink chemistries are likely to affect the impact, stability, and repair of these lesions. As well, a number of different methods have been used for DPC measurements, which has probably contributed to the variability seen in DPC analyses.

Ionizing radiation (IR) is an important environmental risk factor for various cancers and also a major therapeutic agent for cancer treatment. Exposure of mammalian cells to IR induces several types of damage to DNA, including double and single strand breaks, base and sugar damage, as well as interstrand crosslinks (ICLs) and DPCs. The biological consequences of DPC-inducing agents, such as IR, include increased mutagenesis, chromosomal aberrations and cytotoxicity, but the contribution of DPCs to these endpoints has not been well characterized. The determination of the consequences of DPC induction will require an assessment of which proteins become crosslinked to DNA and the stability of these linkages.

This work describes the development and validation of novel methodology for the isolation of DPCs from mammalian cells using chaotropic agents to isolate genomic DNA and stringently remove non-crosslinked proteins followed by nuclease digestion to release covalently crosslinked proteins. This method

generates high quality protein samples in sufficient quantities for analysis by mass spectrometry.

Using our DPC isolation method in combination with mass spectrometry, we have identified 29 proteins belonging to numerous functional categories that can become crosslinked to DNA by γ-radiation under aerated and/or hypoxic conditions. Several aspects of DPC induction were examined by staining 1-D SDS-PAGE gels with SYPRO Tangerine followed by analysis using fluorescence imaging. DPCs were induced linearly with IR dose at low doses, but appeared to reach a plateau with higher doses. There was no dramatic influence of oxygen on total IR-induced DPCs observed. DPC removal was observed to be limited in repair-deficient cell lines. Measurements of the extent and timecourse of protein crosslinking will ultimately contribute to the understanding of the effect of DPCs.

Acknowledgements

I am very grateful to Michael Weinfeld and David Murray for taking me on as a graduate student and for allowing me the independence to develop and work on various projects. I would like to thank my supervisory committee members Liang Li and Susan Andrew for their helpful suggestions and their support. I thank the members of the Weinfeld lab, especially Jane Lee and Louise Enns, for their help during my time here. I would also like to thank John Hanson for his assistance with the statistical analyses and Jing Zheng for all of her hard work on our mass spectrometry. I am indebted to Karen Kerswell for her outstanding organizational and editorial assistance. I would like to thank my brother, Ken Barker, for very generously providing me with a laptop computer because it made writing up more pleasant!

I would like to express my appreciation for the enormous support provided by true friendship. I would like to thank some of the wonderful people who have come into my life for their support, encouragement, and comic relief: Amber Martin, Carolyn Slack, Laurina Turcotte, April Scott, David Ballantyne, Michelle Lee, Wendy Stevenson, Melanie Martilla, Anita Grewal, and many others.

Table of Contents

CHAPTER 1: DNA-PROTEIN CROSSLINKS: THEIR INDUCTION, REPAIR AND BIOLOGICAL CONSEQUENCES **1**

1.1. Introduction **2**

1.2. Detection of DPCs **4**

1.3. Chemical-induced DPC formation **6**
a. Formaldehyde-induced DPCs 6
b. Metal-induced DPCs 7

1.4. DPCs induced by IR and ROS **10**
a. Ionizing radiation-induced DPCs in cells 10
b. Ionizing radiation-induced DPC structures 15
c. Protein radicals and DPCs 17

1.5. Stability of DPCs *in vitro* **20**

1.6. Biological consequences of DPCs **20**
a. Nickel 22
b. Chromium 22
c. Arsenic 23
d. Formaldehyde 24
e. Methylglyoxal and glyoxal 25
f. Pyrrolizidine alkaloids 26
g. Ionizing radiation 26
h. Cumulative/background lesions 27

1.7. Proteins involved in DPCs **27**
a. Crosslinking of DNA replication/repair enzymes to DNA 34

1.8. Crosslinking of DNA to the nuclear matrix **36**

1.9. Enzymatic repair of DPCs **39**
a. How are DPCs sensed at the cellular level? 40
b. How are covalent DPCs repaired? 41
c. How are IR-induced DPCs repaired? 47
d. Might protease activity be involved in DPC repair? 48

1.10. Conclusions **49**

1.11. Research Objectives **51**

References for Chapter 1 ..... **53**

CHAPTER 2: A METHOD FOR THE ISOLATION OF COVALENT DNA-PROTEIN CROSSLINKS SUITABLE FOR PROTEOMICS ANALYSIS 66

2.1. Introduction 67

2.2. Materials and Methods 71
a. Cell Culture 71
b. Radiation and chemical treatments 71
c. DNAzol DPC isolation method (Figure 2-1A) 72
d. DNAzol-Strip DPC isolation method (Figure 2-1B) 72
e. DNAzol-Silica DPC isolation method (Figure 2-1C) 74
f. SDS/K^+ DPC isolation method 75
g. Nuclei isolation 75
h. Nuclear extract preparation 76
i. Quantitation of DNA 76
j. Quantitation of protein 77
k. SDS-PAGE analysis 77
l. Mass Spectrometry 78

2.3. Results 78
a. DPC isolation by DNAzol 78
b. DPC isolation by DNAzol-Strip method 82
c. DPC isolation by DNAzol-Silica method 85
d. Isolation of γ-radiation-induced DPCs by DNAzol-Strip and DNAzol-Silica methods 86
e. Preliminary identification of a crosslinked protein by mass spectrometry 90
f. Isolation of camptothecin-induced DPCs by DNAzol-Strip and DNAzol-Silica methods 93

2.4. Discussion 95

References for Chapter 2 100

CHAPTER 3: THE IDENTIFICATION OF MAMMALIAN PROTEINS CROSSLINKED TO DNA BY Γ-RADIATION 103

3.1. Introduction 104

3.2. Materials and Methods 106
a. Cell culture 106
b. Radiation and chemical treatments of cells 106
c. Quantitation of DNA 107
d. Nuclei isolation 107
e. Nuclear extract preparation 107
f. DNAzol-Strip DPC isolation method 107
g. DNAzol-Silica DPC isolation method 108
h. SDS-PAGE analysis 108

i. Quantitation of protein on SDS-PAGE gels 108
j. Protein identification by Mass spectrometry 109
k. Western blots 110
l. Antibodies 111

3.3. Results 112
a. Isolation and PAGE analysis of γ-radiation-induced DPCs in hamster and human cells 112
b. Identification of proteins involved in γ-radiation-induced DPCs in hamster cells 114
c. Confirmation of individual proteins involved in DPCs by Western blot analysis 123
d. Identification of additional novel proteins involved in DPCs by Western blot analysis 125
e. Quantitation of γ-radiation-induced DPCs in mammalian cells 127

3.4. Discussion 132

References for Chapter 3 144

CHAPTER 4: ANALYSIS OF THE TIMECOURSE OF Γ-RADIATION-INDUCED DNA-PROTEIN CROSSLINKS IM MAMMALIAN CELLS 150

4.1. Introduction 151

4.2. Materials and Methods 154
a. Cell culture 154
b. Radiation and chemical treatments of cells 155
c. Quantitation of DNA 156
d. Nuclei isolation 156
e. Nuclear extract preparation 156
f. DNAzol-Silica DPC isolation method 156
g. SDS-PAGE analysis 156
h. Quantitation of protein on SDS-PAGE gels 157
i. Western blots 157
j. Antibodies 158

4.3. Results 158
a. Time course of Formaldehyde-induced DPCs in mammalian cells 158
b. Time course of γ-radiation-induced DPCs in mammalian cells 160
c. Time course of γ-radiation-induced DPCs in repair-deficient mammalian cells 160
d. Time course of individual DPCs in normal mammalian cells 162
e. Time course of low-dose γ-radiation-induced DPCs in mammalian cells .. 166

4.4. Discussion 169

List of Tables

Table 1-1: Proteins Identified in DNA-Protein Crosslinks.....289

Table 2-1: Peptides used for mass-spectral identification of proteins 92

Table 3-1: Proteins identified in γ-radiation-induced DNA-protein crosslinks.....117-122

Table 3-2: Relevant roles and/or nuclear localization for identified proteins. 137-138

List of Figures

Figure 1-1: Crosslink Structures 3

Figure 1-2: Formaldehyde Crosslinking Mechanism 8

Figure 1-3: Generation of ROS by IR 11

Figure 1-4: Oxygen Dependence of DPCs and Survival in γ-Irradiated AA8 CHO Cells 13

Figure 1-5: Potential DPC Repair Routes 42

Figure 2-1: DNAzol-based DPC isolation methods 70

Figure 2-2: Effect of DNAzol on protein integrity 80

Figure 2-3: Modification of the DNAzol protocol to reduce the level of background protein 81

Figure 2-4: Comparison of background protein levels using different DPC isolation methods 84

Figure 2-5: Isolation of formaldehyde- and γ-ray-induced DPCs from CHO cells using the DNAzol-Strip method 87

Figure 2-6: Isolation of formaldehyde- and γ-ray-induced DPCs from CHO cells using the DNAzol-Silica method 89

Figure 2-7: Mass-spectrometric identification of GRP78 as an ionizing-radiation crosslinked protein in CHO AA8 cells 91

Figure 2-8: Isolation of camptothecin-induced DPCs from CHO cells 94

Figure 3-1: Analysis of DPCs from hamster cells 113

Figure 3-2: Analysis of DPCs from human cells 115

Figure 3-3: Confirmation and quantitation of individual proteins in γ-radiation-induced DPCs 124

Figure 3-4: Identification and quantitation of additional proteins in γ-radiation-induced DPCs 126

Figure 3-5: Quantitation of DPCs from hamster cells, 0-4 Gy 128

Figure 3-6: Quantitation of DPCs from hamster cells, 0-1.5 Gy 130

Figure 3-7: Quantitation of DPCs from human cells, 0-4 Gy 131

Figure 3-8: Quantitation of DPCs from human cells, 0-1.5 Gy 133

Figure 3-9: Quantitation of an individual DPC from human cells, 0-1.5 Gy 134

Figure 4-1: Time course of formaldehyde-induced DPCs in AA8 hamster cells 159

Figure 4-2: Time course of γ-radiation-induced DPCs in AA8 hamster cells, 0-50 h, after 1.5 Gy 161

Figure 4-3: Time course of γ-radiation-induced DPCs in UV41 hamster cells, 0-50 h, after 1.5 Gy 163

Figure 4-4: Time course of γ-radiation-induced DPCs in UV20 hamster cells, 0-50 h, after 1.5 Gy 164

Figure 4-5: Time course of γ-radiation-induced DPCs in irs1SF hamster cells, 0-50 h, after 1.5 Gy 165

Figure 4-6: Time course of individual γ-radiation-induced DPCs in AA8 hamster cells, 0-50 h, after 1.5 Gy 167

Figure 4-7: Time course of γ-radiation-induced DPCs in AA8 hamster cells, 0-96 h, after 0.5 Gy 168

Figure 4-8: Time course comparisons of γ-radiation-induced DPCs in AA8, UV41, UV20, and irs1SF hamster cells, 0-50 h after 1.5 Gy 174

Figure 6-1: Quantitation of DPCs using Deep Purple 194

Figure 6-2: DPCs induced by DMSO 202

Figure 6-3: Melphalan-induced DPCs in CHO cells 204

Figure 6-4: Design of the interstrand crosslinked substrate 206-207

Figure 6-5: Construction of the interstrand crosslinked duplex 208

Figure 6-6: Restriction test of the interstrand crosslinked duplex 209

Figure 6-7: Restriction map of the interstrand crosslinked substrate 211

Figure 6-8: Restriction digest of the full-length interstrand crosslinked substrate 212

Figure 6-9: Characterization of the full-length biotin-tagged interstrand crosslinked substrate 214

Figure 6-10: Schematic of the Electrophoretic Mobility Shift Assay (EMSA)..... 216

Figure 6-11: Detection of formation of protein complexes by EMSA..... 218

Figure 6-12: Schematic of the protein capture assay..... 220

Figure 6-13: Proteins isolated by protein capture assay 221

List of Abbreviations, Symbols, and Nomenclature

~	approximately
+/-	with/without
1-D and 2-D	1-dimensional and 2-dimensional
AA8	CHO parental cell line
alk. phos.	alkaline phosphatase conjugated
AT	ataxia telangiectasia
ATCC	American Type Culture Collection
bp	base pair
BS	Bloom's syndrome
BSA	bovine serum albumin
°C	celcius
ChIP	chromatin immunoprecipitation
CHO	Chinese hamster ovary
CO_2	carbon dioxide
CP	camptothecin
Cr	chromium
CsCl	cesium chloride
Da	Dalton
DMEM	Dulbecco's modified eagle medium
DMSO	dimethylsulfoxide
DNA	deoxyribonucleic acid
DPC	DNA-protein crosslink
DSB	double strand break
DTT	dithiothreitol
E. coli	Eschericia coli
EDTA	ethylenediamminetetraacetic acid
EGTA	ethylene glycol-bis(β-aminoethyl ether) N, N, N', N' – tetraacetic acid
ESI-MS	electrospray ionization - mass spectrometry
FA	Fanconi anemia
FAPY	formamidopyrimidine
FBS	fetal bovine serum
FEN-1	flap endonuclease 1
g	acceleration of gravity
GC/MS	gas chromatography/mass spectrometry
GDP/GTP	guanosine diphosphate/guanosine triphosphate
GM00637	human SV40 transformed fibroblast cell line

GRP78	glucose regulated protein 78
Gy	Gray
h	hour
H_2O	water
HCHO	formaldehyde
HCl	hydrochloric acid
Hepes	N-(2-hydroxyethyl)piperazine-N'-(2-ethanesulfonic acid)
HMG	high mobility group
hnRNP	heterogeneous ribonuclear protein
HOCl	hypochlorous acid
HRR	homologous recombinational repair
HSP	heat shock protein
ICL	DNA-DNA interstrand crosslink
IR	ionizing radiation
irs1SF	NER deficient CHO cell line (XRCC3-)
KCl	potassium chloride
KDa	kilodalton
LC-MS/MS	liquid chromatography-tandem mass spectrometry
LET	linear energy transfer
LPAM	melphalan
LPAM-FAPY	melphalan; ring opened, formamidopyrimidine derivative
M	molar
mA	milliamp
MALDI-TOF MS	matrix assisted laser desorption-ionization – time of flight mass spectrometry
MAR	matrix attachment region
mg	milligram
MG132	Z-Leu-Leu-Leu-H; proteasome inhibitor
$MgCl_2$	magnesium chloride
min	minute
ml	milliliter
mm	millimeter
mM	millimolar
mOGG1	mouse 8-oxoguanine DNA glycosylase
MS	mass spectrometry
MS/MS	tandem mass spectrometry
MW	molecular weight
MWCO	molecular weight cut off

N_2	nitrogen
NaCl	sodium chloride
NaOH	sodium hydroxide
NEIL2	mammalian DNA glycosylase/AP lyase
NER	nucleotide excision repair
ng	nanogram
nm	nanometer
NO	nitric oxide
NP-40	nonidet P-40
O_2	oxygen
OD	optical density
$^{\bullet}OH$	hydroxyl radical
^{32}P	radiolabeled
PAGE	polyacrylamide gel electrophoresis
PARP	poly(ADP)ribose polymerase
PBS	phosphate buffered saline
pH	potential of hydrogen
PMSF	phenylmethylsulfonyl fluoride
PNK	polynucleotide kinase
PSF	polypyrimidine tract binding protein associated splicing factor
PTB	polypyrimidine tract binding protein
RNA	ribonucleic acid
ROS	reactive oxygen species
S. cerevisiae	Saccharomyces cerevisiae
SCE	sister chromatid exchange
SDS/K^+	sodium dodecyl sulphate/potassium
SDS	sodium dodecyl sulphate
sec	second
SR protein	Serine/Arginine-residue proteins
SSB	single strand break
TASR	TLS-associated SR protein
TBST	Tris buffered saline with 0.5 % Tween 20
Tdp1	tyrosyl-DNA phosphodiesterase 1
TLS	translocated in liposarcoma
µL	microlitre
µg	microgram
UV	ultraviolet

UV5, UV20, UV41	NER deficient CHO cell lines (XPB-, ERCC1-, XPF-)
V	volts
v/v	volume/volume
XP (XPA, XPC, XPF, XPG)	Xeroderma Pigmentosum (proteins)
$ZnCl_2$	zinc chloride

Chapter 1: DNA-protein crosslinks: their induction, repair and biological consequences

A version of this paper has been published:

Barker, S.L., Weinfeld, M., and Murray, D. DNA-protein crosslinks: Their induction, repair and biological consequences. Mutation Research, 589(2): 111-35, 2005.

1.1. Introduction

The purpose of this overview is to summarize our current understanding of the mechanisms of induction and repair, as well as the biological consequences, of the types of DNA lesion known as DNA-protein crosslinks (DPCs). A DPC is created when a protein becomes covalently bound to DNA. Such events occur following exposure of cells to a variety of cytotoxic, mutagenic and carcinogenic agents, including ultraviolet light and ionizing radiation (IR), metals and metalloids such as chromium, nickel and arsenic, various aldehydes, and some important chemotherapeutic drugs including cisplatin, melphalan and mitomycin C. Humans are continuously exposed to DPC-inducing agents present in environmental pollutants such as cigarette smoke and automotive and diesel exhaust, industrial chemicals and foodstuffs, as well as physiological metabolites, such as products of lipid peroxidation. Understanding the biology of these lesions is complicated by several factors. For example, different agents induce DPCs by different mechanisms (Figure 1-1). Proteins can become crosslinked to DNA directly through oxidative free radical mechanisms or they can be crosslinked indirectly through a chemical or drug linker or through coordination with a metal atom. A subtype of these crosslinking mechanisms involves a sulfhydryl linkage to the amino acid. The combined result is numerous types of DPCs that are chemically distinct and whose formation is influenced by factors such as cellular metabolism, cell-cycle phase, and temperature. It is likely that these different types of crosslinks will be more or less susceptible to various mechanisms of reversal (e.g., hydrolysis) and enzyme-catalyzed repair, given

A) drug/chemical

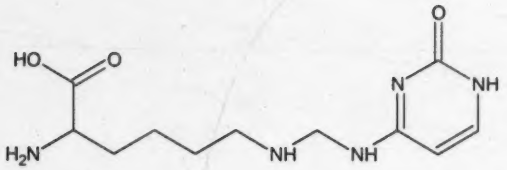

B) reactive oxygen species

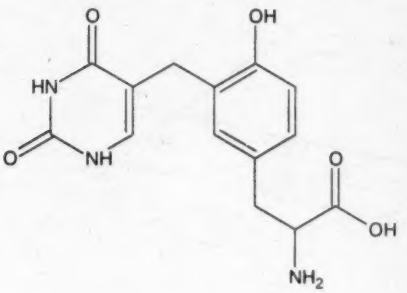

Figure 1-1: Crosslink structures

A schematic representation of two of the chemistries by which proteins may become crosslinked to DNA. A) a formaldehyde induced crosslink between cytosine and lysine (taken from [1]). B) an IR-induced crosslink between thymine and tyrosine (taken from [2]).

their different chemical structures and physical conformations. They may also have different cellular consequences.

The timing of this review coincides with the emergence of proteomics as a tool for studying biological complexes involving unknown proteins, so that the identification and quantification of specific proteins that become crosslinked to DNA is now possible without the necessity for presumption. This approach has been recently highlighted because of its success in identifying proteins involved in complex cellular structures such as the spliceosome [3] and lipid rafts [4]. Such studies have highlighted an important issue that may have compromised earlier studies of this type, namely that of protein abundance and solubility under a given set of assays conditions, which may greatly influence the proteins that are identified to the exclusion of others. These issues may have contributed to discrepancies among earlier studies.

Two classes of DPC, the attachment of topoisomerases to DNA and the association of DNA and protein caused by hyperthermia, have been reviewed recently [5,6] and will not be discussed in depth in this chapter.

1.2. Detection of DPCs

Early studies of DPCs tended to focus on the issue of whether cellular protein became associated with DNA and quantifying these DPCs following exposure of a test system to a given genotoxic agent. Existing techniques for the quantitation of DPCs differ in their detection limit/sensitivity level and associated problems. DPC induction can be measured using the comet assay because the

crosslinking of proteins to DNA retards the migration of DNA fragments, resulting in a reduced tail moment [7,8]. However, this method does not allow for isolation of DPCs. Gradient separation methods (e.g., CsCl, sucrose) [9,10] separate most DPCs from the bulk of the DNA and protein by density, but DPCs are found throughout the DNA and protein fractions [11].

A filter-based DPC isolation method employing nitrocellulose membranes is useful for obtaining dose response curves for total DNA-protein binding based on DNA retention, but is not useful for the identification of specific proteins involved in DPCs because nitrocellulose binds all cellular proteins [12-14]. A method developed by Zhitkovich and Costa [15,16] measures DPC induction as the extent of DNA associated with protein after the protein is precipitated using sodium dodecyl sulfate/potassium (SDS/K^+). However, SDS/K^+ precipitation is expected to result in the precipitation of some non-covalently linked proteins because SDS binds selectively to proteins and is then precipitated (with bound DNA) by the potassium.

An alternative approach to DPC quantitation is to isolate DNA and measure the associated protein. The alkaline elution assay traps high molecular weight DNA (with attached proteins) on a polyvinylchloride or polycarbonate filter while non-covalently bound proteins are washed away [17,18]. However, recovering DPCs from the filters is difficult and poorly reproducible (unpublished data). Total genomic DNA can be isolated using a chaotrope/detergent mix and ethanol precipitation. This DNA isolation method can be combined with additional steps to stringently dissociate non-covalent protein-DNA complexes to

allow the isolation of proteins truly crosslinked to the DNA. Modifications of this method have been used to isolate and identify nuclear matrix proteins crosslinked to DNA by cisplatin [19,20].

The lack of stringency of DPC isolation methods has been part of the problem in assessing the biological relevance of DPC analyses to date. It is known that nuclear matrix proteins are tightly associated with the DNA; their complete dissociation is crucial for the identification of those less abundant proteins that are covalently crosslinked to DNA by a given agent. As well, proteins are usually crosslinked at low levels, and it can be difficult to isolate sufficient quantities for the sequencing of proteins for identification. Detection limits of the various techniques have contributed to variability in results. Several studies have made use of 2-dimensional polyacrylamide gel electrophoresis (2-D PAGE) to analyse proteins present in crosslinked samples or in nuclear matrix fractions [10,19-24], but this technique does not itself identify the proteins. However, the emerging field of proteomics, which combines the separating capacity of 2-D PAGE analysis with powerful protein sequencing technology, should greatly facilitate the identification of these proteins.

1.3. Chemical-induced DPC formation

1.3. a. Formaldehyde-induced DPCs

Formaldehyde is a widely studied DPC-inducing agent, and the crosslinking of proteins to DNA by formaldehyde is used for the investigation of DNA-protein interactions in a technique called chromatin immunoprecipitation

(ChIP). To perform ChIP, cells are treated with formaldehyde, resulting in the covalent crosslinking of proteins to the DNA sequences with which they are associated. The DNA is then fragmented and the protein-DNA complex is isolated by immunoprecipitation with an antibody to the protein of interest.

Formaldehyde can react with amine, thiol, hydroxyl and amide groups to form various types of adducts, but the major class of DNA lesions induced by this compound are DPCs (reviewed in [25], [26]). DPC induction involves the reaction of formaldehyde with amino and imino groups of proteins (e.g., lysine and arginine side chains) or of nucleic acids (e.g., cytosine) to form a Schiff base; which then reacts with another amino group (Figure 1-2) [27,28].

1.3. b. Metal-induced DPCs

Among the DPC-inducing agents commonly found as environmental and workplace pollutants are a number of metal compounds. DPCs induced by nickel compounds have been suggested to involve oxidative mechanisms [29,30]. Nickel ions have a high affinity for proteins, especially for histidine, cysteine and aspartic acid residues [29,30]. In one study [29], DPCs were isolated by SDS/K^+ precipitation from rat lymphocytes treated with various nickel compounds. Co-incubation of lymphocytes with nickel compounds and either metal chelators, free amino acids, or scavengers of reactive oxygen species (ROS) all decreased the yield of DPCs.

Analysis of metal ion-induced crosslinks demonstrated that not all putative

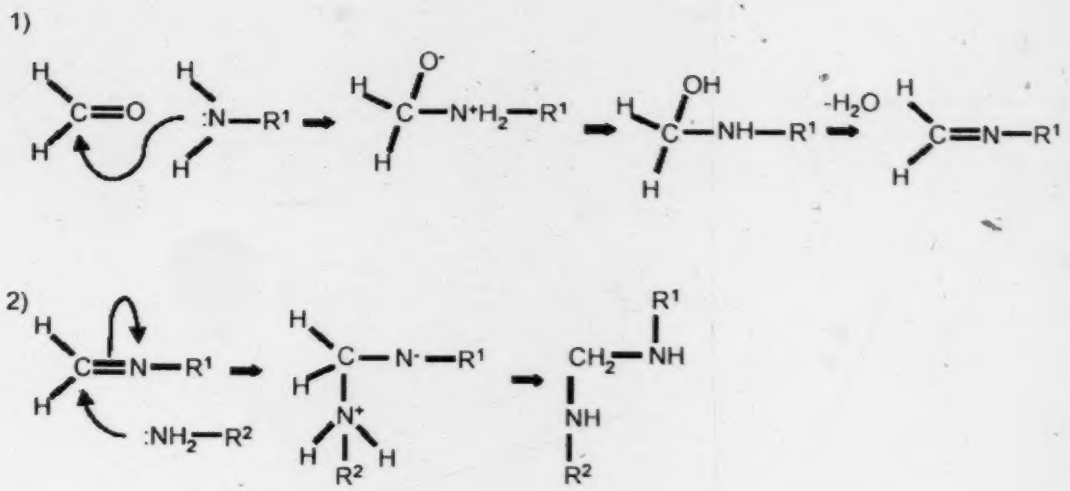

Figure 1-2: Formaldehyde crosslinking mechanism

This figure depicts the steps in the reaction of formaldehyde with an amino group (e.g., of a protein side chain) to form a Schiff base (in step 1) which can then go on and react with another amino group (of a DNA base) to complete the crosslink.

DPCs are due to covalent linkages [24] and that one agent can induce more than one chemical type of crosslink. DPCs were induced in human leukemic cells or isolated nuclei by treatment with potassium chromate, chromium (III) chloride or IR. DPCs were isolated by SDS/K^+ precipitation/ethanol precipitation and analysed by 2-D SDS-PAGE. Some crosslinked proteins were liberated by treatment with EDTA, indicating that they were not covalently crosslinked to DNA but rather were bound to DNA through a chelatable form of chromium. Some crosslinked proteins were liberated by treatment with thiourea, indicating that they were crosslinked to DNA through a sulfhydryl linkage. The majority of IR-induced DPCs were not reversed by EDTA or thiourea treatment and were only released from the DNA by DNase I digestion, and therefore represent covalent crosslinks formed through oxidative mechanisms. Some of the DPCs induced by chromate were also resistant to EDTA or thiourea treatment, and were thus likely to be covalent linkages formed via ROS.

Zhitkovich *et al.* [31] reported that a considerable proportion (~50% at biologically relevant doses) of chromium-DNA adducts were in fact DNA-metal-protein complexes. The amino acids most frequently involved in these complexes were cysteine, histidine and glutamic acid. Reactions of cysteine or histidine with trivalent or hexavalent chromium were analysed, and it was shown that Cr(VI) must be reduced to Cr(III) and that Cr(III) must first complex with an amino acid before reacting with DNA to form the crosslink. No complex was formed between DNA and amino acid if the DNA alone was first incubated with Cr(III) and then separated from unreacted Cr(III) and reacted with protein.

Additionally, these investigators reacted the Cr(III)-histidine complex with nucleosides and nucleotide monophosphates and showed that nucleotides could participate in crosslinks but nucleosides could not, indicating that the phosphate group is essential for the crosslinking reaction. However, this crosslinking utilized free amino acid and free nucleotide and thus may not be identical to that which would occur *in vivo*. The different types of linkages seen with chromium treatment (chelation complexes, sulfhydryl linkages, and linkages generated by ROS) raise the interesting question as to whether other DPC-inducers can generate more than one type of crosslink and what factors might influence the spectrum and yield of various types of crosslinks produced by a given agent.

1.4. DPCs induced by IR and ROS

1.4.a. Ionizing radiation-induced DPCs in cells

Exposure of cells to IR results in the generation of ROS, many of which are localized within a short distance of each other and of the DNA (Figure 1-3). Many of these ROS, including the extremely reactive hydroxyl radical ($^{\bullet}OH$), will be generated at high levels within small discrete regions known as spurs, blobs and short tracks [32]. When these ionization-dense regions overlap a DNA molecule, this can result in what are variously referred to as "locally multiply damaged sites" or "clustered lesions", because each radical within the region can potentially generate damage to the DNA. The result is multiple types of damage – single strand breaks (SSBs), double strand breaks (DSBs), base damage or base loss, ICLs, and/or DPCs – generated within a short distance of each other

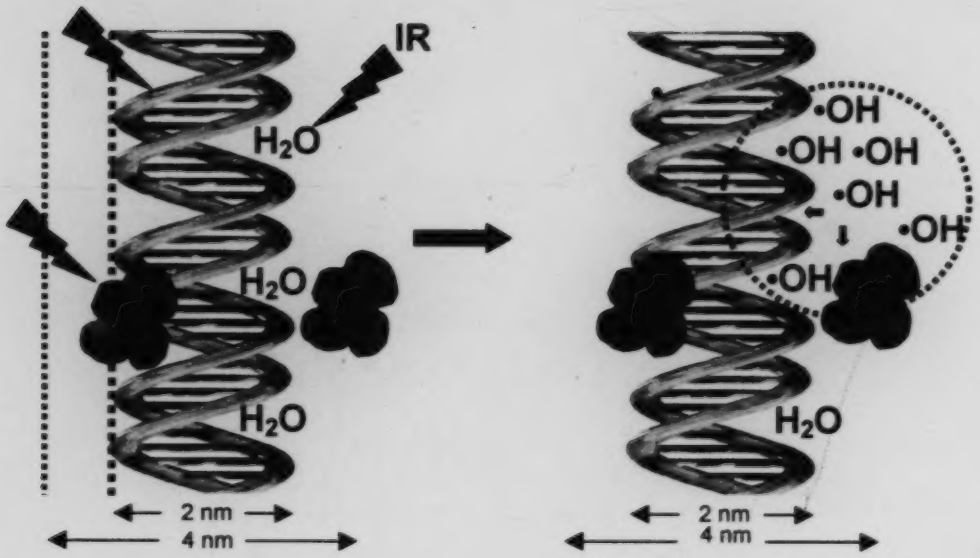

Figure 1-3: Generation of ROS by ionizing radiation (IR)

IR can directly ionize DNA or protein in its path, generating DNA or protein radicals. Indirectly-ionizing events include the ionization of water molecules surrounding the DNA or protein, generating the reactive hydroxyl radical (•OH) which can then react with DNA or protein, rendering it reactive. The dashed line represents the boundary of the spur [32].

in the DNA. Most studies of the biological effects of the cellular lesions induced by IR have focused on DSBs, and not much attention has been paid to the DPC. However, measurements of the amounts of each type of damage induced per mammalian cell per unit absorbed dose of IR reveal that the yield of DPCs (~150/cell/Gy) is actually higher than that of either DSBs (20-40/cell/Gy) or ICLs (~30/cell/Gy) [33].

Early studies by Fornace and Little [34,35] using alkaline elution demonstrated the induction of DPCs in aerated human cells exposed to very high doses of X-rays. They also showed an increase in DPC induction efficiency under hypoxic conditions. A similar observation was made by Meyn and colleagues using Chinese hamster ovary (CHO) cells [36,37] and by Radford [38] using mouse L cells, again using alkaline elution, and by Xue and colleagues [13] in V79 hamster cells using a filter binding assay. Zhang *et al.* [39-41] suggested that negligible levels of DPCs are formed at oxygen concentrations above 1%, that there is maximal DPC induction at oxygen concentrations below 0.1%, and that oxygenated cells are 10-100 fold less susceptible to forming DPCs than hypoxic cells. Similarly, vanAnkeren, Murray and Meyn (unpublished data) examined the relationship between oxygenation and DPC induction in CHO cells exposed to γ-radiation and found that the yield of DPCs decreases as oxygen levels increase (Figure 1-4). Several other studies have also shown a marked increase over background in cellular DPCs induced by IR [2,42-45].

Zhang *et al.* [40] showed that pH, nutrient depletion, temperature, and growth phase did not significantly influence the yield of IR-induced DPCs in

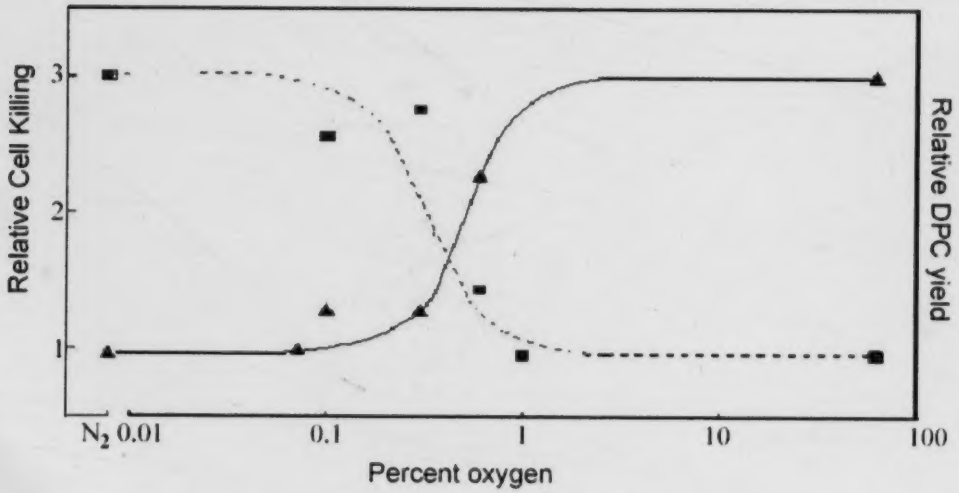

Figure 1-4: Oxygen dependence of DPCs and cell killing in γ–irradiated AA8 CHO cells

DPCs (■) were measured by the alkaline elution assay using polyvinylchloride filters, and cell killing (▲) was measured by colony-forming assay. The x-axis represents the percent oxygen in the gassing mixture. Single-cell suspensions were stirred at 4°C while being gassed with a mixture of 5% CO_2, varying concentrations of O_2, balance N_2, for 3 h prior to irradiation. (S. vanAnkeren, D. Murray, R.E. Meyn, unpublished data)

aerated normal and tumor cells as measured by alkaline elution. Similarly, pH and nutrient status had no effect on cellular DPC induction when oxygen was absent [46]. Importantly, Zhang *et al.* [40] pointed out that it is difficult to compare DPC studies because the various techniques used to measure DPCs differ in their detection limits.

Given that the yield of DPCs in cells decreases markedly as oxygen is introduced, whereas the effect of oxygen on IR-induced cell killing goes in the opposite direction, and because the yield of other types of DNA damage such as DSBs closely parallels cell killing under these conditions, the role of DPCs in the biological effects of IR has been largely disregarded. However, as will be discussed in section 1.9.c, these lesions may contribute to the radiosensitivity of hypoxic cells if their repair is compromised. Also, as will become apparent from the findings to be presented in Chapter 3 of this thesis, the study of individual proteins involved in DPCs suggests a very different scenario than was suggested by these gross DPC studies.

The situation with respect to DPCs and high linear energy transfer (LET) radiation has received some theoretical consideration. One unresolved question is whether DPCs, either alone or in association with clustered lesions, might differentially contribute to cell killing induced by radiations of differing LET. The thinking is that higher LET tracks will generate more complex clustered lesions, possibly with a higher probability of involving a DPC. Putative high-LET "specific" lesions could include complex clustered-damaged sites wherein DSBs are associated with DPCs [47-49]. Some experimental studies have addressed

the issue of whether the yields and/or repair of DPCs might differ with LET. Blakely and colleagues [50] showed that the **initial** DPC yields in normal hamster cells were similar for X-rays and high energy Ne-ions of 32, 100 and 183 keV/μm at low doses, although N-ions (120 keV/μm) generated a lower DPC yield. Another study suggests that a high-LET beam of N-ions appeared to induce **higher** levels of **residual** (6 h post-IR) DPCs per unit dose than low-LET X-rays in human melanoma cells (data from Eguchi *et al.* [51], re-calculated by Frankenberg-Schwager [52]). This difference may be attributable to the above-mentioned induction of lesions of greater complexity at higher LET, rendering DPCs more difficult to repair.

1.4.b. Ionizing radiation-induced DPC structures

To understand the cellular consequences of DPCs and to investigate their possible repair pathways, it will be important to delineate the chemistries of these linkages (e.g., see Figure 1-1). Extensive work with cell-free models has demonstrated the covalent nature of IR-induced DPCs, and the chemical structure of some DPCs has been determined using gas chromatography/mass spectrometry (GC/MS) analyses [53-55]. These reports examined γ-irradiated aqueous mixtures of thymine and amino acids (lysine, glycine, alanine, valine, leucine, isoleucine, tyrosine and threonine) and demonstrated that particular DNA-amino acid crosslinks exist as several isomers [53-55]. The involvement of these amino acids in DPCs was also shown *in vitro* in isolated irradiated mixtures of calf thymus nucleohistone [53-55].

The GC/MS experiments were extended to analyse the formation of DPCs *in vivo* using cultured mammalian cells [2,56] and rat renal tissue [57]. These samples were treated with ferrous ions, hydrogen peroxide, or IR, and the chromatin was isolated, subjected to acid hydrolysis, and analysed by GC/MS. Crosslinking of DNA to protein through a thymine-tyrosine linkage was detected in these samples. In both the *in vitro* and *in vivo* studies, the induction of DNA-amino acid complexes and DPCs increased linearly with IR dose. Hydrogen peroxide treatment of cultured cells also resulted in the concentration-dependent induction of DPCs in chromatin [2]. Addition of radical scavengers/metal chelators (dimethylsulfoxide or *o*-phenanthroline) partially inhibited DPC formation [2].

Dizdaroglu [55] has proposed that the $^{\bullet}OH$ radical is involved in the formation of the crosslink whether these DPCs are induced by ferrous ions, hydrogen peroxide or IR. Free radicals/ROS are also generated through biological redox reactions and under conditions causing oxidative stress, such as malnutrition, numerous disease states, exposure to particular drugs, and environmental pollution. The crosslinking mechanism involves H-atom abstraction from the methyl group of thymine by $^{\bullet}OH$, addition of the resultant thymine radical to the carbon-3 position of the tyrosine ring, and oxidation of the resulting adduct radical [55].

Electrospray-ionization mass spectrometry (ESI-MS) analysis of an irradiated solution containing angiotensin and thymine demonstrated the formation of a covalent bond between the methyl group of thymine and C3 of the

angiotensin tyrosine ring [58] and also indicated C2 of tyrosine as another major site of bond formation. Crosslinks between thymine and tyrosine were detected at IR doses as low as 0.1 Gy, and the yield of crosslinks was linear up to 100 Gy. Reaction of •OH with thymine most frequently resulted in addition to the C5-C6 double bond (~60% and ~30%, respectively, at the 5 and 6 positions), and abstraction of an H-atom from the methyl group occurred only ~10% of the time.

It will be of interest to determine whether specific proteins found to be covalently crosslinked to DNA *in vivo* will prove to be linked through any of these identified target residues. Additionally, this information may be of use in predicting which proteins are likely targets for DPC formation because of their amino acid composition and their contact with the DNA. Identifying a crosslinked protein and the residue through which the linkage forms may also provide information on molecular geometry because the DNA and protein must be in close proximity during free radical generation.

1.4.c. Protein radicals and DPCs

DNA is not the only site of free radical generation or the only target for free radical attack following IR exposure (Figure 1-3). Proteins and amino acids are also susceptible to attack by ROS. Indeed, an alternative mechanism for DPC induction involves an initial protein radical created by abstraction of an H-atom by •OH from the amino acid, followed by addition of the amino acid radical to the C6 position of thymine and oxidation of the adduct radical [53]. ESI-MS studies by Weir-Lipton *et al.* [58] show that •OH adds to the tyrosine ring at C3 ~50% of the time and at C2 ~35% of the time. The C3 tyrosine adduct radical loses water to

generate a phenoxyl radical, which can then react with DNA. Thus, a DPC may be formed by the addition of a protein radical to DNA or vice versa, or from a combination of two radicals.

Exposure of proteins to ROS can generate protein hydroperoxides or other reactive protein species as well as additional free radicals. An *in vitro* study [59] used several purified proteins (insulin, α-casein, apotransferrin and bovine serum albumin (BSA)) irradiated in aqueous solution in the presence of oxygen or nitrous oxide to generate protein hydroperoxides, and tested these for DPC formation with plasmid DNA based on the retardation of DNA migration on an agarose gel. The observation that inclusion of anti-oxidants did not reduce the yield of DPCs suggested that these lesions were not generated from long-lived radical species produced at the irradiation step. However, the formation of DPCs was reduced by including metal chelators in the reaction, suggesting that at least some of the DPCs were dependent on metal atoms associated with the DNA. Other reports have indicated that proteins that do not bind to DNA (e.g., BSA [60]) cannot generate DPCs *in vitro*, so there is some question as to whether or not non-DNA-binding proteins can be involved in DPCs. It is likely that the conflicting reports reflect differences in *in vitro* experimental parameters such as DNA and/or protein concentrations, presence of radical scavengers, and presence of salts or metals or reductants that would interfere with the DPC-formation reaction.

Further work examining the role of reactive protein species in DPC formation used hypochlorous acid (HOCl), an oxidant that is produced by normal

metabolic processes such as phagocyte activity [61]. HOCl can react with protein amino groups, generating chloramines that decompose to protein radicals which can react with DNA. HOCl can also interact with DNA to form chloramines. Hawkins and colleagues [61] investigated the formation of DPCs by HOCl in nucleosomes of eukaryotic-cell nuclei using electron paramagnetic spin resonance spectroscopy. The reaction of protein radicals with pyrimidine nucleosides was observed to yield nucleobase radicals which could result in covalent crosslinking of DNA to protein. These authors [61] suggested that reaction of HOCl occurs predominantly with the protein and not the DNA, and that 50-80% of these reactions are with lysine or histidine residues. The finding that adduct formation was decreased in the presence of radical scavengers suggested that a radical is involved in this reaction.

Similar steps in DPC formation were suggested by analysis of malondialdehyde-induced DPCs *in vitro* [60]. These investigators reacted malondialdehyde with either protein or DNA in aqueous solution, purified away non-reacted material, and then attempted the second half of the DPC reaction (by introducing DNA or protein). For the formation of a DPC, it was apparent that the malondialdehyde must first react with the protein to generate an adduct that subsequently reacts with the DNA to form the crosslink.

Although both DNA- and protein-radical formation have been suggested as the first step in DPC formation *in vitro*, it remains to be seen which mechanism predominates *in vivo*. Both mechanisms are probably operative for various agents, and other factors may influence the levels of each type of radical

produced. For example, in the case of IR, the spatial distribution of DNA and proteins in the radiation track may be critical in this regard [49].

1.5. Stability of DPCs *in vitro*

Different types of DPCs appear to have very different chemical stability. Aldehyde-induced DPCs are reversed by spontaneous hydrolysis and are also reversible by incubation at elevated temperatures (discussed in [26]). Acetaldehyde-induced DPCs are hydrolytically unstable, and in *in vitro* experiments only ~25% of these DPCs remained after 8 h at 37°C [62,63]. By comparison, malondialdehyde-induced DPCs formed *in vitro* using purified DNA and histone protein had a much longer half-life of 13.4 days at 37°C [60].

The lifetime of formaldehyde-induced DPCs *in vitro* was investigated by Quievryn and Zhitkovich [26] using purified DNA and histone H1. Inclusion of either SDS or 0.8 M sodium chloride with the formaldehyde during the crosslinking reaction reduced crosslinking of histone H1 by preventing its binding to DNA. Addition of SDS after the formaldehyde crosslinking reaction decreased the lifetime of the histone H1-DNA DPC from 26.3 h to 18.3 h at 37°C, suggesting that if the protein is allowed to stay associated with the DNA, the crosslinks can reform under physiological conditions.

1.6. Biological consequences of DPCs

The covalent crosslinking of proteins to DNA is expected to interrupt DNA metabolic processes such as replication, repair, recombination, transcription,

chromatin remodeling, etc. Indeed, the effect of agents that cause DPCs on DNA replication has been widely investigated ([64-66] and others). DPCs are expected to act as bulky helix-distorting adducts and would therefore be likely to physically block the progression of replication or transcription complexes and/or prevent access of proteins required either for synthesis along the template strand, for transcription, or for repair recognition and/or incision. They may also affect all of these processes by anchoring the chromatin and preventing its remodeling.

Unfortunately, our understanding of the biological consequences of DPCs is hampered by the fact that no agent exclusively induces these lesions in genomic DNA (although studies using plasmid DNA have provided some insight into the processing of these lesions by cells; see section 1.6.b). Thus, all known DPC-inducing agents generate other forms of DNA damage in addition to DPCs, and direct attribution of any observed effect such as mutagenesis or carcinogenesis to DPCs is inevitably confounded by the concomitant impact of these other lesions. Nonetheless, several studies have reported that the induction of DPCs by many agents correlates with genetic damage such as sister chromatid exchanges (SCEs), transformation, and cytotoxicity [67-71]. Thus, DPCs may contribute to the genotoxic effects of many different DNA-damaging agents, some of which are discussed below.

1.6.a. Nickel

Various types of chromosome damage (e.g., DNA gaps and breaks, SCEs) have been shown to persist in lymphocytes of nickel workers for years after exposure [72,73]. Earlier studies demonstrated an increased incidence of alveolar/bronchial/adrenal medulla neoplasms in rats exposed to nickel compounds [74].

1.6.b. Chromium

Chromium exposure has been associated with an increased incidence of respiratory cancers (reviewed in [75]). Voitkun *et al.* [76] used amino acid-chromium-DNA adducts (model DPCs) in a shuttle vector to show that processing of these lesions by human cells can result in mutagenesis. Plasmids containing DNA-Cr(III)-glutathione or DNA-Cr(III)-amino acid adducts were transfected into human fibroblasts, re-isolated after a 48-h incubation, and sequenced. The types of mutations caused by the DPCs were mainly single base substitutions at G:C base pairs, with G:C→A:T transitions and G:C→T:A transversions being induced with similar frequency. Chromium-DNA complexes also resulted in sequence mutations, although this effect was weaker.

The feasibility of using DPCs as biomarkers for exposure to chromium in human cells has been investigated [75]. Higher levels of DPCs were detected in lymphocytes of individuals exposed to chromium compounds than in non-exposed individuals, although the DPC level was found to plateau in individuals exposed to high levels of chromium.

1.6.c. Arsenic

Arsenic has been implicated in the induction of skin, lung, bladder and liver cancers [77-79]. Although it is carcinogenic, arsenic has not been found to be mutagenic. Earlier studies suggested that arsenic only induces DNA damage at high concentrations; however, a recent study [80] suggests that different cell types differ in their sensitivity to arsenic. Arsenic does in fact induce DNA damage at concentrations that are biologically relevant, the major forms of arsenic-induced DNA damage being oxidative DNA adducts and DPCs [80]. As well, multiple pathways have been proposed for arsenic-induced cytotoxicity [80]. Treatment with arsenite may result in DNA damage through the production of HOCl because there is an activation of NADH oxidase and an increase in superoxide production after NADH addition in arsenite-treated human vascular smooth muscle cells [81]. This pathway can result in DNA damage because superoxide is converted to hydrogen peroxide by superoxide dismutase, and the resulting hydrogen peroxide can react with chloride ions to form HOCl or with transition metal ions to produce $^{\bullet}OH$ [81-83].

Evidence that arsenic cytotoxicity may not be due to DNA damage comes from Mei *et al.* [84]. Similar sensitivity was seen for normal human cells and various DNA repair-deficient cell lines (Xeroderma Pigmentosum (XP), Bloom Syndrome (BS), and Fanconi Anemia (FA)) after treatment with sodium arsenite; however, Ataxia-Telangiectasia (AT) cells were significantly more sensitive. This sensitivity did not appear to be related to DSB repair because additional cell lines defective in DSB repair did not display increased sensitivity to arsenic. As well,

there was no induction of DSBs (as measured by histone H2AX phosphorylation) and no activation of p53 upon treatment of normal cells with sodium arsenite. One parameter that did seem to be affected by arsenic treatment was cell cycle distribution. Normal cells showed a significant increase in the percentage of cells in S-phase and a modest increase in the percentage of cells in G2/M phase after arsenic treatment, whereas the cell cycle distribution of AT cells was unaffected. Thus, the sensitivity of AT cells to arsenic may be due to an effect on cell cycle regulation and not necessarily due to DNA damage. Current evidence indicates that heavy metal exposure has effects on cell cycle checkpoints and progression [85]. However, Bau *et al.* [80] provided evidence that arsenic induces DPCs that are converted to DSBs over time. Thus, measurements of DSBs and DPCs will be inaccurate as DPCs become converted to DSBs. The disruption of cell cycle seen with arsenic treatment may be due to DPCs. Although there is little knowledge on the effect of DPCs on cell cycle progression, these lesions are expected to disrupt multiple functions of DNA metabolism/organization.

1.6.d. Formaldehyde

Formaldehyde is mutagenic in bacteria, lower eukaryotes, and human lymphoblasts, inducing primarily point mutations and deletions. Formaldehyde also causes micronuclei [86] and is implicated in the induction of nasal tumors in experimental animals [87,88]. The induction of DPCs by formaldehyde has been shown to be dose-dependent and to correlate with tumorigenesis [89,90]. The extent of DNA-protein crosslinking has been used as a biomarker of

formaldehyde exposure in mammalian cells [89,91,92] and may have similar applicability in assessing risk factors for exposure to other DPC-inducers.

1.6.e. Methylglyoxal and glyoxal

Methylglyoxal [pyruvic aldehyde: CH_3COCHO] is another endogenous aldehyde metabolite known to induce DPCs. It is found widely in food and beverages and in cigarette smoke. Methylglyoxal reacts with free amino acids, proteins, and nucleic acids (mainly guanines thereof) resulting in DNA adducts, strand breaks, ICLs, and extensive DNA-protein crosslinking through lysine and cysteine residues [93], including crosslinking of histones, (reviewed in [94-96]). Mutations induced by methylglyoxal in mammalian cells were predominantly (~50%) deletions but included a significant proportion of base-pair substitutions (~35%) [95]. The DNA-damaging effects of methylglyoxal include the induction of SCEs, chromosomal aberrations and micronuclei [95].

Glyoxal [$(CHO)_2$] is a related, endogenously produced, aldehyde that induces DNA strand breaks but ~10 fold fewer DPCs than methylglyoxal. Glyoxal also induces ~10 fold fewer frameshift mutations than methylglyoxal, suggesting that DPCs might be the cause of these events (which are a common result of bulky adducts) [96]. Roberts *et al.* [96] compared the effects of glyoxal and methylglyoxal on human skin cells using both the comet assay and an *in vitro* plasmid assay. In the comet assay, the tail moment increased when cells were treated with glyoxal, indicating DNA strand breakage. However, following

methylglyoxal treatment, there was compaction of the nucleus and reduced migration, indicating the presence of DPCs.

1.6.f. Pyrrolizidine alkaloids

Pyrrolizidine alkaloids are cytotoxic compounds found in many plant species that are used in herbal remedies and teas. These compounds can cause liver disease and are carcinogenic [97]. They are metabolically activated and form DPCs and ICLs in similar proportions when assessed by alkaline elution [98]. The cytotoxic and anti-mitotic activities of pyrrolizidine alkaloids correlates with their ability to form both DPCs and ICLs [98-100].

1.6.g. Ionizing radiation

As noted earlier, the role of DPCs in the biological effects of IR has been largely ignored because these lesions are more abundant following irradiation in the absence of oxygen, a condition that is protective for most other IR-induced end-points such as cell killing and mutation. Certainly, this observation suggests that DPCs are minor lesions in irradiated oxygenated cells. However, there is some evidence that DPCs can contribute to the killing of mammalian cells when their repair is inhibited. In particular, certain DNA repair-deficient hamster cell lines such as UV41 (XPF^-) and UV20 ($ERCC1^-$) (reviewed in [101,102]) are significantly more sensitive than wild-type cells to killing by IR under hypoxic conditions, a phenotype that has been attributed to a deficiency in the repair of DPCs [102].

It should be noted that many human tumors contain a significant proportion of hypoxic cells, and this represents a problem in the use of radiation therapy for cancer treatment because hypoxic cells are more resistant to IR-induced killing. The findings that DPCs are induced by IR to a greater extent in hypoxic versus aerated cells and that certain repair deficiencies specifically increase the radiosensitivity of hypoxic cells might provide an avenue for improving radiation therapy if the repair of DPCs can be effectively inhibited.

1.6.h. Cumulative/background lesions

DPC accumulation may be associated with breast cancer [103]. The base-level of DPCs, presumably caused by environmental factors and metabolic byproducts, was found to be significantly elevated in breast cancer patients compared to healthy individuals. It is far from clear, however, whether these DPCs are secondary to the many cellular changes that accompany cancer development or treatment or if these DPCs are in fact causative in breast carcinogenesis.

1.7. Proteins involved in DPCs

Determining which proteins become crosslinked to DNA by these various genotoxic agents and how they are bound may help to unravel the biological consequences of DPCs as well as the mechanisms of their repair. A number of investigators have tried to identify proteins that can become crosslinked to DNA using *in vitro* systems with purified proteins and DNA or by isolating DPCs from

cells exposed to various DNA-damaging agents. Several proteins have been shown to be amenable to crosslinking *in vitro* when they are combined with DNA and treated with a DPC-inducing agent, although the relevance of this information to the *in vivo* situation is uncertain. Some reports suggest that only DNA-binding proteins can be crosslinked to DNA, while others suggest that any protein can become crosslinked to DNA. Potentially biologically-relevant proteins that have been shown to be crosslinked to DNA *in vivo* include actin, lectin, aminoglycoside nucleotidyl transferase, histones, a heat shock protein (GRP78), cytokeratins, vimentin, protein disulfide isomerase, and transcription factors/co-factors (estrogen receptor, histone deacetylase 1, hnRNP K, HET/SAF-B) (Table 1-1) [9,20,21,24,104-107].

Actin was shown to be crosslinked to DNA in human leukemic cells or isolated nuclei treated with chromium compounds or IR [23,24]. DPCs were isolated by SDS/K^+-urea precipitation/ethanol precipitation, followed by analysis by 2-D SDS-PAGE. In this study, ~20 proteins were found to be crosslinked to DNA by chromium and IR. Three of these were identified as actin, aminoglycoside nucleotidyl transferase and lectin. Similarly, Miller *et al.* [21] demonstrated the crosslinking of actin to DNA in hamster cells exposed to chromium or cisplatin. DPCs were isolated by SDS/K^+-urea precipitation/acetone precipitation. DNA was digested with DNase I, and the isolated proteins were analysed by SDS-PAGE. This procedure isolated several proteins, one of which was identified as actin on the basis of molecular weight and pI, and confirmed using immunological methods. Actin-DNA crosslinks comprised ~20% of the

Table 1-1: Proteins Identified in DNA-Protein Crosslinks

Protein	Crosslinking Agent	Reference
Actin	Chromium	[21,24]
	Cisplatin	[108]
	Mitomycin C	[108]
	Pyrrolizidine Alkaloids	[108]
Lectin	Chromium	[24]
Aminoglycoside nucleotidyl transferase	Chromium	[24]
Histones H1, H2A, H2B, H4	Formaldehyde	[106]
Histone H3	Formaldehyde	[106]
	Gilvocarcin V	[104]
Glucose Regulated Protein 78	Gilvocarcin V	[104]
Cytokeratins	Arsenic	[105]
Vimentin	Formaldehyde	[9]
	Metabolic byproducts	[9]
Protein Disulfide Isomerase	Cisplatin	[107]
Estrogen receptor	Cisplatin	[20]
HET/SAF-B	Cisplatin	[20]
hnRNP K	Cisplatin	[20]
Histone deacetylase 1	Cisplatin	[20]

total DPCs isolated. Additional proteins were found to be crosslinked by chromium at higher metal concentrations.

Actin was also found to be crosslinked to DNA by pyrrolizidine alkaloids [108]. Bovine kidney cells and human breast cancer cells were treated with these compounds, and DPCs were isolated by repeated extraction/precipitation with SDS and urea. Crosslinked proteins were released from the DNA by DNase I digestion and analysed by SDS-PAGE. Participation of different isoforms of actin in DPCs was confirmed by immunoblotting. Actin was also identified as a component of DPCs isolated from cells treated with cisplatin or mitomycin C. Another study [107] demonstrated the cisplatin-induced crosslinking of at least four proteins to DNA in human cells and identified protein disulfide isomerase as one of these using immunological methods. If the association of proteins with DNA was disrupted by extracting the cells with DTT prior to cisplatin treatment, protein disulfide isomerase was no longer crosslinked. Several proteins have been shown to be crosslinked to DNA by arsenic [105]. DPCs were isolated from arsenic-treated cultured human hepatic cells using SDS/K^+ precipitation (without urea). Crosslinked proteins were separated by SDS-PAGE, and the presence of several different cytokeratins was confirmed using antibodies. However, these arsenic concentration-dependent crosslinks could be reversed by high salt, suggesting that they may be non-covalent associations rather than true covalent DPCs.

One protein identified as being closely associated with DNA *in vivo* by virtue of its susceptibility to crosslinking by formaldehyde is vimentin, which is a

structural/scaffold protein [9]. DPCs were isolated from formaldehyde-treated mouse and human cells by sucrose gradient sedimentation followed by repeated SDS/K^+ precipitation/ethanol precipitation, followed by immunoprecipitation using anti-vimentin antibodies. The vimentin could be released from the DPC by boiling, which may indicate thermolability of the crosslinkage or a non-covalent association. Vimentin DPCs were also observed in oxidatively-stressed and senescent cells, indicating that metabolic byproducts can crosslink this protein to DNA.

Gilvocarcins are naturally occurring antitumor antibiotics that can crosslink proteins to DNA. Normal human fibroblasts treated with gilvocarcins were subjected to lysis and DPC isolation using SDS/K^+ precipitation with a sodium chloride wash step, followed by immunoprecipitation with an antibody to double stranded DNA [104]. The DPCs were separated by SDS-PAGE, and two proteins – histone H3 and heat shock protein GRP78 - were identified by amino-terminal amino acid sequencing and confirmed by immunoblotting [104].

There are conflicting reports regarding the involvement of histones in DPCs. Several investigations have focused on the *in vitro* induction of histone-involving DPCs in aqueous solution. Miller *et al.* [21] treated a combination of purified actin or histone and bacteriophage DNA with chromium compounds *in vitro* and found that histones were not as efficiently crosslinked to DNA as actin. This may be due to the fact that chromate has a high affinity for sulfhydryl groups and thus induces crosslinks through a sulfhydryl linkage, but there are few sulfhydryl groups in histone proteins [23]. However, histones have been found to

be readily crosslinkable to DNA by formaldehyde through an amine to amine linkage [106,109,110] and mammalian histones can be crosslinked to DNA by treatment with aldehydes both in cells and in cell-free systems [26,60,62,111,112]. The choice of DPC-inducing agent may explain why some studies found histones to be highly crosslinked to DNA while others did not.

Induction of DNA-histone crosslinks by IR has proven controversial. Several studies [53-55] have shown the IR dose-dependent crosslinking of histones to DNA *in vitro* using calf nucleohistone. Studies from Xue *et al.* [113] and Oleinick *et al.* [114] using irradiated hamster cell nuclei demonstrated that DPCs were induced in histone-depleted chromatin [114] and that extraction of nuclei with 1.6 M NaCl showed little depletion of DNA-associated histones but was associated with a significant decrease in DPC induction, indicating that other proteins are involved in these DPCs [113]. However, Mee and Adelstein [43] also examined the induction of DPCs by γ-radiation using chromatin isolated from Chinese hamster lung fibroblasts and obtained different results. They suggested that the core histones (H2A, H2B, H3 and H4) are in fact the major proteins involved in DPCs because they observed no difference in induction of DPCs between *in vitro*-prepared whole chromatin and chromatin stripped of other nuclear matrix proteins. These contradictory results may be due to differences in the efficiencies of the extraction procedures, and thus the true extent of the involvement of histones in cellular DPCs is yet to be resolved.

The conflicting data on the formation of histone-DNA crosslinks may reflect the fact that these studies used different methods of inducing, isolating,

and quantitating DPCs. Given that DPC-inducing agents have different mechanisms of action, it is possible that histones are substrates for only some types of reactions. Different methods of isolation and analysis may result in a failure to detect crosslinked proteins of low abundance, and detectability may be affected by the solubilities of these proteins. These types of problems are also likely to affect the analyses of other proteins involved in DPCs.

Like the histone proteins, high mobility group (HMG) proteins are likely targets for DPC induction given that they are highly abundant and frequently associated with DNA. These proteins have roles in modifying the compaction of the chromatin fiber, promoting access to nucleosomes, and stimulating transcription and replication [115-118]. Additionally, the high affinity of HMG proteins for unusual structures (e.g. chromium- or cisplatin-damaged DNA) may also predispose them to crosslinking. There is little experimental evidence for the involvement of HMG proteins in DPCs. HMG proteins were shown to be crosslinked *in vitro* to a synthetic nitric oxide-damaged DNA substrate [119]. It has been shown [120,121] that a novel anti-tumour drug (FR-66979) covalently crosslinks a DNA duplex with a synthetic peptide corresponding to the HMGA (formerly HMGI/Y [122]) binding domain. Extending this work, Beckerbauer *et al.* [123] reported the crosslinking of HMGA and of HMGB1 and HMGB2 (formerly HMG1 and HMG2 [122]) to DNA *in vivo* by a related drug (FR900482). Complexes of HMGA and DNA were isolated from drug-treated cells but not control cells using a modified ChIP procedure and HMGA antibodies. In this study, the "crosslinked" protein was released from the DNA by proteinase K

digestion, making it difficult to determine if these complexes were in fact covalent. Although the affinity of HMGB1 for undamaged DNA is very weak, it does have very high affinity for unusual DNA structures [115]. HMG proteins bind tightly to chromium-damaged DNA, and HMG-Cr-DNA complexes are stable in 0.5 M NaCl [124], and the affinity of HMGB2 for cisplatin-modified DNA is 10-fold stronger than that for chromium-damaged DNA [125].

The question of whether or not HMG proteins are involved in DPCs requires further investigation. As their name suggests, HMG proteins are known to be extremely mobile [115-118] and, although they are highly abundant and frequently associated with DNA, their association with DNA could be too transient for them to be "trapped" in the crosslinking reaction. The above-mentioned affinity of these proteins for damaged DNA may favour such reactions during extended treatments, increasing the likelihood of a cross-linking event.

1.7.a. Crosslinking of DNA replication/repair enzymes to DNA

The potential for crosslink formation between DNA replication/repair proteins and the substrate DNA has been demonstrated by *in vitro* experiments. HOCl is capable of crosslinking purified DNA single-stranded binding protein to single-stranded oligonucleotides *in vitro* [126]. Methylglyoxal was similarly shown to crosslink purified Klenow fragment to a synthetic DNA substrate [95]. The 2-deoxyribonolactone lesion is an abasic site produced by a variety of DNA damaging agents, including IR. This lesion and it's β-elimination product were prepared in a synthetic substrate and incubated in separate reactions with

protein (*E. coli* endonuclease III, endonuclease VIII, FPG (formamidopyrimidine glycosylase), or NEIL1 (a mammalian DNA glycosylase [127])) resulting in the crosslinking of each of these proteins to the lesions [128]. Another study demonstrated that the 2-deoxyribonolactone lesion could be crosslinked to DNA polymerase β [129].

Nitric oxide (NO) is a product of inflammation, and chronic inflammation is a known risk factor for many cancers. NO-induced damage includes DPCs [130-132]. One type of DNA damage induced by the nitrosation of guanine by NO is oxanine (Oxa). A synthetic duplex DNA containing Oxa was shown to form covalent crosslinks between the Oxa moiety and DNA repair proteins [119]. The *E. coli* DNA repair proteins endo VIII, FPG, AlkA and mammalian hOGG1 (which bind such types of base damage) formed DPCs rapidly, while histones and HMG proteins formed DPCs more slowly and the *E.coli* Endo III and mammalian hNTH1 and mMPG did **not** form DPCs. Furthermore, heat inactivation of the glycosylases prior to incubation with the Oxa substrate abolished DPC formation, indicating that the active form of the protein was needed; however, the same was not true for histone proteins as heat inactivation had no effect on DPC formation. These *in vitro* studies used large excesses of purified proteins and therefore may not be biologically relevant, although DPC species were also detected (as retarded migration in gel shift studies) when the Oxa substrate was incubated with HeLa cell extract.

These findings suggest that some types of DNA damage are reactive suicide substrates for DNA repair proteins, leading to the further generation of

damage (i.e., DPCs), and may thereby prevent their own repair. However, it is not clear if HMG proteins bind damaged DNA to recruit repair factors, as in the case of HMG binding of deoxythioguanosine DNA [133], or bind damaged DNA non-specifically because they recognize any bend in DNA which results in shielding the lesion from DNA repair, as is the case for binding of HMG proteins to cisplatin-modified DNA [134,135].

Thus, it is also important to determine which proteins are responsible for recognizing various types of DPCs and activating their repair. Clearly, the crosslinking of DNA repair proteins to DNA would be expected to interfere with the repair process. It may be that repair proteins can become covalently trapped as the repairosome moves along the DNA looking for its specific lesion substrate.

1.8. Crosslinking of DNA to the nuclear matrix

The nuclear matrix is a 3-D network that is necessary for DNA organization and nuclear structure and function. This framework consists of the nuclear membrane with the nuclear lamina and pore proteins, the internal network of ribonuclear proteins, and nucleolar proteins [136]. The nuclear matrix contains anchoring sites for the DNA called "matrix attachment regions" (MARs) and the DNA is organized into loops of 50-200 kbp between these anchor sites. Loop domain anchoring allows for differential control of supercoiling between loops during processes such as replication and transcription [137] which are known to alter DNA topology.

Nuclear matrix proteins are associated with processes such as DNA replication, transcription, and repair [136]. Some proteins isolated from DPCs, such as actin, are known to be associated with the nuclear matrix and to be involved in these processes [21,138-141]. Other proteins, such as the intermediate filament protein vimentin, have recently been shown to be crosslinked to DNA and to be associated with the nuclear matrix [9,142]. Because vimentin can bind to and become crosslinked to DNA, particularly to sequences that resemble sequences at MARs, and because it can also bind to histones, it has been proposed that this protein is involved in chromatin remodeling [142].

Cisplatin has been shown to crosslink nuclear matrix proteins to DNA [20,143]. Nuclear matrix fractions and cisplatin-crosslinked fractions were isolated from human breast cancer cells and protein profiles were compared by 2-D SDS-PAGE [20,143]. Most of the cisplatin-crosslinked proteins were nuclear matrix proteins. Cisplatin crosslinked several transcription factors to the DNA, leading to the suggestion that this is a mechanism of transcription inhibition by crosslinking agents [20]. Additionally, profiles of crosslinked nuclear matrix proteins changed in breast cancer cells at different stages of the disease [143].

The effect of IR on the integrity of DNA loop supercoiling was investigated in mouse lymphoma cells using the propidium iodide fluorescence halo assay, which allows the visualization of the unwinding of anchored DNA loops [137]. The supercoiling ability of DNA loops was examined in both radioresistant and radiosensitive cells, with and without the presence of IR-induced damage, but

DPCs were not specifically analysed. The supercoiling of DNA loops containing IR-induced damage was inhibited to a greater degree in radiosensitive cells, suggestive of alterations in DNA anchoring. This study also used 2-D PAGE to examine the proteins in nucleoids (DNA with associated, extraction-resistant, nuclear matrix proteins) from both types of cells. Several proteins associated with nucleoids derived from radioresistant cells were absent from nucleoids from radiosensitive cells, but none of these proteins correlated directly with radioresistance [137]. This work provides evidence of a relationship between IR-induced damage and the DNA supercoiling ability of DNA loop domains [137]. Balasubramaniam and Oleinick [144] demonstrated that IR can crosslink MAR-containing DNA to the nuclear matrix. Clearly, the covalent attachment of DNA to the nuclear matrix should result in serious disregulation of DNA metabolic processes. Several studies have indicated that nuclear matrix proteins are indeed involved in DPCs ([21,113,144,145] and others). Stripping histones from the DNA with high salt extractions does not completely eliminate the formation of DPCs, indicating that other proteins, such as nuclear matrix proteins that remain bound to DNA despite high salt extraction, are susceptible to crosslinking by IR [113,114].

Thus, DPC-mediated alterations in the control of DNA supercoiling by altering the anchoring and/or unwinding of DNA loops might influence DNA repair and other processes by altering DNA conformation, remodeling abilities, and/or accessibility. Clearly, the effect of DPCs on the dynamic control of DNA metabolic processes warrants further investigation.

1.9. Enzymatic repair of DPCs

Studies on some types of cellular DPCs indicate that these lesions can be longer-lived than other types of DNA damage and persist through several DNA-replication cycles [146,147] and are only partially repaired [148], which may result in permanent DNA alterations and have serious consequences for replication, transcription, and repair processes [149]. A significant background level of accumulated DPCs has been reported in some types of mammalian cells [2,60], and in mice this frequency increases with age [150,151]. In mammalian cells, the processes of aging and other cellular stresses (illness, exposure to drugs, IR, pollutants, etc.) may result in the accumulation of different types of DNA lesions, including DPCs, due to oxidative mechanisms [150,151]. Nonetheless, the majority of DPCs induced by exogenous agents are clearly removed from the genome with time (although it should be noted that studies of the removal of DPCs from biological systems are complicated by the known chemical instability of many types of DPCs). DPCs were detected in rat kidney cells up to 48 h following treatment with nickel compounds [30]. Levels of ferric nitriloacetate-induced thymine-tyrosine DPCs in renal cells of Wistar rats peaked at 24 h (corresponding to the onset of mitosis), but DPC levels had returned to control level by the 19th day of ongoing treatment, suggesting active repair of these lesions [57]. Quieveryn and Zhitkovich [26] reported a half-life for formaldehyde-induced DPCs of 11.6-13.0 h in three human cell lines (skin, lung, and kidney cell lines) and suggested that the differences in DPC half-lives among these cell lines might be due to an active repair process. The half-life of

formaldehyde-induced DPCs in peripheral human lymphocytes was found to be longer (~18 h), likely due to inefficient active repair in lymphocytes [152]. Chromium-induced crosslinks were also reported to be relatively long lived in human lymphocytes (reviewed in [75]).

At this point, it should be stressed that many of the DPC-inducing agents discussed in this chapter, such as IR, methylglyoxal and cisplatin, generate DNA intra- and ICLs as well as DPCs. Both ICLs and DPCs are expected to present special steric challenges to the DNA repair machinery because of their large size and/or local covalent involvement of both strands of DNA. Indeed, both of these types of lesions, or at least some sub-classes thereof, may be repaired by the same pathway or using some common elements. For example, as will become apparent, the nucleotide excision repair (NER) enzymes ERCC1 and XPF appear to be involved in the repair of some types of ICLs as well as DPCs. There are a number of outstanding issues in this regard that we will consider in turn.

1.9.a. How are DPCs sensed at the cellular level?

The association of proteins with DNA is a common occurrence in cellular processes. The mechanisms by which a cell will distinguish between a protein associated with DNA appropriately and one that is bound by a covalent linkage are unknown. Is the DPC recognized due to its bulk and/or distortion of the helix? Is the DPC recognized because it blocks the progression of complexes

involved in processes such as chromatin remodeling, DNA replication, transcription, or the repair of other types of lesions?

1.9.b. How are covalent DPCs repaired?

Depending on the chemistry of the crosslink and the size and orientation of the protein involved in the crosslink (i.e., on steric issues), these lesions may be substrates for different repair pathways. Direct reversal by chelation (Figure 1-5A) is possible in the case where the protein is bound through complexation with a metal. Direct reversal by hydrolysis (Figure 1-5B) has been demonstrated for some aldehyde-induced DPCs.

At least some DPCs could represent the typical bulky/helix distorting adducts that are expected to be substrates for the NER pathway (Figure 1-5C). It may be that the crosslinking of a protein with extensive DNA interaction might prevent access to repair enzymes, and these lesions may first need to be de-bulked by proteases before they can be processed by the NER machinery or other repair pathways (Figure 1-5D). Alternatively, they may require recombination-dependent pathways (Figure 1-5E). Several lines of evidence suggest that DNA crosslinks are repaired through an incisional-recombinational repair mechanism that involves components of NER and homologous recombinational repair (HRR) [153,154], which, in bacteria, is suggested to be the mechanism involved in restarting stalled replication forks [155].

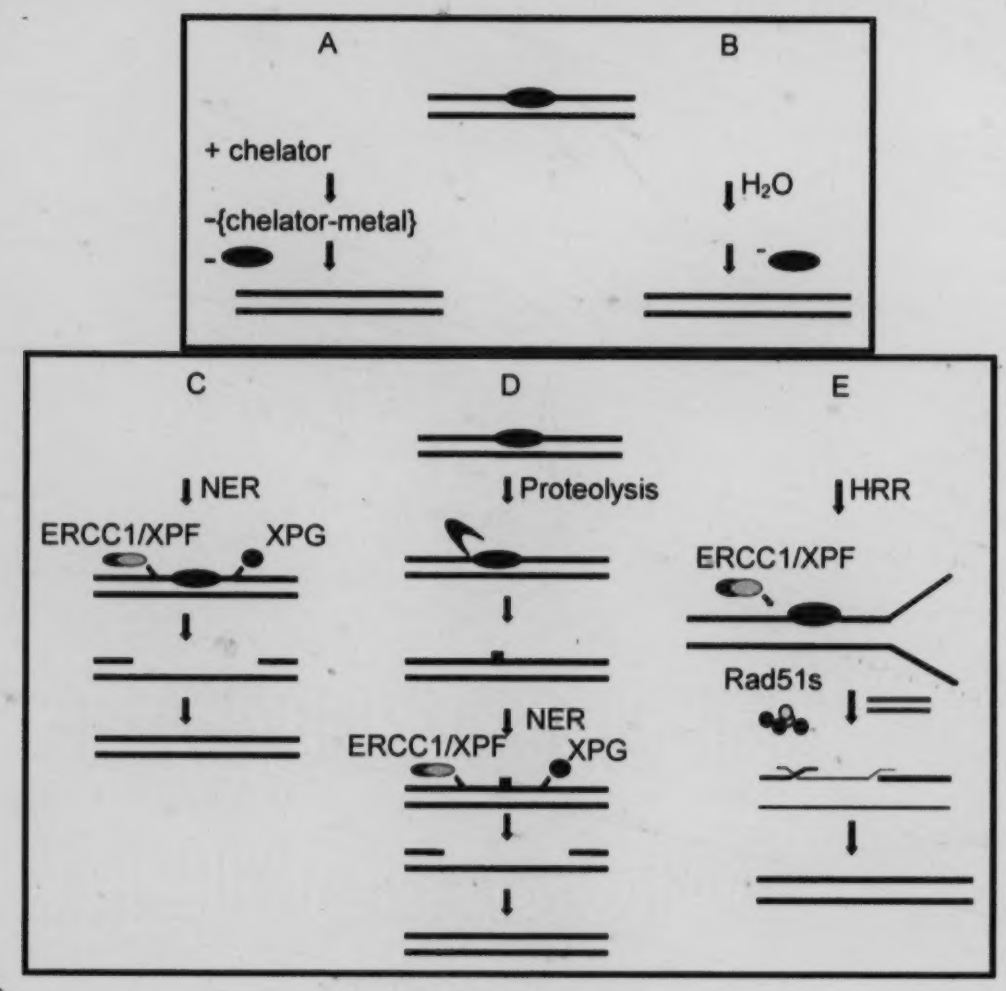

Figure 1-5: Potential DPC Repair Routes

DPCs may be repaired by A) direct reversal by chelation B) direct reversal by hydrolysis C) NER D) partial proteolytic degradation followed by NER or other repair E) incisional-homologous recombinational repair

Previous studies have suggested that there is indeed active repair of DPCs in mammalian cells and that this may involve more than one repair pathway [35,149,156,157], with NER likely to be involved. However, the involvement of NER or HRR in DPC repair remains unclear.

The involvement of the NER pathway in removal of formaldehyde-induced DPCs was examined in several types of human cells and *in vitro* with histone H1 using the SDS/K^+ precipitation method [26]. Formaldehyde-induced DPCs were found to be removed from *in vitro* samples by hydrolysis. DPCs in human lung, kidney and fibroblast cells were observed to have a reduced half-life compared to formaldehyde-induced DPCs studied *in vitro*, suggesting that an active repair process is involved in DPC loss in cells. Human lymphocytes, which are known to have less efficient NER due to their terminally differentiated status, were shown to have reduced DPC removal compared to other human cells studied. However, the human NER-deficient cell lines, XPA and XPF, were found to have DPC half-lives similar to that of normal human cells, implying that NER may not be involved in DPC removal. Interestingly, XPA cells and, more markedly, XPF cells are hypersensitive to formaldehyde-induced cell killing. Although formaldehyde induces other types of DNA damage that are substrates for NER, the differential sensitivity of the XPA and XPF cells argues for the involvement of the XPF protein in the repair of DNA damage through another pathway. A differential sensitivity to crosslinking agents is also seen for XPF cells as compared to XPA cells [158], and other studies have suggested the involvement

of the XPF protein but not the XPA protein in a recombination-dependent crosslink repair pathway [159].

It should be noted, however, that the chemical instability of many DPCs means that direct measurements of crosslink repair in different cell types may not be informative for identifying proteins involved in the repair of DPCs, and that studies of the sensitivity of mutant cells to killing by DPC-inducing agents may be more relevant in this regard.

Assessments of DPC induction and removal are affected by the limitations of the DPC isolation and quantitation method being used. When chromium-induced DPCs generated in V79 hamster cells were analysed, no reduced tail moment (i.e., DPCs) was detected [7] by the alkaline comet assay, but a dose-dependent reduction of the tail moment was detected using a neutral comet assay. The removal of formaldehyde-induced DPCs from normal, NER-deficient (XPA), or ICL repair-deficient (FA-A) human cells was analysed using the alkaline comet assay [160]. The XPA and FA-A cells showed a similar tail moment to the normal cells after formaldehyde treatment, indicating no differences in DPC induction. The tail moments were also similar for all three formaldehyde-treated cell lines after various repair times were allowed, indicating no differences in DPC removal between the normal and repair deficient cell lines. However, there was a dose-dependent relationship between formaldehyde concentration and the induction of micronuclei in these human cell lines. The induction of micronuclei might be due to reduced repair of DPCs and was

significantly greater in the repair-deficient cell lines, particularly the XPA cell line, which argues for a role for NER in the proper repair of DPCs.

Alternatively, it may be that chemically distinct crosslinks are repaired by different mechanisms and that NER may be involved in the repair of some types of DPCs and not others. Transplatin-induced DPCs have previously been reported to be more persistent in human XPA cells [35]. A more recent study [161] examined the effectiveness of NER in removing DPCs induced by a transplatin analog, *trans*-[$PtCl_2$(*E*-iminoether)$_2$] (*trans*-EE). Synthetic DPCs were generated by reacting *trans*-EE with an oligonucleotide to induce the monoadduct, which was then combined with histone H1 to generate the DPC. Double-stranded crosslinked substrate was used in *in vitro* reactions to assess the efficiency of incision of this lesion by human or rodent cell-free extracts. Incubation of control NER substrates containing a *trans*-EE-induced monoadduct or a cisplatin-induced intrastrand crosslink each generated 24-30mer oligonucleotide NER excision products, whereas the *trans*-EE-induced DPC substrate showed no excision, indicating that NER is unable to recognize and/or incise this type of lesion *in vitro*. These repair assays were performed *in vitro*, and the protein crosslinking was done using single-stranded DNA. It will be of interest to see if protein-crosslinking is the predominant reaction induced by this transplatin analog *in vivo* when the complementary DNA strand is present and if those *trans*-EE induced lesions are also refractory to NER.

It has recently been shown that the NER system is effective in removing chromium-induced DNA damage. This was quantitated by measuring the initial

and residual amounts of chromium bound to DNA in human XPA, XPC, and XPF cells [162]. Since chromium induces a number of different types of DNA damage, this study tried to dissect the influence of NER specifically on the repair of chromium-induced crosslinks. Cysteine was crosslinked to a plasmid by chromium treatment and these plasmids were transfected into XPA cells and XPA-complemented XPA cells (XPA^+ cells). The XPA cells exhibited significantly greater mutagenic and genotoxic effects after replication of the crosslink-containing plasmid, suggesting the importance of the NER pathway in dealing with chromium-induced DPCs. However, this analysis involved only a single amino acid crosslinked to DNA, and the effect of an entire protein or even a peptide fragment crosslinked to DNA may be different.

Using a synthetic substrate with an enzyme (T4-pyrimidine dimer-DNA glycosylase) covalently crosslinked to it, it was shown that the *E. coli* UvrABC complex was capable of incising DNA at the site of a DPC [163]. Two incisions were made on the same DNA strand; one incision was made at the eighth phosphodiester bond on the 5′ side of the DPC and the second incision was made at the fifth and sixth phosphodiester bonds on the 3′ side of the DPC. This *in vitro* incision process was more efficient than incisions made on a reduced apurinic/apyrimidinic-site substrate, but was only half as efficient as that for a trans-benzo[a]pyrene diol epoxide adduct. The extent to which this type of repair might be carried out *in vivo* is unclear.

Although topoisomerase cleavage complexes are a distinct type of protein-DNA covalent complex, the mechanisms of their repair may provide some

insight into the repair of other DPCs. Tyrosyl-DNA phosphodiesterase I (Tdp1) is an enzyme capable of removing a topoisomerase I-covalent complex from a DNA end. The activity is specific for hydrolysing 3'-phosphodiester linkages but could remove a protein other than topoisomerase I from the DNA end (reviewed in [5]). Tdp1 may also act in strand break repair pathways as DNA-protein complexes may be processed into SSBs or DSBs during replication, transcription, or repair [5]. Cleavage complexes are also substrates for DSB repair pathways, and these pathways have been shown in yeast to be separate from the Tdp1 pathway through the use of NER and HRR mutants (reviewed in [5]).

1.9.c. How are IR-induced DPCs repaired?

The involvement of NER in the repair of IR-induced DPCs was investigated by assessing the rate of removal of the DPCs induced following irradiation of NER-deficient hamster cells under hypoxic conditions [37]. As measured by alkaline elution, wild-type AA8 cells removed ~80% of their DPCs in 24 h, whereas NER-deficient UV41 (XPF^-) cells removed only ~20% of their DPCs in the same period. As was noted earlier, UV41 cells are significantly more sensitive than wild-type AA8 cells to killing by IR under hypoxic conditions, suggesting that a deficiency in the repair of DPCs (which are formed preferentially in hypoxia) increases the cells' radiosensitivity. Almost identical cell survival data were reported for the NER-deficient UV20 ($ERCC1^-$) hamster cell line, although the ability of these cells to repair DPCs was not measured [101]. Surprisingly, the repair of DPCs induced in UV41 cells by IR under aerated

conditions appears to be normal [164]. Thus, DPCs induced under hypoxic conditions appear to be distinct from those induced under aerated conditions, which in turn influences their repair. Evidence in support of this suggestion will be presented in Chapter 3 of this thesis.

Several other NER-deficient hamster cell lines, notably those with defects in the XPB and XPD genes, did not exhibit this radiosensitive phenotype under hypoxic conditions [102], suggesting that these DPCs are not repaired by NER *per se*. Rather, the phenomenon of hypoxia-specific radiosensitization appears to be restricted to genetic defects that influence both NER and HRR [102,158], suggesting that the latter pathway is responsible for the repair of DPCs induced by IR in hypoxia. It cannot, however, be ruled out that IR-induced DNA ICLs underlie some aspects of these findings.

1.9.d. Might protease activity be involved in DPC repair?

Proteolytic degradation of the proteins involved in DPCs has been suggested to occur in cells. Quievryn and Zhitkovich [26] demonstrated that formaldehyde-induced DPCs were removed in part by proteolytic degradation because the loss of DPCs was partially inhibited when cells were incubated with lactacystin, a specific inhibitor of proteosomes.

However, DNA repair proteins, cell-cycle regulatory proteins, transcription factors and signaling molecules are also substrates for proteolytic degradation [165]; therefore, inhibiting proteolysis may affect the induction/removal/repair of

DPCs by mechanisms other than inhibiting direct proteolytic degradation of the crosslinked protein.

An earlier study demonstrated that covalent complexes of topoisomerase I and DNA induced by camptothecin were ubiquitinated and then underwent proteolytic degradation [166], and this mechanism may be active on other types of DPCs as well. Proteolytic degradation may not remove the entire protein but rather could leave a small peptide or amino acid adduct, which might then be a substrate for another repair pathway, such as NER (Figure 1-5D).

Studies of the Tdp1 enzyme have demonstrated that it is more effective on substrates containing a denatured or proteolytically digested protein than it is on substrates containing a native protein [5]. Although this enzyme has not been shown to be active for other protein-DNA covalent complexes, it is possible that this or a similarly active enzyme might be involved in a DPC repair step secondary to proteolytic digestion.

1.10. Conclusions

Because DPCs have received less attention than other types of DNA damage, their biological consequences and mechanisms of repair are not well understood. In part, this is because DPC-inducing agents inevitably induce other types of DNA and protein damage. Possible biochemical consequences of the covalent crosslinking of proteins to DNA are blockage of replication, transcription and recombination. Evidence is mounting that DPCs contribute to the cytotoxic, mutagenic and carcinogenic effects of a number of agents. Further information

regarding the mechanisms of the formation and removal of DPCs would help to delineate the biological relevance of this type of lesion, and may provide insights into cellular processes such as the interaction of the nuclear matrix with DNA metabolism. Because DPCs are induced by some bifunctional chemotherapy drugs [167,168], the role of DPCs in the cytotoxicity of these agents may be relevant to further understanding of clinical responses and drug-resistance mechanisms, which in turn may lead to novel anti-tumour drug development. For example, a new analog of transplatin (*trans*-EE) has been shown to be more cytotoxic than cisplatin and to demonstrate significant anti-tumour activity in both cisplatin-sensitive and -resistant cells [169-171]. Compared to cisplatin and *cis*-EE, the *trans*-EE analog readily crosslinks proteins to DNA, leading to more efficient inhibition of DNA polymerases and resistance to processing by the NER pathway [161]. Determining the proteins involved in DPCs will also allow us to gain further insight into the consequences of these lesions and their repair. The involvement of particular proteins in DPCs induced by various environmental and occupational agents may prove useful in biomonitoring for mutagenesis/carcinogenesis. This chapter highlights the advances in DPC analysis and at the same time underscores the need for the identification of the proteins involved in these lesions and for clarification of the mechanisms of their repair.

1.11. Research Objectives

DPCs have not received as much attention as other types of radiation-induced DNA damage. This is partly due to the known inverse relationship between DPC induction and cytotoxicity (see Figure 1-4). However, this supposition was based entirely on studies of gross overall protein binding; the situation for individual proteins is unknown, and addressing this deficiency is a major objective of the studies described in this thesis. Previous studies suggest that DPCs are induced to a greater degree than either DSBs or ICLs [33] and that these lesions persist longer than other forms of DNA damage. Also, previous studies have shown that DPCs are induced to a greater extent under hypoxic conditions [37,41] and that hypoxia is a commonly encountered condition in human tumours. Hypoxic cells are radioresistant, which limits the effectiveness of radiotherapy in cancer treatment. An interesting observation is the fact that hypoxic NER/HRR-deficient cells, but not NER-deficient/HRR competent cells, are more radiosensitive than their parental strains. The relevance of NER/HRR in this increased sensitivity to radiation is confirmed by the fact that these cells become more radioresistant when repair activity is restored by tranfection with a wild-type gene [102]. However, there is considerable variation in the literature as to the extent of the influence of oxygen on DPC induction. The involvement of NER *per se* in DPC repair is also unclear. Many other questions remain to be answered before the role of DPCs in the effects of radiation and other DNA-damaging agents will be understood.

To fully understand the induction and repair of these lesions, it will be important to identify the individual DNA-crosslinked proteins involved therein. In order to take advantage of dramatic improvements in instrument sensitivity that have facilitated the identification of proteins by proteomic approaches, improved methods are required for the isolation of proteins involved in DPCs. As a first step, we therefore developed and compared several novel methods for the isolation of DPCs from mammalian cells that use chaotropic agents to isolate genomic DNA and stringently remove non-crosslinked proteins, followed by nuclease digestion to release covalently crosslinked proteins. As will be discussed in Chapter 2, these methods do in fact generate protein samples of sufficient quality and quantity for analysis by mass spectrometry.

These methods represent a significant improvement in resolution and specificity, enabling more accurate analyses of DPCs. The high quality protein samples isolated by these methods can then be analyzed by a variety of methods. We applied these protein isolation protocols to re-evaluate some important questions regarding DPCs induced by low LET radiation, specifically γ-radiation, including i) the influence of oxygen on the induction of DPCs by γ-radiation, ii) the extent of DPC induction in mammalian cells, and iii) the trends of induction and removal of DPCs by γ-radiation in both parental and DNA repair deficient cell lines. The interpretation of these data with regard to the understanding of the role of DPCs in γ-radiation-induced cell death is discussed.

References for Chapter 1

[1] V. Orlando, H. Strutt and R. Paro Analysis of chromatin structure by *in vivo* formaldehyde cross-linking, Methods 11 (1997) 205-214.

[2] R. Olinski, Z. Nackerdien and M. Dizdaroglu DNA-protein cross-linking between thymine and tyrosine in chromatin of gamma-irradiated or H_2O_2-treated cultured human cells, Arch. Biochem. Biophys. 297 (1992) 139-143.

[3] G. Neubauer, A. King, J. Rappsilber, C. Calvio, M. Watson, P. Ajuh, J. Sleeman, A. Lamond and M. Mann Mass spectrometry and EST-database searching allows characterization of the multi-protein spliceosome complex, Nat. Genet. 20 (1998) 46-50.

[4] N. Li, A. Mak, D.P. Richards, C. Naber, B.O. Keller, L. Li and A.R. Shaw Monocyte lipid rafts contain proteins implicated in vesicular trafficking and phagosome formation, Proteomics 3 (2003) 536-548.

[5] J.C. Connelly and D.R. Leach Repair of DNA covalently linked to protein, Mol. Cell 13 (2004) 307-316.

[6] J.L. Roti Roti, H.H. Kampinga, R.S. Malyapa, W.D. Wright, R.P. vanderWaal and M. Xu Nuclear matrix as a target for hyperthermic killing of cancer cells, Cell Stress Chaperones 3 (1998) 245-255.

[7] O. Merk, K. Reiser and G. Speit Analysis of chromate-induced DNA-protein crosslinks with the comet assay, Mutat. Res. 471 (2000) 71-80.

[8] O. Merk and G. Speit Detection of crosslinks with the comet assay in relationship to genotoxicity and cytotoxicity, Environ. Mol. Mutagen. 33 (1999) 167-172.

[9] G.V. Tolstonog, E. Mothes, R.L. Shoeman and P. Traub Isolation of SDS-stable complexes of the intermediate filament protein vimentin with repetitive, mobile, nuclear matrix attachment region, and mitochondrial DNA sequence elements from cultured mouse and human fibroblasts, DNA Cell Biol. 20 (2001) 531-554.

[10] A.E. Cress, K.M. Kurath, M.J. Hendrix and G.T. Bowden Nuclear protein organization and the repair of radiation damage, Carcinogenesis 10 (1989) 939-943.

[11] T. Moss, S.I. Dimitrov and D. Houde UV-laser crosslinking of proteins to DNA, Methods 11 (1997) 225-234.

[12] S.M. Chiu, N.M. Sokany, L.R. Friedman and N.L. Oleinick Differential processing of ultraviolet or ionizing radiation-induced DNA-protein cross-links in Chinese hamster cells, Int. J. Radiat. Biol. Relat. Stud. Phys. Chem. Med. 46 (1984) 681-690.

[13] L.Y. Xue, L.R. Friedman and N.L. Oleinick Repair of chromatin damage in glutathione-depleted V-79 cells: comparison of oxic and hypoxic conditions, Radiat. Res. 116 (1988) 89-99.

[14] A.E. Cress, K.M. Kurath, B. Stea and G.T. Bowden The crosslinking of nuclear protein to DNA using ionizing radiation, J. Cancer Res. Clin. Oncol. 116 (1990) 324-330.

[15] A. Zhitkovich and M. Costa A simple, sensitive assay to detect DNA-protein crosslinks in intact cells and *in vivo*, Carcinogenesis 13 (1992) 1485-1489.
[16] M. Costa, A. Zhitkovich, M. Gargas, D. Paustenbach, B. Finley, J. Kuykendall, R. Billings, T.J. Carlson, K. Wetterhahn, J. Xu, S. Patierno and M. Bogdanffy Interlaboratory validation of a new assay for DNA-protein crosslinks, Mutat. Res. 369 (1996) 13-21.
[17] K.W. Kohn DNA as a target in cancer chemotherapy: measurement of macromolecular DNA damage produced in mammalian cells by anticancer agents and carcinogens, in: Methods in Cancer Research, Academic Press, New York, 1979, pp. 291-345.
[18] K.W. Kohn, R.A. Ewig, L.C. Erickson, L.A. Zwelling Measurement of strand breaks and crosslinks by alkaline elution, in: E.C. Friedberg and P.C. Hanawalt (Eds.), DNA Repair: A Laboratory Manual of Research Procedures, M. Dekker, New York, 1981, pp. 379-401.
[19] A. Ferraro, P. Grandi, M. Eufemi, F. Altieri and C. Turano Crosslinking of nuclear proteins to DNA by cis-diamminedichloroplatinum in intact cells. Involvement of nuclear matrix proteins, FEBS Lett. 307 (1992) 383-385.
[20] S.K. Samuel, V.A. Spencer, L. Bajno, J.M. Sun, L.T. Holth, S. Oesterreich and J.R. Davie In situ cross-linking by cisplatin of nuclear matrix-bound transcription factors to nuclear DNA of human breast cancer cells, Cancer Res. 58 (1998) 3004-3008.
[21] C.A.I. Miller, M.D. Cohen and M. Costa Complexing of actin and other nuclear proteins to DNA by cis-diamminedichloroplatinum(II) and chromium compounds, Carcinogenesis 12 (1991) 269-276.
[22] A.E. Cress and K.M. Kurath Identification of attachment proteins for DNA in Chinese hamster ovary cells, J. Biol. Chem. 263 (1988) 19678-19683.
[23] S.N. Mattagajasingh and H.P. Misra Mechanisms of the carcinogenic chromium(VI)-induced DNA-protein cross-linking and their characterization in cultured intact human cells, J. Biol. Chem. 271 (1996) 33550-33560.
[24] S.N. Mattagajasingh and H.P. Misra Analysis of EDTA-chelatable proteins from DNA-protein crosslinks induced by a carcinogenic chromium (VI) in cultured intact human cells, Mol. Cell. Biochem. 199 (1999) 149-162.
[25] T.H. Ma and M.M. Harris Review of the genotoxicity of formaldehyde, Mutat. Res. 196 (1988) 37-59.
[26] G. Quievryn and A. Zhitkovich Loss of DNA-protein crosslinks from formaldehyde-exposed cells occurs through spontaneous hydrolysis and an active repair process linked to proteosome function, Carcinogenesis 21 (2000) 1573-1580.
[27] J.D. McGhee and P.H. von Hippel Formaldehyde as a probe of DNA structure. II. Reaction with endocyclic imino groups of DNA bases, Biochemistry 14 (1975) 1297-1303.
[28] J.D. McGhee and P.H. von Hippel Formaldehyde as a probe of DNA structure. I. Reaction with exocyclic amino groups of DNA bases, Biochemistry 14 (1975) 1281-1296.

[29] S.K. Chakrabarti, C. Bai and K.S. Subramanian DNA-Protein crosslinks induced by nickel compounds in isolated rat renal cortical cells and its antagonism by specific amino acids and magnesium ion, Toxicol. Appl. Pharmacol. 154 (1999) 245-255.

[30] S.K. Chakrabarti, C. Bai and K.S. Subramanian DNA-protein crosslinks induced by nickel compounds in isolated rat lymphocytes: role of reactive oxygen species and specific amino acids, Toxicol. Appl. Pharmacol. 170 (2001) 153-165.

[31] A. Zhitkovich, V. Voitkun and M. Costa Formation of the amino acid-DNA complexes by hexavalent and trivalent chromium in vitro: importance of trivalent chromium and the phosphate group, Biochemistry 35 (1996) 7275-7282.

[32] A. Mozumder Early production of radicals from charged particle tracks in water, Radiat. Res. Suppl. 8 (1985) S33-39.

[33] E.C. Woudstra Chromatin Structure, DNA Damage, DNA Repair and Cellular Radiosensitivity, Radiobiology, (PhD Thesis) University of Groningen, The Netherlands, 1999, pp. 270.

[34] A.J. Fornace, Jr. and J.B. Little DNA crosslinking induced by x-rays and chemical agents, Biochim. Biophys. Acta 477 (1977) 343-355.

[35] A.J. Fornace, Jr. and D.S. Seres Repair of trans-Pt(II) diamminedichloride DNA-protein crosslinks in normal and excision-deficient human cells, Mutat. Res. 94 (1982) 277-284.

[36] R.E. Meyn, W.T. Jenkins and D. Murray Radiation damage to DNA in various animal tissues: Comparison of yields and repair *in vivo* and *in vitro*, in: M.G. Simic, L. Grossman and A.C. Upton (Eds.), Mechanisms of DNA Damage and Repair: Implications to Carcinogenesis and Risk Assessment, Plenum Press, New York, 1986, pp. 151-158.

[37] R.E. Meyn, S.C. vanAnkeren and W.T. Jenkins The induction of DNA-protein crosslinks in hypoxic cells and their possible contribution to cell lethality, Radiat. Res. 109 (1987) 419-429.

[38] I.R. Radford Effect of radiomodifying agents on the ratios of X-ray-induced lesions in cellular DNA: use in lethal lesion determination, Int. J. Radiat. Biol. Relat. Stud. Phys. Chem. Med. 49 (1986) 621-637.

[39] H. Zhang and K.T. Wheeler Radiation-induced DNA damage in tumors and normal tissues. I. Feasibility of estimating the hypoxic fraction, Radiat. Res. 136 (1993) 77-88.

[40] H. Zhang and K.T. Wheeler Radiation-induced DNA damage in tumors and normal tissues. II. Influence of dose, residual DNA damage and physiological factors in oxygenated cells, Radiat. Res. 140 (1994) 321-326.

[41] H. Zhang, C.J. Koch, C.A. Wallen and K.T. Wheeler Radiation-induced DNA damage in tumors and normal tissues. III. Oxygen dependence of the formation of strand breaks and DNA-protein crosslinks, Radiat. Res. 142 (1995) 163-168.

[42] I. Al-Nabulsi and K.T. Wheeler Temperature dependence of radiation-induced DNA-protein crosslinks formed under hypoxic conditions, Radiat. Res. 148 (1997) 568-574.
[43] L.K. Mee and S.J. Adelstein Predominance of core histones in formation of DNA-protein crosslinks in gamma-irradiated chromatin, Proc. Natl. Acad. Sci. USA 78 (1981) 2194-2198.
[44] A.E. Cress and G.T. Bowden Covalent DNA-protein crosslinking occurs after hyperthermia and radiation, Radiat. Res. 95 (1983) 610-619.
[45] S.M. Chiu, L.R. Friedman and N.L. Oleinick Formation and repair of DNA-protein crosslinks in newly replicated DNA, Radiat. Res. 120 (1989) 545-551.
[46] I. Al-Nabulsi and K.T. Wheeler Radiation-induced DNA damage in tumors and normal tissues: V. Influence of pH and nutrient depletion on the formation of DNA-protein crosslinks in irradiated partially and fully hypoxic tumor cells, Radiat. Res. 151 (1999) 188-194.
[47] J.F. Ward Biochemistry of DNA lesions, Radiat. Res. Suppl. 8 (1985) S103-111.
[48] H. Nikjoo, P. O'Neill, M. Terrissol and D.T. Goodhead Modelling of radiation-induced DNA damage: the early physical and chemical event, Int. J. Radiat. Biol. 66 (1994) 453-457.
[49] D.T. Goodhead Molecular and cell models of biological effects of heavy ion radiation, Radiat. Environ. Biophys. 34 (1995) 67-72.
[50] E.A. Blakely, P.Y. Chang and K.A. Bjornstad LET dependence of DNA-protein crosslinks, in: U. Hagen, H. Jung and C. Streffer (Eds.), Radiation Research 1895-1995 Congress Proceedings, ICRR Society, 1995, pp. 136-139.
[51] K. Eguchi, T. Inada, M. Yaguchi, S. Satoh and I. Kaneko Induction and repair of DNA lesions in cultured human melanoma cells exposed to a nitrogen-ion beam, Int. J. Radiat. Biol. Relat. Stud. Phys. Chem. Med. 52 (1987) 115-123.
[52] M. Frankenberg-Schwager Radiation-induced DNA lesions in eukaryotic cells, their repair and biological relevance, in: C.E. Swenberg, G. Horneck and E.G. Stassinopoulos (Eds.), Biological Effects and Physics of Solar and Galactic Cosmic Radiation, Plenum Press, New York, 1993, pp. 1-31.
[53] E. Gajewski, A.F. Fuciarelli and M. Dizdaroglu Structure of hydroxyl radical-induced DNA-protein crosslinks in calf thymus nucleohistone in vitro, Int. J. Radiat. Biol. 54 (1988) 445-459.
[54] M. Dizdaroglu and E. Gajewski Structure and mechanism of hydroxyl radical-induced formation of a DNA-protein cross-link involving thymine and lysine in nucleohistone, Cancer Res. 49 (1989) 3463-3467.
[55] M. Dizdaroglu, E. Gajewski, P. Reddy and S.A. Margolis Structure of a hydroxyl radical induced DNA-protein cross-link involving thymine and tyrosine in nucleohistone, Biochemistry 28 (1989) 3625-3628.
[56] S.A. Altman, T.H. Zastawny, L. Randers-Eichhorn, M.A. Cacciuttolo, S.A. Akman, M. Dizdaroglu and G. Rao Formation of DNA-protein cross-links in

cultured mammalian cells upon treatment with iron ions, Free Radicals Biol. Med. 19 (1995) 897-902.

[57] S. Toyokuni, T. Mori, H. Hiai and M. Dizdaroglu Treatment of Wistar rats with a renal carcinogen, ferric nitrilotriacetate, causes DNA-protein cross-linking between thymine and tyrosine in their renal chromatin, Int. J. Cancer 62 (1995) 309-313.

[58] M.S. Weir Lipton, A.F. Fuciarelli, D.L. Springer and C.G. Edmonds Characterization of radiation-induced thymine-tyrosine crosslinks by electrospray ionization mass spectrometry, Radiat. Res. 145 (1996) 681-686.

[59] S. Gebicki and J.M. Gebicki Crosslinking of DNA and proteins induced by protein hydroperoxides, Biochem. J. 338 (1999) 629-636.

[60] V. Voitkun and A. Zhitkovich Analysis of DNA-protein crosslinking activity of malondialdehyde in vitro, Mutat. Res. 424 (1999) 97-106.

[61] C.L. Hawkins, D.I. Pattison and M.J. Davies Reaction of protein chloramines with DNA and nucleosides: evidence for the formation of radicals, protein-DNA cross-links and DNA fragmentation, Biochem. J. 365 (2002) 605-615.

[62] J.R. Kuykendall and M.S. Bogdanffy Reaction kinetics of DNA-histone crosslinking by vinyl acetate and acetaldehyde, Carcinogenesis 13 (1992) 2095-2100.

[63] M. Costa, A. Zhitkovich, M. Harris, D. Paustenbach and M. Gargas DNA-protein cross-links produced by various chemicals in cultured human lymphoma cells, J. Toxicol. Environ. Health 50 (1997) 433-449.

[64] P. Bedinger, M. Hochstrasser, C.V. Jongeneel and B.M. Alberts Properties of the T4 bacteriophage DNA replication apparatus: the T4 dda DNA helicase is required to pass a bound RNA polymerase molecule, Cell 34 (1983) 115-123.

[65] A.L. Pinto and S.J. Lippard Sequence-dependent termination of in vitro DNA synthesis by cis- and trans-diamminedichloroplatinum (II), Proc. Natl. Acad. Sci. USA 82 (1985) 4616-4619.

[66] J.A. Briggs and R.C. Briggs Characterization of chromium effects on a rat liver epithelial cell line and their relevance to in vitro transformation, Cancer Res. 48 (1988) 6484-6490.

[67] M.O. Bradley, I.C. Hsu and C.C. Harris Relationship between sister chromatid exchange and mutagenicity, toxicity and DNA damage, Nature 282 (1979) 318-320.

[68] M.O. Bradley and K.W. Kohn X-ray induced DNA double strand break production and repair in mammalian cells as measured by neutral filter elution, Nucleic Acids Res. 7 (1979) 793-804.

[69] A.J. Fornace, Jr. and J.B. Little Malignant transformation by the DNA-protein crosslinking agent trans-Pt(II) diamminedichloride, Carcinogenesis 1 (1980) 989-994.

[70] A.J. Fornace, Jr. Detection of DNA single-strand breaks produced during the repair of damage by DNA-protein cross-linking agents, Cancer Res. 42 (1982) 145-149.

[71] O. Merk and G. Speit Significance of formaldehyde-induced DNA-protein crosslinks for mutagenesis, Environ. Mol. Mutagen. 32 (1998) 260-268.
[72] H. Waksvik and M. Boysen Cytogenetic analyses of lymphocytes from workers in a nickel refinery, Mutat. Res. 103 (1982) 185-190.
[73] H. Waksvik, M. Boysen and A.C. Hogetveit Increased incidence of chromosomal aberrations in peripheral lymphocytes of retired nickel workers, Carcinogenesis 5 (1984) 1525-1527.
[74] J.K. Dunnick, M.R. Elwell, A.E. Radovsky, J.M. Benson, F.F. Hahn, K.J. Nikula, E.B. Barr and C.H. Hobbs Comparative carcinogenic effects of nickel subsulfide, nickel oxide, or nickel sulfate hexahydrate chronic exposures in the lung, Cancer Res. 55 (1995) 5251-5256.
[75] A. Zhitkovich, V. Voitkun, T. Kluz and M. Costa Utilization of DNA-protein cross-links as a biomarker of chromium exposure, Environ. Health Perspect. 106 Suppl 4 (1998) 969-974.
[76] V. Voitkun, A. Zhitkovich and M. Costa Cr(III)-mediated crosslinks of glutathione or amino acids to the DNA phosphate backbone are mutagenic in human cells, Nucleic Acids Res. 26 (1998) 2024-2030.
[77] M.N. Bates, A.H. Smith and C. Hopenhayn-Rich Arsenic ingestion and internal cancers: a review, Am. J. Epidemiol. 135 (1992) 462-476.
[78] C.J. Chen, C.W. Chen, M.M. Wu and T.L. Kuo Cancer potential in liver, lung, bladder and kidney due to ingested inorganic arsenic in drinking water, Br. J. Cancer 66 (1992) 888-892.
[79] M.E. Gonsebatt, L. Vega, A.M. Salazar, R. Montero, P. Guzman, J. Blas, L.M. Del Razo, G. Garcia-Vargas, A. Albores, M.E. Cebrian, M. Kelsh and P. Ostrosky-Wegman Cytogenetic effects in human exposure to arsenic, Mutat. Res. 386 (1997) 219-228.
[80] D.T. Bau, T.S. Wang, C.H. Chung, A.S. Wang and K.Y. Jan Oxidative DNA adducts and DNA-protein cross-links are the major DNA lesions induced by arsenite, Environ. Health Perspect. 110 Suppl 5 (2002) 753-756.
[81] S. Lynn, J.R. Gurr, H.T. Lai and K.Y. Jan NADH oxidase activation is involved in arsenite-induced oxidative DNA damage in human vascular smooth muscle cells, Circ. Res. 86 (2000) 514-519.
[82] M. Whiteman and B. Halliwell Loss of 3-nitrotyrosine on exposure to hypochlorous acid: implications for the use of 3-nitrotyrosine as a biomarker *in vivo*, Biochem. Biophys. Res. Commun. 258 (1999) 168-172.
[83] M. Whiteman, J.P. Spencer, A. Jenner and B. Halliwell Hypochlorous acid-induced DNA base modification: potentiation by nitrite: biomarkers of DNA damage by reactive oxygen species, Biochem. Biophys. Res. Commun. 257 (1999) 572-576.
[84] N. Mei, J. Lee, X. Sun, J.Z. Xing, J. Hanson, X.C. Le and M. Weinfeld Genetic predisposition to the cytotoxicity of arsenic: the role of DNA damage and ATM, FASEB J. 17 (2003) 2310-2312.
[85] J.L. Yen, N.Y. Su and P. Kaiser The yeast ubiquitin ligase SCFMet30 regulates heavy metal response, Mol Biol Cell 16 (2005) 1872-1882.

[86] G. Speit and O. Merk Evaluation of mutagenic effects of formaldehyde in vitro: detection of crosslinks and mutations in mouse lymphoma cells, Mutagenesis 17 (2002) 183-187.
[87] W.D. Kerns, K.L. Pavkov, D.J. Donofrio, E.J. Gralla and J.A. Swenberg Carcinogenicity of formaldehyde in rats and mice after long-term inhalation exposure, Cancer Res. 43 (1983) 4382-4392.
[88] L. Recio, S. Sisk, L. Pluta, E. Bermudez, E.A. Gross, Z. Chen, K. Morgan and C. Walker p53 mutations in formaldehyde-induced nasal squamous cell carcinomas in rats, Cancer Res. 52 (1992) 6113-6116.
[89] USEPA Formaldehyde Risk Assessment Update, Office of Toxic Substances, Washington, D.C., 1991.
[90] E.A. Hubal, P.M. Schlosser, R.B. Conolly and J.S. Kimbell Comparison of inhaled formaldehyde dosimetry predictions with DNA-protein cross-link measurements in the rat nasal passages, Toxicol. Appl. Pharmacol. 143 (1997) 47-55.
[91] M. Casanova, K.T. Morgan, W.H. Steinhagen, J.I. Everitt, J.A. Popp and H.D. Heck Covalent binding of inhaled formaldehyde to DNA in the respiratory tract of rhesus monkeys: pharmacokinetics, rat-to-monkey interspecies scaling, and extrapolation to man, Fundam. Appl. Toxicol. 17 (1991) 409-428.
[92] M. Casanova, K.T. Morgan, E.A. Gross, O.R. Moss and H.A. Heck DNA-protein cross-links and cell replication at specific sites in the nose of F344 rats exposed subchronically to formaldehyde, Fundam. Appl. Toxicol. 23 (1994) 525-536.
[93] N. Murata-Kamiya, H. Kamiya, H. Kaji and H. Kasai Methylglyoxal induces G:C to C:G and G:C to T:A transversions in the supF gene on a shuttle vector plasmid replicated in mammalian cells, Mutat. Res. 468 (2000) 173-182.
[94] B.M. Barnett and E.R. Munoz Genetic damage induced by methylglyoxal and methylglyoxal plus X-rays in Drosophila melanogaster germinal cells, Mutat. Res. 421 (1998) 37-43.
[95] N. Murata-Kamiya and H. Kamiya Methylglyoxal, an endogenous aldehyde, crosslinks DNA polymerase and the substrate DNA, Nucleic Acids Res. 29 (2001) 3433-3438.
[96] M.J. Roberts, G.T. Wondrak, D.C. Laurean, M.K. Jacobson and E.L. Jacobson DNA damage by carbonyl stress in human skin cells, Mutat. Res. 522 (2003) 45-56.
[97] R.J. Huxtable Human health implications of pyrrolizidine alkaloids and herbs containing them, in: P.R. Cheeke (Ed.), Toxicants of Plant Origin. Vol. I. Alkaloids, CRC Press Inc., Boca Raton, FL, 1989, pp. 41-86.
[98] J.R. Hincks, H.Y. Kim, H.J. Segall, R.J. Molyneux, F.R. Stermitz and R.A. Coulombe, Jr. DNA cross-linking in mammalian cells by pyrrolizidine alkaloids: structure-activity relationships, Toxicol. Appl. Pharmacol. 111 (1991) 90-98.
[99] H.Y. Kim, F.R. Stermitz and R.A. Coulombe, Jr. Pyrrolizidine alkaloid-induced DNA-protein cross-links, Carcinogenesis 16 (1995) 2691-2697.

[100] H.Y. Kim, F.R. Stermitz, J.K. Li and R.A. Coulombe, Jr. Comparative DNA cross-linking by activated pyrrolizidine alkaloids, Food Chem. Toxicol. 37 (1999) 619-625.
[101] D. Murray, A. Macann, J. Hanson and E. Rosenberg ERCC1/ERCC4 5'-endonuclease activity as a determinant of hypoxic cell radiosensitivity, Int. J. Radiat. Biol. 69 (1996) 319-327.
[102] D. Murray and E. Rosenberg The importance of the ERCC1/ERCC4[XPF] complex for hypoxic-cell radioresistance does not appear to derive from its participation in the nucleotide excision repair pathway, Mutat. Res. 364 (1996) 217-226.
[103] F.Y. Wu, Y.J. Lee, D.R. Chen and H.W. Kuo Association of DNA-protein crosslinks and breast cancer, Mutat. Res. 501 (2002) 69-78.
[104] A. Matsumoto and P.C. Hanawalt Histone H3 and heat shock protein GRP78 are selectively cross-linked to DNA by photoactivated Gilvocarcin V in human fibroblasts, Cancer Res. 60 (2000) 3921-3926.
[105] P. Ramirez, L.M. Del Razo, M.C. Gutierrex-Ruiz and M.E. Gonsebatt Arsenite induces DNA-protein crosslinks and cytokeratin expression in the WRL-68 human hepatic cell line, Carcinogenesis 21 (2000) 701-706.
[106] P.M. O'Connor and B.W. Fox Isolation and characterization of proteins cross-linked to DNA by the antitumor agent methylene dimethanesulfonate and its hydrolytic product formaldehyde, J. Biol. Chem. 264 (1989) 6391-6397.
[107] R.P. VanderWaal, D.R. Spitz, C.L. Griffith, R. Higashikubo and J.L. Roti Roti Evidence that protein disulfide isomerase (PDI) is involved in DNA-nuclear matrix anchoring, J. Cell. Biochem. 85 (2002) 689-702.
[108] R.A.J. Coulombe, G.L. Drew and F.R. Stermitz Pyrrolizidine alkaloids crosslink DNA with actin, Toxicol. Appl. Pharmacol. 15 (1999) 198-202.
[109] B. Singer and D. Grunberger Reactions of directly acting agents with nucleic acids, in: B. Singer and D. Grunberger (Eds.), Molecular Biology of Mutagens and Carcinogens, Plenum Publishing Corp., New York, 1983, pp. 53-55.
[110] C.A. Miller, 3rd and M. Costa Analysis of proteins cross-linked to DNA after treatment of cells with formaldehyde, chromate, and cis-diamminedichloroplatinum(II), Mol. Toxicol. 2 (1989) 11-26.
[111] J.R. Kuykendall and M.S. Bogdanffy Efficiency of DNA-histone crosslinking induced by saturated and unsaturated aldehydes in vitro, Mutat. Res. 283 (1992) 131-136.
[112] J.R. Kuykendall and M.S. Bogdanffy Formation and stability of acetaldehyde-induced crosslinks between poly-lysine and poly-deoxyguanosine, Mutat. Res. 311 (1994) 49-56.
[113] L.Y. Xue, L.R. Friedman, N.L. Oleinick and S.M. Chiu Induction of DNA damage in gamma-irradiated nuclei stripped of nuclear protein classes: differential modulation of double-strand break and DNA-protein crosslink formation, Int. J. Radiat. Biol. 66 (1994) 11-21.

[114] N.L. Oleinick, U. Balasubramaniam, L. Xue and S. Chiu Nuclear structure and the microdistribution of radiation damage in DNA, Int. J. Radiat. Biol. 66 (1994) 523-529.
[115] A. Agresti and M.E. Bianchi HMGB proteins and gene expression, Curr. Opin. Gen. Devel. 13 (2003) 170-178.
[116] M. Bustin HMGN dynamics and chromatin function, Biochem. Cell Biol. 81 (2003) 113-122.
[117] R. Reeves HMGA proteins: flexibility finds a nuclear niche? Biochem. Cell Biol. 81 (2003) 185-195.
[118] A.A. Travers Priming the nucleosome: a role for HMGB proteins? EMBO Rep. 4 (2003) 131-136.
[119] T. Nakano, H. Terato, K. Asagoshi, A. Masaoka, M. Mukuta, Y. Ohyama, T. Suzuki, K. Makino and H. Ide DNA-protein cross-link formation mediated by oxanine. A novel genotoxic mechanism of nitric oxide-induced DNA damage, J. Biol. Chem. 278 (2003) 25264-25272.
[120] S.R. Rajski, S.B. Rollins and R.M. Williams FR-66979 covalently cross-links the binding domain of the high-mobility group I/Y proteins to DNA, J. Am. Chem. Soc. 120 (1998) 2192-2193.
[121] S.R. Rajski and R.M. Williams Observations on the covalent cross-linking of the binding domain (BD) of the high mobility group I/Y (HMG I/Y) proteins to DNA by FR66979, Bioorg. Med. Chem. 8 (2000) 1331-1342.
[122] M. Bustin Revised nomenclature for high mobility group (HMG) chromosomal proteins, Trends Biochem. Sci. 26 (2001) 152-153.
[123] L. Beckerbauer, J.J. Tepe, J. Cullison, R. Reeves and R.M. Williams FR900482 class of anti-tumor drugs cross-links oncoprotein HMG I/Y to DNA in vivo, Chem. Biol. 7 (2000) 805-812.
[124] J.F. Wang, M. Bashir, B.N. Engelsberg, C. Witmer, H. Rozmiarek and P.C. Billings High mobility group proteins 1 and 2 recognize chromium-damaged DNA, Carcinogenesis 18 (1997) 371-375.
[125] P.C. Billings, R.J. Davis, B.N. Engelsberg, K.A. Skov and E.N. Hughes Characterization of high mobility group protein binding to cisplatin-damaged DNA, Biochem. Biophys. Res. Commun. 188 (1992) 1286-1294.
[126] P.A. Kulcharyk and J.W. Heinecke Hypochlorous acid produced by the myeloperoxidase system of human phagocytes induces covalent cross-links between DNA and protein, Biochemistry 40 (2001) 3648-3656.
[127] T.A. Rosenquist, E. Zaika, A.S. Fernandes, D.O. Zharkov, H. Miller and A.P. Grollman The novel DNA glycosylase, NEIL1, protects mammalian cells from radiation-mediated cell death, DNA Repair (Amst) 2 (2003) 581-591.
[128] M. Hashimoto, M.M. Greenberg, Y.W. Kow, J.-T. Hwang and R.P. Cunningham The 2-Deoxyribonolactone lesion produced in DNA by Neocarzinostatin and other damaging agents forms cross-links with the base-excision repair enzyme Endonuclease III, J. Am. Chem. Soc. 123 (2001) 3161-3162.
[129] M.S. DeMott, E. Beyret, D. Wong, B.C. Bales, J.T. Hwang, M.M. Greenberg and B. Demple Covalent trapping of human DNA polymerase

beta by the oxidative DNA lesion 2-deoxyribonolactone, J. Biol. Chem. 277 (2002) 7637-7640.
[130] T. Suzuki, M. Yamada, H. Ide, K. Kanaori, K. Tajima, T. Morii and K. Makino Identification and characterization of a reaction product of 2'-deoxyoxanosine with glycine, Chem. Res. Toxicol. 13 (2000) 227-230.
[131] T. Suzuki, M. Yamada, T. Nakamura, H. Ide, K. Kanaori, K. Tajima, T. Morii and K. Makino Products of the reaction between a diazoate derivative of 2'-deoxycytidine and L-lysine and its implication for DNA-nucleoprotein cross-linking by NO or HNO(2), Chem. Res. Toxicol. 13 (2000) 1223-1227.
[132] T. Suzuki, T. Nakamura, M. Yamada, H. Ide, K. Kanaori, K. Tajima, T. Morii and K. Makino Isolation and characterization of diazoate intermediate upon nitrous acid and nitric oxide treatment of 2'-deoxycytidine, Biochemistry 38 (1999) 7151-7158.
[133] E.Y. Krynetski, N.F. Krynetskaia, M.E. Bianchi and W.E. Evans A nuclear protein complex containing high mobility group proteins B1 and B2, heat shock cognate protein 70, ERp60, and glyceraldehyde-3-phosphate dehydrogenase is involved in the cytotoxic response to DNA modified by incorporation of anticancer nucleoside analogues, Cancer Res. 63 (2003) 100-106.
[134] Q. He, C.H. Liang and S.J. Lippard Steroid hormones induce HMG1 overexpression and sensitize breast cancer cells to cisplatin and carboplatin, Proc. Natl. Acad. Sci. USA 97 (2000) 5768-5772.
[135] G. Nagatani, M. Nomoto, H. Takano, T. Ise, K. Kato, T. Imamura, H. Izumi, K. Makishima and K. Kohno Transcriptional activation of the human HMG1 gene in cisplatin-resistant human cancer cells, Cancer Res. 61 (2001) 1592-1597.
[136] E.S. Leman and R.H. Betzenberg Nuclear matrix proteins as biomarkers in prostate cancer, J. Cell. Biochem. 86 (2002) 213-223.
[137] R.S. Malyapa, W.D. Wright and J.L. Roti Roti DNA supercoiling changes and nucleoid protein composition in a group of L5178Y cells of varying radiosensitivity, Radiat. Res. 145 (1996) 239-242.
[138] D. Rungger, E. Rungger-Brandle, C. Chaponnier and G. Gabbiani Intranuclear injection of anti-actin antibodies into Xenopus oocytes blocks chromosome condensation, Nature 282 (1979) 320-321.
[139] J.M. Egly, N.G. Miyamoto, V. Moncollin and P. Chambon Is actin a transcription initiation factor for RNA polymerase B? EMBO J. 3 (1984) 2363-2371.
[140] J.W. Hamilton, C.A. Louis, K.A. Doherty, S.R. Hunt, M.J. Reed and M.D. Treadwell Preferential alteration of inducible gene expression in vivo by carcinogens that induce bulky DNA lesions, Mol. Carcinog. 8 (1993) 34-43.
[141] W. Hofmann, B. Reichart, A. Ewald, E. Muller, I. Schmitt, R.H. Stauber, F. Lottspeich, B.M. Jockusch, U. Scheer, J. Hauber and M.C. Dabauvalle Cofactor requirements for nuclear export of Rev response element (RRE)-

and constitutive transport element (CTE)-containing retroviral RNAs. An unexpected role for actin, J. Cell Biol. 152 (2001) 895-910.
[142] G.V. Tolstonog, M. Sabasch and P. Traub Cytoplasmic intermediate filaments are stably associated with nuclear matrices and potentially modulate their DNA-binding function, DNA Cell Biol. 21 (2002) 213-239.
[143] V.A. Spencer, S.K. Samuel and J.R. Davie Altered profiles in nuclear matrix proteins associated with DNA in situ during progression of breast cancer cells, Cancer Res. 61 (2001) 1362-1366.
[144] U. Balasubramaniam and N.L. Oleinick Preferential cross-linking of matrix-attachment region (MAR) containing DNA fragments to the isolated nuclear matrix by ionizing radiation, Biochemistry 34 (1995) 12790-12802.
[145] N.L. Oleinick, S.M. Chiu, L.R. Friedman, L.Y. Xue and N. Ramakrishnan DNA-protein cross-links: new insights into their formation and repair in irradiated mammalian cells, Basic Life Sci. 38 (1986) 181-192.
[146] M.J. Tsapakos, T.H. Hampton and K.E. Wetterhahn Chromium(VI)-induced DNA lesions and chromium distribution in rat kidney, liver, and lung, Cancer Res. 43 (1983) 5662-5667.
[147] D.Y. Cupo and K.E. Wetterhahn Binding of chromium to chromatin and DNA from liver and kidney of rats treated with sodium dichromate and chromium(III) chloride in vivo, Cancer Res. 45 (1985) 1146-1151.
[148] M. Sugiyama, S.R. Patierno, O. Cantoni and M. Costa Characterization of DNA lesions induced by $CaCrO_4$ in synchronous and asynchronous cultured mammalian cells, Mol. Pharmacol. 29 (1986) 606-613.
[149] N.L. Oleinick, S.M. Chiu, N. Ramakrishnan and L.Y. Xue The formation, identification, and significance of DNA-protein cross-links in mammalian cells, Br. J. Cancer. Suppl. 8 (1987) 135-140.
[150] A. Izzotti, C. Cartiglia, M. Taningher, S. De Flora and R. Balansky Age-related increases of 8-hydroxy-2'-deoxyguanosine and DNA-protein crosslinks in mouse organs, Mutat. Res. 446 (1999) 215-223.
[151] R.K. Zahn, G. Zahn-Daimler, S. Ax, M. Hosokawa and T. Takeda Assessment of DNA-protein crosslinks in the course of aging in two mouse strains by use of a modified alkaline filter elution applied to whole tissue samples, Mech. Ageing Dev. 108 (1999) 99-112.
[152] J.M. Barret, P. Calsou and B. Salles Deficient nucleotide excision repair activity in protein extracts from normal human lymphocytes, Carcinogenesis 16 (1995) 1611-1616.
[153] L.H. Thompson Evidence that mammalian cells possess homologous recombinational repair pathways, Mutat. Res. 363 (1996) 77-88.
[154] R.J. Legerski and C. Richie Mechanisms of repair of interstrand crosslinks in DNA, Cancer Treat. Res. 112 (2002) 109-128.
[155] M.M. Cox The nonmutagenic repair of broken replication forks via recombination, Mutat. Res. 510 (2002) 107-120.
[156] R.C. Grafstrom, A. Fornace, Jr. and C.C. Harris Repair of DNA damage caused by formaldehyde in human cells, Cancer Res. 44 (1984) 4323-4327.

[157] R. Gantt A cell cycle-associated pathway for repair of DNA-protein crosslinks in mammalian cells, Mutat. Res. 183 (1987) 75-87.
[158] D. Murray, L. Vallee-Lucic, E. Rosenberg and B. Andersson Sensitivity of nucleotide excision repair-deficient human cells to ionizing radiation and cyclophosphamide, Anticancer Res. 22 (2002) 21-26.
[159] L. Li, C.A. Peterson, X. Lu, P. Wei and R.J. Legerski Interstrand cross-links induce DNA synthesis in damaged and undamaged plasmids in mammalian cell extracts, Mol. Cell. Biol. 19 (1999) 5619-5630.
[160] G. Speit, P. Schutz and O. Merk Induction and repair of formaldehyde-induced DNA-protein crosslinks in repair-deficient human cell lines, Mutagenesis 15 (2000) 85-90.
[161] O. Novakova, J. Kasparkova, J. Malina, G. Natile and V. Brabec DNA-protein cross-linking by trans-[PtCl(2)(E-iminoether)(2)]. A concept for activation of the trans geometry in platinum antitumor complexes, Nucleic Acids Res. 31 (2003) 6450-6460.
[162] M. Reynolds, E. Peterson, G. Quievryn and A. Zhitkovich Human nucleotide excision repair efficiently removes chromium-DNA phosphate adducts and protects cells against chromate toxicity, J. Biol. Chem. 279 (2004) 30419-30424.
[163] I.G. Minko, Y. Zou and R.S. Lloyd Incision of DNA-protein crosslinks by UvrABC nuclease suggests a potential repair pathway involving nucleotide excision repair, Proc. Natl. Acad. Sci. USA 99 (2002) 1905-1909.
[164] S.-M. Chiu, L.-Y. Xue, L.R. Friedman and N.L. Oleinick DNA-protein crosslinks: Formation and repair in irradiated cells, in: U. Hagen, H. Jung and C. Streffer (Eds.), Radiation Research 1895-1995, Congress Proceedings, Volume 2: Congress Lectures, ICRR Society, 1995, pp. 400-403.
[165] W.H. McBride, K.S. Iwamoto, R. Syljuasen, M. Pervan and F. Pajonk The role of the ubiquitin/proteasome system in cellular responses to radiation, Oncogene 22 (2003) 5755-5773.
[166] S.D. Desai, L.F. Liu, D. Vazquez-Abad and P. D'Arpa Ubiquitin-dependent destruction of topoisomerase I is stimulated by the antitumor drug camptothecin, J. Biol. Chem. 272 (1997) 24159-24164.
[167] W.J. DeNeve, C.K. Everett, J.E. Suminski and F.A. Valeriote Influence of WR2721 on DNA cross-linking by nitrogen mustard in normal mouse bone marrow and leukemia cells in vivo, Cancer Res. 48 (1988) 6002-6005.
[168] J.Y. Wang, G. Prorok and W.P. Vaughan Cytotoxicity, DNA cross-linking, and DNA single-strand breaks induced by cyclophosphamide in a rat leukemia in vivo, Cancer Chemother. Pharmacol. 31 (1993) 381-386.
[169] M. Coluccia, A. Nassi, F. Loseto, A. Boccarelli, M.A. Mariggio, D. Giordano, F.P. Intini, P. Caputo and G. Natile A trans-platinum complex showing higher antitumor activity than the cis congeners, J. Med. Chem. 36 (1993) 510-512.
[170] M. Coluccia, A. Boccarelli, M.A. Mariggio, N. Cardellicchio, P. Caputo, F.P. Intini and G. Natile Platinum(II) complexes containing iminoethers: a trans platinum antitumour agent, Chem. Biol. Interact. 98 (1995) 251-266.

[171] M. Coluccia, A. Nassi, A. Boccarelli, D. Giordano, N. Cardellicchio, F.P. Intini, G. Natile, A. Barletta and A. Paradiso In vitro antitumour activity and cellular pharmacological properties of the platinum-iminoether complex trans-[PtCl2[E-HN=C(OMe)Me]2], Int. J. Oncol. 15 (1999) 1039-1044.

Chapter 2: A method for the isolation of covalent DNA-protein crosslinks suitable for proteomics analysis

A version of this paper has been accepted for publication:

Sharon Barker, David Murray, Jing Zheng, Liang Li and Michael Weinfeld A method for the isolation of covalent DNA-protein crosslinks suitable for proteomics analysis. Analytical Biochemistry. 344(2):204-215. 2005.

2.1. Introduction

A DPC is created when a protein becomes covalently bound to DNA. These lesions are induced by UV and IR, by metals and metalloids such as chromium, nickel and arsenic, and by various aldehydes and anticancer drugs [1]. It has been suggested that, in mammalian cells, cellular stresses (illness, exposure to drugs, radiation, pollutants, etc.) result in the accumulation of different types of DNA-damage, including DPCs, due to oxidative mechanisms [2-4]. There are numerous chemically distinct types of DPCs; indeed, proteins can become crosslinked to DNA directly through oxidative free radical mechanisms, or indirectly through aldehydes generated by oxidative stress, or they can be crosslinked through a chemical or drug linker or through coordination with a metal atom [5]. These chemically-distinct DPCs may also differ in their biological consequences depending on their structure and persistence in the genome. Gross DPC half-lives have been measured *in vitro* and *in vivo* in mammalian cells and range from hours to days depending on the system and agent being studied [6-10].

Determining the biological relevance of DPCs is a complicated task. The covalent crosslinking of proteins to DNA is expected to physically block the access/assembly or progression of replication, repair, recombination, or transcription complexes. The induction of DPCs has been shown to correlate with the incidence of genetic damage such as SCEs, transformation, and cytotoxicity [11-15], although the contribution of specific DPCs to these events remains to be determined. Efforts to elucidate the biological consequences of DPCs are

confounded by several factors, including the simultaneous induction of other classes of lesions by DPC-inducing agents. DPCs are therefore inevitably induced in a background of multiple types of damage, and ascribing particular consequences to one type of damage is not yet possible. A second complication is the background of tightly, but non-covalently, bound proteins. Methods that would permit the separation and study of genuinely covalently bound proteins would greatly facilitate this effort.

Early studies of DPCs tended to focus on whether cellular proteins became associated with DNA following exposure of a test system to a given genotoxic agent and, if so, to what extent. With the advent of high-throughput proteomics methodologies, the emphasis has shifted to the possibility of recovering and identifying the proteins that become covalently linked to DNA. The latter studies will, however, require methodologies that recover the DNA component and those (rare) covalently bound proteins that are extracted along with the DNA. The more commonly used DPC investigation methods, such as nitrocellulose filter binding [16-18] and SDS/K^+ precipitation [19,20], quantitate DPCs as the amount of DNA isolated when proteins are trapped, and will therefore not be informative for the isolation and study of specific crosslinked proteins without extensive modification. A DPC isolation method that isolates proteins by virtue of their association with DNA should provide much cleaner DPC samples with respect to non-covalently associated proteins.

The stringency of isolating covalently-bound proteins has been part of the problem in assessing the biological relevance of DPCs to date. For example, it is

known that nuclear matrix proteins are tightly associated with the DNA [21]; their complete dissociation is therefore crucial for the identification of those less abundant proteins that are covalently crosslinked to DNA by a given agent. Previous studies [22-24] have isolated cisplatin-crosslinked proteins and nuclear matrix fractions from mammalian cells and shown by 2-D SDS-PAGE that the majority of the crosslinked proteins are present in the nuclear matrix fraction. However, this method involves binding of DNA/DPCs to hydroxylapatite, which is also capable of binding non-crosslinked proteins.

Applying proteomic approaches to the study of DPCs requires the development of novel methods that allow the isolation of the proteins covalently crosslinked to DNA as a pure sample and in sufficient quantities for further analysis and detection. To this end, we have developed two protocols to recover proteins covalently bound to DNA. Both protocols involve isolation of total genomic DNA using a commercial chaotrope/detergent mix (DNAzol) that lyses cells, hydrolyzes RNA, and dissociates non-covalent protein-DNA complexes. In the DNAzol-Strip method (Figure 2-1B), DNAzol treatment is followed by salt washes to strip non-covalently-bound proteins from the DNA. In the DNAzol-Silica method (Figure 2-1C), the genomic DNA is adsorbed onto silica in the presence of a chaotrope (DNAzol, urea, sodium chloride) under alkaline conditions to remove non-covalently associated proteins from the DNA. These DNA isolation methods were followed by additional steps to allow the recovery of truly covalently crosslinked proteins.

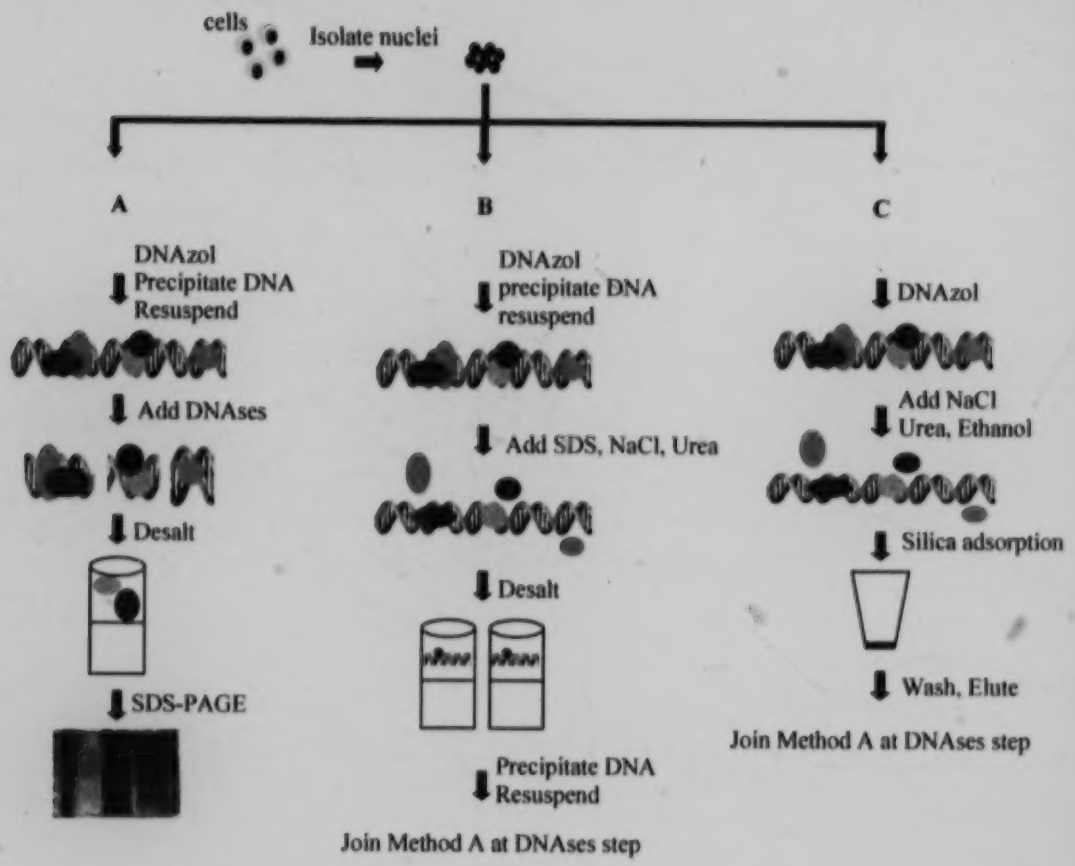

Figure 2-1: DNAzol-based DPC isolation methods

A schematic representation of the steps involved in the isolation and analysis of DPCs using the DNAzol method (A), the DNAzol-Strip method (B), and the DNAzol-Silica method (C). Proteins are represented by shaded circles/ovals.

2.2. Materials and Methods

2.2.a. Cell Culture

The CHO cell line, AA8, was maintained as a monolayer culture in αDMEM-F12 medium (Invitrogen) with 10% fetal bovine serum (Invitrogen) and 5% penicillin/streptomycin in a humidified 5% CO2/95% air atmosphere at 37°C.

2.2.b. Radiation and chemical treatments

For all experiments, low LET radiation, specifically γ-radiation, was used because all of the previous data on radiation-sensitive mutants and DPC induction and repair used these types of beams (e.g. [25-28]). As noted in Chapter 1, high LET radiations potentially result in a very different damage profile that is not well characterized. For γ-radiation treatments, cells (~85% confluency) were irradiated in a ^{60}Co irradiator (Gammacell 220; Atomic Energy of Canada Limited, Ottawa, ON) with doses of 0-4 Gy.

For formaldehyde treatment, 37% formaldehyde (Sigma) was added to the medium to a final concentration of 1% and the sample was incubated at 37°C for 1 h.

For topoisomerase I inhibitor treatment, cells were washed with phosphate buffered saline (PBS) and transferred to serum-free medium (10 mL). The cultures received either 10 µL of DMSO or 10 µg/mL camptothecin (Sigma) in 10 µL of DMSO and were incubated for 1.5 h at 37°C.

For proteasome inhibitor treatment, AA8 cells were treated with 10 µM MG132 (Cedarlane) in 10 mL medium for 3 h at 37°C. After 3 h, the medium was

replaced with serum-free medium and both proteasome inhibitor (to a final concentration of 10 μM) and camptothecin (to a final concentration of 10 μg/mL) were added as above and the cells were incubated at 37°C for 1.5 h.

2.2.c. DNAzol DPC isolation method (Figure 2-1A)

After treatment, the culture medium was removed and the cells were washed on the tissue culture dish with ice-cold PBS. Cells (or in later experiments, nuclei) were lysed by the addition of 500 μL DNAzol (Invitrogen) per 7×10^7 cells. DNA was precipitated from each sample using ½ volume of ice-cold 99% ethanol. The pellets were resuspended in 8 mM NaOH (3 mL per 9×10^6 cells) overnight at 37°C with a protease inhibitor mixture (Sigma). For DNA digestion, digestion buffer (5X) (1 mL of 50 mM $MgCl_2$, 50 mM $ZnCl_2$, 0.5 M sodium acetate, pH 5.0) was added to each sample and the samples were digested for 1 h at 37°C with 5 units of DNase I (Sigma) and 5 units of S1 nuclease (Invitrogen). After digestion, the DNA concentration was determined by UV absorbance and the samples were concentrated to 1 mL using Centricon concentrators with a molecular weight cut off (MWCO) of 5 kDa (Millipore). Samples were then reduced to dryness by lyophilization.

2.2.d. DNAzol-Strip DPC isolation method (Figure 2-1B)

Nuclei were isolated as described in section 2.2-g. Isolated nuclei were lysed by the addition of 500 μL DNAzol per 7×10^7 nuclei. DNA was precipitated from each sample using ½ volume of ice-cold 99% ethanol. The pellets were air-

dried briefly and resuspended in 8 mM NaOH (3 mL per 9 x 10^6 cells) at 37°C. An equal volume of 5 M urea was added and the samples were incubated at 37°C for 30 min on a rotating shaker. 10% SDS was added to a final concentration of 2% and the samples were incubated as above. The solute level was reduced using Centricon concentrators with an MWCO of 3 kDa. When the volume had been reduced to ~5 mL, an equal volume of 5 M NaCl was added. Samples were mixed at 37°C for 30 min on a rotating shaker and then filtered and washed with distilled deionized water three times, using Centricon concentrators with an MWCO of 3 kDa to reduce the volume and the salt concentration. The DNA from each sample was then re-precipitated by the addition of 1/10 volume of 3 M sodium acetate and 3 volumes of ice-cold 99% ethanol. Precipitated DNA was collected by centrifugation at 200x*g* at 4°C for 30 min and dried. The DNA was dissolved in 8 mM NaOH (3 mL per 9 x 10^6 cells). For DNA digestion, digestion buffer (5X) (1 mL of 50 mM $MgCl_2$, 50 mM $ZnCl_2$, 0.5 M sodium acetate, pH 5.0) was added to each sample and the samples were digested for 1 h at 37°C with 5 units of DNase I and 5 units of S1 nuclease. After digestion, the DNA concentration was determined by UV absorbance and the samples were washed with distilled deionized water (3 x 10 mL) and concentrated to 1 mL using Centricon concentrators with an MWCO of 5 kDa. Samples were then reduced to dryness by lyophilization.

2.2.e. DNAzol-Silica DPC isolation method (Figure 2-1C)

Silica fines were activated as detailed elsewhere [29]. Briefly, silica fines (EM Science, New Jersey) were heated to near boiling in 5 M nitric acid, washed three times in distilled deionized water and resuspended in an equal volume of distilled deionized water. The pH of the solution was adjusted to 7.0 using 1 M Tris-HCl, pH 8.0, and the silica fines were sedimented, resuspended in an equal volume of distilled deionized water and autoclaved. After lysing the nuclei with DNAzol as described above, 2 mL of pre-warmed (65°C) 10 mM Tris-HCl, pH 7.0, was added and each sample was drawn through a 21-gauge needle three times then through a 25-gauge needle three times to shear the DNA. NaCl (5 M) was added to a final concentration of 4 M, and this mixture was incubated at 37°C with shaking for 20 min. Urea (8 M) was added to a final concentration of 4 M and the samples were incubated as above. An equal volume of 99% ethanol was added to each sample. The activated silica slurry was then added (1 mL per 7×10^7 cells) and the samples were gently rocked for 20 min at room temperature to allow for binding. The silica was collected by centrifugation for 4 min at 35x*g* and the supernatant discarded. The silica was washed three times in 50% ethanol and collected by gentle centrifugation each time. The DNA was eluted two times using 2 mL of 8 mM NaOH at 65°C for 5 min and eluates were combined. For DNA digestion, 1 mL of 5X digestion buffer (50 mM $MgCl_2$, 50 mM $ZnCl_2$, 0.5 M sodium acetate, pH 5.0) was added to each sample and the samples were digested for 1 h at 37°C with 5 units of DNase I and 5 units S1 nuclease. After digestion, the DNA concentration was determined by UV

absorbance and the samples were washed with distilled deionized water (3 x 10 mL) and concentrated to 1 mL using Centricon concentrators with an MWCO of 5 kDa. Samples were then reduced to dryness by lyophilization.

2.2.f. SDS/K^+ DPC isolation method

We also employed the method of Zhitkovitch and Costa [19] to isolate DPCs. Nuclei were lysed by addition of ¼ volume of 4% SDS in 20 mM Tris-HCl, pH 7.4, followed by heating at 65°C for 10 min to allow complete binding of SDS to proteins. The SDS and protein-bound SDS was then precipitated by the addition of an equal volume of 200 mM KCl in 20 mM Tris-HCl, pH 7.4, and incubation on ice for 20 min. Precipitated proteins and protein-DNA complexes were collected by centrifugation at 12,000x*g* at 4°C for 10 min. The supernatant was discarded and the pellet was resuspended in 8 mM NaOH (3 mL per 9 x 10^6 cells) overnight at 37°C.

2.2.g. Nuclei isolation

Cultures were trypsinized at room temperature for 3 min and collected by centrifugation at 200x*g* at 4°C for 5 min. Cells were washed in ice-cold PBS and collected as before. The cell pellet was gently resuspended in Buffer 1 (400 µL per 10^7 cells) using a wide-bore pipette tip (Buffer 1: 10 mM Hepes pH 7.9, 10 mM KCl, 100 mM EDTA, 100 mM EGTA, 1 mM DTT, 0.5 mM phenylmethylsulfonyl fluoride (PMSF), 1% (v/v) aprotinin). Cells were chilled on ice for 15 min and then lysed by the addition of 0.6% (v/v) Nonidet P-40 and

mixing by inversion. Nuclei were pelleted at 200x*g* for 5 min at 4°C and the supernatant was removed.

2.2.h. Nuclear extract preparation

Nuclear extracts of CHO AA8 cells were prepared for control purposes. After nuclei isolation (above), the pellet was resuspended gently in ice-cold Buffer 2 (100 µL per 10^7 cells) using a wide-bore pipette tip (Buffer 2: 20 mM Hepes pH 7.9, 400 mM NaCl, 1 mM EDTA, 1 mM EGTA, 1 mM DTT, 1 mM PMSF, 1% (v/v) aprotinin, 10% (v/v) glycerol) and incubated, with shaking, at 4°C for 30 min. The lysate was centrifuged at 12,000x*g* for 10 min at 4°C. The supernatant was aliquoted into ice-cold 1.5 mL microcentrifuge tubes supplemented with 0.025 mg/mL leupeptin and aliquots were flash frozen in liquid nitrogen and stored at -80°C.

2.2.i. Quantitation of DNA

The UV absorbance at 260 nm was measured for each sample to determine the DNA concentration. A value of 32 µg (oligonucleotide) per 1 OD unit was used to calculate the amount of DNA in each sample. The relative amounts of DNA were determined within each experiment and used to determine sample loads for SDS-PAGE analysis. The 260/280 nm absorbance ratios were also determined. Ratios of 1.5-1.7 were invariably obtained, indicating that the contribution of protein to the 260 nm reading was not significant. For

optimization experiments, the amount of DNA was also assessed by 1% agarose gel electrophoresis and ethidium bromide staining.

2.2.j. Quantitation of protein

Protein content of DPC isolates was determined using the Bradford reagent (BioRad) and standard Bradford assay procedure with BSA as a standard.

2.2.k. SDS-PAGE analysis

Laemmli buffer (BioRad) was added to each sample in amounts determined to equalize the DNA concentration of each sample. In later experiments, dried protein samples were dissolved in 20 μL of Laemmli buffer (BioRad) and sample loads were determined to equalize the DNA concentration of each sample. Samples were analyzed by 1-D SDS-PAGE using 12% separating gels (180 x 160 x 0.75 mm for MS analysis or 80 x 60 x 0.75 mm for standard protein analysis), or 10-20% gradient gels (80 x 60 x 0.75 mm, BioRad) in later experiments. In separate experiments, gels were silver stained using the ammoniacal-silver nitrate staining procedure or by standard Coomassie blue staining and destaining procedures, or by SYPRO Tangerine (Invitrogen) staining according to the manufacturer's protocol.

2.2.1. Mass Spectrometry

MS analysis was performed at the Alberta Cancer Board Proteomics Facility (Department of Chemistry, University of Alberta). Samples were subjected to digestion with trypsin. Peptide extracts were analyzed on a Bruker REFLEX III (Bremen/Leipzig, Germany, Serial # FM 2413) time of flight mass spectrometer using MALDI in positive ion mode. The peptide maps obtained were used for database searching to identify proteins. Furthermore, selected peptides were fragmented using MALDI MS/MS analysis using a PE Sciex API-QSTAR Pulsar instrument (MDS-Sciex, Toronto, ON, Serial # K0940105). The obtained partial sequence information for each peptide was used to confirm the previously-obtained results from the peptide map search.

2.3. Results

2.3.a. DPC isolation by DNAzol

DPCs can be detected using the alkaline elution assay [30,31]. In the first steps of this method, cells are lysed on a polyvinylchloride or polycarbonate filter which traps DNA based on its high molecular weight (MW) [32]. Repeated washing causes smaller fragments of DNA to be lost along with free proteins. Large fragments of DNA and any covalently bound proteins are trapped on the filter. We initially evaluated the utility of the polycarbonate filter trapping method for protein recovery because these filters do not strongly bind DNA or protein and therefore might provide the stringency necessary for the isolation of pure DPCs.

However, we found that this method resulted in poor protein recovery and poor reproducibility (data not shown), and we therefore sought to develop an alternative procedure.

Genomic DNA isolation kits currently available are not useful for DPC isolation because most of them include a Proteinase K digestion step (which will destroy the crosslinked proteins) and because they are not amenable to scaling up to the level necessary to isolate sufficient quantities of DPCs for protein identification purposes. One currently available genomic DNA isolation reagent is DNAzol, a proprietary reagent (US patent no. 5,945,515), which contains a guanidine salt and detergent in alkali conditions. This reagent lyses cells, dissociates proteins, and hydrolyzes RNA. The DNA is precipitated by the addition of ethanol (DNAzol method; Figure 2-1A). The DNAzol reagent does not contain proteinases and is not overtly damaging to proteins (Figure 2-2). No obvious degradation of proteins was seen after incubation of AA8 nuclear extract with DNAzol (5 min at room temperature) and analysis of the proteins by SDS-PAGE and Coomassie Blue staining (Figure 2-2, lane 2). In contrast, the complete degradation of proteins was apparent following incubation of AA8 nuclear extract with Proteinase K (Figure 2-2, lane 3), as expected.

Although the DNAzol reagent contains detergent and the chaotropic agent guanidine hydrochloride, the isolation of DNA from untreated AA8 cells using the standard DNAzol method does not fully dissociate proteins from the DNA as detected by both SDS-PAGE and Bradford analyses (Figure 2-3, lane 1). We

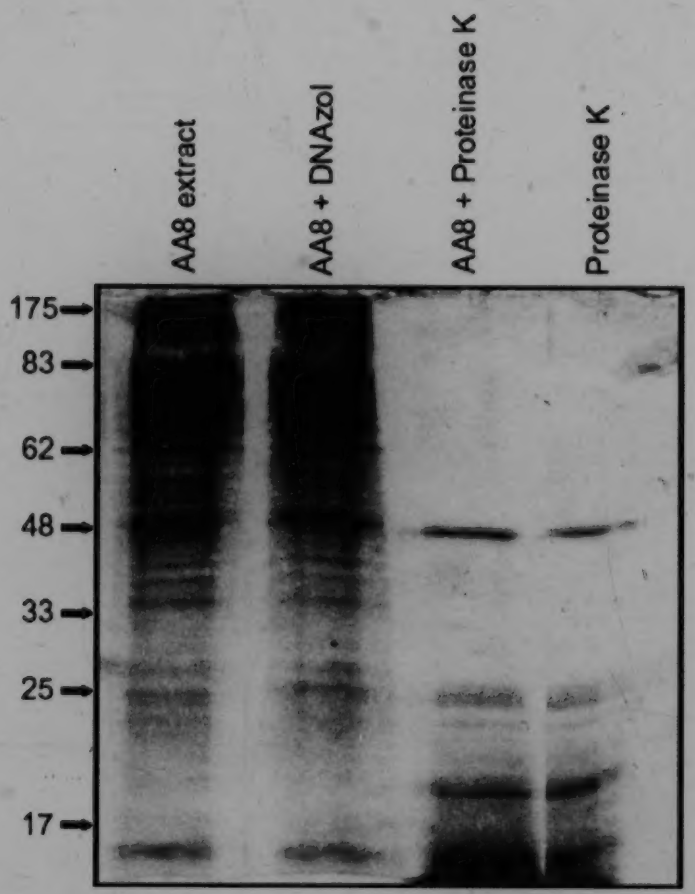

Figure 2-2: Effect of DNAzol on protein integrity

AA8 nuclear extract was incubated with DNAzol for 5 min at room temperature and analyzed by SDS-PAGE. For comparison, an equal amount of AA8 nuclear extract was incubated with Proteinase K for 5 min at room temperature to fully digest the proteins. For reference, the Proteinase K reagent and AA8 nuclear extract were also each run on their own. Protein MWs are indicated in kDa.

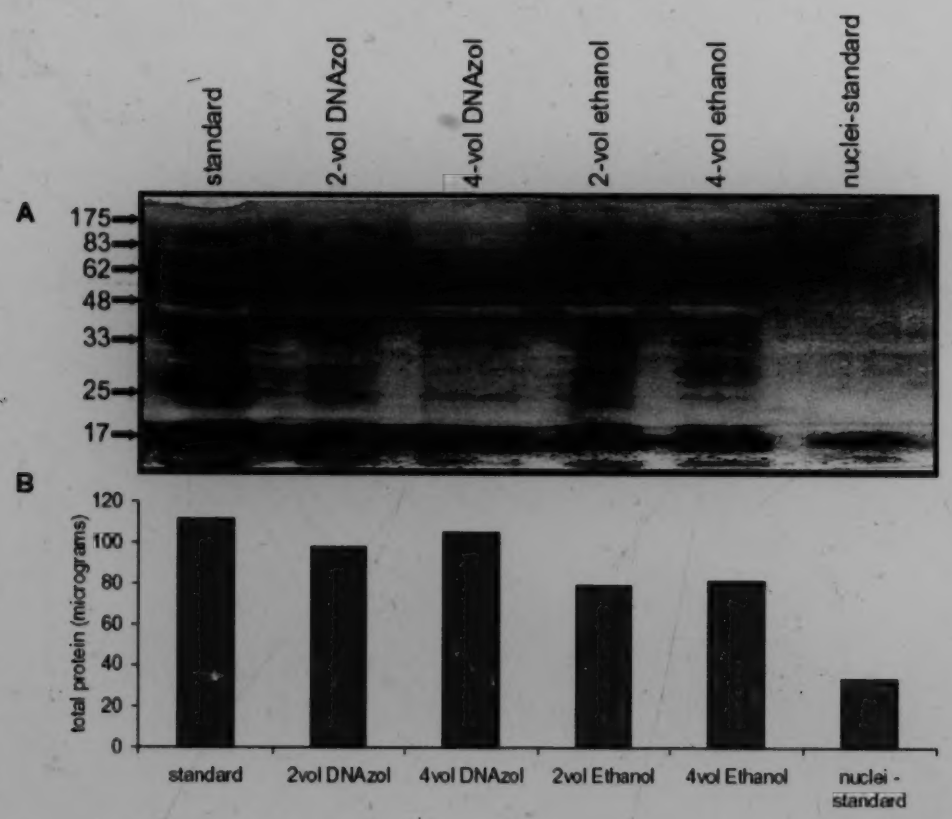

Figure 2-3: Modification of the DNAzol protocol to reduce the level of background protein

To minimize the isolation of non-covalently bound protein, several modifications to the standard DNAzol method were tested. DNA and bound protein was isolated from untreated AA8 cells using different volumes of DNAzol or different volumes of ethanol to precipitate the DNA and associated protein. We also tested the DNAzol protocol using isolated nuclei. Sample loads were normalized based on the amount of digested DNA present in the sample (approximately 35 µg of DNA loaded for each sample) and proteins were analyzed by 12% SDS-PAGE and silver staining (A) and Bradford protein quantitation (B) to assess the level of recovered protein. Protein MWs are indicated in kDa.

attempted to optimize the stripping of proteins from the DNA by varying both the amounts of the detergent/chaotrope (i.e., genomic DNA isolation using twice or four times the volume of DNAzol used in the standard DNAzol method) and ethanol (i.e., DNA precipitation using twice or four times the volume of ethanol used in the standard DNAzol isolation method) (Figure 2-3, lanes 2–5). Although these modifications did reduce the background level of associated proteins, the purity of the samples was not adequate because there was still a significant level of protein isolated from the untreated sample. To further modify this method to obtain the level of stringency that would be necessary for DPC isolation, we first carried the AA8 cells through a nuclei isolation procedure and then isolated DNA using the DNAzol method (Figure 2-3, lane 6), which greatly reduced the background level of protein isolated. However, these modifications were not sufficient to remove **all** non-covalently associated proteins from the DNA as there was still some staining observed on the SDS-PAGE gel as well as protein detected in these samples by Bradford analysis (Figure 2-3, lane 6). Nonetheless, these experiments demonstrated that the isolation of nuclei and the use of an increased volume of ethanol or chaotropic agent did reduce the level of background proteins isolated, and these modifications formed the basis for further method development.

2.3.b. DPC isolation by DNAzol-Strip method

We developed a method from this point (DNAzol-Strip method; Figure 2-1B) exclusively using isolated nuclei. We combined the DNAzol reagent to lyse

nuclei, hydrolyse RNA and dissociate bulk proteins from DNA with additional chaotropic agents to strip non-covalently bound proteins from the DNA. Isolated nuclei were lysed by the addition of DNAzol and the DNA (with attached proteins) was precipitated with ethanol. The DNA was then resuspended and washed in an SDS/urea/sodium chloride mixture to optimize removal of non-covalently bound proteins. The samples were subjected to extensive desalting and volume reduction. The DNA was then isolated by ethanol precipitation and resuspended. The DNA was digested with DNase I and S1 nucleases, and the proteins were collected and reduced to dryness. Because this DPC isolation method isolates crosslinked proteins as a function of their attachment to DNA, sample loads were always normalized for DNA content within each experiment as determined after DNA digestion. Proteins were separated by 1-D SDS-PAGE and the gels were stained for visualization.

Using nuclei from untreated AA8 cells, various forms of the DNAzol isolation method were compared with the SDS/K^+ precipitation method to assess the background level of proteins isolated (Figure 2-4). (It should be noted that others have combined additional isolation and wash steps with the SDS/K^+ protocol [5,33] to reduce the background level of non-covalently bound proteins). Protein sample loads were normalized based on the cell number determined at plating (24 million cells plated per sample) (Figure 2-4A) or DNA content determined after DNA digestion (Figure 2-4B). As expected, the unmodified SDS/K^+ method resulted in the recovery of a high level of non-covalently associated protein. In contrast, the DNAzol-Strip method (Figure 2-4A, lane 4

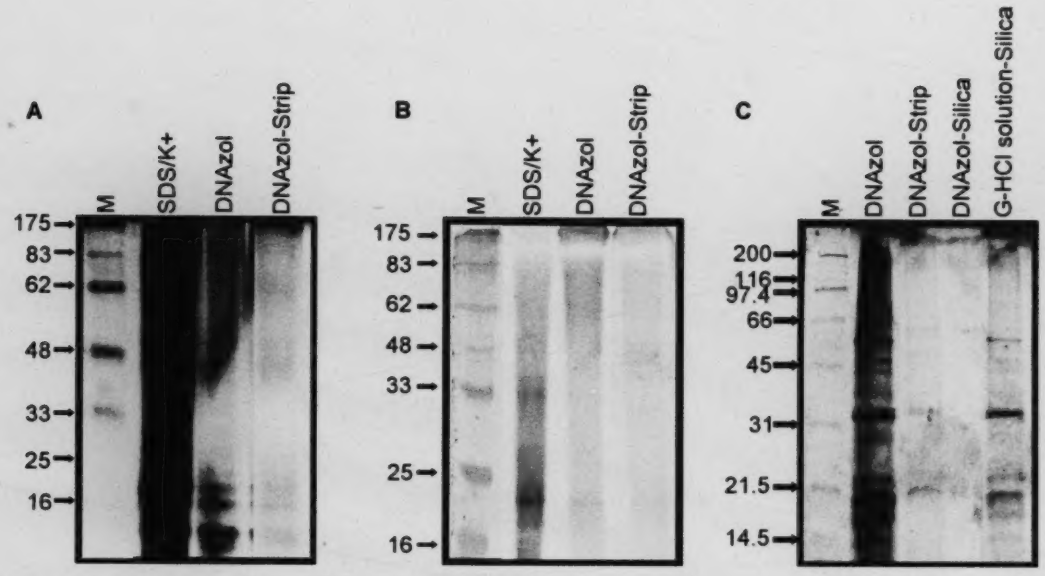

Figure 2-4: Comparison of background protein levels using different DPC isolation methods

Untreated AA8-cell nuclei were subjected to DPC isolation by the SDS/K^+ method, the DNAzol method, or the DNAzol-Strip method. Sample volumes were adjusted for (A) cell number (equal number of cells determined at plating; 24 million cells per plate) or (B) DNA content (determined after DNA digestion; ~70 µg of DNA loaded for each sample) and were analyzed by 12% SDS-PAGE and silver staining. (C) Using untreated AA8-cell nuclei, the DNAzol (Figure 2-1A), DNAzol-Strip (Figure 2-1B) and DNAzol-Silica (Figure 2-1C) methods were directly compared. Sample volumes were adjusted for DNA content (measured after DNA digestion) and proteins were analyzed by 10-20% SDS-PAGE gradient gel and SYPRO-Tangerine staining. The Silica-based isolation method (Figure 2-1C) was also performed using a non-commercial genomic DNA isolation reagent (G-HCl solution) instead of DNAzol. The "M" lanes are the MW markers with the MWs shown in kDa. Lanes within each panel are from the same gel with intervening lanes removed.

and Figure 2-4B, lane 4) isolated relatively little non-covalently associated protein. Thus, combining the use of DNAzol with additional wash steps reduces the background level of proteins to almost zero and represents an improvement over the SDS/K^+ and standard DNAzol (Figure 2-4A, lanes 2 & 3 and Figure 2-4B, lanes 2 & 3) isolation methods.

2.3.c. DPC isolation by DNAzol-Silica method

We have modified the DNAzol-based DPC isolation procedure to make it considerably faster and more economical (Figure 2-1C). The modification relies on the ability of DNA (but not proteins) to bind to silica in the presence of chaotropic/dissociative agents such as guanidinium hydrochloride, sodium chloride, and urea, which strip the DNA of associated proteins [29]. This protocol substitutes an adsorption step for the desalting/concentration step, resulting in the DNA (and covalently-attached proteins) being bound to the silica and the non-covalently associated proteins being removed in the supernatant and subsequent wash steps. The DNA (with DPCs) is then eluted from the silica and digested, releasing the proteins, which are collected and analyzed by 1-D SDS-PAGE.

Using nuclei from untreated AA8 cells, the DNAzol-Silica method (Figure 2-4C, lane 4) was compared with the DNAzol (Figure 2-4C, lane 2) and the DNAzol-Strip (Figure 2-4C, lane 3) methods to assess the background level of proteins isolated by each protocol. Protein sample loads were normalized based on DNA content determined after DNA digestion. As demonstrated in Figure 2-4,

the DNAzol-Strip and DNAzol-Silica methods both isolated relatively little non-covalently associated protein.

We also examined the impact of substitution of DNAzol by a non-commercial DNA extraction solution (Figure 2-4C, lane 5; "G-HCl solution") composed of 6 M guanidinium hydrochloride, 0.5% SDS and 8 mM sodium hydroxide in this silica-based isolation method. As seen in Figure 2-4C, this solution proved less effective than DNAzol in reducing background protein recovery.

2.3.d. Isolation of γ-radiation-induced DPCs by DNAzol-Strip and DNAzol-Silica methods

Both the DNAzol-Strip and DNAzol-Silica methods successfully dissociated non-covalently bound proteins from genomic DNA. The utility of each of these methods for the isolation of covalently crosslinked proteins from biological samples was investigated. The DNAzol-Strip method was used in preliminary experiments to isolate and analyze DPCs induced in AA8 cells exposed to formaldehyde or γ-radiation (Figure 2-5). AA8 cells were exposed to 0 or 1 Gy of γ-radiation, or to 1% formaldehyde at 37°C for 1 h, and nuclei were isolated. DPCs were isolated using the DNAzol-Strip method as outlined above. Dried protein samples were resuspended in Laemmli loading buffer and volumes were adjusted based on DNA content. Proteins were analyzed by 12% SDS-PAGE and silver staining. Only a few faint distinct protein bands were visible in the unirradiated sample (Figure 2-5, lane 2), while a greater number and intensity

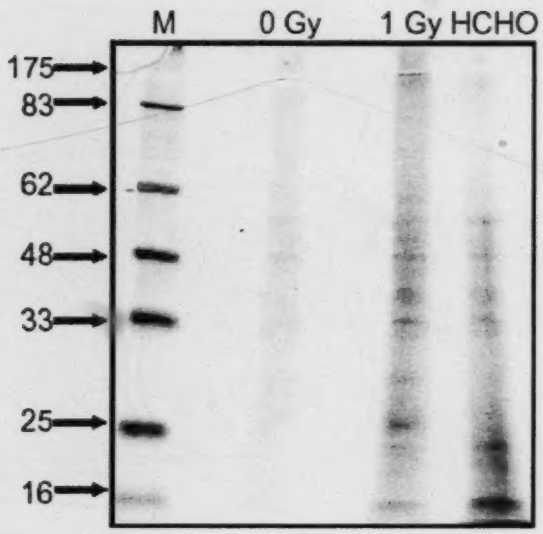

Figure 2-5: Isolation of formaldehyde- and γ-ray-induced DPCs from CHO cells using the DNAzol-Strip method

AA8 cells received 0 or 1 Gy of γ-radiation, or were treated with 1% formaldehyde (HCHO) at 37°C for 1h. DPCs were isolated using the DNAzol-Strip method. Sample volumes were adjusted for DNA content (determined after DNA digestion) and proteins were analyzed by 12% SDS-PAGE and silver staining. The "M" lane is the MW markers with the MWs shown in kDa. Lanes in the figure are from the same gel with intervening lanes removed.

of distinct protein bands were routinely observed in both irradiated and formaldehyde-treated samples (Figure 2-5, lanes 3 and 4), demonstrating that the DNAzol-Strip method isolated reasonably pure, presumably covalently-crosslinked proteins and little background protein. The protein concentration measurements routinely demonstrated that the level of protein in the irradiated sample (1Gy) was ~3-fold higher than that in the unirradiated sample. The suitability of the SDS-PAGE bands for further analysis by MS was then addressed (see section 2.3.e.).

We also assessed the potential utility of the more convenient DNAzol-Silica method in isolating DPCs from biological samples. Additional modifications in the analysis involved the use of a quantitative, reversible protein stain, SYPRO Tangerine. AA8 cells were exposed to 0 or 1 Gy of γ-radiation, or to 1% formaldehyde at 37°C for 1 h. DPCs were isolated using the DNAzol-Silica method as outlined above. Dried protein samples were resuspended in Laemmli loading buffer and volumes were adjusted based on DNA content. Proteins were analyzed by 10-20% gradient SDS-PAGE and SYPRO-Tangerine staining (Figure 2-6). This method generated similar results to the DNAzol-Strip method. There was a low level of background protein isolated as evidenced by the few distinct protein bands observed in the untreated sample (Figure 2-6, lane 2). The DNAzol-Silica method allowed the isolation of relatively pure, presumably covalently-crosslinked, proteins from both the 1 Gy-irradiated and formaldehyde-treated samples (Figure 2-6, lanes 3 and 4) as evidenced by the appearance of distinct protein bands. Some smearing of the protein bands is expected on 1-D

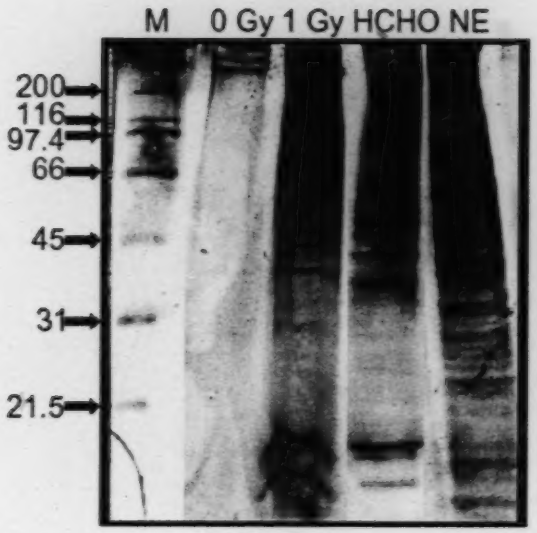

Figure 2-6: Isolation of formaldehyde- and γ-ray-induced DPCs from CHO cells using the DNAzol-Silica method

AA8 cells received 0 or 1 Gy of γ-radiation, or were treated with 1% formaldehyde (HCHO) at 37°C for 1 h. DPCs were isolated using the DNAzol-Silica method. Sample volumes in the "0 Gy", "1 Gy", and "HCHO" lanes were adjusted to equalize the DNA concentrations determined by UV absorbance after DNA digestion. Proteins were analyzed by 10-20% gradient SDS-PAGE and SYPRO-Tangerine staining. "M" represents MW markers with the MWs shown in kDa and "NE" represents AA8 nuclear extract from untreated cells. Lanes in the figure are from the same gel with intervening lanes removed.

SDS-PAGE as there may be multiple protein species of similar size. This behaviour was more marked in the case of formaldehyde crosslinking, probably because of the potency of this crosslinking agent and the extended treatment interval used (1 h) compared to irradiation (10 sec) as well as the different lifetimes of the various intermediates involved in these two chemically distinct crosslinking mechanisms. Nonetheless, individual bands were readily visible.

2.3.e. Preliminary identification of a crosslinked protein by mass spectrometry

The DNAzol-Strip method yielded excellent quality protein samples of sufficient quantity to allow identification of a number of γ-radiation-crosslinked proteins by MS. Figure 2-7 shows an example of a mass spectrum (Figure 2-7B) of peptides isolated from pooled SDS-PAGE gel bands excised from identical samples of irradiated CHO cells (Figure 2-7A). Several of the peptides isolated from the excised bands (Table 2-1) led to the identification of the hamster heat shock protein, glucose regulated protein 78 (GRP78), which has previously been shown to be crosslinked to DNA by the antitumour antibiotic gilvocarcin [33]. A more extensive analysis of γ-radiation-induced DPCs is the subject of the studies described in Chapter 3.

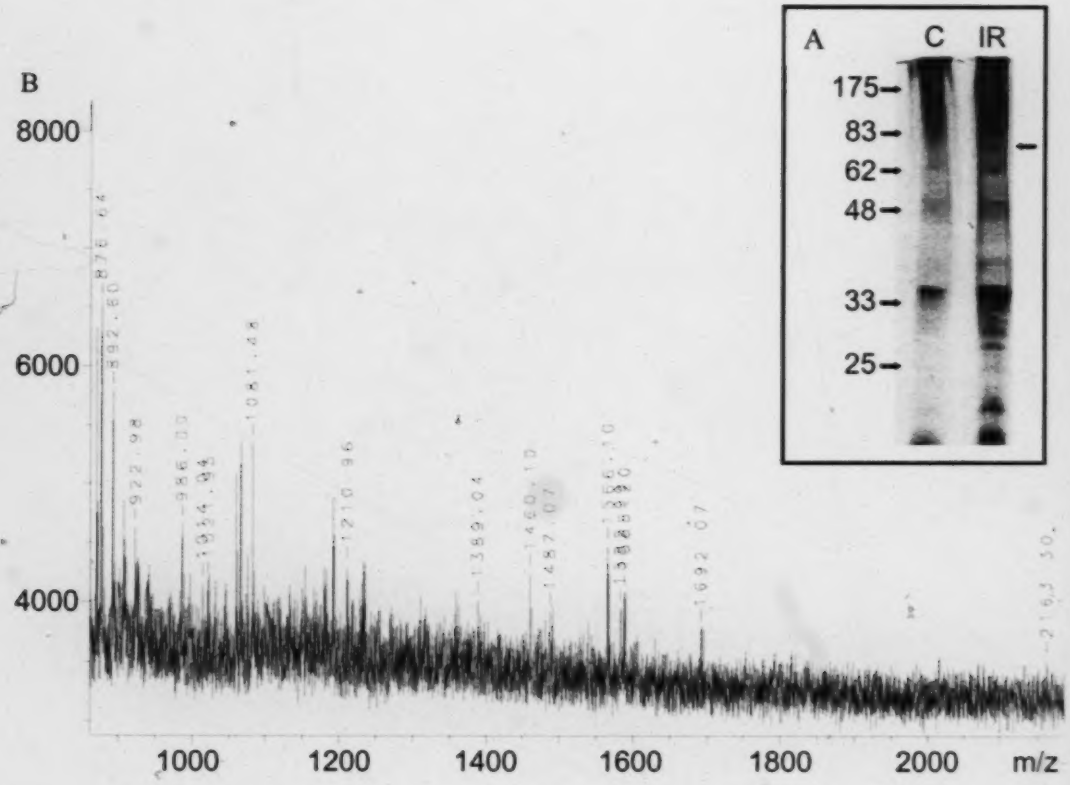

Figure 2-7: Mass-spectrometric identification of GRP78 as an ionizing-radiation crosslinked protein in CHO AA8 cells

(A) Peptides were obtained from the 12% SDS-PAGE silver-stained gel band indicated by the arrow in the γ-irradiated "IR" lane and pooled with the same band from multiple γ-irradiated samples. The "C" lane is the un-irradiated control. (B) The mass/charge (m/z) ratios for peptides isolated from the indicated protein band. Database searching identified several of these peptides as part of the amino acid sequence of the hamster 78-kDa glucose regulated protein (GRP78) (see Table 2-1). The intensely stained band at ~35 kDa is due to DNase I.

Table 2-1: Peptides used for mass-spectral identification of proteins

Protein	Peptide	Mass observed
GRP78	SDIDEIVLVGGSTR	1460.10
	ITPSYVAFTPEGER	1566.10
	KSDIDEIVLVGGSTR	1588.20
Topoisomerase I Sample A	EMTNDEK *	882.15
	ITVAWCKK	1004.69
	QRAVALYFIDK	1323.16
	YIMLNPSSRIK *	1338.04
	AVQRLEEQLMK *	1360.14
	CDFTQMSQYFKDQSEAR	2139.48
	MSGDHLHNDSQIEADFRLNDSHK *	2680.77
Topoisomerase I Sample B	IEPPGLFR	927.27
	DQLADARR	943.93
	ILSYNRANR	1105.34
	TYNASITLQQQLK	1507.71
	IMPEDIIINCSKDAK *	1761.16
Topoisomerase I Sample C	EENKQIALGTSK	1316.53
	RIMPEDIIINCSK *	1602.52
	QIALGTSKLNYLDPR	1687.44
	LNYLDPRITVAWCK	1747.47
	LLKEYGFCVMDNHR	1782.03
Topoisomerase I Sample E	EDIKPLK	841.67
	GNHPKMGMLK *	1128.21
	QRAVALYFIDK	1322.48
	WGVPIEKIYNK	1345.41
	SMMNLQSKIDAK *	1380.74
	TFEKSMMNLQSK **	1473.44
	IMPEDIIINCSKDAK	1745.77
	CDFTQMSQYFKDQSEAR	2140.21

A listing of the peptides and peptide masses that were used to identify GRP78 from the samples in Figure 2-7A and to confirm the presence of DNA topoisomerase I in the samples indicated in Figure 2-8. The asterisk(s) indicate the presence of oxidized methionines in the peptide.

2.3.f. Isolation of camptothecin-induced DPCs by the DNAzol-Strip and DNAzol-Silica methods

The utility of each of these methods for the isolation of genuinely covalently crosslinked proteins from biological samples was also investigated using a known target DPC. Mammalian DNA topoisomerase I (91 kDa) becomes transiently covalently crosslinked to DNA during DNA processing [34], and these DPCs can be trapped using inhibitors such as camptothecin. AA8 cells were treated with 10 μg/mL camptothecin for 1.5 h at 37°C and nuclei were isolated. DPCs were isolated using the DNAzol-Strip method (Figure 2-8, lanes 1-3) or the DNAzol-Silica method (Figure 2-8, lanes 5-7). Dried protein samples were resuspended in Laemmli loading buffer and volumes were adjusted based on DNA content previously determined after DNA digestion. Proteins were analyzed by 10-20% gradient SDS-PAGE and SYPRO-Tangerine staining. As shown in Figure 2-8, lane 3, the DNAzol-Strip method primarily isolated smaller bands from the camptothecin-treated cells, many of which were probably degradation products. The DNAzol-Silica method (Figure 2-8, lane 6), on the other hand, isolated a band of ~100 kDa as well as several smaller and larger sized protein bands. The higher MW species probably represent ubiquitinated topoisomerase I [35], which are seen to an even greater extent in cells treated simultaneously with camptothecin and a proteasome inhibitor, MG132 ([35] and Figure 2-8, lane 7). The presence of DNA topoisomerase I in DPCs isolated from these

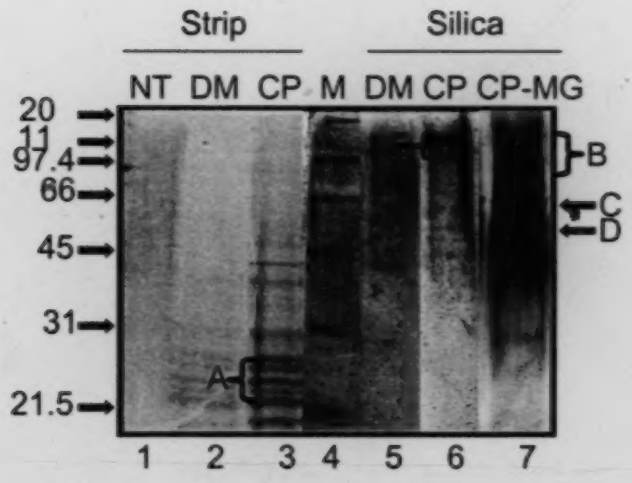

Figure 2-8: Isolation of camptothecin-induced DPCs from CHO cells

AA8 cells received no treatment "NT", 1 µL/mL DMSO (DM), or 10 µg/mL camptothecin for 1.5 h at 37°C "CP", or 10 µM MG132 for 3 h at 37°C followed by 10 µg/mL camptothecin and 10 µM MG132 for 1.5 h at 37°C "CP-MG". DPCs were isolated using the DNAzol-Strip method (lanes 1-3) or the DNAzol-Silica method (lanes 5-7). Dried protein samples were resuspended in Laemmli loading buffer and sample volumes were adjusted for DNA content (measured after DNA digestion). Proteins were analyzed by 10-20% gradient SDS-PAGE and SYPRO-Tangerine staining. Bands from within the indicated regions (A-E) were excised and bands within regions A, B, and E were pooled separately, The "M" lane is the MW markers with MWs shown in kDa.

experiments (Figure 2-8: lane 3 Sample A, lane 6 Sample E, lane 7 Samples B and C) was confirmed by MS (Table 2-1). Sample D (Figure 2-8, lane 7) was not found to contain topoisomerase I. (Pooling of excised bands within sample areas A, B, and E was performed to ensure sufficient material for MS identification because we were concerned that the recovery of topoisomerase I may be limited by its rapid degradation. Furthermore, the detection limit of SYPRO Tangerine is lower than the detection limit of the MS technology.)

2.4. Discussion

The study of covalent protein-DNA complexes has been limited by the lack of availability of techniques that overcome a number of challenges [1]. DPCs will involve a small fraction of the proteome, and may involve low-abundance proteins and proteins of differing solubilities and stability. DPC isolation must be rigorous because DPCs must be distinguished from various DNA-protein associations that are non-covalent but may nonetheless be relatively abundant and strong enough to resist dissociation by commonly-used isolation methods. Detection and chemical analysis of DPCs will require sufficiently large, pure samples and sensitive protein analytical techniques. Current methods used for the isolation of DPCs from cells fail to provide adequate stringency, specificity and scalability of isolation [1]. We have described here the development of novel methods for the isolation of pure, enriched and intact DPCs that is applicable to large numbers of cells and is economical, rapid, and amenable to high-throughput. The methods are based on the use of the DNAzol reagent and high

concentrations of additional chaotropes to dissociate non-covalent DNA-protein associations. The two variations of the DNAzol-based DPC isolation procedure allow the isolation of highly pure, covalently crosslinked, proteins from cells.

The SDS-PAGE analyses (Figures 2-5 and 2-6) indicate that the background level of protein isolated from untreated AA8 cells, while extremely low, is not zero. However, it should be noted that endogenous DPC-inducing agents (e.g., free radicals, aldehydes, and lipid peroxidation products) will be present in a cell at any given time. Indeed, it has been proposed that DNA crosslink repair mechanisms actually evolved in response to the damage induced by such intracellular crosslinking agents [36]. We have now used both the DNAzol-Strip and DNAzol-Silica methods extensively for DPC isolations and have routinely observed very little signal in the unirradiated samples on SDS-PAGE analysis in a larger study of γ-radiation-crosslinked proteins (see Chapter 3). Considering the evidence from the present study showing that measured background DPC levels are very sensitive to small methodological alterations, it is not surprising that the level of background endogenously-induced DPCs reported in different studies varies greatly with the method used for DPC detection [2,4,37].

The two method variations presented here involve relatively mild conditions for the elution and resuspension of DNA and DPCs and release the crosslinked proteins by nuclease digestion, making these methods suitable for analysis of DPCs induced by various agents. As well, the crosslinked proteins isolated in the present study are in a sufficiently pure and enriched form to be

useful for proteomics analysis as we were able to use MALDI-TOF MS and MS/MS to identify GRP78 as a protein crosslinked to DNA by γ-radiation in two independent experiments. GRP78 was described here only to illustrate the usefulness of this protein isolation method for interfacing with high-throughput proteomics technologies, and in fact we have to date isolated and identified 29 cellular proteins that appear to participate in such lesions (see Chapter 3).

The comparison of the DNAzol-Strip and DNAzol-Silica methods for isolation of the DNA-toposimerase I complex revealed that the DNAzol-Strip method probably isolated degraded complex (Figure 2-8 and Table 2-1, Sample A). This was most likely due to the lengthy processing time in high salt conditions involved in the DNAzol-Strip method. Previous studies have shown that a) camptothecin treatment induces a time- and dose-dependent degradation of topoisomerase I [38], and b) camptothecin-induced topoisomerase I-DNA complexes are rapidly lost once the drug is removed *in vivo* [38] and are reversed *in vitro* with the addition of 0.5 M sodium chloride [34]. The DNAzol-Silica method isolated these degradation products as well as larger products which may represent ubiquitinated forms of topoisomerase I (Figure 2-8 and Table 2-1, Samples B and C), which are seen as higher MW bands on SDS-PAGE analysis [35]. The comparison of the DNAzol-Strip and DNAzol-Silica method indicates that the latter is faster, thereby permitting the isolation of the shorter-lived population of DPCs.

With respect to the resolution of exogenously-induced DPCs, the DNAzol-Strip and DNAzol-Silica methods can detect DPCs at γ-ray doses as low as 1 Gy

(Figures 2-5 and 2-6). Bradford analyses performed on DNAzol-Strip experiments demonstrated an average of 3-fold more protein isolated from 1 Gy-irradiated samples over the unirradiated samples. This detection level can be compared with the alkaline elution/polycarbonate filter method in which DPC detection was only possible at much higher doses of IR (50 Gy) [39], and with the nitrocellulose filter binding technique, which can detect DPCs in irradiated cells at doses as low as 30 Gy but which does not allow specific protein recovery [39].

During preparation of this manuscript we became aware of a method devised for the isolation of cisplatin-induced crosslinks [22-24]. The method used was developed for analyzing a specific type of DPC rather than for the isolation of any/all crosslinked proteins, but it underscores the utility of chaotropic agents for dissociating non-covalently crosslinked proteins. However, the background level of proteins isolated from untreated cells was not reported in those studies [22-24]; therefore, the contribution of non-covalently bound but tightly associated nuclear matrix proteins cannot be evaluated. That method involved binding DNA with attached proteins to a hydroxylapatite matrix, which can also bind proteins. The DNAzol-Strip method described here does not involve adsorption to a solid phase, and the DNAzol-Silica method utilizes a solid phase that does not bind protein significantly.

In summary, we have developed DPC isolation methods that optimize the isolation of proteins covalently crosslinked to DNA in a pure and concentrated sample. The isolation procedures are readily scaleable and economical. DPCs were isolated in sufficient quantities for use with proteomics technology for

protein separation and identification. The next objective was to utilize this technology to identify a larger number of proteins that become covalently crosslinked to DNA following exposure of mammalian cells to γ-radiation. The results of such studies are described in Chapter 3.

References for Chapter 2

[1] S.L. Barker, M. Weinfeld and D. Murray DNA-protein crosslinks: their induction, repair and biological consequences, Mutat Res 589 (2005) 111-135.

[2] A. Izzotti, C. Cartiglia, M. Taningher, S. De Flora and R. Balansky Age-related increases of 8-hydroxy-2'-deoxyguanosine and DNA-protein crosslinks in mouse organs, Mutat. Res. 446 (1999) 215-223.

[3] S. Gebicki and J.M. Gebicki Crosslinking of DNA and proteins induced by protein hydroperoxides, Biochem. J. 338 (1999) 629-636.

[4] R.K. Zahn, G. Zahn-Daimler, S. Ax, M. Hosokawa and T. Takeda Assessment of DNA-protein crosslinks in the course of aging in two mouse strains by use of a modified alkaline filter elution applied to whole tissue samples, Mech. Ageing Dev. 108 (1999) 99-112.

[5] C.A.I. Miller, M.D. Cohen and M. Costa Complexing of actin and other nuclear proteins to DNA by cis-diamminedichloroplatinum(II) and chromium compounds, Carcinogenesis 12 (1991) 269-276.

[6] J.R. Kuykendall and M.S. Bogdanffy Reaction kinetics of DNA-histone crosslinking by vinyl acetate and acetaldehyde, Carcinogenesis 13 (1992) 2095-2100.

[7] J.R. Kuykendall and M.S. Bogdanffy Formation and stability of acetaldehyde-induced crosslinks between poly-lysine and poly-deoxyguanosine, Mutat. Res. 311 (1994) 49-56.

[8] M. Costa, A. Zhitkovich, M. Harris, D. Paustenbach and M. Gargas DNA-protein cross-links produced by various chemicals in cultured human lymphoma cells, J. Toxicol. Environ. Health 50 (1997) 433-449.

[9] V. Voitkun and A. Zhitkovich Analysis of DNA-protein crosslinking activity of malondialdehyde in vitro, Mutat. Res. 424 (1999) 97-106.

[10] S. Toyokuni, T. Mori, H. Hiai and M. Dizdaroglu Treatment of Wistar rats with a renal carcinogen, ferric nitrilotriacetate, causes DNA-protein cross-linking between thymine and tyrosine in their renal chromatin, Int. J. Cancer 62 (1995) 309-313.

[11] A.J. Fornace, Jr. and J.B. Little Malignant transformation by the DNA-protein crosslinking agent trans-Pt(II) diamminedichloride, Carcinogenesis 1 (1980) 989-994.

[12] A.J. Fornace, Jr. Detection of DNA single-strand breaks produced during the repair of damage by DNA-protein cross-linking agents, Cancer Res. 42 (1982) 145-149.

[13] M.O. Bradley, I.C. Hsu and C.C. Harris Relationship between sister chromatid exchange and mutagenicity, toxicity and DNA damage, Nature 282 (1979) 318-320.

[14] M.O. Bradley and K.W. Kohn X-ray induced DNA double strand break production and repair in mammalian cells as measured by neutral filter elution, Nucleic Acids Res 7 (1979) 793-804.

[15] O. Merk and G. Speit Significance of formaldehyde-induced DNA-protein crosslinks for mutagenesis, Environ. Mol. Mutagen. 32 (1998) 260-268.

[16] L.Y. Xue, L.R. Friedman and N.L. Oleinick Repair of chromatin damage in glutathione-depleted V-79 cells: comparison of oxic and hypoxic conditions, Radiat. Res. 116 (1988) 89-99.

[17] S.M. Chiu, N.M. Sokany, L.R. Friedman and N.L. Oleinick Differential processing of ultraviolet or ionizing radiation-induced DNA-protein cross-links in Chinese hamster cells, Int J Radiat Biol Relat Stud Phys Chem Med 46 (1984) 681-690.

[18] A.E. Cress, K.M. Kurath, B. Stea and G.T. Bowden The crosslinking of nuclear protein to DNA using ionizing radiation, J. Cancer Res. Clin. Oncol. 116 (1990) 324-330.

[19] M. Costa, A. Zhitkovich, M. Gargas, D. Paustenbach, B. Finley, J. Kuykendall, R. Billings, T.J. Carlson, K. Wetterhahn, J. Xu, S. Patierno and M. Bogdanffy Interlaboratory validation of a new assay for DNA-protein crosslinks, Mutat. Res. 369 (1996) 13-21.

[20] A. Zhitkovich and M. Costa A simple, sensitive assay to detect DNA-protein crosslinks in intact cells and *in vivo*, Carcinogenesis 13 (1992) 1485-1489.

[21] J.W. Bodnar, C.J. Jones, D.H. Coombs, G.D. Pearson and D.C. Ward Proteins tightly bound to HeLa cell DNA at nuclear matrix attachment sites, Mol Cell Biol 3 (1983) 1567-1579.

[22] A. Ferraro, P. Grandi, M. Eufemi, F. Altieri and C. Turano Crosslinking of nuclear proteins to DNA by cis-diamminedichloroplatinum in intact cells. Involvement of nuclear matrix proteins, FEBS Lett 307 (1992) 383-385.

[23] S.K. Samuel, V.A. Spencer, L. Bajno, J.M. Sun, L.T. Holth, S. Oesterreich and J.R. Davie In situ cross-linking by cisplatin of nuclear matrix-bound transcription factors to nuclear DNA of human breast cancer cells, Cancer Res 58 (1998) 3004-3008.

[24] V.A. Spencer, S.K. Samuel and J.R. Davie Altered profiles in nuclear matrix proteins associated with DNA in situ during progression of breast cancer cells, Cancer Res 61 (2001) 1362-1366.

[25] R.E. Meyn, S.C. vanAnkeren and W.T. Jenkins The induction of DNA-protein crosslinks in hypoxic cells and their possible contribution to cell lethality, Radiat. Res. 109 (1987) 419-429.

[26] D. Murray, A. Macann, J. Hanson and E. Rosenberg ERCC1/ERCC4 5'-endonuclease activity as a determinant of hypoxic cell radiosensitivity, Int. J. Radiat. Biol. 69 (1996) 319-327.

[27] D. Murray and E. Rosenberg The importance of the ERCC1/ERCC4[XPF] complex for hypoxic-cell radioresistance does not appear to derive from its participation in the nucleotide excision repair pathway, Mutat. Res. 364 (1996) 217-226.

[28] D. Murray, L. Vallee-Lucic, E. Rosenberg and B. Andersson Sensitivity of nucleotide excision repair-deficient human cells to ionizing radiation and cyclophosphamide, Anticancer Res. 22 (2002) 21-26.

[29] M.S. Elphinstone, G.N. Hinten, M.J. Anderson and C.J. Nock An inexpensive and high-throughput procedure to extract and purify total genomic DNA for population studies, Mol Ecol Notes 3 (2003) 317-320.

[30] K.W. Kohn Methods in Cancer Research, Academic Press, New York, 1967.

[31] K.W. Kohn DNA Repair: A Laboratory Manual of Research Procedures, M. Dekker, New York, 1981.

[32] D. Murray, S.C. vanAnkeren and R.E. Meyn Applicability of the alkaline elution procedure as modified for the measurement of DNA damage and its repair in nonradioactively labeled cells, Anal Biochem 160 (1987) 149-159.

[33] A. Matsumoto and P.C. Hanawalt Histone H3 and heat shock protein GRP78 are selectively cross-linked to DNA by photoactivated Gilvocarcin V in human fibroblasts, Cancer Res. 60 (2000) 3921-3926.

[34] Y.H. Hsiang, R. Hertzberg, S. Hecht and L.F. Liu Camptothecin induces protein-linked DNA breaks via mammalian DNA topoisomerase I, J Biol Chem 260 (1985) 14873-14878.

[35] Q. Fu, S.W. Kim, H.X. Chen, S. Grill and Y.C. Cheng Degradation of topoisomerase I induced by topoisomerase I inhibitors is dependent on inhibitor structure but independent of cell death, Mol Pharmacol 55 (1999) 677-683.

[36] G. Weeda, I. Donker, J. de Wit, H. Morreau, R. Janssens, C.J. Vissers, A. Nigg, H. van Steeg, D. Bootsma and J.H. Hoeijmakers Disruption of mouse ERCC1 results in a novel repair syndrome with growth failure, nuclear abnormalities and senescence, Curr Biol 7 (1997) 427-439.

[37] R. Olinski, Z. Nackerdien and M. Dizdaroglu DNA-protein cross-linking between thymine and tyrosine in chromatin of gamma-irradiated or H_2O_2-treated cultured human cells, Arch. Biochem. Biophys. 297 (1992) 139-143.

[38] D.R. Beidler and Y.C. Cheng Camptothecin induction of a time- and concentration-dependent decrease of topoisomerase I and its implication in camptothecin activity, Mol Pharmacol 47 (1995) 907-914.

[39] I. Al-Nabulsi and K.T. Wheeler Temperature dependence of radiation-induced DNA-protein crosslinks formed under hypoxic conditions, Radiat. Res. 148 (1997) 568-574.

Chapter 3: The identification of mammalian proteins crosslinked to DNA by γ-radiation

A version of this paper has been accepted for publication:

Barker, S.L., Weinfeld, M., Zheng, J., Li, L., and Murray, D. The identification of mammalian proteins crosslinked to DNA by ionizing radiation. Journal of Biological Chemistry. 2005.

3.1. Introduction

DPCs can be induced by a variety of agents, including UV light and IR, metals and semimetals such as chromium, nickel, and arsenic, various aldehydes including metabolic by-products, and some important chemotherapeutic drugs such as cisplatin, melphalan, and mitomycin C [1]. Measurements of the amount of DNA damage induced by IR indicate that, in a mammalian cell, a 1-Gy exposure induces 1,000-2,000 damaged bases, 800-1,600 damaged sugars, 500-1,000 SSBs, 200-300 alkali-labile sites, 20-40 DSBs, ~30 ICLs, and ~150 DPCs [2-4]. Studies of DPCs induced by various agents have shown half lives of hours to days [5,6]. This removal is a reflection of both chemical instability and enzymatic repair processes.

Early studies of the DNA-damaging effects of high/supralethal doses of IR [7-10] demonstrated the induction of DPCs by this agent in aerated mammalian cells. IR has also been shown to induce DPCs in hypoxic mammalian cells and to do so more efficiently (1.5-5.5 fold) than in aerated cells [8,10-13]. In addition, cells that are deficient in some DNA repair factors related to crosslink removal show an increased sensitivity to the cytotoxic effects of IR under hypoxic, but not aerated, conditions [14]. An interesting implication of these observations is that abrogating the repair of DPCs might be clinically advantageous in radiation therapy because this could render hypoxic tumor cells more radiosensitive [15,16]. However, there are many questions to answer before such a therapeutic strategy might be realized. For example, how are DPCs repaired? How does the presence of a DPC activate a particular repair pathway; is there a specific damage-recognition event, and is it protein specific, or is it a general mechanism,

such as blockage of the progression of protein complexes that mediate various DNA transactions? What are the biological consequences of unrepaired DPCs? Identifying the actual proteins involved in these DPCs may help to answer these questions. As well, high doses (typically >30 Gy) have been used in previous studies to measure DPCs. The effect of oxygen on DPC induction at low, clinically relevant, doses has not yet been examined.

To date, various methods (nitrocellulose filter binding, polycarbonate filter trapping, SDS/K^+ precipitation, and others (reviewed in [1]) have been used to quantitate and/or isolate IR-induced DPCs with varying levels of success. Trying to purify DPCs by any method that isolates all cellular proteins is clearly going to be non-informative for protein identification, whereas an approach that isolates DPCs by first isolating the DNA should be useful in combination with protein-identification methods such as MS. Although MS is a sensitive technique, it is possible that only a small percentage of the ~30,000 proteins in the cell can be significantly crosslinked to DNA, so it is essential to obtain a high yield of these proteins with very little contamination in order to identify them. Accordingly, we developed a novel method for the isolation of proteins covalently crosslinked to DNA that yields a sufficient quantity of protein for MS analysis [17] (see Chapter 2 of this thesis). In this study, we have employed this method to purify γ-radiation-induced DPCs from mammalian cells and have combined this method with MS identification of the isolated proteins. We have also examined the dose dependence of γ-radiation-induced DPCs and confirmed the involvement of some of these proteins in γ-radiation-induced DPCs using immunological techniques.

3.2. Materials and Methods

3.2.a. Cell culture

The parental CHO cell line, AA8, was obtained from Dr. Keith Caldecott (University of Sussex, UK) and maintained as a monolayer culture in αDMEM-F12 medium with 10% fetal bovine serum and 5% penicillin/streptomycin in a humidified 5% CO_2 and 95% air atmosphere at 37°C. The human fibroblast cell line, GM00637, was obtained from American Type Culture Collection (Manassas, VA) and maintained as a monolayer culture in αDMEM-F12 medium with 10% serum and 5% penicillin/streptomycin as above.

3.2.b. Radiation and chemical treatments of cells

Cells were grown as monolayer cultures to ~85% confluency. Aerated cells were irradiated in 150-mm plastic dishes. To render cells hypoxic [18], the cultures were washed with PBS and trypsinized. Fresh medium was added to a final volume of 5 ml per 2.4 $x10^7$ cells and the cells were transferred to 60-mm glass Petri dishes. The dishes were placed in air-tight aluminium chambers and the chambers were evacuated using a vacuum manifold. The chambers were then filled with pure nitrogen gas and the cells were incubated at room temperature in nitrogen for 8 sec, with the process being repeated four times. This process was repeated another four times using 8-min incubations, and the cells were then incubated at 37°C for 20 min to allow them to metabolize residual oxygen (adapted from [18]).

For γ-radiation treatments, cells were irradiated in a ^{60}Co irradiator (Gammacell) at a dose rate of 0.1 Gy/sec. For formaldehyde treatment, 37% formaldehyde was added to the growth medium to a final concentration of 1% and the sample was incubated at 37°C for 1 h.

3.2.c. Quantitation of DNA

The UV absorbance at 260 nm was measured for each sample to determine the DNA concentration after DNA digestion, as described in Chapter 2, section 2.2.i. The relative amounts of DNA were determined within each experiment and were used to determine sample loads for SDS-PAGE analysis.

3.2.d. Nuclei isolation

Nuclei isolation was performed as described in Chapter 2, section 2.2.g.

3.2.e. Nuclear extract preparation

Nuclear extracts were prepared as described in Chapter 2, section 2.2.h.

3.2.f. DNAzol-Strip DPC isolation method

We followed the protocol of Barker *et al.* [17] as described in Chapter 2, section 2.2.d.

3.2.g. DNAzol-Silica DPC isolation method

Again, we followed the method of Barker *et al.* [17] as described in Chapter 2, section 2.2.e. The method of Elphinstone *et al.* [19] was used to prepare the silica fines (VWR, Mississauga, Ontario).

3.2.h. SDS-PAGE analysis

Laemmli buffer (BioRad) was added to each sample in amounts determined to equalize the DNA concentration of each sample. Samples were analyzed by 1-D SDS-PAGE using 15% separating gels (for MS analysis) or pre-cast 10-20% gradient gels (BioRad) in later experiments. In separate experiments, gels were stained using either ammoniacal-silver nitrate or SYPRO Tangerine (Invitrogen).

3.2.i. Quantitation of protein on SDS-PAGE gels

SYPRO Tangerine-stained 1-D SDS-PAGE gels were scanned using a Typhoon 7400 imager (GE Healthcare). These images were analyzed using the ImageQuant 5.2 software (GE Healthcare) by measuring fluorescence signal. Known quantities of broad-range marker proteins (Biorad) were run on each gel and stained with SYPRO-Tangerine. Representative background regions were subtracted for each band and marker bands were quantified. Quantitation was based on comparison to the fluorescence signal in the marker protein bands after subtraction of representative background regions. Linear regression analysis

was performed using the Prism software and ANOVA single factor analyses were performed using Microsoft Excel.

3.2.j. Protein identification by Mass Spectrometry

Protein bands excised from silver-stained SDS-PAGE gels were reduced with DTT, carbamidomethylated using iodoacetamide, and digested in-gel with trypsin. The resulting peptides were analyzed on a Bruker REFLEX III time of flight mass spectrometer (Bremen/Leipzig, Germany, Serial #FM 2413) and the obtained peptide mass maps were searched against databases to identify proteins (peptide mass mapping). Furthermore, selected peptides were fragmented on a PE Sciex API-QSTAR Pulsar mass spectrometer (MDS-Sciex, Toronto, Ontario, Canada, Serial #K0940105) to acquire MS/MS spectra, which contain sequence-specific information, and were then subjected to database searching (MS/MS ion search) to either confirm the previously-acquired results from the peptide mass mapping or to identify proteins if no positive results were obtained by peptide mapping.

The MASCOT search engine (http://www.matrixscience.com/search_form_select.html) was used for both peptide mass mapping and MS/MS ion searching. Database search criteria are listed below. Two of the most up-to-date and complete proteome databases, SwissProt and NCBInr, were selected in our database search. Mass tolerance was set according to instrument mass accuracy. For peptide mass mapping, the peptide mass tolerance was set at 100 ppm. For MS/MS ion searching, the mass tolerance was set at 0.3 Da for both the parent ion and fragment ions.

Carbamidomethylation of cysteine was set as a fixed modification while methionine oxidation was set as a variable modification.

3.2.k. Western blots

Crosslinked proteins isolated by the DNAzol-Silica method were resuspended in Laemmli Buffer, equalized for total amounts of DNA, separated on 10-20% gradient gels and stained with SYPRO Tangerine protein stain. Gels were visualized by scanning with the Typhoon 7400 instrument. Gels were then de-stained briefly in 10% methanol and transferred to nitrocellulose membranes (Biorad) for 1.5 h at 4°C and 80 V. Blots were blocked in 5% milk-Tris buffered saline with 0.5% Tween (TBST) for 1 h at room temperature with gentle agitation. After overnight incubation (4°C) with primary antibody, the blots were washed 4 times (15 min per wash) in 10 mL of 5% milk-TBST at room temperature. Secondary antibodies were incubated with the blots for 1 h at room temperature with gentle agitation. After the secondary antibody incubation, the blots were washed again as above, with a final wash in PBS. Blots were developed using chemiluminescent reagents by mixing equal portions of the two reagents and incubating each blot with 1 mL of prepared reagent for 5 min at room temperature. Signals were captured using X-OMAT K film (Kodak). The films were scanned as image files and the optical densities (ODs) of the bands in these image files were quantified using the ImageJ software/shareware available from the NIH (www.ncbi.nlm.nih.gov). Alternatively, fluorescent secondary antibodies were used and the blots were analyzed using a LI-COR Odyssey infra-red imager and the ImageJ software to quantitate the band ODs. The

average relative band intensities were plotted after normalizing the most intense signal of the irradiated samples within each determination as 100%.

3.2.I. Antibodies

Primary polyclonal antibodies to mammalian vimentin, histone H2B, histone H4, actin, cofilin, hnRNP, poly-ADP ribose polymerase (PARP), and HSP10 were obtained from Santa Cruz Biotechnology (Santa Cruz, CA). Primary monoclonal antibody to tubulin was also obtained from Santa Cruz. Primary monoclonal antibody to mammalian (mouse) ninein was generously provided by Dr. Gordon Chan, (Department of Oncology, University of Alberta). Polyclonal anti-polynucleotide kinase (PNK) antibody has been previously described [20]. Primary antibodies to hnRNP A3 and C1/C2 were generously provided by Dr. Gideon Dreyfuss, (University of Pennsylvania School of Medicine). Secondary antibodies, peroxidase conjugated rabbit anti-goat and goat anti-rabbit, were also obtained from Santa Cruz. Primary antibodies were used at dilutions of 1:1,000 in 5% milk-TBST in a total volume of 3 mL. Fluorescently-tagged secondary antibodies, goat anti-rabbit IR800, rabbit anti-goat 700, were obtained from Rockland Immunologicals (Gilbertsville, PA) and used at a dilution of 1:5,000 in 5% milk-TBST in a total volume of 5 mL.

3.3. Results

3.3.a. Isolation and PAGE analysis of γ-radiation-induced DPCs in hamster and human cells

CHO AA8 cells were exposed to 0 or 1 Gy of γ-radiation under either aerated or hypoxic conditions, and DPCs were isolated using the DNAzol-Strip method. Sample volumes were normalized for the amount of DNA isolated, and crosslinked proteins were analyzed by SDS-PAGE and silver staining. Figure 3-1 shows a representative composite gel from these analyses. In the unirradiated sample (Figure 3-1; aerated 0 Gy) very little protein was detected, confirming that this method successfully strips the DNA of associated proteins and that we are in fact isolating predominantly covalently-crosslinked proteins following γ-radiation exposure. This level of isolated protein can be compared with that isolated from irradiated cells (Figure 3-1; aerated 1 Gy) or from formaldehyde-treated cells (Figure 3-1; F) where each lane contains a greater number and intensity of bands than the control.

Figure 3-1 shows similar data for hypoxic cells. Compared with aerated cells, more protein was isolated from the hypoxic untreated sample (Figure 3-1; hypoxic 0 Gy), indicating that removal of oxygen leads to modestly increased background DPC induction, although the level of protein was still quite low. Several protein bands observed in the hypoxic-irradiated samples were not detected or were less intense in the aerated-irradiated samples (Figure 3-1; hypoxic 1 Gy).

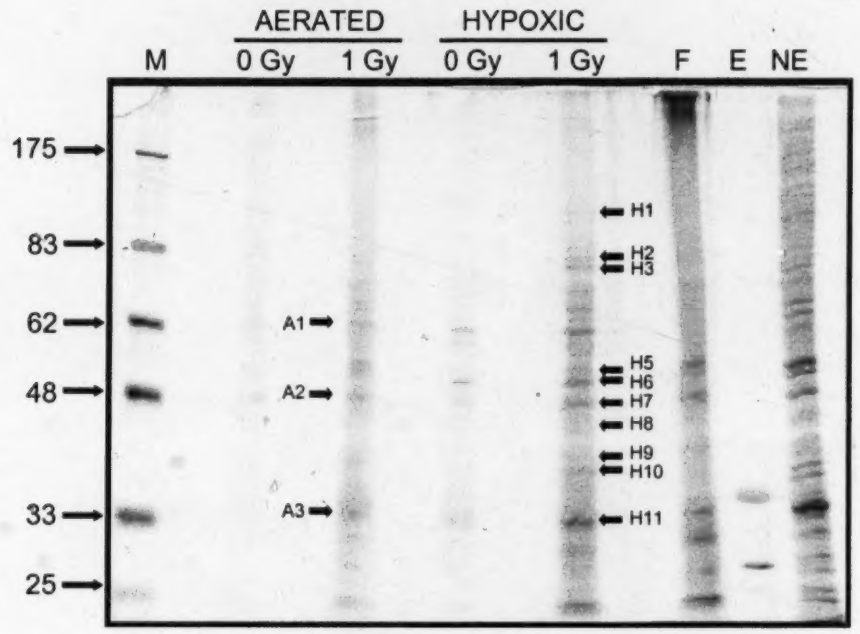

Figure 3-1: Analysis of DPCs from hamster cells

DPCs were isolated from CHO AA8 cells using the DNAzol-Strip method (see Chapter 2, section 2.2.d) and analyzed by SDS-PAGE and silver staining. The cells received 0 or 1 Gy of γ-radiation, or 1% formaldehyde "F" for 1 h at 37°C, under either aerated or hypoxic conditions. The "NE" lane is a total AA8 nuclear extract and lane "E" shows the nucleases used for digestion. The black arrows with sample numbers (A1-3 and H1-11) indicate some of the bands from which proteins were extracted and identified by MS (Table 3-1). The "M" lane is MW markers with the MW indicated in kDa.

The γ-radiation-induced crosslinking of proteins to DNA was also examined in human GM00637 fibroblasts (Figure 3-2). Cells received 0 or 4 Gy of γ-radiation under either aerated or hypoxic conditions and DPCs were isolated using the DNAzol-Strip method. Again, analysis of isolated proteins by SDS-PAGE and silver staining (a representative composite gel is shown in Figure 3-2) revealed that little protein was isolated from the unirradiated control samples and that a greater number and intensity of bands were observed in the irradiated samples.

3.3.b. Identification of proteins involved in γ-radiation-induced DPCs in hamster cells

To identify crosslinked proteins, protein bands were excised from several gels. Some of the sample bands that were excised for MS analysis are indicated in Figure 3-1 (A1-3 and H1-11). Although similar patterns of bands were seen in each experiment, band selection for MS analysis was based on the intensity and sharpness of band staining in an individual gel. The more intensely and sharply stained bands were chosen as they were more likely to yield a positive identification in MS analysis.

As described in Materials and Methods (section 3.2.j), the search engine, Mascot, was used for protein identification by searching MS data against primary sequence databases. Mascot uses a statistical scoring algorithm, mowse score, to calculate the matching scores that represent the identification significance. According to its calculation, significance thresholds vary between peptides in the

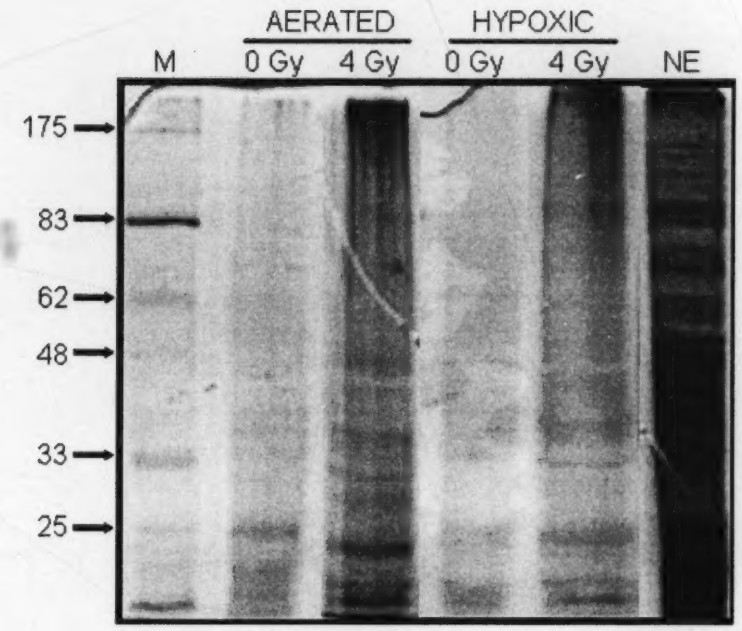

Figure 3-2: Analysis of DPCs from human cells

DPCs were isolated from GM00637 cells using the DNAzol-Strip method and analyzed by SDS-PAGE and silver staining. The cells received 0 or 4 Gy of γ-radiation under either aerated or hypoxic conditions. The "NE" lane is a total nuclear extract. The "M" lane is MW markers with the MW indicated in kDa.

search. Therefore, in our results both mowse scores and significance thresholds are considered. MS/MS spectra were also manually inspected to ensure that the identifications were reasonable and confident. In some cases, a single peptide's score may be low (lower than the threshold), but correlation with other identified peptides from the same protein and peptide mass mapping results increased the confidence of the protein identification. If the Mascot MS/MS ion search did not yield positive results (due to internal or side chain fragmentation that Mascot does not account for), a potential peptide match was submitted to the MS-product (http://prospector.ucsf.edu/) program and the theoretical fragments of the peptide were compared with those shown in the MS/MS spectrum.

To date, we have identified 29 proteins involved in γ-radiation-induced DPCs (Table 3-1). Table 3-1 shows the protein identification results: identified proteins, sequences of peptides selected for MS/MS experiments, peptide masses, Mascot scores for MS/MS ion searches, and the corresponding significance thresholds. Some of the identified proteins were from bands excised from the gel shown in Figure 3-1. Tubulin α-6 chain was identified by peptide mass mapping and confirmed by manually matching the MS/MS spectrum with the theoretical fragments. Ninein was identified by peptide mass mapping only because of the unavailability of MS/MS instrumentation at that time.

The proteins identified include: structural nuclear-matrix proteins, such as actin and vimentin; spliceosome components, such as heterogeneous nuclear ribonuclear proteins (hnRNPs) and the polypyrimidine tract binding protein associated splicing factor (PSF); stress-response proteins, such as heat-shock proteins HSP10 and the 78 kDa glucose-regulated protein (GRP78); and

Table 3-1: Proteins identified in γ-radiation-induced DNA-protein crosslinks

Protein	Peptides subjected to MS/MS	Peptide mass	Mascot score	Significance threshold	Aerated*	Hypoxic*	Fig.1
Architectural/ Structural and associated proteins							
††Actin, beta	IIAPPERK	923.50	35	27	5	3	H7, H8
	AGFAGDDAPR	976.45	25	24			
	VAPEEHPVLLTEA PLNPK	1954.07	50	12			
	GYSFTTTAER	1132.53	47	15			
	QEYDESGPSIVHR	1516.71	62	21			
	DSYVGDEAQSKR	1354.63	26	15			
	SYELPDGQVITIG NER	1790.89	24	12			
	IWHHTFYNELR	1515.75	16	10			
	AVFPSIVGR	945.50	35	27			
	QEYDESGPSIVHR +Pyro-glu (N-term Q)	1499.68	53	15			
Cofilin	EDLVFIFWAPESA PLK	1861.98	28	55	1	1	
	KEDLVFIFWAPES APLK	1990.00	20	14			
†Vimentin	VELQELNDR	1115.57	17	24	2	3	A1, H5
	MALDIEIATYR	1295.67	39	15			

Protein	Peptides subjected to MS/MS	Peptide mass	Mascot score	Significance threshold	Aerated*	Hypoxic*	Fig.1
	EEAESTLQSFR	1296.61	26	19			
	SLYSSSPGGAYVTR	1444.71	47	20			
	LGDLYEEEMR	1254.57	12	18			
	QVQSLTCEVDALKGTNESLER	2377.17	23	14			
	ISLPLPNFSSLNLR	1570.90	42	24			
Tropomyosin, alpha 3 chain and alpha 4 chain	KYEEVAR	894.46	37	30	2	1	A3, H11
	KIQVLQQQADDAEER	1770.90	50	22			
	IQVLQQQADDAEER	1642.81	17	15			
	IQLVEEELDR	1243.66	37	25			
	AGLNSLEAVKR	1199.68	28	21			
Tubulin, alpha-6 chain	EDAANNYARGHYTIGK	1780.01	manually matched			1	
Radixin	IQNWHEEHR	1248.59	15	13		1	H2
	EIHKPGYLANDR	1412.73	7	17			
Ninein	Identified by peptide mass mapping only					1	
Cell cycle proteins/ Chromatin regulators							
Histone H1	KASGPPVSELITK	1326.77	8	15		1	

Protein	Peptides subjected to MS/MS	Peptide mass	Mascot score	Significance threshold	Aerated*	Hypoxic*	Fig.1
	ALAAAGYDVEKN NSR	1578.79	19	28			
††Histone H2A	VTIAQGGVLPNIQ AVLLPK	1931.17	18	14		1	
††Histone H2B	AMGIMNSFVNDIF ER	1743.82	38	16	1	3	
	AMGIMNSFVNDIF ER 2Oxidation(M)	1775.81	23	16			
	STITSREIQTAVR	1461.80	34	61			
††Histone H3	KLPFQR	788.48	22	31		3	
	STELLIR	831.50	46	31			
	YQKSTELLIR	1250.71	43	21			
	EIAQDFKTDLR	1335.69	159	55			
	YRPGTVALR	1032.60	5	16			
	KPHRYRPGTVAL R	1550.91	188	55			
††Histone H4	VFLENVIR	989.58	39	30		3	
	ISGLIYEETR	1180.62	33	28			
	DNIQGITKPAIR	1325.76	30	22			
CGI-55 protein	AKVEFNIR	976.56	23	28		1	H5
	RFEKPLEEK	1175.64	26	25			

Protein	Peptides subjected to MS/MS	Peptide mass	Mascot score	Significance threshold	Aerated*	Hypoxic*	Fig.1
	RPDQQLQGEGK	1255.64	40	23			
Nuclease sensitive element binding protein 1	RPENPKPQDGK	1265.66	62	29		1	H6
	RRPENPKPQDGK	1421.76	10	13			
	NEGSESAPEGQAQQR	1587.70	46	29			
PTBP-associated splicing factor (PSF)	FGQGGAGPVGGQGPR	1341.67	53	31		1	H1
	FAQHGTFEYEYSQR	1762.78	20	16			
	GIVEFASKPAAR	1245.70	18	22			
Cellular homeostasis							
Calumenin (Crocalbin)	EQFVEFR	954.47	49	38		1	H6
	TFDQLTPEESKER	1579.76	36	18			
Serotransferrin precursor	TYDSYLGDDYVR	1466.65	6	13	1		
thioredoxin peroxidase II	ATAVMPDGQFR	1192.58	27	14	1		A5
Alpha-2-macroglobulin receptor-associated protein	LAELHSDLK	1025.57	21	25		1	H8
	LVHNLNVILAR	1261.78	20	16			
Glyceraldehyde-3-phosphate dehydrogenase (GAPDH)	GALQNIIPASTGAAK	1411.78	15	27		2	H10
	VPTANVSVVDLTCR	1530.80	17	30			

Protein	Peptides subjected to MS/MS	Peptide mass	Mascot score	Significance threshold	Aerated*	Hypoxic*	Fig.1
	AITIFQER	977.54	18	24			
	VPTPNVSVVDLTCR	1556.81	63	15			
	LISWYDNEFGYSNR	1763.81	11	14			
GDP/GTP binding proteins							
Rho GDP-dissociation inhibitor 1	IDKTDYMVGSYGPR	1601.77	6	15		1	
	AEEYEFLTPMEEAPK	1783.81	10	10			
Stress Response							
†78 kDa glucose-regulated protein (GRP78)	IEIESFFEGEDFSETLTR	2149.00	31	14		2	H3
	KSDIDEIVLVGGSTR	1588.86	78	24			
	DNHLLGTFDLTGIPPAPR	1933.02	19	14			
	SDIDEIVLVGGSTR	1460.76	39	21			
	ITPSYVAFTPEGER	1566.78	19	17			
10 kDa heat shock protein	FLPLFDR	907.51	37	25	1	1	
	VVLDDKDYFLFR	1529.80	33	21			
Transcription regulators/ RNA splicing components							
Heterogeneous nuclear ribonucleo-protein A1	SSGPYGGGGQYFAKPR	1628.78	25	17		1	

Protein	Peptides subjected to MS/MS	Peptide mass	Mascot score	Significance threshold	Aerated*	Hypoxic*	Fig.1
	KLFIGGLSFETTDESLR	1913.00	10	13			
Heterogeneous nuclear ribonucleo-protein (hnRNP) A2/B1	EVYQQQQYGSGGR	1499.69	17	15		2	H9
	KLFIGGLTFETTDESLR	1927.02	5	14			
similar to Heterogeneous nuclear ribonucleo-protein (hnRNP) A3	IFVGGIKEDTEEYNLR	1882.96	32	24	1	1	
40S ribosomal protein S24/SA	TTPDVIFVFGFR	1398.74	25	14		2	H9
	FAAATGATPIAGR	1203.65	29	19			
Elongation factor 1-alpha 1	IGGIGTVPVGR	1025.61	48	28	1	1	H6
	YYVTIIDAPGHR	1404.73	25	16			
TLS-associated protein,TASR-2	GFAYVQFEDVR	1330.65	13	26	1	1	
	YGPIVDVYVPLDFYTR	1916.98	25	27			

†These proteins have been found to be crosslinked to DNA by other agents (††by IR) [21-26].

*The DPC isolation and protein identification experiments were carried out seven times. The same set of bands was NOT excised in each experiment. This number represents the number of times that this protein was identified in the seven sets of intensely stained bands that were selected for MS analysis.

Note: most peptides were detected in multiple experiments and modified peptides were also detected (oxidized, acetylated, etc). The mascot score indicates how likely it is that the observed masses were generated from the suggested sequences in the database search. Generally, higher the score, the better the match. The significance threshold is an indication of the identification confidence level; it depends on the database, species, mass tolerance and other parameters used for the database search. In our research, protein identifications with mascot scores greater than the significance threshold are considered a confident match (see section 3.3.b.).

chromatin-regulatory proteins, such as histones. Some of the proteins identified may be crosslinked to DNA specifically under hypoxic conditions, for example, hnRNP A2/B1, histones H3 and H4, and GRP78.

3.3.c. Confirmation of individual proteins involved in DPCs by Western blot analysis

Confirmation and relative quantitation of selected individual proteins identified by the MS analyses was performed by Western blotting of DPC samples from both hamster AA8 and human GM00637 cells. DPC samples, prepared as above, were transferred to nitrocellulose membranes. Samples from hamster cells were probed with antibodies to histone H2B (Figure 3-3A) or vimentin (data not shown), and human samples were probed with antibodies to actin (Figure 3-3B), or tubulin (Figure 3-3C), or ninein (data not shown). The Western blotting results confirmed the involvement of each of these proteins in γ-radiation-induced crosslinks. Based on the relative quantitation from data pooled from multiple independent experiments, the crosslinking of actin and histone H2B increased following γ-irradiation under hypoxic conditions but was not ignificantly increased over background levels under aerated conditions. The opposite was true for the crosslinking of tubulin, which showed an increase in crosslinking following γ-irradiation under aerated conditions, but no significant increase over background after γ-irradiation under hypoxic conditions. As well, actin, histone

H2B, and tubulin were each shown to crosslink to DNA when cells were treated with formaldehyde, which is a well-known DPC inducer. Proteins identified to be involved in γ-radiation-induced crosslinks by MS but that were

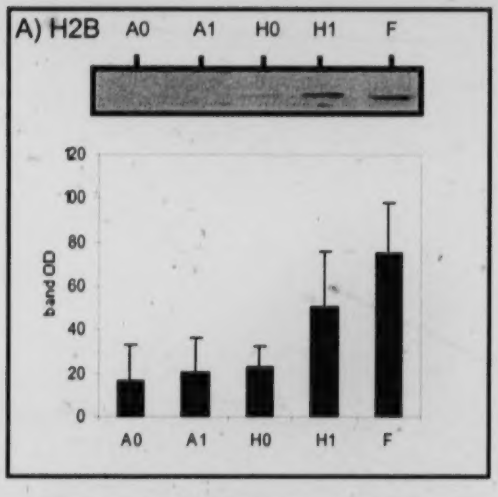

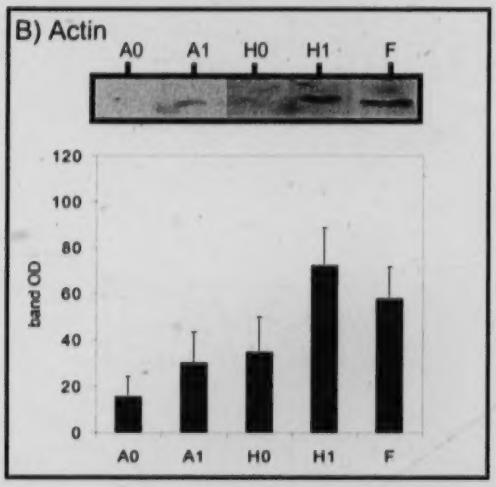

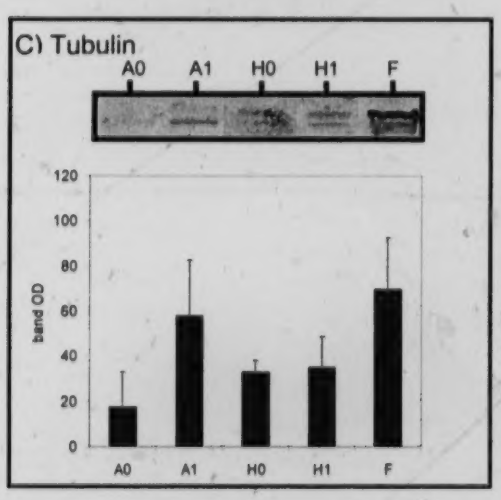

Figure 3-3: Confirmation and quantitation of individual proteins in γ-radiation-induced DPCs

Western blot analysis and quantitation of (A) histone H2B, (B) actin, and (C) tubulin in γ-irradiation-induced DPCs hamster (A) and human cells (B-C). Samples are labeled to indicate 0 Gy or 1 Gy γ-radiation under aerated "A0 and A1" or hypoxic "H0 or H1" or formaldedhyde "F" treatment. Quantitations were performed on pooled data from independent experiments as described in Materials and Methods (section 3.2.k).

negative on all Western blots attempted (n = 9) were the hnRNP A/B proteins; this may be due to antibody quality or masked/destroyed epitopes, although most of the proteins examined in our analyses showed no size reductions/proteolysis (i.e., they migrated at the expected sizes).

3.3.d. Identification of additional novel proteins involved in DPCs by Western blot analysis

Our list of proteins involved in γ-radiation-induced DPCs is not exhaustive, and no doubt further MS analyses would lead to the identification of additional proteins. Because our MS data indicated the involvement of hnRNP A2/B1 and A3 in γ-radiation-induced DPCs, we probed for the related proteins hnRNP C1/C2 (Figure 3-4A). Western blotting demonstrated the involvement of these splicing components in γ-radiation-induced DPCs as the level of protein crosslinked to DNA increased after γ-irradiation under both aerated and hypoxic conditions.

Given that any proteins that are frequently in contact with the DNA, such as DNA repair proteins, are potential targets for crosslinkage by IR, we investigated the involvement of several additional proteins in γ-radiation-induced DPCs by Western blotting. Both PARP (Figure 3-4B) and PNK (Figure 3-4C) were found to be involved in γ-radiation-induced DPCs in human cells. Based on relative quantitation from data from multiple independent analyses, PARP and PNK each demonstrated an increased crosslinking to DNA after γ-irradiation under hypoxic conditions. PARP demonstrated a more marked increase in crosslinking after γ-irradiation under aerated conditions, while PNK showed a

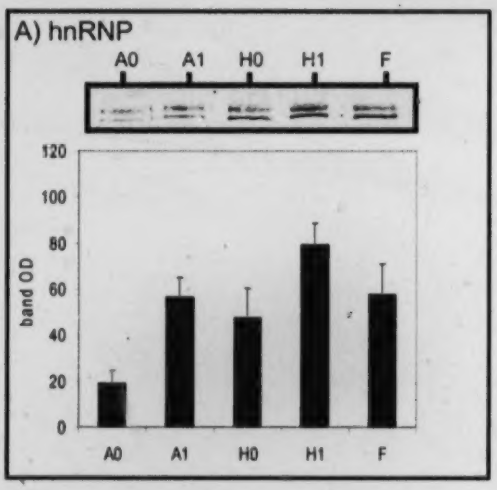

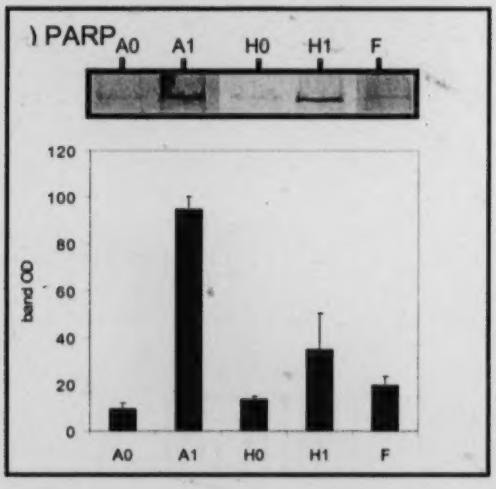

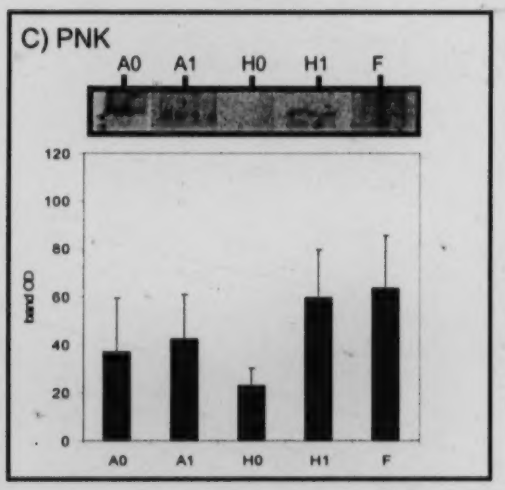

Figure 3-4: Identification and quantitation of additional proteins in γ-radiation-induced DPCs

Western blot analysis and quantitation of A) hnRNP C1/C2, B) PARP, and C) PNK in γ-irradiation-induced DPCs in hamster (A-B) and human cells (C). Samples are labeled to indicate 0 Gy or 1 Gy γ-radiation under aerated "A0 and A1" or hypoxic "H0 or H1" or formaldedhyde "F" treatment. Quantitations were performed on pooled data from independent experiments as described in Materials and Methods (section 3.2.k).

background level of DPC induction under aerated conditions.

The PNK and hnRNP C1/C2 proteins also showed increased crosslinking after treatment of cells with formaldehyde, but PARP showed only a slight increase above background.

3.2.e. Quantitation of γ-radiation-induced DPCs in mammalian cells

As shown above, Western blotting allowed for the relative quantitation of crosslinking of individual proteins to DNA. The next step was to examine the dose dependence of total DPC induction by γ-radiation. The DNAzol-Strip method is useful for isolating high yields of crosslinked proteins (which is important for MS), but previous work with topoisomerase poison-induced DPCs [17] (see Chapter 2, section 2.3-f of this thesis) indicated that the lengthy processing time and conditions may result in the loss of some DPCs. For quantitation work, we switched to the DNAzol-Silica method as it is more rapid, thus reducing the opportunity for DPC reversal or degradation. We also switched from silver staining (Figures 3-1 and 3-2) to SYPRO Tangerine staining (Figures 3-5 to 3-8) because the latter method has a lower detection limit, low protein-to-protein staining variability and is quantitative, whereas silver staining is not. Figures 3-5A and B show typical SYPRO Tangerine-stained SDS-PAGE analyses of crosslinked proteins from aerated (3-5A) and hypoxic (3-5B) CHO AA8 cells exposed to increasing doses (0-4 Gy) of γ-radiation. Again, the stringency of the removal of non-crosslinked proteins was confirmed by examining the lane for the unirradiated aerated cell sample, which contained little

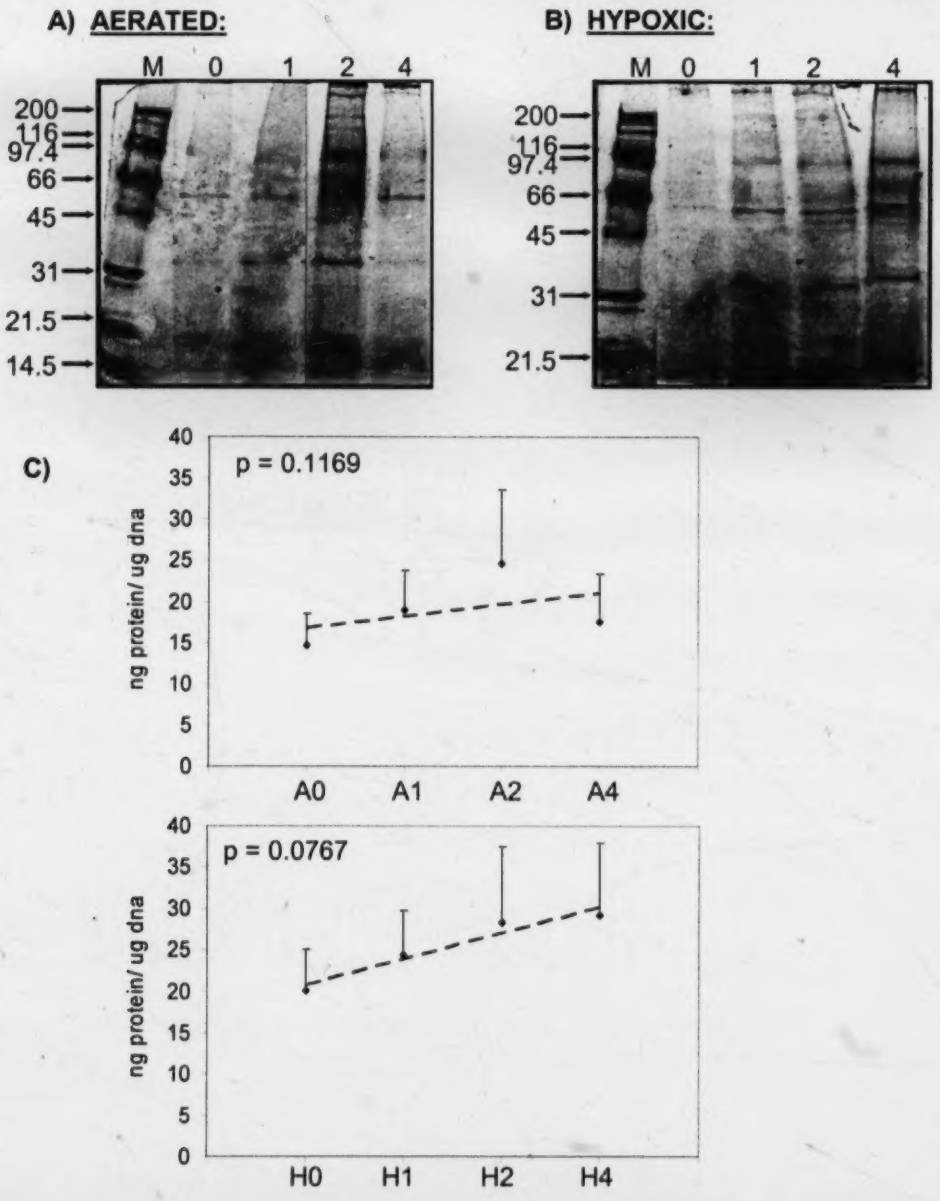

Figure 3-5: Quantitation of DPCs from hamster cells, 0-4 Gy

CHO AA8 cells received 0, 1, 2, or 4 Gy of γ-radiation under either aerated (panel A) or hypoxic (panel B) conditions. DPCs were isolated using the DNAzol-Silica method and analyzed by SDS-PAGE and SYPRO Tangerine staining. The dose in Gy is indicated above each lane. C) Plot of total protein isolated per μg of DNA for each sample. Means, standard error and linear regression analysis were performed on data accumulated from 7 independent experiments.

protein. The extent of crosslinking was quantified for the total protein for each sample (Figure 3-5C) using known quantities of the size-marker proteins for calibration and the ImageQuant 5.2 software on the Typhoon 7400 imager and subtracting a representative background region for each sample. This was performed on 7 independent experiments. Under aerated conditions, there appeared to be a dose-responsive crosslink induction that plateaued at 2 Gy. The dose-response was not the same under hypoxic conditions where the induction of DPCs with increasing doses of γ-radiation approached linearity ($p = 0.077$), but possibly reaching a plateau by the higher doses.

We then analyzed the dose-dependence of γ-radiation-induced crosslinking in these cells in a lower dose range; 0-1.5 Gy (Figure 3-6). Representative gels of isolated DPCs from aerated and hypoxic cells are shown in Figure 3-6A and B, respectively. The statistical analyses were carried out on pooled data ($n = 10$) and demonstrated that there is a linear dose-responsive relationship for DPC-induction in aerated and hypoxic cells below 2 Gy ($p = 0.035$ and 0.048, respectively).

Similar analyses were performed for γ-radiation-induced protein crosslinking to DNA in human cells. Figure 3-7 shows a typical analysis of crosslinked proteins isolated from GM00637 normal human fibroblasts exposed to 0-4 Gy of γ-radiation under aerated (Figure 3-7A) or hypoxic (Figure 3-7B) conditions. Under aerated conditions, the γ-radiation-induced crosslinking of protein to DNA did increase linearly over the 0-4 Gy dose range ($p = 0.042$, $n = 6$), but this linearity was not observed under hypoxic conditions ($p = 0.1$, $n = 6$).

Additional analyses were also performed in human cells using a lower

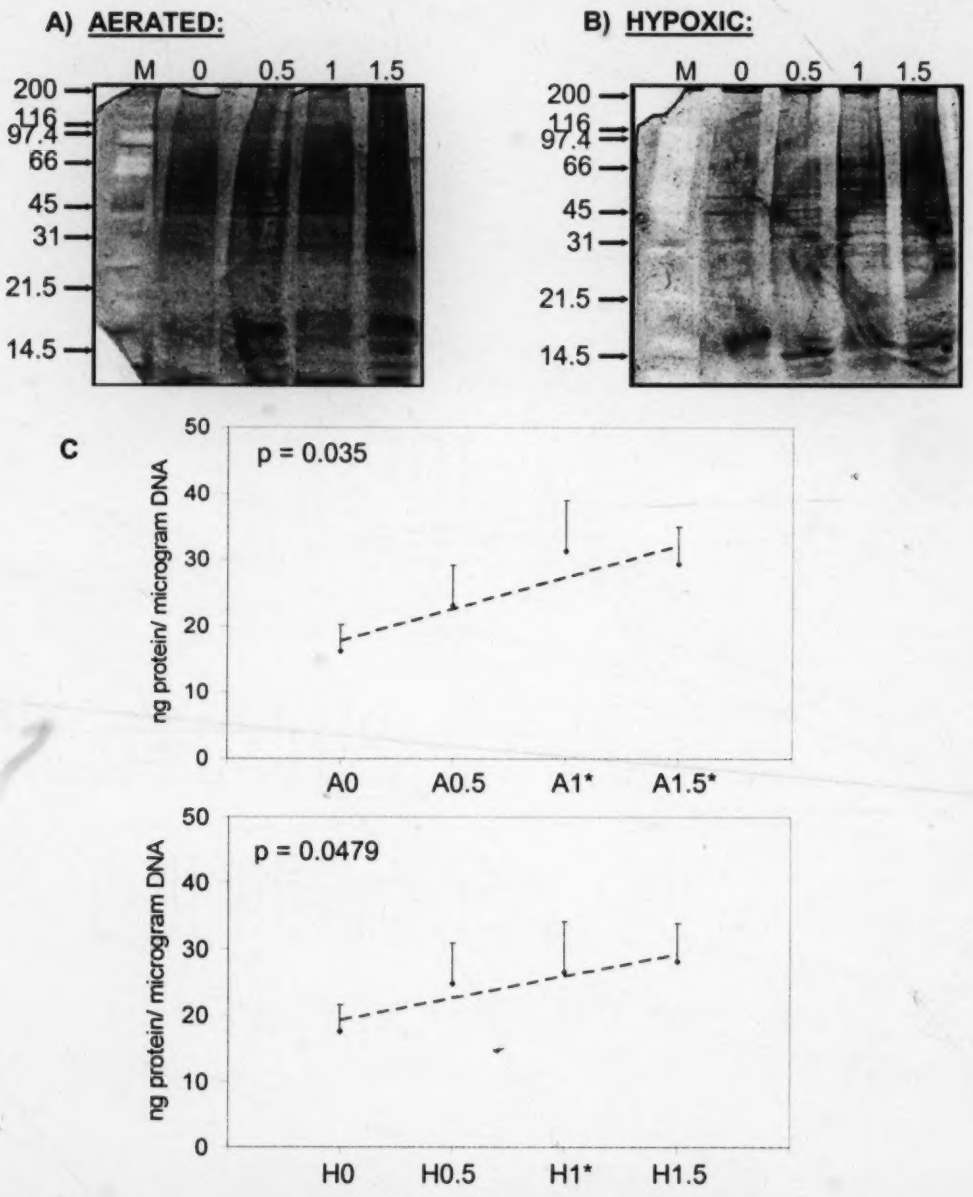

Figure 3-6: Quantitation of DPCs from hamster cells, 0-1.5 Gy

CHO AA8 cells received 0, 0.5, 1.0, or 1.5 Gy of γ-radiation under either aerated (panel A) or hypoxic (panel B) conditions. DPCs were isolated using the DNAzol-Silica method and analyzed by SDS-PAGE and SYPRO Tangerine staining. The dose in Gy is indicated above each lane. (C) Plot of total protein isolated per μg of DNA for each sample. Means, standard error and linear regression analysis were performed on data accumulated from 10 independent experiments. (*) indicates that the data point is significantly different from the 0 Gy sample.

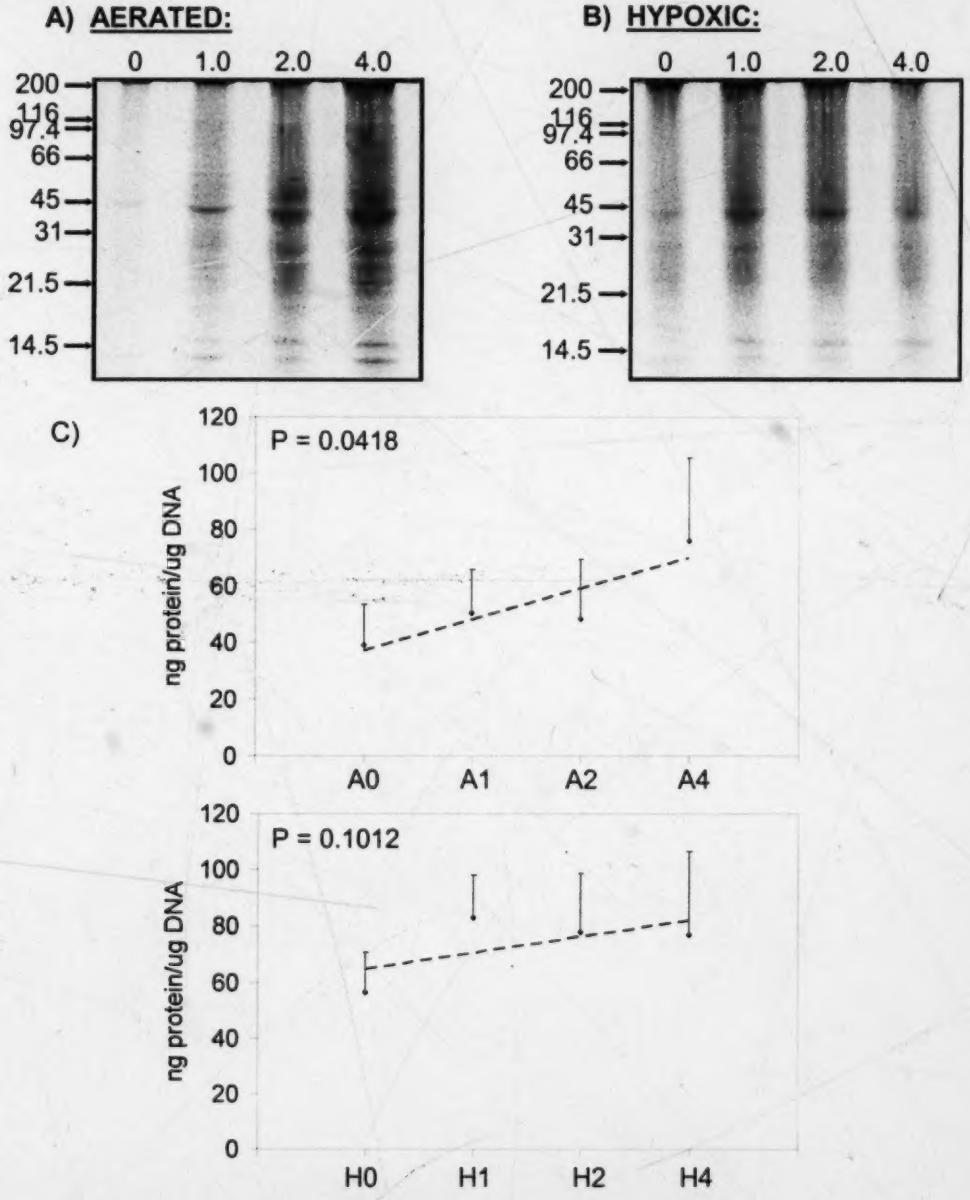

Figure 3-7: Quantitation of DPCs from human cells, 0-4 Gy

GM00637 cells received 0, 1, 2, or 4 Gy of γ-radiation under either aerated (panel A) or hypoxic (panel B) conditions. DPCs were isolated using the DNAzol-Silica method and analyzed by SDS-PAGE and SYPRO Tangerine staining. The dose in Gy is indicated above each lane. (C) Plot of total protein isolated per μg of DNA for each sample. Means, standard error and linear regression analysis were performed on data accumulated from 6 independent experiments.

dose range (Figure 3-8). Representative gels for DPCs isolated from aerated (Figure 3-8A) and hypoxic (Figure 3-8B) cells exposed to 0-1.5 Gy of γ-radiation are shown. The results were similar (Figure 3-8C) for both aerated and hypoxic conditions, with neither condition revealing a linear dose-dependent induction of DPCs by γ-radiation ($p = 0.082$ and 0.089 ($n = 12$) for aerated and hypoxic cells, respectively).

An advantage of this approach is that SYPRO Tangerine staining and ImageQuant software enable analysis of the crosslinking response of individual protein bands, as shown in Figure 3-8D, where we have analyzed the protein content of two sample bands (H1 and H2 in Figure 3-8B). We further compared the quantitation of a specific band with the Western blot for a specific protein constituent of that band (PARP) in an individual experiment (Figure 3-9). DPCs isolated from hypoxic CHO AA8 cells exposed to 0-1.5 Gy of γ-radiation were separated on SDS-PAGE and stained with SYPRO Tangerine. The total protein in the band migrating with an approximate MW of 116 kDa (Figure 3-9A) was quantified (Figure 3-9B). After protein transfer to nitrocellulose, the blot was probed with antibodies to PARP and the signal intensities determined (Figure 3-9C and 3-9D). These data highlight the applicability of this DPC analysis approach to the eventual dissection of the biological relevance of the crosslinking of individual proteins.

3.4. Discussion

Several proteins involved in DPCs induced by various agents have been

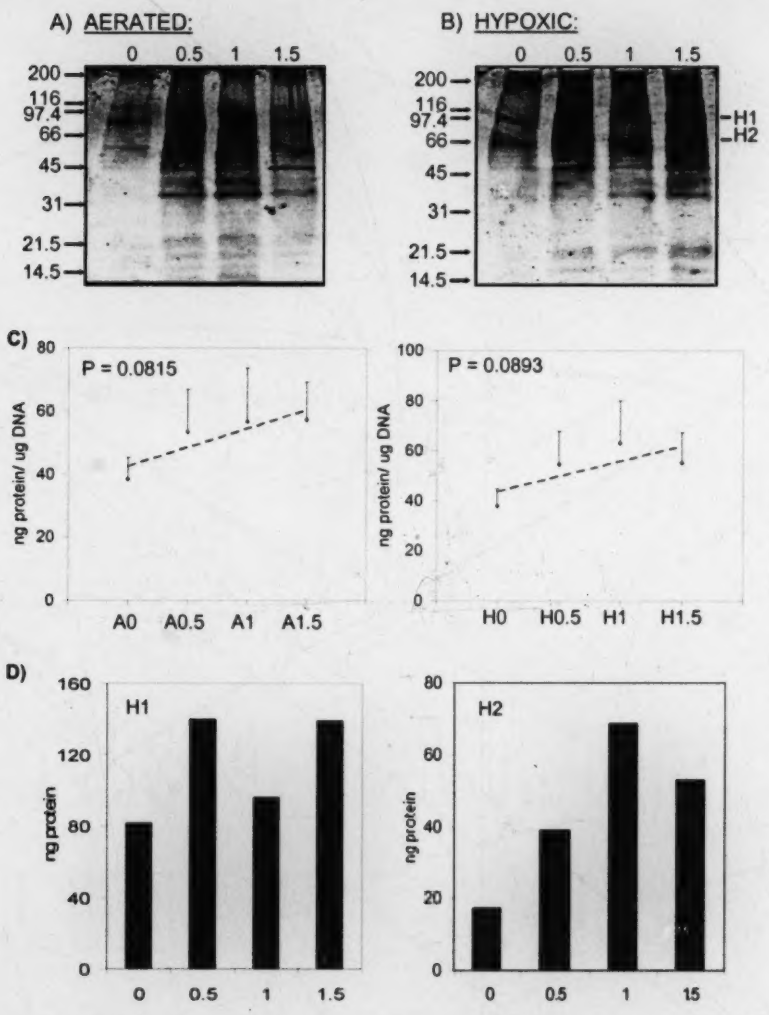

Figure 3-8: Quantitation of DPCs from human cells, 0-1.5 Gy

GM00637 cells received 0, 0.5, 1.0, or 1.5 Gy of γ-radiation under either aerated (panel A) or hypoxic (panel B) conditions. DPCs were isolated using the DNAzol-Silica method and analyzed by SDS-PAGE and SYPRO Tangerine staining. The dose in Gy is indicated above each lane. (C) Plot of total protein isolated per µg of DNA for each sample. Means, standard error and linear regression analysis were performed on data accumulated from 12 independent experiments. (D) Quantitation of individual protein bands H1 and H2 from the gel shown in B.

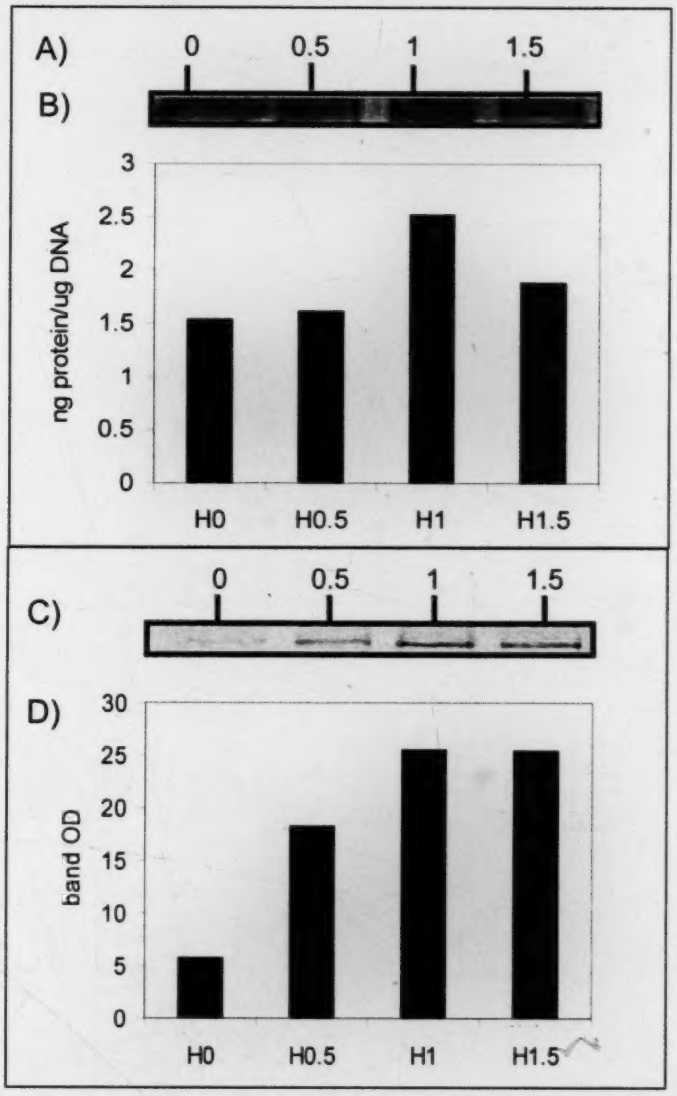

Figure 3-9: Quantitation of an individual DPC from human cells, 0-1.5 Gy

CHO AA8 cells received 0, 0.5, 1.0, or 1.5 Gy of γ-radiation under hypoxic conditions. (A) DPCs were isolated using the DNAzol-Silica method and analyzed by SDS-PAGE and SYPRO Tangerine staining. (B) Total protein isolated per μg of DNA for each band was quantified. (C) Western blot analysis with anti-PARP antibody was performed and quantitation of optical density was performed for each band (D). The dose in Gy is indicated above each lane.

identified previously using immunological methods [1,21-28]. Early studies of formaldehyde- and IR-induced crosslinking logically focused on histones because of their known close association with DNA, and these proteins were indeed shown to be crosslinkable by both of these agents, although the studies with IR were performed *in vitro* using cell-free systems. One study [22] did examine the crosslinking of proteins to DNA by IR *in vivo* and identified three such proteins: actin, lectin, and aminoglycoside nucleotidyl transferase; there is information about a role for actin in the nucleus [29], but the biological relevance of these other crosslinked proteins within the nucleus is unknown.

In this study, we have successfully combined stringent protein removal with SDS-PAGE separation and sensitive MS analysis to identify a set of proteins crosslinked to DNA in mammalian cells following exposure to γ-radiation. We have presented here the identification of 29 proteins that appear to be involved in γ-radiation-induced DPCs. These proteins fall into several categories according to their nuclear functions. Among these are structural/nuclear-matrix proteins such as actin and vimentin, spliceosome components such as hnRNPs and PSF, stress-response proteins such as HSP10 and GRP78, chromatin-regulatory and structural proteins such as histones, as well as proteins involved in other DNA transactions such as the chromatin remodeling protein CGI-55, and proteins whose nuclear functions are not yet fully known. These proteins must be located within several nanometers of the DNA to become crosslinked. Therefore, such proteins are in direct association with the DNA or in very close proximity at the time of irradiation or shortly thereafter. Some of the proteins identified here have already been shown to be involved in DNA metabolic processes and in

association with DNA, for example the histones, while others have not. Another factor affecting the likelihood that a protein will be identified as being involved in DPCs is whether it is sufficiently abundant that it can be visualized as a distinct band on SDS-PAGE and in sufficient yield to be identifiable by MS.

The nuclear localization of some of these proteins, for example glyceraldehyde-3-phosphate dehydrogenase and vimentin, was originally discounted as artifactual, and yet further work on such proteins has led to the proposal of new and additional roles in DNA repair and recombination processes [30,31]. Other proteins on our list also have roles in these processes, which may explain their association with DNA (Table 3-2). A number of mRNA-processing components were identified in this study, and their presence was probably not a result of their crosslinking to ribonucleic acid because DNAzol effectively hydrolyzes RNA. We must therefore consider the possible association of these proteins with DNA directly, and thus what roles they might be performing in this regard. For example, a recent study has shown the involvement of hnRNPA1 in Okazaki fragment maturation during DNA replication as a stimulator of the FEN-1 nuclease [55]. A novel role of another ribonucleoprotein, this time in genome maintenance, has also been demonstrated; the TLS/FUS protein has been shown to mediate homologous pairing and to be involved in the DNA damage response [62]. The TASR (TLS-associated SR) proteins, identified as being involved in DPCs in our study, may also be involved in these processes due to their association with TLS.

We were not able to find evidence of nuclear localization or a nuclear function for every protein that we identified. It may be that the fingerprint

Table 3-2: Relevant roles and/or nuclear localization for identified proteins.

Protein	Roles
Histone H2A, H4	DNA organization, modified forms involved in DNA repair [32]
Histone H2B	DNA organization
Histone H3	DNA organization, telomere binding [33]
CGI-55 Protein	potential chromatin remodeling factor [34]
Ninein	microtubule anchoring; localizes to nuclei in interphase [35]
Tubulin	component of microtubule organizing centre in nucleus [36]
Vimentin	chromatin remodeling, recombination [31]
Actin	nuclear scaffold, chromatin remodeling [37], regulation of DNA replication and/or transcription [38,39], senescence marker [40]
Cofilin	actin-regulatory protein; nuclear accumulation in senescence [40]
Elongation Factor 1 alpha 1	actin organization, transcription; nuclear localization in apoptotic cells [41]
Tropomyosin	actin-regulatory protein
Radixin	actin organizing protein, localizes to nucleus [42]
78kDa Glucose Regulated Protein (GRP78)	stress response, protein folding; localizes to ER [43]
Calumenin/Crocalbin	Ca++ regulatory protein, localizes to the endoplasmic reticulum (ER) and Golgi [44]
Alpha-2-Macroglobulin Receptor-Associated Protein	protein folding, localizes to ER [45]

10kDa Heat Shock Protein, mitochondrial (chaperonin10)	stress response, protein folding, localizes to mitochondria and secretory compartments [46]
Thioredoxin Peroxidase II	oxidative stress response [47,48], apoptosis inhibitor [49], maintenance of genome stability [50]
Serotransferrin Precursor	iron transport, transferrin localizes to endosomes [51]
TLS-Associated SR Protein, TASR-2	mRNA splicing factor; TLS is nuclear [52,53]
Heterogeneous Nuclear Ribonuclear Protein A3	mRNA splicing factor, nuclear localization [54]
Heterogeneous Nuclear Ribonuclear Protein A1	mRNA splicing factor, FEN-1 stimulator [55], telomere formation and/or stabilization [56], control of apoptosis [57]
Heterogeneous Nuclear Ribonuclear Protein A2/B1	mRNA splicing factor, telomere formation and/or stabilization [56], control of apoptosis [57]
40S Ribosomal Protein S24	part of hnRNP complex involved in mRNA processing
Rho GDP-Dissociation Inhibitor 1 (GDI 1)	modulator of Rho GTPases; nuclear localization? [58,59]
Splicing Factor - PTB Protein Associated	homologous pairing promoter [60]
Nuclease Sensitive Element Binding Protein 1	recognizes unusual DNA structures [61]
Glyceraldehyde 3-Phosphate Dehydrogenase	repair of thioguanylated DNA [30], transcription [39]

peptides used for identification will also be found in novel nuclear proteins. More likely, there may be yet unknown nuclear functions for some of the proteins we have identified. Indeed, new nuclear functions have been found for other proteins. For example, recent studies have shown that the centriole protein, Centrin 2, localizes to the nucleus and binds the NER protein, XPC, suggesting a link between cell division and DNA repair [63]. Similarly, the DNA ligase IV protein has recently been shown to interact with a subunit of the human condensin complex, defining a new link between chromatin structure and DNA repair [64]. Identification of proteins as being in close proximity to the DNA may also provide insight into the content and organization of the protein complexes involved in various processes in the nucleus.

Any protein involved in DNA-metabolic processes (repair, replication, recombination, etc.) is a potential candidate for involvement in this form of IR-induced lesion. Based on their known association with DNA, we investigated the involvement of two additional DNA-repair proteins, PARP and PNK, in γ-radiation-induced DPCs through immunoblotting experiments. The PARP proteins are involved in DNA damage signalling [65,66] and PNK is involved in strand break repair. Both of these proteins were indeed shown to be crosslinked to DNA in response to γ-radiation.

Other important aspects of the γ-radiation-induced crosslinking of proteins to DNA are the background level of crosslinks and the dose- and oxygen-dependence of these events. The SDS-PAGE analysis of DPC isolates demonstrated that the DPC isolation method was sufficiently stringent to strip non-covalent DNA-protein complexes from the DNA based on the low level of

protein observed in the unirradiated-aerated sample (Figure 3-1, 0 Gy sample). As with other forms of DNA damage, DPCs can be induced by endogenous agents (e.g., free radicals generated during normal cellular metabolism). Human cells have been reported to have a baseline level of DPC induction of 0.5-4.5 per 10^7 bases [67] and a baseline level of thymine-tyrosine DPCs of ~7 molecules/10^6 bases [68]. However, the detection limit of the DPC isolation and measurement methods will have a major impact on this parameter. For example, the alkaline elution/polycarbonate filter method failed to detect DPCs in unirradiated cells, and only detected DPCs in irradiated cells at doses of 50 Gy [69]. The nitrocellulose filter binding technique is more sensitive and can detect DPCs in irradiated cells at doses of ~30 Gy [69]. The method presented here has allowed, for the first time, the detection of DPCs in irradiated cells at biologically relevant doses as low as 0.5 Gy.

Based on previous observations, it has been suggested that molecular oxygen favours DNA fragmentation reactions at the expense of DNA-protein radical reactions following exposure to IR [70]. Consistent with this suggestion, several previous studies [10,11,13,71] have reported an increased induction of DPCs under hypoxic conditions; however, these studies typically used much higher doses of IR and used the alkaline elution assay for DPC measurements, which are indirect and influenced by other forms of DNA damage and is not very sensitive. In many studies, the alkaline elution method cannot detect background DPCs because X-rays were used to fragment the DNA in order to allow it to flow through the filter. As well, DPCs in hypoxic cells were not detected by this method at doses below 5 Gy [11]. Using our new, sensitive method for DPC

detection and low doses of γ-radiation (0-4 Gy) we did not observe a dramatic effect of hypoxia on gross DPC induction. Quantitation of the crosslinking of individual proteins; however, revealed an oxygen dependence of crosslinking for some proteins (e.g., H2B, actin, hnRNPC1/C2, PNK) but not others (e.g., PARP, tubulin). These results suggest that proteins become crosslinked to DNA by different mechanisms. Indeed, it has been shown that there are chemically different forms of crosslinks and that the induction of some crosslinks is not influenced by the presence of oxygen *in vitro* [72-75]. Proteins can become crosslinked to DNA directly through the intermediacy of IR-induced radicals. Because the lifetime of these radicals is very short, only those proteins that are located within several nanometers of the DNA at the time of irradiation can become crosslinked. Alternatively, IR exposure can potentially produce crosslinks on a delayed time scale as a result of the generation of reactive aldehydes or possibly other longer-lived species [75,76].

The dose dependence of DPC induction revealed a linear relationship in hamster cells under aerated and hypoxic conditions in the low-dose range (0-1.5 Gy). In human cells, DPC induction under aerated and hypoxic conditions approached linearity in the same low-dose range (0-1.5 Gy). At a higher dose range (0-4 Gy), DPC induction in hamster cells appeared to plateau or decline under aerated conditions, but approached linearity under hypoxic conditions. The opposite effect was seen in human cells; DPC induction in the 0-4 Gy dose range was linear under aerated conditions but appeared to plateau or decline under hypoxic conditions. A non-linear dose response for crosslink induction has previously been reported for other genotoxic agents. A decline in damage

frequency with dose was reported for the crosslinking of nuclear matrix proteins to DNA by the antitumor agent, cisplatin [27]. In the cisplatin study, SDS-PAGE indicated that there was little change in the extent of crosslinking of abundant proteins to DNA with cisplatin concentrations between 35 and 1,000 μM. Drug concentration-responsiveness of DPC induction was demonstrated for individual proteins in that study [27] using immunoblot analysis. A similar phenomenon has also been reported for laser-induced DNA-protein crosslinking [77] and for UV-induced recombination [78], although the cause of this effect is not yet known. It is inevitable that cellular DPC induction will be a saturable process given that there are a finite number of proteins per cell in contact with the DNA and available for crosslinking reactions. Also, because of the differing protein abundances, this plateau will occur at different doses and with differing amplitudes for individual proteins. The existence of different dose-responses was demonstrated by the quantitation of individual proteins. It may also be that at higher doses of IR there are other types of damage that are occurring which may affect either DPC induction or the efficiency of DPC detection.

It should be noted that other studies demonstrating the dose-dependence of IR-induced DPCs used higher doses (and therefore, longer irradiation times) than the present study. It is known that exposing cells to IR rapidly induces changes in chromatin structure [79]. It may also be the case that the stress induced by hypoxia also alters chromatin structure. Also, in the present study we have used unsynchronized cell populations, and there may be variations in the efficiency of chromatin stripping depending on the cell type and growth phase [80,81]. Work from the Oleinick group [82-85] has shown that actively-

transcribing DNA regions are more susceptible to DPC induction and that cells in metaphase not only display a higher background level of DPCs but also show a more gradual dose response for IR-induced DPCs compared to asynchronous cell populations.

The crosslinking of nuclear proteins to DNA would be expected to have serious consequences for DNA-metabolic processes such as the progression of replication, transcription, and repair complexes. Determining which proteins become covalently crosslinked to DNA may help to unravel the consequences of DPCs for these DNA transactions and enable a better understanding of the contribution of different types of DPCs to IR-induced responses such as mutagenicity, transformation and cytotoxicity. It is not unreasonable to imagine that there may be as yet undiscovered cooperative interactions between the machinery that controls various aspects of the cell cycle and organization of DNA/chromatin and members of the protein complexes that perform replication, recombination, transcription, etc., and/or multiple roles for some of these proteins in different nuclear metabolic processes. The identification of the proteins involved in DPCs should therefore provide useful information towards determining the consequences and repair of these DNA lesions and may also provide some insight into the structural and temporal arrangements of protein complexes in cellular chromatin.

References for Chapter 3

[1] S.L. Barker, M. Weinfeld and D. Murray DNA-protein crosslinks: their induction, repair and biological consequences, Mutat. Res. 589 (2005) 111-135.

[2] E.C. Friedberg, G.C. Walker and W. Siede DNA Repair and Mutagenesis, ASM Press, Washington D.C., 1995.

[3] W. Vermeulen, J.H.J. Hoeijmakers and D. Bootsma Maintaining nature's perfection, Helix 1 (1996) 22-29.

[4] J.-M.H. Vos DNA Repair Mechanisms: Impact on Human Diseases and Cancer, Springer-Verlag, New York, 1996.

[5] V. Voitkun and A. Zhitkovich Analysis of DNA-protein crosslinking activity of malondialdehyde in vitro, Mutat. Res. 424 (1999) 97-106.

[6] G. Quievryn and A. Zhitkovich Loss of DNA-protein crosslinks from formaldehyde-exposed cells occurs through spontaneous hydrolysis and an active repair process linked to proteosome function, Carcinogenesis 21 (2000) 1573-1580.

[7] N. Ramakrishnan, S.M. Chiu and N.L. Oleinick Yield of DNA-protein cross-links in gamma-irradiated Chinese hamster cells, Cancer Res. 47 (1987) 2032-2035.

[8] R.E. Meyn, W.T. Jenkins and D. Murray Radiation damage to DNA in various animal tissues: Comparison of yields and repair *in vivo* and *in vitro*, in: M.G. Simic, L. Grossman and A.C. Upton (Eds.), Mechanisms of DNA Damage and Repair: Implications to Carcinogenesis and Risk Assessment, Plenum Press, New York, 1986, pp. 151-158.

[9] L.K. Mee and S.J. Adelstein Radiolysis of chromatin extracted from cultured mammalian cells: formation of DNA-protein cross links, Int. J. Radiat. Biol. Relat. Stud. Phys. Chem. Med. 36 (1979) 359-366.

[10] A.J. Fornace, Jr. and J.B. Little DNA crosslinking induced by x-rays and chemical agents, Biochim. Biophys. Acta 477 (1977) 343-355.

[11] L.Y. Xue, L.R. Friedman and N.L. Oleinick Repair of chromatin damage in glutathione-depleted V-79 cells: comparison of oxic and hypoxic conditions, Radiat. Res. 116 (1988) 89-99.

[12] A.J. Fornace, Jr. Detection of DNA single-strand breaks produced during the repair of damage by DNA-protein cross-linking agents, Cancer Res. 42 (1982) 145-149.

[13] R.E. Meyn, S.C. vanAnkeren and W.T. Jenkins The induction of DNA-protein crosslinks in hypoxic cells and their possible contribution to cell lethality, Radiat. Res. 109 (1987) 419-429.

[14] D. Murray, A. Macann, J. Hanson and E. Rosenberg ERCC1/ERCC4 5'-endonuclease activity as a determinant of hypoxic cell radiosensitivity, Int. J. Radiat. Biol. 69 (1996) 319-327.

[15] M. Hockel and P. Vaupel Biological consequences of tumor hypoxia, Semin. Oncol. 28 (2001) 36-41.

[16] P. Vaupel, D.K. Kelleher and M. Hockel Oxygen status of malignant tumors: pathogenesis of hypoxia and significance for tumor therapy, Semin. Oncol. 28 (2001) 29-35.

[17] S.L. Barker, D. Murray, J. Zheng, L. Li and M. Weinfeld A method for the isolation of covalent DNA-protein crosslinks suitable for proteomics analysis, Anal. Biochem. In Press (2005).

[18] C.J. Koch, C.C. Stobbe and E.A. Bump The effect on the Km for radiosensitization at 0 degree C of thiol depletion by diethylmaleate pretreatment: quantitative differences found using the radiation sensitizing agent misonidazole or oxygen, Radiat Res 98 (1984) 141-153.

[19] M.S. Elphinstone, G.N. Hinten, A. M.J. and N. C.J. An inexpensive and high-throughput procedure to extract and purify total genomic DNA for population studies, Mol. Ecol. Notes 3 (2003) 317-320.

[20] M. Fanta, H. Zhang, N. Bernstein, M. Glover, F. Karimi-Busheri and M. Weinfeld Production, characterization, and epitope mapping of monoclonal antibodies against human polydeoxyribonucleotide kinase, Hybridoma 20 (2001) 237-242.

[21] R.A.J. Coulombe, G.L. Drew and F.R. Stermitz Pyrrolizidine alkaloids crosslink DNA with actin, Toxicol. Appl. Pharmacol. 15 (1999) 198-202.

[22] S.N. Mattagajasingh and H.P. Misra Analysis of EDTA-chelatable proteins from DNA-protein crosslinks induced by a carcinogenic chromium (VI) in cultured intact human cells, Mol. Cell. Biochem. 199 (1999) 149-162.

[23] C.A.I. Miller, M.D. Cohen and M. Costa Complexing of actin and other nuclear proteins to DNA by cis-diamminedichloroplatinum(II) and chromium compounds, Carcinogenesis 12 (1991) 269-276.

[24] P.M. O'Connor and B.W. Fox Isolation and characterization of proteins cross-linked to DNA by the antitumor agent methylene dimethanesulfonate and its hydrolytic product formaldehyde, J. Biol. Chem. 264 (1989) 6391-6397.

[25] G.V. Tolstonog, E. Mothes, R.L. Shoeman and P. Traub Isolation of SDS-stable complexes of the intermediate filament protein vimentin with repetitive, mobile, nuclear matrix attachment region, and mitochondrial DNA sequence elements from cultured mouse and human fibroblasts, DNA Cell Biol. 20 (2001) 531-554.

[26] A. Matsumoto and P.C. Hanawalt Histone H3 and heat shock protein GRP78 are selectively cross-linked to DNA by photoactivated Gilvocarcin V in human fibroblasts, Cancer Res. 60 (2000) 3921-3926.

[27] S.K. Samuel, V.A. Spencer, L. Bajno, J.M. Sun, L.T. Holth, S. Oesterreich and J.R. Davie In situ cross-linking by cisplatin of nuclear matrix-bound transcription factors to nuclear DNA of human breast cancer cells, Cancer Res. 58 (1998) 3004-3008.

[28] P. Ramirez, L.M. Del Razo, M.C. Gutierrex-Ruiz and M.E. Gonsebatt Arsenite induces DNA-protein crosslinks and cytokeratin expression in the WRL-68 human hepatic cell line, Carcinogenesis 21 (2000) 701-706.

[29] A. Zimber, Q.D. Nguyen and C. Gespach Nuclear bodies and compartments: functional roles and cellular signalling in health and disease, Cell Signal. 16 (2004) 1085-1104.

[30] E.Y. Krynetski, N.F. Krynetskaia, M.E. Bianchi and W.E. Evans A nuclear protein complex containing high mobility group proteins B1 and B2, heat shock cognate protein 70, ERp60, and glyceraldehyde-3-phosphate dehydrogenase is involved in the cytotoxic response to DNA modified by incorporation of anticancer nucleoside analogues, Cancer Res. 63 (2003) 100-106.

[31] G.V. Tolstonog, M. Sabasch and P. Traub Cytoplasmic intermediate filaments are stably associated with nuclear matrices and potentially modulate their DNA-binding function, DNA Cell Biol. 21 (2002) 213-239.

[32] J.A. Downs, S. Allard, O. Jobin-Robitaille, A. Javaheri, A. Auger, N. Bouchard, S.J. Kron, S.P. Jackson and J. Cote Binding of chromatin-modifying activities to phosphorylated histone H2A at DNA damage sites, Mol Cell 16 (2004) 979-990.

[33] J.E. Lowell and G.A. Cross A variant histone H3 is enriched at telomeres in Trypanosoma brucei, J Cell Sci 117 (2004) 5937-5947.

[34] T.A. Lemos, D.O. Passos, F.C. Nery and J. Kobarg Characterization of a new family of proteins that interact with the C-terminal region of the chromatin-remodeling factor CHD-3, FEBS Lett 533 (2003) 14-20.

[35] V. Bouckson-Castaing, M. Moudjou, D.J. Ferguson, S. Mucklow, Y. Belkaid, G. Milon and P.R. Crocker Molecular characterisation of ninein, a new coiled-coil protein of the centrosome, J Cell Sci 109 (Pt 1) (1996) 179-190.

[36] Y. You, T. Huang, E.J. Richer, J.E. Schmidt, J. Zabner, Z. Borok and S.L. Brody Role of f-box factor foxj1 in differentiation of ciliated airway epithelial cells, Am. J. Physiol. Lung Cell. Mol. Physiol. 286 (2004) L650-657.

[37] K. Zhao, W. Wang, O.J. Rando, Y. Xue, K. Swiderek, A. Kuo and G.R. Crabtree Rapid and phosphoinositol-dependent binding of the SWI/SNF-like BAF complex to chromatin after T lymphocyte receptor signaling, Cell 95 (1998) 625-636.

[38] H. Fidlerova, M. Masata, J. Malinsky, M. Fialova, Z. Cvackova, A. Louzecka, K. Koberna, R. Berezney and I. Raska Replication-coupled modulation of early replicating chromatin domains detected by anti-actin antibody, J Cell Biochem (2005).

[39] H. Mitsuzawa, M. Kimura, E. Kanda and A. Ishihama Glyceraldehyde-3-phosphate dehydrogenase and actin associate with RNA polymerase II and interact with its Rpb7 subunit, FEBS Lett 579 (2005) 48-52.

[40] I.H. Kwak, H.S. Kim, O.R. Choi, M.S. Ryu and I.K. Lim Nuclear accumulation of globular actin as a cellular senescence marker, Cancer Res 64 (2004) 572-580.

[41] O. Billaut-Mulot, R. Fernandez-Gomez, M. Loyens and A. Ouaissi Trypanosoma cruzi elongation factor 1-alpha: nuclear localization in parasites undergoing apoptosis, Gene 174 (1996) 19-26.

[42] C.L. Batchelor, A.M. Woodward and D.H. Crouch Nuclear ERM (ezrin, radixin, moesin) proteins: regulation by cell density and nuclear import, Exp Cell Res 296 (2004) 208-222.

[43] D.G. Bole, R. Dowin, M. Doriaux and J.D. Jamieson Immunocytochemical localization of BiP to the rough endoplasmic reticulum: evidence for protein sorting by selective retention, J Histochem Cytochem 37 (1989) 1817-1823.

[44] H. Vorum, H. Hager, B.M. Christensen, S. Nielsen and B. Honore Human calumenin localizes to the secretory pathway and is secreted to the medium, Exp. Cell. Res. 248 (1999) 473-481.

[45] M. Albate, D. Bachinsky, G. Zheng, I. Stamenkovic, M. McLaughlin, J.L. Niles, R.T. McCluskey and D. Brown Location of gp330/alpha 2-m receptor-associated protein (alpha 2-MRAP) and its binding sites in kidney: distribution of endogenous alpha 2-MRAP is modified by tissue processing, Eur. J. Cell Biol. 61 (1993) 139-149.

[46] S.K. Sadacharan, A.C. Cavanagh and R.S. Gupta Immunoelectron microscopy provides evidence for the presence of mitochondrial heat shock 10-kDa protein (chaperonin 10) in red blood cells and a variety of secretory granules, Histochem. Cell Biol. 116 (2001) 507-517.

[47] S.N. Radyuk, R.S. Sohal and W.C. Orr Thioredoxin peroxidases can foster cytoprotection or cell death in response to different stressors: over- and under-expression of thioredoxin peroxidase in Drosophila cells, Biochem. J. 371 (2003) 743-752.

[48] S.J. Ross, V.J. Findlay, P. Malakasi and B.A. Morgan Thioredoxin peroxidase is required for the transcriptional response to oxidative stress in budding yeast, Mol. Biol. Cell 11 (2000) 2631-2642.

[49] M.I. Berggren, B. Husbeck, B. Samulitis, A.F. Baker, A. Gallegos and G. Powis Thioredoxin peroxidase-1 (peroxiredoxin-1) is increased in thioredoxin-1 transfected cells and results in enhanced protection against apoptosis caused by hydrogen peroxide but not by other agents including dexamethasone, etoposide, and doxorubicin, Arch. Biochem. Biophys. 392 (2001) 103-109.

[50] M.E. Huang, A.G. Rio, A. Nicolas and R.D. Kolodner A genomewide screen in Saccharomyces cerevisiae for genes that suppress the accumulation of mutations, Proc. Natl. Acad. Sci. USA 100 (2003) 11529-11534.

[51] S. Gruenheid, F. Canonne-Hergaux, S. Gauthier, D.J. Hackam, S. Grinstein and P. Gros The iron transport protein NRAMP2 is an integral membrane glycoprotein that colocalizes with transferrin in recycling endosomes, J Exp Med 189 (1999) 831-841.

[52] H. Zinszner, D. Immanuel, Y. Yin, F.X. Liang and D. Ron A topogenic role for the oncogenic N-terminus of TLS: nucleolar localization when transcription is inhibited, Oncogene 14 (1997) 451-461.

[53] H. Zinszner, J. Sok, D. Immanuel, Y. Yin and D. Ron TLS (FUS) binds RNA in vivo and engages in nucleo-cytoplasmic shuttling, J Cell Sci 110 (Pt 15) (1997) 1741-1750.

[54] E.V. Laz, C.A. Wiwi and D.J. Waxman Sexual dimorphism of rat liver nuclear proteins: regulatory role of growth hormone, Mol Cell Proteomics 3 (2004) 1170-1180.

[55] Q. Chai, L. Zheng, M. Zhou, J.J. Turchi and B. Shen Interaction and stimulation of human FEN-1 nuclease activities by heterogeneous nuclear ribonucleoprotein A1 in alpha-segment processing during Okazaki fragment maturation, Biochemistry 42 (2003) 15045-15052.

[56] L.P. Ford, W.E. Wright and J.W. Shay A model for heterogeneous nuclear ribonucleoproteins in telomere and telomerase regulation, Oncogene 21 (2002) 580-583.

[57] R. Hermann, F. Hensel, E.C. Muller, M. Keppler, M. Souto-Carneiro, S. Brandlein, H.K. Muller-Hermelink and H.P. Vollmers Deactivation of regulatory proteins hnRNP A1 and A2 during SC-1 induced apoptosis, Hum. Antibodies 10 (2001) 83-90.

[58] G.A. Murphy, S.A. Jillian, D. Michaelson, M.R. Philips, P. D'Eustachio and M.G. Rush Signaling mediated by the closely related mammalian Rho family GTPases TC10 and Cdc42 suggests distinct functional pathways, Cell Growth Differ. 12 (2001) 157-167.

[59] M. Tsuda, Y. Makino, T. Iwahara, H. Nishihara, H. Sawa, K. Nagashima, H. Hanafusa and S. Tanaka Crk associates with ERM proteins and promotes cell motility toward hyaluronic acid, J. Biol. Chem. 279 (2004) 46843-46850.

[60] A.T. Akhmedov and B.S. Lopez Human 100-kDa homologous DNA-pairing protein is the splicing factor PSF and promotes DNA strand invasion, Nucleic Acids Res. 28 (2000) 3022-3030.

[61] R. Kolluri, T.A. Torrey and A.J. Kinniburgh A CT promoter element binding protein: definition of a double-strand and a novel single-strand DNA binding motif, Nucleic Acids Res. 20 (1992) 111-116.

[62] P. Bertrand, A.T. Akhmedov, F. Delacote, A. Durrbach and B.S. Lopez Human POMp75 is identified as the pro-oncoprotein TLS/FUS: both POMp75 and POMp100 DNA homologous pairing activities are associated to cell proliferation, Oncogene 18 (1999) 4515-4521.

[63] M. Araki, C. Masutani, M. Takemura, A. Uchida, K. Sugasawa, J. Kondoh, Y. Ohkuma and F. Hanaoka Centrosome protein centrin 2/caltractin 1 is part of the xeroderma pigmentosum group C complex that initiates global genome nucleotide excision repair, J. Biol. Chem. 276 (2001) 18665-18672.

[64] M.R. Przewloka, P.E. Pardington, S.M. Yannone, D.J. Chen and R.B. Cary In vitro and in vivo interactions of DNA ligase IV with a subunit of the condensin complex, Mol. Biol. Cell 14 (2003) 685-697.

[65] V.J. Bouchard, M. Rouleau and G.G. Poirier PARP-1, a determinant of cell survival in response to DNA damage, Exp. Hematol. 31 (2003) 446-454.

[66] J.C. Ame, C. Spenlehauer and G. de Murcia The PARP superfamily, Bioessays 26 (2004) 882-893.

[67] R.K. Zahn, G. Zahn-Daimler, S. Ax, M. Hosokawa and T. Takeda Assessment of DNA-protein crosslinks in the course of aging in two mouse strains by use of a modified alkaline filter elution applied to whole tissue samples, Mech. Ageing Dev. 108 (1999) 99-112.

[68] R. Olinski, Z. Nackerdien and M. Dizdaroglu DNA-protein cross-linking between thymine and tyrosine in chromatin of gamma-irradiated or H_2O_2-treated cultured human cells, Arch. Biochem. Biophys. 297 (1992) 139-143.

[69] I. Al-Nabulsi and K.T. Wheeler Temperature dependence of radiation-induced DNA-protein crosslinks formed under hypoxic conditions, Radiat. Res. 148 (1997) 568-574.

[70] P. Alexander and J.T. Lett Role of oxygen in the cross-linking and degradation of deoxyribonucleic acid by ionizing radiations, Nature 187 (1960) 933-934.

[71] I.R. Radford Effect of radiomodifying agents on the ratios of X-ray-induced lesions in cellular DNA: use in lethal lesion determination, Int J Radiat Biol Relat Stud Phys Chem Med 49 (1986) 621-637.

[72] E. Gajewski, A.F. Fuciarelli and M. Dizdaroglu Structure of hydroxyl radical-induced DNA-protein crosslinks in calf thymus nucleohistone in vitro, Int. J. Radiat. Biol. 54 (1988) 445-459.

[73] M. Dizdaroglu, E. Gajewski, P. Reddy and S.A. Margolis Structure of a hydroxyl radical induced DNA-protein cross-link involving thymine and tyrosine in nucleohistone, Biochemistry 28 (1989) 3625-3628.

[74] Z. Nackerdien, G. Rao, M.A. Cacciuttolo, E. Gajewski and M. Dizdaroglu Chemical nature of DNA-protein cross-links produced in mammalian chromatin by hydrogen peroxide in the presence of iron or copper ions, Biochemistry 30 (1991) 4873-4879.

[75] J.P. Pouget and S.J. Mather General aspects of the cellular response to low- and high-LET radiation, Eur. J. Nucl. Med. 28 (2001) 541-561.

[76] M. Quintiliani The oxygen effect in radiation inactivation of DNA and enzymes, Int J Radiat Biol Relat Stud Phys Chem Med 50 (1986) 573-594.

[77] S. Lejnine, G. Durfee, M. Murnane, H.C. Kapteyn, V.L. Makarov and J.P. Langmore Crosslinking of proteins to DNA in human nuclei using a 60 femtosecond 266 nm laser, Nucleic Acids Res 27 (1999) 3676-3684.

[78] C.A. Bill and J.A. Nickoloff Spontaneous and ultraviolet light-induced direct repeat recombination in mammalian cells frequently results in repeat deletion, Mutat. Res. 487 (2001) 41-50.

[79] I.Y. Belyaev, S. Czene and M. Harms-Ringdahl Changes in chromatin conformation during radiation-induced apoptosis in human lymphocytes, Radiat. Res. 156 (2001) 355-364.

[80] L.Y. Xue, L.R. Friedman, N.L. Oleinick and S.M. Chiu Induction of DNA damage in gamma-irradiated nuclei stripped of nuclear protein classes: differential modulation of double-strand break and DNA-protein crosslink formation, Int. J. Radiat. Biol. 66 (1994) 11-21.

[81] M.C. Elia and M.O. Bradley Influence of chromatin structure on the induction of DNA double strand breaks by ionizing radiation, Cancer Res. 52 (1992) 1580-1586.

[82] S.M. Chiu, L.R. Friedman, L.Y. Xue and N.L. Oleinick Modification of DNA damage in transcriptionally active vs. bulk chromatin, Int J Radiat Oncol Biol Phys 12 (1986) 1529-1532.

[83] S.M. Chiu, L.R. Friedman, N.M. Sokany, L.Y. Xue and N.L. Oleinick Nuclear matrix proteins are crosslinked to transcriptionally active gene sequences by ionizing radiation, Radiat Res 107 (1986) 24-38.

[84] S.M. Chiu, N.M. Sokany, L.R. Friedman and N.L. Oleinick Differential processing of ultraviolet or ionizing radiation-induced DNA-protein cross-links in Chinese hamster cells, Int J Radiat Biol Relat Stud Phys Chem Med 46 (1984) 681-690.

[85] S.M. Chiu, L.R. Friedman and N.L. Oleinick The fate of DNA-protein crosslinks formed in gamma-irradiated metaphase cells, Int J Radiat Biol 58 (1990) 235-247.

Chapter 4: Analysis of the timecourse of γ-radiation-induced DNA-protein crosslinks in mammalian cells.

4.1. Introduction

DPCs are induced by a number of agents including UV, IR, metals, aldehydes and some chemotherapeutic agents [1]. The crosslinks created by these various agents are likely to be chemically distinct from each other as evidenced by the fact that the crosslinked proteins can be released from the DNA by different methods. The study of any DPC-inducing agent is further complicated by the existence of additional DPC-induction pathways. Cells are regularly exposed to DPC-inducing agents both exogenously and endogenously through normal metabolic processes that generate aldehydes or free radicals. Background DPC levels were measured in human peripheral lymphocytes and found to have a frequency of between 0.5 and 4.5 adducts per 10^7 bases [2]. Although some linkages have been conclusively shown to be covalent [3-6], many studies have assumed that DPCs are covalent because of their persistence despite the use of stringent dissociating conditions such as urea, guanidine hydrochloride, boiling, detergent, etc. [7-9].

Reports on the cellular lifetime of DPCs indicate that they are longer lived than many other forms of damage and that persistence varies depending on the agent used, the dose used, and the cell type studied. Using CHO cells, it was shown that ~50% of the DPCs induced by 50 Gy of X-rays were removed within 45 min at 37°C and ~90% were removed within 2 h [8,10]. Chiu *et al.* [11] measured DPC levels in Chinese hamster V79 cells exposed to 60 Gy of γ-rays and demonstrated that ~50% of DPCs were removed within 1 h of exposure at 37°C, ~80% were removed within 5 h after exposure, and ~90% were removed

by 24 h. Chromium-induced DPCs in CHO cells produced by a 6-h incubation with 10 μM $CaCrO_4$ were repaired within 24 h, but there was no removal of DPCs after treatment with 25 μM $CaCrO_4$ despite little cytotoxicity [12]. Chromium-induced DPCs persisted after 36 h in rat kidney and lung cells, but not in liver cells [13]. Malondialdehyde is a DPC-inducing agent that is generated endogenously through lipid peroxidation. The half-life of malondialdehyde-induced DPCs *in vitro* was found to be 13.4 days [2]. Ferric nitriloacetate is a known renal carcinogen associated with lipid peroxidation processes and oxidative damage; DPC levels in rats treated with this agent peaked at 24 h, were still significantly above background by 48 h, and returned to control levels by day 19 [14]. Acetaldehyde-induced DPCs have been shown to be hydrolytically unstable, with up to 75% of the lesions being lost after an 8-h incubation at 37°C [15,16], while formaldehyde-induced DPCs have been shown to have a half-life of ~12.5 h in human cells [17]. DPCs induced by formaldehyde *in vitro* exhibited a half-life of ~26 h at 37°C; however, if agents that prevent DNA-protein re-association (i.e., salt and/or detergent) were present, the half-life of these DPCs was decreased to ~18 h. This observation suggests that crosslinks can reform if the DNA and proteins remain in contact. The fact that the *in vivo* removal rate is shorter than that predicted by hydrolytic instability and from that seen *in vitro* suggests that there are additional, active repair processes that contribute to the removal of DPCs *in vivo*.

Because of the induction of many forms of damage by endogenous agents, specialized DNA repair systems have evolved for removing various types

of damage (strand breaks, base damage, etc.) from the genome. This may also be the case for DPCs, although these lesions may also be substrates for known repair pathways. DPCs are expected to be bulky and potentially helix-distorting and may therefore be substrates for NER [18]. Evidence for the involvement of the NER pathway in DPC repair is contradictory. The removal of formaldehyde-induced DPCs was examined in NER deficient cells (XPA and XPF) and was found to be similar to that of normal cells, suggesting that NER is ***not*** involved in DPC removal [17,19,20]. In contrast, Meyn *et al.* [21] reported that the UV41 (XPF deficient) CHO cell line removed only ~20% of the DPCs induced by 50 Gy of X-rays under hypoxic conditions, while the parental AA8 cells removed ~80% of these DPCs in the same 24 h period. The mutagenicity and toxicity of a cysteine-Cr-DNA adduct in a shuttle plasmid was significantly greater towards XPA cells than their corrected counterpart (XPA^+ cells) [22]. Gantt [23] found that transplatin-induced DPCs were removed from normal human cells within 24 h, but XPA cells required 4-6 days to remove them. Further support for the possibility of DPC repair or partial repair by NER comes from Lloyd and coworkers [24,25]. These investigators constructed a synthetic protein-DNA substrate and synthetic peptide-DNA substrates of different sizes and different crosslinking chemistries and showed that the *E. Coli* UvrABC complex could incise each of these substrates *in vitro* in a manner identical to the bacterial NER reaction. The efficiency of incising activity on the DPC substrates was comparable to, or greater than, that seen for standard NER substrates even in

the presence of one of these competing adducts, implicating NER as a potential contributing pathway to DPC repair [24,25].

As is apparent from the above discussion, the existing data on DPC lifetimes and repair is extremely variable and limited. This variability may be due in part to the use of different DPC-inducing agents and different DPC-detection methods. There is an urgent need for clarification of the biological relevance of these lesions, and such clarification will require a detailed dissection of the stability, persistence, and possible repair routes of the various types of DPCs. The present study examines the lifetime of -induced DPCs in repair-proficient and NER/HRR and HRR –deficient mammalian cells due to the potential involvement of these pathways in DPC repair.

4.2. Materials and Methods

4.2.a. Cell culture

The parental CHO cell line, AA8, was obtained from Dr. Keith Caldecott (University of Sussex, UK). The mutant cell lines irs1SF, UV20, and UV41 were obtained from the American Type Culture Collection (ATCC) (Manassas, VA). Each cell line was maintained as a monolayer culture in αDMEM-F12 medium supplemented with 10% fetal bovine serum and 5% penicillin/streptomycin in a humidified 5% CO_2 and 95% air atmosphere at 37°C.

4.2.b. Radiation and chemical treatments of cells

Cells were grown as monolayer cultures to ~85% confluency. Aerated cells were irradiated in 150-mm plastic dishes. To render cells hypoxic, the cells were washed with PBS and trypsinized. Fresh medium was added to a final volume of 5 ml per 2.4 $x10^7$ cells and the cells were transferred to 60-mm glass Petri dishes. The dishes were placed in air-tight aluminium chambers and the chambers were evacuated using a vacuum manifold. The chambers were then filled with pure nitrogen gas and the cells were incubated at room temperature in nitrogen for 8 sec, with the process being repeated four times. This process was repeated another four times using 8-min incubations, and the cells were then incubated at 37°C for 20 min to allow them to metabolize residual oxygen [26]. After irradiation, the cells were released from hypoxia and returned to 150-mm plates. Fresh medium was then added, and the cultures were returned to the 37°C incubator.

For γ-radiation exposures, cells were irradiated in a ^{60}Co irradiator (Gammacell; Atomic Energy of Canada Limited, Ottawa) at a dose rate of 0.1 Gy/sec. For formaldehyde treatment, 37% formaldehyde was added to the growth medium to a final concentration of 1% and the sample was incubated at 37°C for 1 h. Cells were either processed immediately (0 h time point) or were washed twice with warm PBS and incubated for between 5 and 30 h at 37°C in fresh growth medium.

4.2.c. Quantitation of DNA

For each sample, the DNA concentration was determined after nuclease digestion by measuring the UV absorbance at 260 nm, as described in Chapter 2, section 2.2.i. The relative amounts of DNA were determined within each experiment and were used to determine sample loads for SDS-PAGE analysis.

4.2.d. Nuclei isolation

Nuclei isolation was performed as described in Chapter 2, section 2.2.g.

4.2.e. Nuclear extract preparation

Nuclear extracts were prepared as described in Chapter 2, section 2.2.h.

4.2.f. DNAzol-Silica DPC isolation method

We followed the method of Barker *et al.* [27] as described in Chapter 2, section 2.2.e. The method of Elphinstone *et al.* [28] was used to prepare the silica fines (VWR, Mississauga, Ontario).

4.2.g. SDS-PAGE analysis

Laemmli buffer (BioRad) was added to each sample to normalize the DNA content among the samples within each individual experiment. Samples were analyzed by 1-D SDS-PAGE using pre-cast 10-20% gradient gels (BioRad). Gels were stained using SYPRO Tangerine (Invitrogen).

4.2.h. Quantitation of protein on SDS-PAGE gels

SYPRO Tangerine-stained 1-D SDS-PAGE gels were scanned using an Amersham Typhoon 7400 imager. The resulting fluorescence images were analyzed using the ImageQuant 5.2 software. Known amounts of broad-range protein markers (Biorad) were run on each gel and stained with SYPRO-Tangerine. Representative background regions were subtracted for each band and marker bands were quantitated. Marker bands were also quantitated and used to determine protein levels in each sample after subtraction of representative background regions.

4.2.i. Western blots

After analysis of SYPRO Tangerine staining with the Typhoon imager, the gels were de-stained in 10% methanol and protein was transferred to nitrocellulose membranes (Bio-Rad) for 1.5 h at 80 V. Blots were blocked in 5% milk-TBST for 1 h, at room temperature, with gentle agitation. Primary antibody incubations were overnight at 4°C with gentle agitation. After incubation with primary antibody, the blots were washed 4 times (15 min per wash) in 10 mL of 5% milk-TBST at room temperature. Fluorescent secondary antibodies were incubated with the blots for 1 h at room temperature, in the dark, with gentle agitation. After the secondary antibody incubation, the blots were kept in the dark while being washed again as above, with a final wash in PBS. Images of the blots were obtained using a LI-COR Odyssey infra-red imager.

4.2.j. Antibodies

Primary polyclonal antibodies to mammalian vimentin, histone H2B, actin, and PARP were obtained from Santa Cruz Biotechnology. Primary antibodies were used at dilutions of 1:1,000 in 5% milk-TBST in a total volume of 3 mL. Fluorescence-tagged secondary antibodies (goat anti-rabbit IR800 and rabbit anti-goat 700) were obtained from Rockland Immunologicals (Gilbertsville, PA) and used at a dilution of 1:5,000 in 5% milk-TBST in a total volume of 5 mL.

4.3. Results

4.3.a. Time course of formaldehyde-induced DPCs in mammalian cells

To validate the method of analysis, the induction and loss/removal of formaldehyde-induced DPCs in mammalian cells was examined. CHO AA8 cells received either no treatment or were treated with 1% formaldehyde for 1 h at 37°C; the formaldehyde was then removed and the cells were further incubated at 37°C for 0, 5, 15 or 30 h. DPCs were isolated using the DNAzol-Silica method. Sample volumes were normalized based on the amount of DNA isolated, and the recovered DPCs were analyzed by SDS-PAGE. A representative SYPRO Tangerine-stained gel from 6 independent experiments is shown in Figure 4-1A. The fluorescent markers were used to quantitate the level of protein in each sample lane. The amount of crosslinked protein isolated at each time point is shown in Figure 4-1B. Similar to the earlier published lifetime of ~12.5 h for formaldehyde-induced DPCs in human cells [17] the level of crosslinked proteins decreased rapidly and returned to background level within ~15 h.

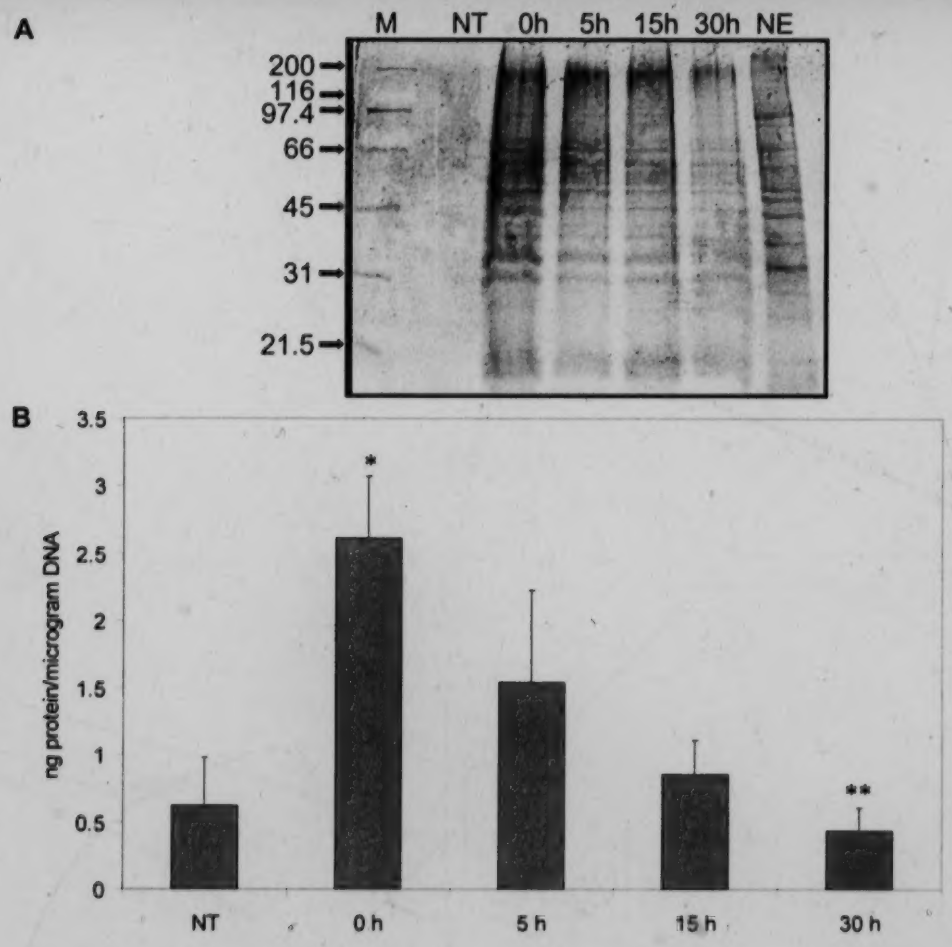

Figure 4-1: Time course of formaldehyde-induced DPCs in AA8 hamster cells

AA8 CHO cells received no treatment "NT" or were treated with 1% formaldehyde for 1 h at 37°C. Cells were either processed immediately or were further incubated for 5-30 h. DPCs were isolated using the DNAzol-Silica method, analyzed, and quantitated as described in sections 4.2.f-h. Gel images (A) were obtained using the Typhoon 7400 instrument and quantitations (B) were performed using the ImageQuant 5.2 software. The "M" lane represents the MW markers, indicated in kDa. The time (h) after treatment is indicated above each lane. The "NE" lane is a total AA8 nuclear extract. The data in panel B represent the means and standard errors of 6 independent experiments. * indicates that the peak value is significantly different from the "NT" sample and ** indicates that the final value is significantly different from the peak value.

4.3.b. Time course of γ-radiation-induced DPCs in mammalian cells

CHO AA8 cells received either no treatment or were exposed to 1.5 Gy of γ-rays under either aerated or hypoxic conditions, then were incubated at 37°C for 0, 5, 15, 30 or 50 h. DPCs were isolated using the DNAzol-Silica method and analyzed by SDS-PAGE. Representative gels for the two conditions (aerated and hypoxic) are shown in Figures 4-2A and B, respectively. DPCs were quantitated using SYPRO Tangerine staining and fluorescence quantitation was performed for 7 independent experiments (Figure 4-2C). There was a similar time dependency for the induction and loss curves in both aerated and hypoxic cells. (Note that the hypoxic cells were re-aerated immediately after irradiation, such that the actual repair phase occurs under aerated conditions). For both sets of cells, DPC levels increased in the first 15 h and decreased after 15 h, but had not returned to background level by 50 h.

4.3.c. Time course of γ-radiation-induced DPCs in repair-deficient mammalian cells

The time course analysis was extended to γ-radiation-induced DPCs in repair-deficient CHO cells to assess the potential involvement of different repair pathways in DPC removal. The NER pathway has been suggested to be involved in DPC removal (see section 4.1 and Figure 1-5) and the HRR pathway has been suggested to be involved in the removal of crosslinks (see section 1.9 and Figure 1-5). The UV20 cell line is deficient in the ERCC1 protein, which is involved in NER and possibly in HRR [29]; the UV41 cell line is deficient in the XPF NER protein, which, like ERCC1, may also be involved in HRR [29]. The

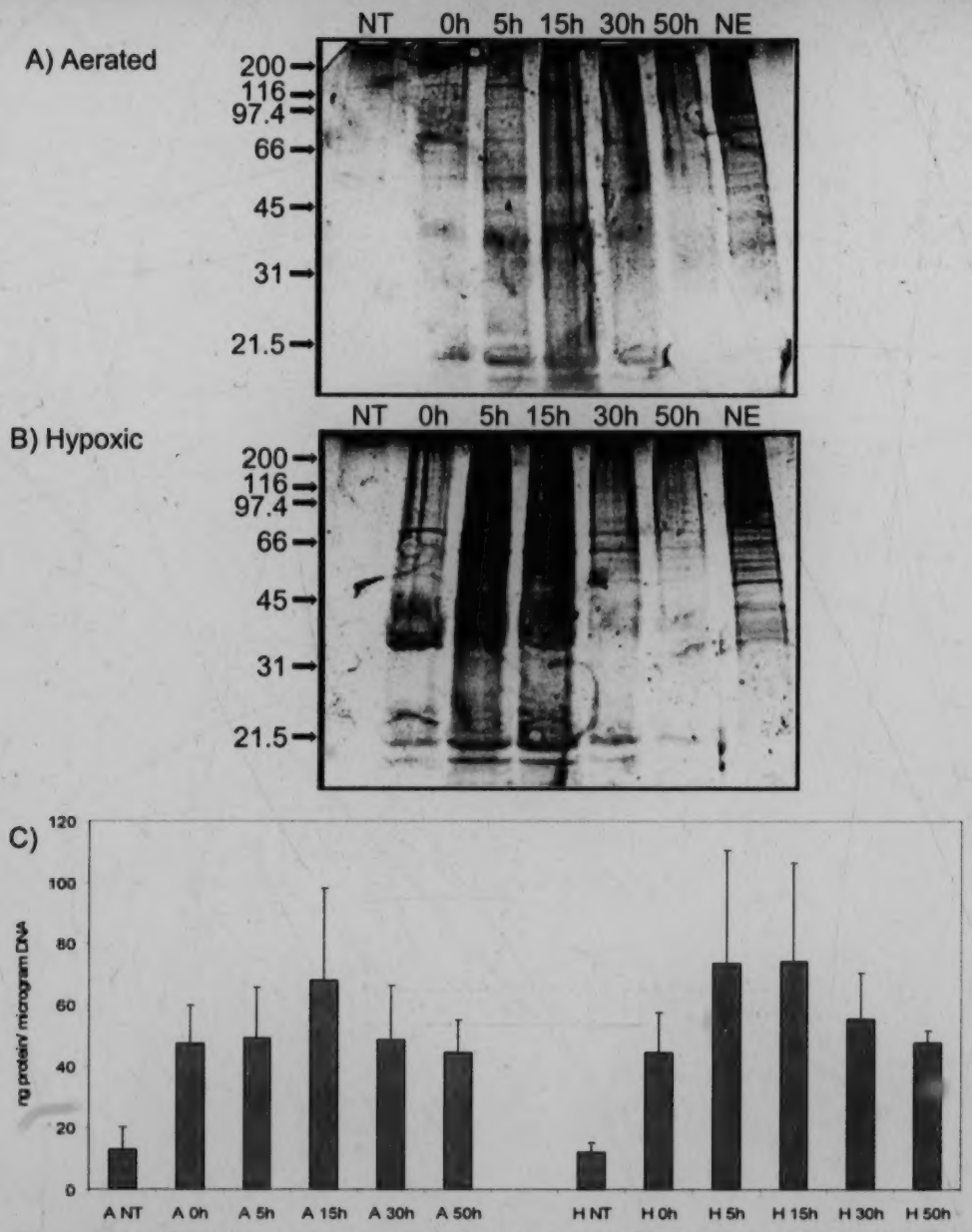

Figure 4-2: Time course of γ-radiation-induced DPCs in AA8 hamster cells, 0-50 h after 1.5 Gy

AA8 CHO cells received no treatment "NT" or were exposed to 1.5 Gy of γ-radiation under either aerated (A) or hypoxic (B) conditions. Cells were either processed immediately or were further incubated for 5-50 h. DPCs were isolated, analyzed, and quantitated (C) as detailed in Figure 4-1. The data in panel C represent the means and standard errors of 7 independent experiments. The MW markers are indicated in kDa. The time (h) after treatment is indicated above each lane. The "NE" lane is a total nuclear extract.

irs1SF cell line is deficient in the XRCC3 protein, which is a homolog of the HRR protein RAD51, and is also involved in HRR, but not in NER [30]. Cells received either no treatment or were exposed to 1.5 Gy of γ-rays under either aerated or hypoxic conditions and were further incubated at 37°C for 0, 5, 15, 30 or 50 h. DPCs were isolated, analyzed, and quantitated as above. Representative gels are shown for UV41 cells in Figures 4-3A and B, for UV20 cells in Figures 4-4A and B, and for irs1SF cells in Figures 4-5A and B. Quantitations of 4 (UV41, irs1SF) or 3 (UV20) separate experiments were performed and the averaged data are shown in the third panel of each figure (4-3C, 4-4C, and 4-5C). For each of the three mutant cell lines a greater level of DPC induction was apparent in the cells irradiated under hypoxic conditions. Furthermore, all three mutant cell lines demonstrated a slower removal of DPCs than that seen in the parental AA8 cell line. Indeed, by 50 h after irradiation, none of the mutant cell lines demonstrated a significant decrease in DPC levels compared with their peak values. Interestingly, the mutant cell lines differed with respect to the total level of DPCs induced, and the DPC levels in the mutants were invariably lower than those seen in the parental cell line.

4.3.d. Time course of individual DPCs in normal mammalian cells

The time course of crosslinking of individual proteins to DNA was also examined by Western blotting. The SDS-PAGE gels from the quantitation analyses were de-stained and the proteins were transferred to a nitrocellulose membrane. The blots were probed with antibodies to three proteins that we had previously shown (see Chapter 3) to be crosslinked to DNA following γ-radiation

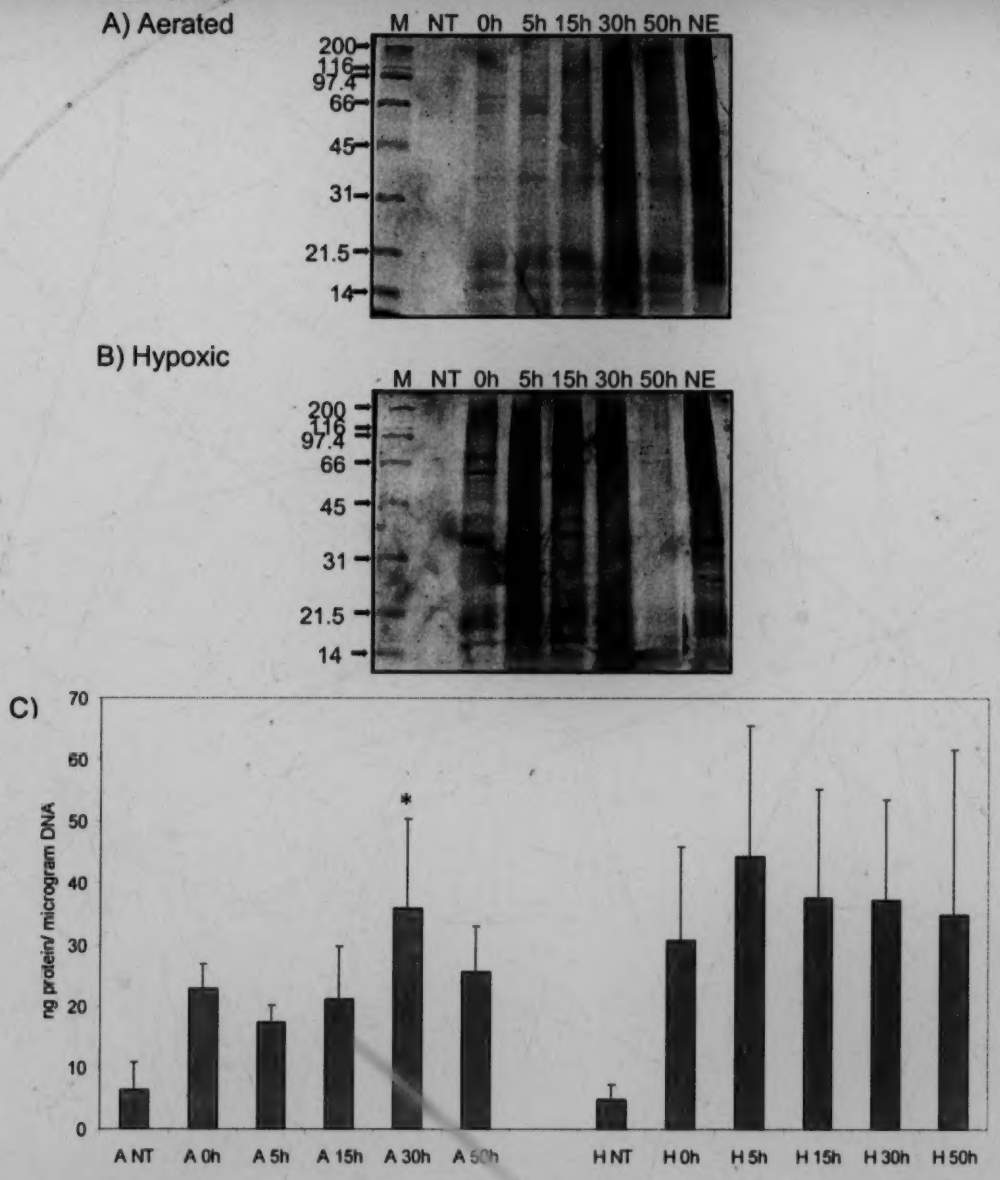

Figure 4-3: Time course of γ-radiation-induced DPCs in UV41 hamster cells, 0-50 h after 1.5 Gy

UV41 CHO cells either received no treatment "NT" or were exposed to 1.5 Gy of γ-rays under either aerated (A) or hypoxic (B) conditions. Cells were either processed immediately (no treatment and 0 h time point) or were further incubated for 5-50 h. DPCs were isolated, analyzed, and quantitated (C) as detailed in Figure 4-1. The data in panel C represent the means and standard errors of 4 independent experiments. The "M" lane represents the MW markers, indicated in kDa. The time (h) after treatment is indicated above each lane. The "NE" lane is a total nuclear extract. * indicates that the peak DPC yield is significantly different from the "NT" sample.

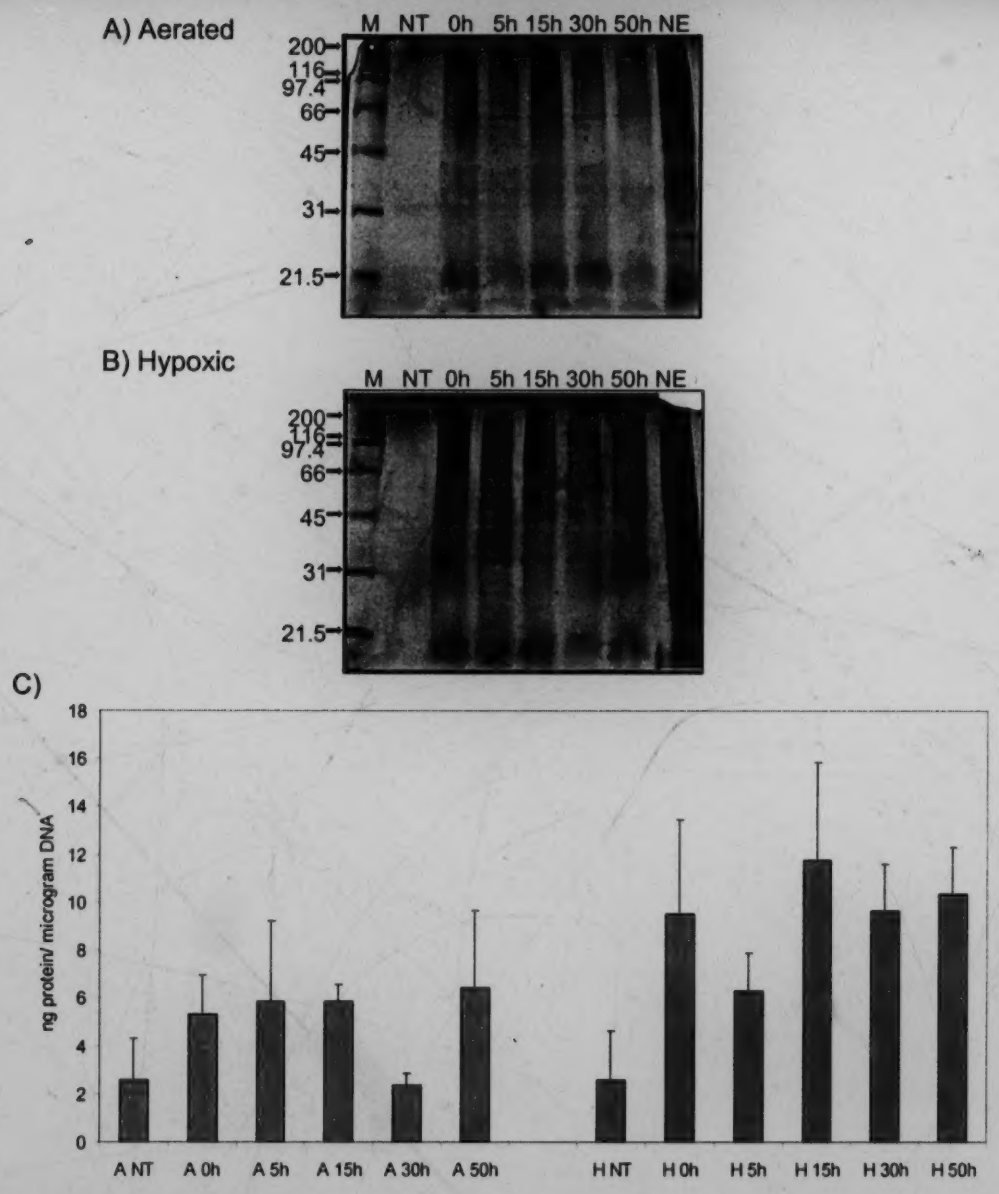

Figure 4-4: Time course of γ-radiation-induced DPCs in UV20 hamster cells, 0-50 h after 1.5 Gy

UV20 CHO cells either received no treatment "NT" or were exposed to 1.5 Gy of γ-rays under either aerated (A) or hypoxic (B) conditions. Cells were either processed immediately or were further incubated for 5-50 h. DPCs were isolated, analyzed, and quantitated (C) as detailed in Figure 4-1. The data in panel C represent the means and standard errors of 3 independent experiments. The "M" lane represents the MW markers, indicated in kDa. The time (h) after treatment is indicated above each lane. The "NE" lane is a total nuclear extract.

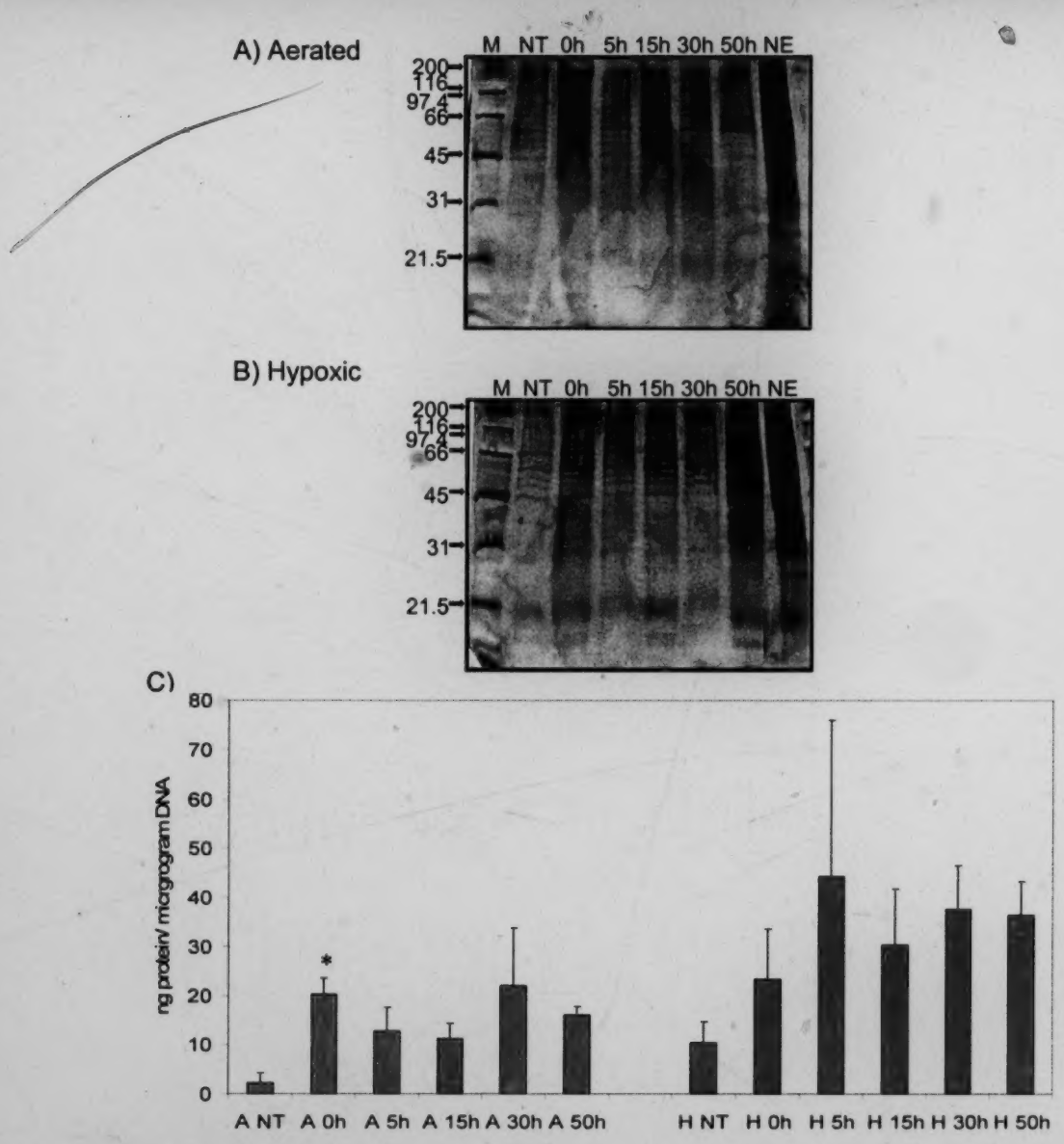

Figure 4-5: Time course of γ-radiation-induced DPCs in irs1SF hamster cells, 0-50 h after 1.5 Gy

Irs1SF CHO cells either received no treatment "NT" or were exposed to 1.5 Gy of γ-rays under either aerated (A) or hypoxic (B) conditions. Cells were either processed immediately or were further incubated for 5-50 h. DPCs were isolated, analyzed, and quantitated (C) as detailed in Figure 4-1. The data in panel C represent the means and standard errors of 4 independent experiments. The "M" lane represents the MW markers, indicated in kDa. The time (h) after treatment is indicated above each lane. The "NE" lane is a total nuclear extract. * indicates that the peak DPC yield is significantly different from the "NT" sample.

exposure, namely vimentin (Figure 4-6A), PARP (Figure 4-6B), and histone H2B (Figure 4-6C). These blots demonstrate that individual proteins are crosslinked to DNA and that this crosslinking exhibits a very different oxygen dependence for the different proteins. Thus, vimentin and PARP both appeared to be crosslinked to DNA to a greater degree under aerated conditions, while the opposite was true for histone H2B. The crosslinks were also removed with different kinetics; for example, vimentin and PARP crosslinks appeared to persist for up to 50 h, while the crosslinking of histone H2B peaked by 5 h post-γ-radiation and was almost resolved by 50 h.

4.3.e. Time course of low-dose γ-radiation-induced DPCs in mammalian cells

We modified the DPC time course analysis to examine an extended time period and a lower dose of γ-radiation. CHO AA8 cells received no treatment or were exposed to 0.5 Gy of γ-rays under either aerated or hypoxic conditions, and the cells were further incubated at 37°C for 0, 5, 15, 30, 50, 72 or 96 h. DPCs were isolated using the DNAzol-Silica method and analyzed by SDS-PAGE. DPC quantitation using SYPRO Tangerine fluorescence was performed for 7 independent experiments for both aerated (Figure 4-7A) and hypoxic (Figure 4-7B) conditions. An interesting trend in DPC induction was observed at this low dose (0.5 Gy). DPC induction under both aerated and hypoxic conditions peaked immediately after irradiation and then declined for 15 h, but then increased again at 24 h after irradiation before decreasing again by 96 h.

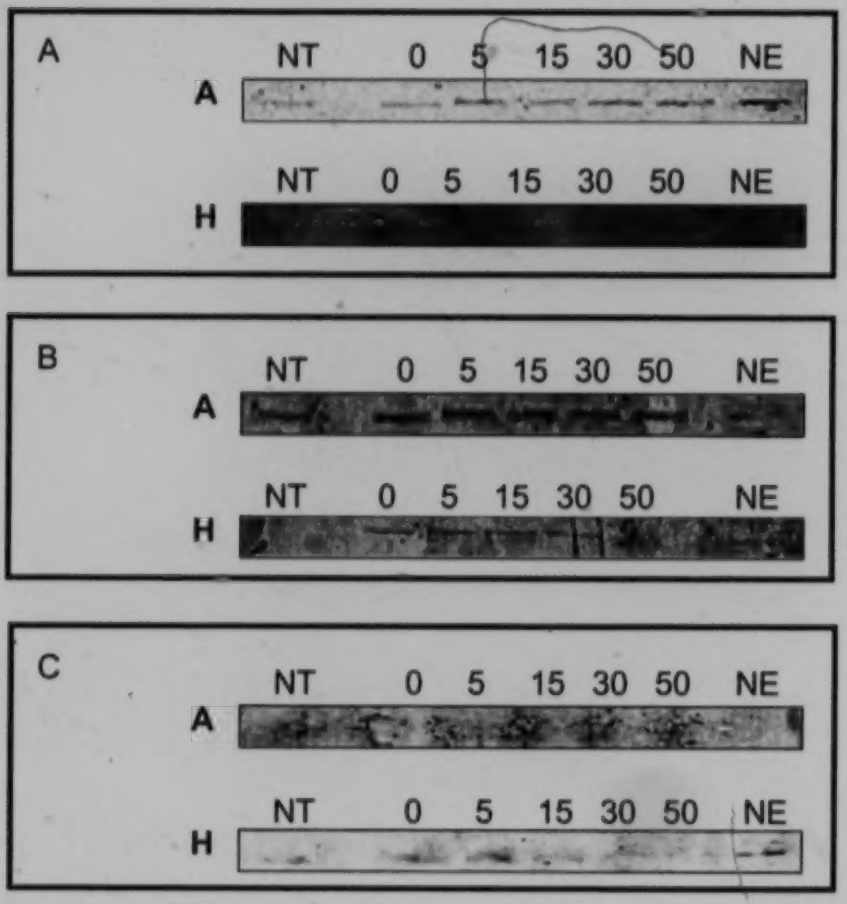

Figure 4-6: Time course of individual γ-radiation-induced DPCs in AA8 hamster cells, 0-50 h after 1.5 Gy

After Typhoon analysis of 1-D SDS-PAGE gels of DPC samples from Figure 4-2, the gels (A-aerated and H-hypoxic) were transferred to nitrocellulose and probed with antibodies to vimentin (A), PARP (B), or histone H2B (C). Fluorescent-secondary antibodies were used and blots were analyzed using a LI-COR odyssey infra-red imager. The time after treatment (h) is indicated above each sample. The no treatment "NT" sample and the total nuclear extract "NE" are also shown.

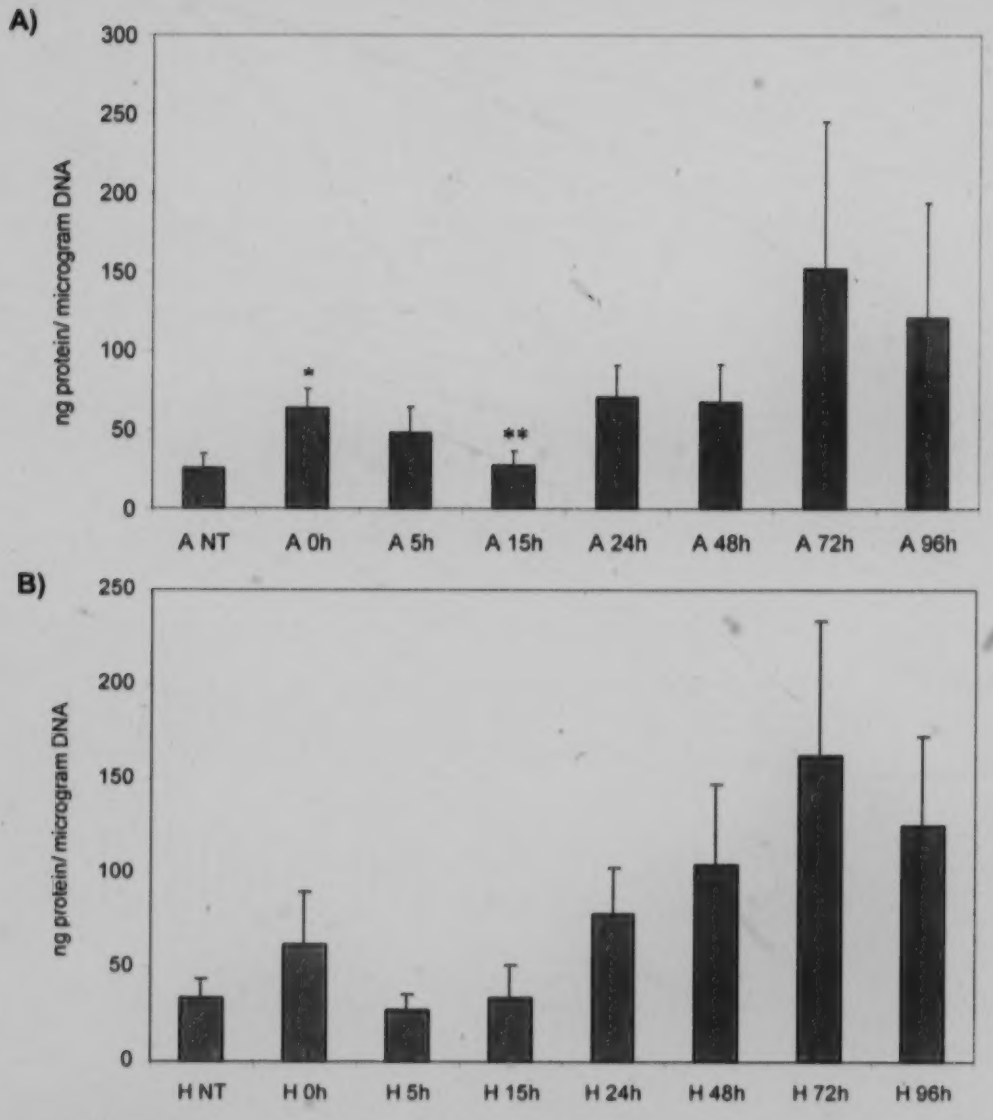

Figure 4-7:Time course of γ-radiation-induced DPCs in AA8 hamster cells, 0-96 h after 0.5 Gy

AA8 CHO cells either received no treatment "NT" or were exposed to 0.5 Gy of γ-rays under either aerated or hypoxic conditions. Cells were either processed immediately or were further incubated for 5-96 h. DPCs were isolated, analyzed, and quantitated (A-aerated, B-hypoxic) as detailed in Figure 4-1. The data represent the means and standard errors of 7 independent experiments. * indicates that the 0 h value is significantly different from the "NT" sample and ** indicates that the 15 h value is significantly different from the 0 h value.

4.4. Discussion

As noted in the Introduction, it is very difficult, based on the existing literature, to develop any real consensus as to the stability and repairability of DPCs induced by various genotoxic agents in mammalian cells. This problem is partly a result of differences in DPC chemistry, isolation methods, cell lines and DPC-inducing agents. Many previous DPC studies used either the alkaline elution or nitrocellulose filter binding assays. These methods and their various modifications have quite different abilities to resolve IR-induced DPCs, and almost invariably require high (supralethal) doses of IR. Indeed, two different groups [21,31] have reported that doses of 50-60 Gy were required to be able to follow the repair of crosslinked proteins using filter-binding techniques over a 24 h period.

The DNAzol-Silica method used in the present study can readily detect IR-induced DPCs in both aerated and hypoxic cells after low doses (~1 Gy) [27] and therefore enables, for the first time, the study of DPC induction and repair in various cell lines following exposure to biologically-relevant doses of IR. It should also be noted that the confluency (85%) of the cells at the time of irradiation would be sufficient to limit the contribution of cell doubling to the dilution of DPCs. The DPC isolation method was first used to confirm the reported short life-time of ~12.5 h for formaldehyde-induced DPCs that has previously been observed in mammalian cells [17]. We observed that formaldehyde-induced DPCs in parental CHO cells were maximal immediately after a 1-h treatment and were removed almost completely within 15 h of

treatment (Figure 4-1), whereas the formation of DPCs induced by 1.5 Gy of γ-radiation peaked by ~15 h and persisted at above background levels for up to 50 h after irradiation (Figure 4-2). At a dose of 0.5 Gy, DPCs were found to persist in these parental cells up to 96 h after irradiation and surprisingly to exhibit two peaks of induction (Figure 4-7). The prolonged presence and even an increase in DPC induction over a period of hours to days post-treatment has been reported previously for DPCs induced by chromium [32], ferric nitriloacetate [14], and UV [11,33].

The early and extended γ-radiation-induced DPC formation may be due to immediate versus delayed/secondary effects of IR, respectively. Crosslinking reactions can occur by a number of chemistries and therefore on a number of timescales. The immediate DNA-damaging events associated with γ-radiation exposure presumably involve the rapid, local generation of many ROS and other radicals, and especially of hydroxyl radicals, which can then react with DNA or protein directly, potentially causing the crosslinking of these two biomolecules if they are in close contact. Processes that occur on a longer time scale as a result of exposure to IR include the post-irradiation generation of hydrogen peroxide, which creates additional hydroxyl radicals, and the generation of reactive but relatively stable molecules such as aldehydes through the activity of lipid peroxidation processes. Protein hydroperoxides generated from protein attack by IR-induced hydroxyl radicals have also been shown to have a lifetime of days [34,35], and it is possible that these species are later converted back to

reactive/crosslinkable species, e.g., through the intermediacy of redox-active transition metal ions such as copper (I) and iron (II).

Other studies have also detected an increased association of protein with DNA over a period of hours following irradiation, but have suggested that this increase is not due to the formation of covalent DPCs, but is instead due to the reorganization of chromatin in response to damage [10]. Chiu *et al.* [36,37] also proposed that a re-organization of chromatin occurs during DPC repair. They suggested that changes in the interaction of DNA with the nuclear matrix occur based on the observation that DPCs induced immediately after IR exposure are enriched in actively transcribing sequences, but this enrichment falls off during the post-IR incubation period [37]. They proposed that DNA loops are reeled into the nuclear matrix scaffold for repair and that DPCs might contribute to cell killing if their repair is inhibited [36]. These authors also speculated that DPCs may be induced to a greater extent in open chromatin because there is more space for proteins to access the DNA and because there is also greater water solvation of these regions that would result in an increased local production of hydroxyl radicals after irradiation. The re-organization of chromatin may in fact be in response to damage or an attempt to repair damage, but it may lead to the induction of additional DPCs if there are still reactive sites or species present. Indeed, crosslinking of DNA repair proteins to repair intermediates, such as abasic sites, has been previously reported [38,39].

The quantitation of DPC induction in HRR and NER/HRR -deficient cell lines (Figures 4-3, 4-4, and 4-5) indicated that the total amount of protein

crosslinked by γ-radiation under either aerated or hypoxic conditions is lower than that in parental cells (Figure 4-2). It is difficult to explain this unexpected observation. One possibility is that this effect may be caused by a decreased availability of proteins for crosslinking reactions in the mutant cells. Previous studies have noted differences in chromatin structure and nuclear matrix protein composition in radiosensitive cells. Maranon *et al.* [40] have shown that radiosensitive IRS-20 cells have a more open chromatin conformation, as demonstrated by the increased sensitivity to DNase I digestion, suggesting fewer sites in association with proteins. Some radiosensitive mutants [41] have been shown to be deficient in nuclear matrix proteins and to have an impaired ability to rewind their DNA after irradiation. In fact, Malyapa *et al.* [41] proposed that the stability of anchorage sites determines the radiosensitivity of cells. Alterations in chromatin structure have also been suggested to underlie the radiosensitivity of the xrs-5 mutant CHO cell line [42].

Alternatively, it may be that deficiency of a particular DNA repair protein leads to increased sensitivity to DPC induction (or indeed lack of DPC removal) not because that particular DNA repair pathway is involved in the removal of these lesions, but because that repair protein is somehow involved in the formation of nuclear matrix anchorage complexes or in the chromatin remodeling steps required to access damage for repair. It has been suggested [43] that modification of chromatin structure is an early response to DNA damage and would be the starting point for mobilization of the downstream effectors of repair. Absence of a protein involved in nuclear matrix anchoring or chromatin

modification might result in fewer opportunities for DPC induction because of a reduction in DNA-bound protein complexes, but would also result in reduced repair of DPCs because of the failure to move the DNA loops into position for repair or in failure to modify the chromatin structure to allow access by repair proteins. It may be that crosslinking of specific proteins is detrimental to the cell in that repair proteins may be sequestered and the contribution of DPCs to cell killing is due to the sequestration of proteins required for the repair of other types of damage. Certainly, several proteins in these functional categories have been shown to be crosslinked to DNA by γ-radiation [44] (see Chapter 3 of this thesis).

A limited removal of DPCs generated under aerated or hypoxic conditions was observed in the HRR and NER/HRR -deficient cells (see Figure 4-8 for data comparison). It may be that DPCs are in fact repaired predominantly by the HRR pathway and this accounts for the lack of repair in both the NER/HRR-deficient cells and the HRR-deficient cells. However, the repair of DPCs is likely to be more complex; DPCs may be substrates for repair by HRR or NER. The XPF and ERCC1 proteins, in addition to their role in HRR/crosslink repair, are also components of the NER pathway; therefore, we evaluated NER/HRR mutants and not strictly NER mutants. As well, other removal mechanisms (e.g., proteolysis; see section 1.9-d of Chapter 1 of this thesis) may alter the repair path utilized. Indeed, loss of formaldehyde-induced DPCs in human cells was seen to decrease in normal human or XPA cells treated with a proteasome inhibitor [17], suggesting involvement of proteolysis in DPC removal. However,

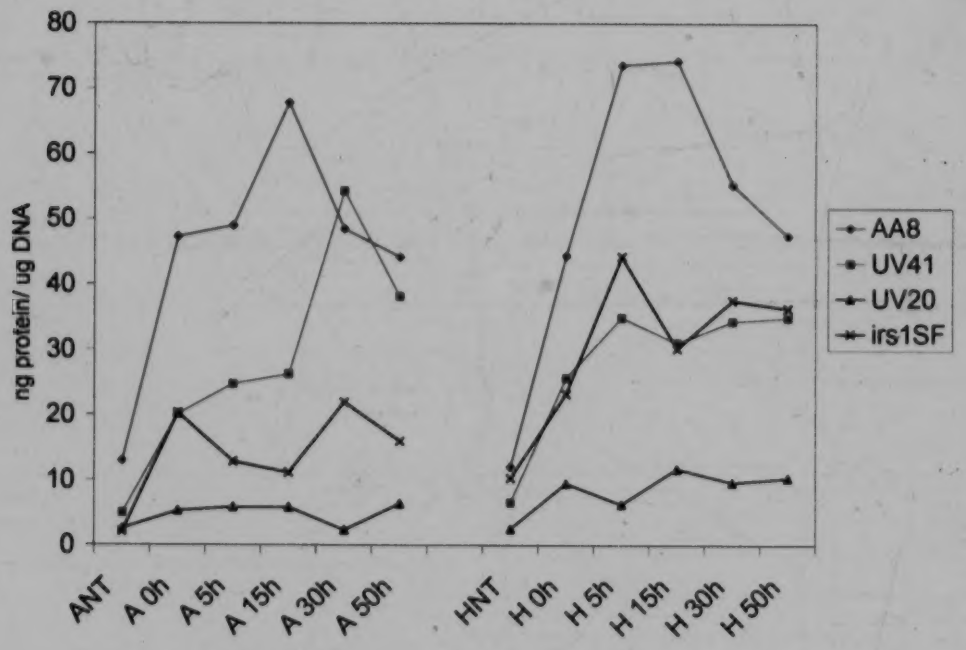

Figure 4-8: Time course comparisons of γ-radiation-induced DPCs in AA8, UV41, UV20, and irs1SF hamster cells, 0-50 h after 1.5 Gy

The data from figures 4-2, 4-3, 4-4, and 4-5 have been plotted together for comparison purposes.

the inhibition of proteolysis can itself directly impact on DNA repair pathways [45].

Further complicating matters is the fact that many DPC-inducing agentscan induce more than one chemical type of DPC. The conflicting reports on DPC repair may therefore reflect differential repair based on DPC chemistry. The NER pathway does exhibit a preference for particular types of DPCs; for example, a DPC generated from an apurinic/apyrimidinic site was incised more effectively than were DPCs generated from a γ-hydroxypropanodeoxyguanosine adduct [24]. The size of the adducted protein/peptide also influenced the effectiveness of *E. coli* UvrABC incision as an intermediate sized adduct (12 amino acids) was incised more effectively than a small (4 amino acid) or a large (16 kDa T4 pyrimidine dimer glycosylase-apurinic/apyrimidinic site lyase protein) adduct [24]. These results allow for the possibility that a DPC might first be acted upon by a proteolytic pathway to reduce the size of the protein moiety to a more manageable peptide that can be processed by the NER complex. Other factors may affect DPC repair pathway choice; for example, the HRR pathway requires the availability of homologous sequence. As will be discussed in section 6.6 of Chapter 6, the role of another pathway that is important for the repair of IR-induced DNA damage, i.e., non-homologous end-joining, in DPC repair is unknown but should be elucidated as it may be possible that DPCs are converted to DSBs as has been proposed for ICLs. It is also possible that the first step toward DPC generation involves base damage, which can be acted upon by the

BER pathway, thus preventing DPC induction; therefore, the involvement of this pathway in DPC repair should also be determined.

In summary, it is clear that γ-radiation-induced cellular DPCs are not as rapidly repaired as other forms of DNA damage. These lesions appear to be relatively long lived and can remain in the genome for days after treatment. NER/HRR-deficient cells demonstrate a limited removal of DPCs induced under either aerated or hypoxic conditions; thus, the involvement of these repair pathways warrants further investigation. At this point we could speculate that it is not the **gross** initial or residual DPC levels that determine the consequences of DPC induction as the total yields are higher in the parental cells, but that it is the extent of and/or persistence of the crosslinking of **particular** proteins that is detrimental. It may be that crosslinking of particular proteins prevents these or other lesions from being repaired or in some way activates or inhibits an important cellular event (e.g., signaling or chromatin anchoring/remodeling). Determining the biological relevance of the crosslinking of proteins to DNA will require further detailed study of the crosslinking of individual proteins involved in DPCs.

References for Chapter 4

[1] S.L. Barker, M. Weinfeld and D. Murray DNA-protein crosslinks: their induction, repair and biological consequences, Mutat. Res. 589 (2005) 111-135.

[2] V. Voitkun and A. Zhitkovich Analysis of DNA-protein crosslinking activity of malondialdehyde in vitro, Mutat. Res. 424 (1999) 97-106.

[3] R. Olinski, Z. Nackerdien and M. Dizdaroglu DNA-protein cross-linking between thymine and tyrosine in chromatin of gamma-irradiated or H_2O_2-treated cultured human cells, Arch. Biochem. Biophys. 297 (1992) 139-143.

[4] E. Gajewski, A.F. Fuciarelli and M. Dizdaroglu Structure of hydroxyl radical-induced DNA-protein crosslinks in calf thymus nucleohistone in vitro, Int. J. Radiat. Biol. 54 (1988) 445-459.

[5] M. Dizdaroglu, E. Gajewski, P. Reddy and S.A. Margolis Structure of a hydroxyl radical induced DNA-protein cross-link involving thymine and tyrosine in nucleohistone, Biochemistry 28 (1989) 3625-3628.

[6] Z. Nackerdien, G. Rao, M.A. Cacciuttolo, E. Gajewski and M. Dizdaroglu Chemical nature of DNA-protein cross-links produced in mammalian chromatin by hydrogen peroxide in the presence of iron or copper ions, Biochemistry 30 (1991) 4873-4879.

[7] A.E. Cress and K.M. Kurath Identification of attachment proteins for DNA in Chinese hamster ovary cells, J. Biol. Chem. 263 (1988) 19678-19683.

[8] A.E. Cress and G.T. Bowden Covalent DNA-protein crosslinking occurs after hyperthermia and radiation, Radiat Res 95 (1983) 610-619.

[9] W. Krauth and D. Werner Analysis of the most tightly bound proteins in eukaryotic DNA, Biochim Biophys Acta 564 (1979) 390-401.

[10] A.E. Cress, K.M. Kurath, M.J. Hendrix and G.T. Bowden Nuclear protein organization and the repair of radiation damage, Carcinogenesis 10 (1989) 939-943.

[11] S.M. Chiu, N.M. Sokany, L.R. Friedman and N.L. Oleinick Differential processing of ultraviolet or ionizing radiation-induced DNA-protein cross-links in Chinese hamster cells, Int J Radiat Biol Relat Stud Phys Chem Med 46 (1984) 681-690.

[12] M. Sugiyama, S.R. Patierno, O. Cantoni and M. Costa Characterization of DNA lesions induced by CaCrO4 in synchronous and asynchronous cultured mammalian cells, Mol Pharmacol 29 (1986) 606-613.

[13] M.J. Tsapakos, T.H. Hampton and K.E. Wetterhahn Chromium(VI)-induced DNA lesions and chromium distribution in rat kidney, liver, and lung, Cancer Res 43 (1983) 5662-5667.

[14] S. Toyokuni, T. Mori, H. Hiai and M. Dizdaroglu Treatment of Wistar rats with a renal carcinogen, ferric nitrilotriacetate, causes DNA-protein cross-linking between thymine and tyrosine in their renal chromatin, Int J Cancer 62 (1995) 309-313.

[15] J.R. Kuykendall and M.S. Bogdanffy Efficiency of DNA-histone crosslinking induced by saturated and unsaturated aldehydes in vitro, Mutat Res 283 (1992) 131-136.

[16] J.R. Kuykendall and M.S. Bogdanffy Reaction kinetics of DNA-histone crosslinking by vinyl acetate and acetaldehyde, Carcinogenesis 13 (1992) 2095-2100.
[17] G. Quievryn and A. Zhitkovich Loss of DNA-protein crosslinks from formaldehyde-exposed cells occurs through spontaneous hydrolysis and an active repair process linked to proteosome function, Carcinogenesis 21 (2000) 1573-1580.
[18] J.R. Horton and X. Cheng PvuII Endonuclease contains two calcium ions in active sites, J. Mol. Biol. 300 (2000) 1049-1056.
[19] G. Speit, P. Schutz and O. Merk Induction and repair of formaldehyde-induced DNA-protein crosslinks in repair-deficient human cell lines, Mutagenesis 15 (2000) 85-90.
[20] A.J. Fornace, Jr. and D.S. Seres Repair of trans-Pt(II) diamminedichloride DNA-protein crosslinks in normal and excision-deficient human cells, Mutat Res 94 (1982) 277-284.
[21] R.E. Meyn, S.C. vanAnkeren and W.T. Jenkins The induction of DNA-protein crosslinks in hypoxic cells and their possible contribution to cell lethality, Radiat. Res. 109 (1987) 419-429.
[22] M. Reynolds, E. Peterson, G. Quievryn and A. Zhitkovich Human nucleotide excision repair efficiently removes chromium-DNA phosphate adducts and protects cells against chromate toxicity, J Biol Chem 279 (2004) 30419-30424.
[23] R. Gantt A cell cycle-associated pathway for repair of DNA-protein crosslinks in mammalian cells, Mutat Res 183 (1987) 75-87.
[24] I.G. Minko, A.J. Kurtz, D.L. Croteau, B. Van Houten, T.M. Harris and R.S. Lloyd Initiation of repair of DNA-polypeptide cross-links by the UvrABC nuclease, Biochemistry 44 (2005) 3000-3009.
[25] I.G. Minko, Y. Zou and R.S. Lloyd Incision of DNA-protein crosslinks by UvrABC nuclease suggests a potential repair pathway involving nucleotide excision repair, Proc Natl Acad Sci U S A 99 (2002) 1905-1909.
[26] C.J. Koch, C.C. Stobbe and E.A. Bump The effect on the Km for radiosensitization at 0 degree C of thiol depletion by diethylmaleate pretreatment: quantitative differences found using the radiation sensitizing agent misonidazole or oxygen, Radiat Res 98 (1984) 141-153.
[27] S.L. Barker, D. Murray, J. Zheng, L. Li and M. Weinfeld A method for the isolation of covalent DNA-protein crosslinks suitable for proteomics analysis, Anal. Biochem. In Press (2005).
[28] M.S. Elphinstone, G.N. Hinten, A. M.J. and N. C.J. An inexpensive and high-throughput procedure to extract and purify total genomic DNA for population studies, Mol. Ecol. Notes 3 (2003) 317-320.
[29] D. Murray and E. Rosenberg The importance of the ERCC1/ERCC4[XPF] complex for hypoxic-cell radioresistance does not appear to derive from its participation in the nucleotide excision repair pathway, Mutat. Res. 364 (1996) 217-226.
[30] L.F. Fuller and R.B. Painter A Chinese hamster ovary cell line hypersensitive to ionizing radiation and deficient in repair replication, Mutat Res 193 (1988) 109-121.

[31] S.M. Chiu, L.R. Friedman and N.L. Oleinick The fate of DNA-protein crosslinks formed in gamma-irradiated metaphase cells, Int J Radiat Biol 58 (1990) 235-247.
[32] S.N. Mattagajasingh and H.P. Misra Mechanisms of the carcinogenic chromium(VI)-induced DNA-protein cross-linking and their characterization in cultured intact human cells, J. Biol. Chem. 271 (1996) 33550-33560.
[33] B.S. Rosenstein, D. Subramanian and M.T. Muller The involvement of topoisomerase I in the induction of DNA-protein crosslinks and DNA single-strand breaks in cells of ultraviolet-irradiated human and frog cell lines, Radiat Res 148 (1997) 575-579.
[34] S. Gebicki and J.M. Gebicki Crosslinking of DNA and proteins induced by protein hydroperoxides, Biochem J 338 (Pt 3) (1999) 629-636.
[35] M. Quintiliani The oxygen effect in radiation inactivation of DNA and enzymes, Int J Radiat Biol Relat Stud Phys Chem Med 50 (1986) 573-594.
[36] S. Chiu, L. Xue, L.R. Friedman, U. Balasubramaniam and N.L. Oleinick DNA-protein crosslinks: formation and repair in irradiated cells, in: D.H. U. Hagen, H. Jung and C. Streffer (Ed.), Radiation Research 1895-1995, Congress Proceedings, Volume 2: Congress Lectures, Universitatsdruckerei H. Sturtz AG, Wurzburg, Germany, 1996, pp. 400-403.
[37] S.M. Chiu, L.R. Friedman, N.M. Sokany, L.Y. Xue and N.L. Oleinick Nuclear matrix proteins are crosslinked to transcriptionally active gene sequences by ionizing radiation, Radiat Res 107 (1986) 24-38.
[38] M.S. DeMott, E. Beyret, D. Wong, B.C. Bales, J.T. Hwang, M.M. Greenberg and B. Demple Covalent trapping of human DNA polymerase beta by the oxidative DNA lesion 2-deoxyribonolactone, J. Biol. Chem. 277 (2002) 7637-7640.
[39] K.M. Kroeger, M. Hashimoto, Y.W. Kow and M.M. Greenberg Cross-linking of 2-deoxyribonolactone and its beta-elimination product by base excision repair enzymes, Biochemistry 42 (2003) 2449-2455.
[40] D.G. Maranon, A.O. Laudicina and M. Muhlmann In situ DNAse I sensitivity assay indicates DNA conformation differences between CHO cells and the radiation-sensitive CHO mutant IRS-20, Cytogenet Genome Res 104 (2004) 100-103.
[41] R.S. Malyapa, W.D. Wright and J.L. Roti Roti DNA supercoiling changes and nucleoid protein composition in a group of L5178Y cells of varying radiosensitivity, Radiat. Res. 145 (1996) 239-242.
[42] J.L. Schwartz, J.M. Cowen, E. Moan, B.A. Sedita, J. Stephens and A.T. Vaughan Metaphase chromosome and nucleoid differences between CHO-K1 and its radiosensitive derivative xrs-5, Mutagenesis 8 (1993) 105-108.
[43] S.P. Jackson Detecting, signalling and repairing DNA double-strand breaks, Biochem Soc Trans 29 (2001) 655-661.
[44] S.L. Barker, M. Weinfeld, L. Li, J. Zheng and D. Murray The identification of mammalian proteins crosslinked to DNA by ionizing radiation, (2005).
[45] W.H. McBride, K.S. Iwamoto, R. Syljuasen, M. Pervan and F. Pajonk The role of the ubiquitin/proteasome system in cellular responses to radiation, Oncogene 22 (2003) 5755-5773.

Chapter 5: Conclusions

IR is an important environmental risk factor for various cancers and paradoxically is also a major therapeutic agent for cancer treatment. However, the exact mechanisms by which exposure to this agent lead to its various harmful and useful effects on biological systems is less clear. Exposure of mammalian cells to IR induces several types of damage to DNA, including DSBs, SSBs, base and sugar damage, as well as DNA interstrand crosslinks and DPCs. As outlined in Chapter 1, not much is known regarding the contribution of DPCs to the biological consequences of exposure to IR, in part because these lesions are not yet well characterized. What has been reported about IR-induced crosslinks is that more than one form of this lesion is induced [1-10], these lesions are induced preferentially when oxygen levels are very low [11-13], and that while the induction of DPCs inversely correlates with cell killing [14] it may be a useful target for modulating the effectiveness of radiotherapy [11]. There is great variability in the literature as to the consequences, half-lives, and proposed repair pathways for DPCs induced by various agents. The different crosslink chemistries are likely to affect the stability and repair of these lesions as well as their biological impact. Furthermore, a number of different methods have been used for analysis of these lesions. To exploit these types of lesion for therapeutic advantage it will be necessary to further characterize their properties in much greater detail.

The existing methods for DPC isolation were not stringent enough for identification of truly crosslinked proteins due to high levels of contamination with non-crosslinked proteins [15]. Thus, the first challenge in our work was the

development of a novel method for the isolation of covalent DPCs from mammalian cells. The method that we developed, and which is described in Chapter 2, uses chaotropic agents to isolate genomic DNA and stringently remove non-crosslinked proteins, followed by nuclease digestion to release the covalently crosslinked proteins for further analysis. The technique generated high quality protein samples in sufficient quantities for analysis by MS. We also developed a modified form of this method, which additionally makes use of chaotropic agents for promoting the adsorption of DNA (with crosslinked proteins) to silica fines, which markedly reduced the DPC isolation time and cost. The SDS-PAGE analysis of DPC isolates demonstrated that the DPC isolation method was sufficiently stringent to strip non-covalent DNA-protein complexes from the DNA based on the consistently low level of protein observed in unirradiated samples. Perhaps for this reason, these methods can readily detect DPCs after γ-ray doses as low as 0.5 Gy. This can be compared with the alkaline elution/polycarbonate filter method or the nitrocellulose filter binding method that can reproducibly detect DPCs only at much higher radiation doses of ~50 Gy and ~30 Gy, respectively [16].

Next, as outlined in Chapter 3, we used this stringent DPC isolation procedure in combination with SDS-PAGE and MS, and identified 29 proteins that can be covalently crosslinked to DNA by IR in mammalian cells under aerated and/or hypoxic conditions [17]. The identified proteins include structural proteins, actin-associated proteins, transcription regulators, RNA splicing components, stress response proteins, cell cycle proteins, GDP/GTP binding

proteins, and proteins whose nuclear functions are not yet known. The involvement of several of these proteins (e.g., actin, histone H2B) in DPCs was confirmed using Western blot analysis. The demonstration of the crosslinking of these proteins to DNA indicates that they are in close contact with the DNA at the time of, or shortly after, irradiation. These findings may suggest new roles for some of these proteins in DNA metabolism, such as in DNA replication or repair, or in chromatin anchoring or remodelling processes.

Quantitation of DPCs was performed by staining 1-D SDS-PAGE gels with SYPRO Tangerine followed by analysis using fluorescence imaging. The dose-dependence of DPC induction revealed a linear relationship in mammalian cells under aerated and hypoxic conditions in the low-dose range (0-1.5 Gy), but appeared to plateau or even decrease at higher doses (2-4 Gy) (Figures 3-5 through 3-8). Previous studies have demonstrated a linear dose-dependence of IR-induced DPCs, but these studies used much higher doses, longer irradiation times, and greater dose increments than the present study and have employed very different DPC isolation methods. It is not unexpected that crosslinking of proteins to DNA might reach a saturation point as there are a finite number of proteins in the nucleus in contact with DNA. Individual proteins will be present at different levels and therefore their crosslinking would be anticipated to plateau at different doses and with differing amplitudes.

While previous studies [11-13] have demonstrated an increased level (1.5-5.5 fold [18]) of DPCs induced by IR under hypoxic conditions, there have also been reports that some IR-induced DPCs are induced independently of oxygen

status [2,10,19]. Perhaps this is not surprising considering that there are several chemically distinct types of DPCs formed by IR and that the formation of these various DPCs may be differentially influenced by the presence of oxygen. Proteins can in fact become crosslinked to DNA by several mechanisms. The immediate effects of IR (either through direct or indirect action) involve radical formation on either the protein or the DNA (or possibly both) and the subsequent reaction of these radicals with another macromolecule (protein or DNA). These types of reactions might be inhibited in the presence of oxygen because the DNA or protein radical could react with oxygen rather than a neighbouring protein or DNA atom. They might also be potentiated for some types of radicals. The delayed effects of IR include the generation of longer-lived species such as the products of the peroxidation of lipids, e.g., leading to the generation of DNA-reactive electrophilic aldehydes, which are potent DPC-inducers, as well as the generation of protein hydroperoxides [20-22] which, as discussed in Chapter 4, section 4.4, may later be converted to reactive species when they encounter redox-active transition metal ions. The generation of these various reactive intermediates differs in the reliance on oxygen. Some reactive intermediates (e.g., products of peroxidation) absolutely require molecular oxygen for their generation and therefore more of these potential crosslinking intermediates will be generated when oxygen is present, leading to an increase in these types of DPCs. In contrast, the generation of other radiochemical products (e.g., 8,5'-cycloadenosine) is independent of oxygen [23], whereas yet other species can be rapidly quenched by reaction with oxygen (e.g., to form a strand break) and

thus prevented from further reaction to form a DPC. These reactions will be occurring on different time scales as some of these reactions are diffusion dependent and the various reactive intermediates differ in their stabilities.

A major finding in this work was that, after low doses of IR (0.5–4 Gy), lesions involving some proteins were favoured by the presence of oxygen, some were suppressed, and some were not affected (see Chapter 3). This is very different from the general picture that has emerged from previous studies, which had two major problems: (1) use of high/supralethal doses (typically >10 Gy); and (2) an inability to look at individual proteins, thus imposing a misleading focus on gross lesions that we now know are extremely heterogeneous and have differing oxygen dependencies. The sensitive DPC isolation method developed here can now be combined with numerous other approaches (MS, protein separation and visualization, protein quantitations, Western blotting) for the re-evaluation of many aspects of DPC induction by low-dose IR (or other agents).

We also extended our analyses of DPC induction to examine the rate of DPC loss/removal from mammalian cells [24]. We confirmed that formaldehyde-induced DPCs were lost within 15 h of treatment (Figure 4-1). We also found that the level of IR-induced DPCs after 1.5 Gy of γ-radiation first increased and later decreased with time, but these lesions were much more persistent, remaining significantly above background levels as late as 50 h after irradiation (Figure 4-2). A longer time period was studied using a lower dose (0.5 Gy), and these data indicated that there may be a biphasic nature to the induction of DPCs, with a second peak of DPC induction occurring after ~24 h (Figure 4-7).

The mechanism of this second reaction phase possibly involves the production of protein hydroperoxides or other longer-lived reactive species. [21,22]. This may be the case for some aldehyde reactions as these reactive moieties can react with protein [25] generating a longer-lived protein-aldehyde intermediate which is still reactive and might subsequently react with DNA to result in a DPC.

The removal of IR-induced DPCs was also examined in repair-deficient mammalian cells to assess the involvement of NER/HRR in this process. Little decrease in DPC levels was seen in NER/HRR- or HRR-deficient cells under either aerated or hypoxic conditions (Figures 4-3 through 4-5); DPC levels remained fairly constant over the time period (up to 50 h) examined, while the DPC levels in the parental cells appeared to decrease over this same time period (Figure 4-2). The lifetime analyses suggest that DPCs are relatively long-lived lesions and that the HRR and NER pathways may be involved in their repair. However, improving the statistical validity of these conclusions will require additional experimentation.

Because of the collateral induction of other forms of damage, our understanding of the contribution of DPCs to the cytotoxic, mutagenic and carcinogenic effects of DPC-inducing agents has been elusive. It would be fair to say that IR-induced DPCs are poorly-characterized lesions and, as such, their biological consequences are not yet fully appreciated. DPCs may potentially block the progression of translocating replication, transcription and recombination complexes and may also prevent necessary manipulations of chromatin structure. The study of DPCs has been complicated by the variety of DPC

chemistries that are possible and by various limitations in DPC isolation and quantitation methods. Identification of proteins involved in IR-induced DPCs using the methodology developed in this thesis may thus be helpful in determining the consequences and repair of these lesions. The crosslinking of individual proteins needs to be further examined to determine which DPCs are of the greatest biological relevance. What is clear is the fact that IR-induced DPCs are not as rapidly repaired as other forms of damage. These lesions appear to be relatively long lived and persist for days after irradiation. NER/HRR- and HRR-deficient cells do demonstrate a trend towards showing impaired DPC removal. Further information regarding the mechanisms of the formation and removal of DPCs would help to delineate the biological relevance of this type of lesion, and may provide insights into cellular processes such as the interaction of the nuclear matrix with DNA metabolism. Determining the mechanisms by which DPCs are repaired may also provide information for developing successful cancer treatment strategies that overcome radioresistance in hypoxic tumours.

References for Chapter 5

[1] M. Dizdaroglu and E. Gajewski Structure and mechanism of hydroxyl radical-induced formation of a DNA-protein cross-link involving thymine and lysine in nucleohistone, Cancer Res. 49 (1989) 3463-3467.

[2] M. Dizdaroglu, E. Gajewski, P. Reddy and S.A. Margolis Structure of a hydroxyl radical induced DNA-protein cross-link involving thymine and tyrosine in nucleohistone, Biochemistry 28 (1989) 3625-3628.

[3] M. Dizdaroglu and M.G. Simic Radiation-induced crosslinking of cytosine, Radiat. Res. 100 (1984) 41-46.

[4] M. Dizdaroglu and M.G. Simic Radiation-induced crosslinks between thymine and phenylalanine, Int. J. Radiat. Biol. Relat. Stud. Phys. Chem. Med. 47 (1985) 63-69.

[5] E. Gajewski, A.F. Fuciarelli and M. Dizdaroglu Structure of hydroxyl radical-induced DNA-protein crosslinks in calf thymus nucleohistone in vitro, Int. J. Radiat. Biol. 54 (1988) 445-459.

[6] L.R. Karam, M. Dizdaroglu and M.G. Simic Intramolecular H atom abstraction from the sugar moiety by thymine radicals in oligo- and polydeoxynucleotides, Radiat. Res. 116 (1988) 210-216.

[7] S.A. Margolis, B. Coxon, E. Gajewski and M. Dizdaroglu Structure of a hydroxyl radical induced cross-link of thymine and tyrosine, Biochemistry 27 (1988) 6353-6359.

[8] R. Olinski, Z. Nackerdien and M. Dizdaroglu DNA-protein cross-linking between thymine and tyrosine in chromatin of gamma-irradiated or H_2O_2-treated cultured human cells, Arch. Biochem. Biophys. 297 (1992) 139-143.

[9] E. Gajewski and M. Dizdaroglu Hydroxyl radical induced cross-linking of cytosine and tyrosine in nucleohistone, Biochemistry 29 (1990) 977-980.

[10] Z. Nackerdien, G. Rao, M.A. Cacciuttolo, E. Gajewski and M. Dizdaroglu Chemical nature of DNA-protein cross-links produced in mammalian chromatin by hydrogen peroxide in the presence of iron or copper ions, Biochemistry 30 (1991) 4873-4879.

[11] R.E. Meyn, S.C. vanAnkeren and W.T. Jenkins The induction of DNA-protein crosslinks in hypoxic cells and their possible contribution to cell lethality, Radiat. Res. 109 (1987) 419-429.

[12] H. Zhang, C.J. Koch, C.A. Wallen and K.T. Wheeler Radiation-induced DNA damage in tumors and normal tissues. III. Oxygen dependence of the formation of strand breaks and DNA-protein crosslinks, Radiat. Res. 142 (1995) 163-168.

[13] L.Y. Xue, L.R. Friedman and N.L. Oleinick Repair of chromatin damage in glutathione-depleted V-79 cells: comparison of oxic and hypoxic conditions, Radiat. Res. 116 (1988) 89-99.

[14] S.L. Barker, M. Weinfeld and D. Murray DNA-protein crosslinks: their induction, repair and biological consequences, Mutat Res 589 (2005) 111-135.

[15] S.L. Barker, D. Murray, J. Zheng, L. Li and M. Weinfeld A method for the isolation of çovalent DNA-protein crosslinks suitable for proteomics analysis, Anal. Biochem. In Press (2005).

[16] I. Al-Nabulsi and K.T. Wheeler Temperature dependence of radiation-induced DNA-protein crosslinks formed under hypoxic conditions, Radiat Res 148 (1997) 568-574.

[17] S.L. Barker, M. Weinfeld, L. Li, J. Zheng and D. Murray The identification of mammalian proteins crosslinked to DNA by ionizing radiation, (2005).

[18] S. Chiu, L. Xue, L.R. Friedman, U. Balasubramaniam and N.L. Oleinick DNA-protein crosslinks: formation and repair in irradiated cells, in: D.H. U. Hagen, H. Jung and C. Streffer (Ed.), Radiation Research 1895-1995, Congress Proceedings, Volume 2: Congress Lectures, Universitatsdruckerei H. Sturtz AG, Wurzburg, Germany, 1996, pp. 400-403.

[19] E. Gajewski, G. Rao, Z. Nackerdien and M. Dizdaroglu Modification of DNA bases in mammalian chromatin by radiation-generated free radicals, Biochemistry 29 (1990) 7876-7882.

[20] J.P. Pouget and S.J. Mather General aspects of the cellular response to low- and high-LET radiation, Eur. J. Nucl. Med. 28 (2001) 541-561.

[21] M. Quintiliani The oxygen effect in radiation inactivation of DNA and enzymes, Int J Radiat Biol Relat Stud Phys Chem Med 50 (1986) 573-594.

[22] S. Gebicki and J.M. Gebicki Crosslinking of DNA and proteins induced by protein hydroperoxides, Biochem. J. 338 (1999) 629-636.

[23] A.F. Fuciarelli, C.J. Koch and J.A. Raleigh Oxygen dependence of product formation in irradiated adenosine 5'-monophosphate, Radiat Res 113 (1988) 447-457.

[24] S.L. Barker, D. Murray and M. Weinfeld Analysis of the stability and lifetime of IR-induced DPCs in mammalian cells, in preparation (2005).

[25] H. Esterbauer, R.J. Schaur and H. Zollner Chemistry and biochemistry of 4-hydroxynonenal, malonaldehyde and related aldehydes, Free Radic Biol Med 11 (1991) 81-128.

Chapter 6: Future Directions

6.1. Introduction

The data presented in this work have provided useful additional insights into the nature of IR-induced DPCs and have started to open up the possibility of understanding the biological impact of these lesions. There are, of course, many further questions to be answered before the full relevance of DPCs is clear.

6.2. Improved control over the study cell population

Several reports suggest that DPC induction, removal, or isolation may be affected by several factors:

6.2.a. Cell cycle

Metaphase cells do not form or repair DPCs at the same rate as asynchronous cells [1], and non-crosslinked proteins require less stringent methods for stripping from stationary cells than from proliferating cells [2,3]. In the present work, we used asynchronous cell populations. In the future, techniques such as centrifugal elutriation that separate cells into the different phases of the cell cycle should be interfaced with such studies. This will be particularly important for studies of DNA repair, as outlined in section 6.5.

6.2.b. Attachment

No repair of DPCs was observed in cells that were normally grown as a monolayer, but that were instead detached and grown in suspension [4]. In the present study, cells under hypoxic conditions were detached from the cell culture

plate and transferred to glass plates for the induction of hypoxia and subsequent irradiation. This was necessary in order to accommodate the large number of cells needed and the small size of the aluminium chambers. It would be of use to determine if this is in fact an issue and did affect the results obtained.

6.2.c. SV40 transformation

A difference in the rate of DPC repair was observed in non-transformed XPA cells versus SV40-transformed XPA cells [5]. This effect may be due to increased proliferation caused by virus transformation or it may be due to activation of some other cellular function (e.g., DNA damage responses) by the virus [5,6]. In the present study, we used a human SV40-transformed fibroblast line. It would be of interest to examine the influence of SV40 transformation on DPC induction and removal, and to extend this line of questioning to examine the influence of proliferation rate on DPC removal. As cells replicate, it is possible that translocating replication complexes trigger the recognition and repair of DPCs. It may also be the case that replication is arrested before the DPC can be reached because of steric constraints in the helix, creating a strand break upstream of the DPC, leading to recombinational repair of both the break and the DPC? It is known that another type of DPC, those induced by topoisomerase poisons, is more toxic in S-phase because it blocks progression of replication [7,8]. This type of DPC is also toxic when it blocks transcription [9]; therefore, it would be of interest to measure both the extent of replication and of transcription and their correlation with DPC induction and removal.

6.2.d. Apoptosis

Another parameter that has not been addressed in the present work is the extent of apoptosis induced and its relationship to the DPC levels in these cells. Because the hypoxic cells were not attached to the dish during treatment (see above discussion on attachment), dead cells were not washed away before DPC levels were quantitated. Hypoxic cells are known to be radioresistant and the IR dose used was not high enough to induce a large degree of cell death, but it might be informative to perform cell counts and Annexin V quantitations of apoptotic cells on the cell populations used for DPC analyses.

Thus, further studies should be conducted on more controlled cell populations. As well, a more complete picture of DPC induction and repair would be obtained by extending the analyses we performed to a larger range of human and hamster repair-proficient and -deficient cells.

6.3. DPC quantitation

The novel methods presented in this work offer a substantial improvement over existing methods in detection limit and purity of the isolated DPCs. The use of a quantitative fluorescent protein stain (SYPRO Tangerine) combined with the Imagequant 5.2 software allowed the quantitation of isolated DPCs. It would be of use to confirm the quantitation data by another method. The protein isolated in the DPC samples could be quantitated using a newer fluorescent protein stain, Deep Purple (GE Healthcare) (Figure 6-1, top panel), which is more sensitive than the Bradford reagent. As with the SYPRO Tangerine staining, samples

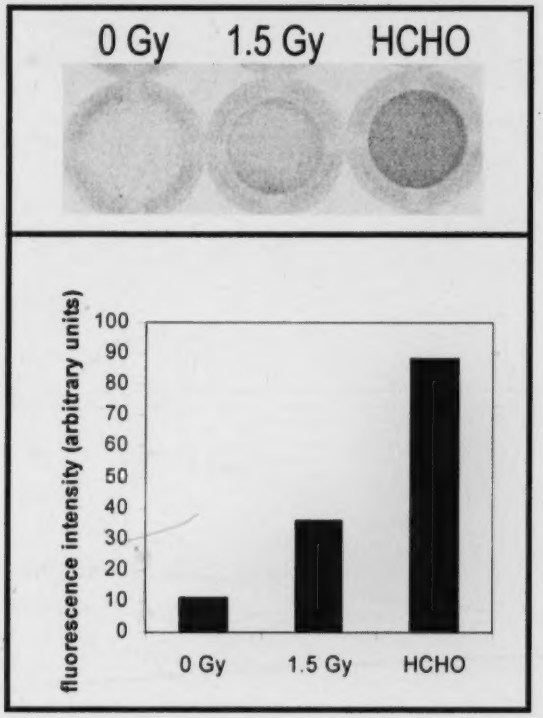

Figure 6-1: Quantitation of DPCs using Deep Purple

The upper panel shows a section of a multi-well plate of DPC samples isolated from CHO cells exposed to 0 or 1.5 Gy of γ-radiation, or treated with 1% formaldehyde (HCHO) for 1 h at 37°C. DPCs were isolated using the DNAzol-Silica method. One-third of the total isolated protein for each sample was incubated with the Deep Purple Total Protein Stain (GE Healthcare) and the fluorescence was analyzed and quantitated (bottom panel) using the Typhoon 7400 instrument.

stained with this dye would be analysed on the Typhoon 7400 instrument and quantitated using the ImageQuant 5.2 software (Figure 6-1, bottom panel). This approach has the advantage of not requiring separation of proteins by gel electrophoresis, which removes the potentially confounding factors of dealing with background gel staining. The Deep Purple stain is only fluorescent upon binding with protein and is not affected significantly by nucleic acids, detergents, or other common biological contaminants and is reported not to cause the gel "speckling" which often complicates quantitation efforts with other dyes. Because the proteins are not separated and the Deep Purple stain is more sensitive (60 pg detection limit) than SYPRO Tangerine, this quantitation approach would require less sample (see figure 6-1).

It is clear that there are different chemical types of DPCs and that these DPCs are likely formed and lost at different rates. Therefore, individual DPCs may contribute differently to the biological relevance of this class of lesions. Individual DPCs can be isolated using a modified ChIP approach. The target DPC protein would be immunoprecipitated from the DPC isolate using an antibody. Immunoprecipitates are then separated by SDS-PAGE and probed with antibody by Western blotting. It may also be possible to immunoprecipitate with a fluorescently-labeled secondary antibody so that quantitation can be performed using a fluorescence scanner rather than SDS-PAGE analysis. These analyses could be done for proteins that we have currently identified and could be extended to "fish" for additional DPCs.

A second immunological approach that could be used for individual DPC isolation is the powerful combination of immunological detection with capillary electrophoresis and laser-induced fluorescence detection [10]. This technique is significantly more sensitive than current techniques for the detection of base damage to DNA. DNA with (covalently) attached protein would be incubated with antibody to a target DPC, followed by incubation with a fluorescently-labeled secondary antibody. This complex would be separated from free antibodies by capillary electrophoresis and the peak corresponding to the complex of protein with bound primary antibody and bound secondary antibody would be quantitated. The use of this approach to quantitate individual DPCs is currently being optimized in conjunction with Dr. Hailin Wang in the laboratory of Dr. Chris Le (Department of Public Health Sciences, University of Alberta).

One final approach that could be used for the quantitation of individual DPCs is MS. In recent years, the technology has improved greatly and the laboratory of Dr. Liang Li (Department of Chemistry, University of Alberta) is equipped with LC-MALDI MS to perform such detailed analyses [11].

6.4. Stability and chemical composition of IR-induced DPCs

Chemical studies have demonstrated that IR induces different chemical forms of crosslinks [12-15] and that crosslinks induced by IR under hypoxic conditions are different from those induced under aerated conditions based on the observation that the formation of these crosslinks did not appear to be influenced by the presence of oxygen [12,13,16]. Cress and Bowden [17]

suggested that ~20% of the DPCs induced by 100 Gy of X-rays are phosphate to nitrogen bonds which can be disrupted by hydroxylamine. However, these DPCs do not appear to be due to phospho-serine or phospho-threonine bonds as they were not affected by guanidine hydrochloride. A study analyzing chromate-induced DPCs in mammalian cells [18] demonstrated that ~19% of these lesions involve crosslinking through the metal atom based on their disruption by EDTA. The remaining ~81% of chromate-induced crosslinks appear to be crosslinked through oxidative mechanisms, and ~45% of these were probably crosslinked through sulfur-containing amino acids because they were released by thiourea treatment [18].

To estimate the reversal of IR-induced crosslinks of various chemistries, the DNAzol-Silica DPC isolation method can be modified to test different DPC reversal methods. The reversal methods to be tested include: i) incubation with 150 mM NaCl at 65°C for 4 h, which is used in ChIP protocols to reverse the (hydrolytically unstable) formaldehyde crosslinks, ii) incubation in 100 mM thiourea at 37°C for 2 h, which is used to release DPCs formed through sulfhydryl linkages [19,20], iii) incubation in 50 mM EDTA, pH 8.0 at 37°C for 2 h, which is used to release DPCs formed through coordination with a metal atom [18]. As a control, the reversal of formaldehyde-induced DPCs (1% formaldehyde treatment for 1 h at 37°C) by heating at 65°C for 4 h in 150 mM NaCl will also be examined. For comparison, a set of samples will also be carried through the standard DNAzol-Silica isolation method, which involves total

DPC release by nuclease digestion. These experiments are currently being optimized in our laboratory.

6.5. Effect of DPCs on chromatin structure

The use of MS for quantitation would be useful for examining the relevance of individual proteins in DPCs. For example, the role of histones in DPCs could be examined in more detail by MS as this technology is also capable of detecting various post-translational modifications [21-23]. It is known that histones exist in different isoforms and can undergo a number of different modifications [24]. These modified histone isoforms are in intimate contact with DNA at different locations, at different times during the cell cycle, and under different cellular circumstances [25]; for example, histone H3 acetylation has been suggested to be involved in the DNA damage response [26], and the phosphorylation of histone H2AX has been shown to be important for DSB repair [27,28]. We have already observed the IR-induced crosslinking of various proteins in mammalian cells that correspond in size to a number of histones and have confirmed the involvement of histones H1-H4 in IR-induced DPCs using MS (see Table 3-1). Determining which histone variants become crosslinked may be informative as to what regions of DNA or regions of activity are more frequent targets for DPC induction.

Analyses of DPC induction could also be applied to other proteins that are involved in chromatin structure. We have shown that a number of such proteins can be crosslinked to DNA by IR. Other studies [29-31] have suggested a link

between nuclear matrix anchoring/chromatin organization and radiosensitivity. The effects of DPCs on chromatin modifications could be examined by the use of an intercalating fluorescent dye such as propidium iodide, which has been used in other studies of nuclear matrix anchoring [32,33]. These analyses could be performed on repair-proficient and repair-deficient cells to analyze the differences in the amount and stability of anchored DNA loops and would provide information on the effect of various DNA repair proteins in forming these complexes. This would also reveal the extent of DNA availability for DPC formation. After irradiation, the extent of dye intercalation would again be analyzed to determine the effect of IR-induced damage on DNA loop anchorage and/or unwinding. The extent of DPC induction by IR in these cells could also be measured to examine any correlation of DPC induction with effect on chromatin anchoring or unwinding. The presence of DPCs might also be demonstrated by repeated high stringency salt extractions prior to propidium iodide staining to confirm that these new protein associations are not disrupted. These assays may provide information on whether or not the induction of DPCs has the effect of disrupting necessary chromatin remodeling or DNA loop unwinding or migrating activities.

6.6. Repair of DPCs

Regardless of the quantitation method(s) used, it would be useful if these assays were applied to a number of different crosslinked proteins as well as total proteins. Because of the lack of clarity on whether and how DPCs are actively repaired, it would be important to quantitate DPCs in a greater number and

variety of repair-proficient and -deficient hamster and human cell lines. The cell lines used should include NER and HRR deficient lines due to the suggestion [34] that these pathways may be involved in DPC repair; as well as the human Scan-1 cell line, which is deficient in the tyrosyl-DNA phosphodiesterase I protein, which is responsible for the reversal of topoisomerase I-induced DPCs [35]. As well, it would be informative to use this sensitive methodology to quantitate the loss/removal of DPCs from cells treated with proteasome inhibitor to assess the contribution, if any, of proteolysis in DPC removal. It may also be of interest to assay DPC removal in cell lines where more than one repair pathway has been targeted for disruption; for example, inhibition of proteasome activity in NER deficient cells [36]. Further information on DPC repair may be provided by analyzing the removal of formaldehyde-induced DPCs in these repair-deficient cell lines and comparing the time-courses for induction and removal of DPCs induced by different agents.

Another experiment that could be done to assess the active repair of DPCs would be to test whether or not there is an inducible repair response. Compared to other studies, we have used low doses of IR: 0-1.5 Gy. Cells could be treated with a low dose (e.g., 0.2 Gy), returned to the incubator for 4 h to allow for activation of repair, and then treated with a higher dose (1.5 Gy). The level and repair of DPCs isolated from these cells would then be compared with the level of DPCs isolated from cells treated with 1.5 Gy alone to see if there is greater removal after the "priming" dose, which would suggest the activation of a repair pathway.

The effect of crosslinking of individual proteins will also be informative as to the involvement of these proteins in DNA metabolic processes. For example, recent data suggest the involvement of various histones in DNA repair [37]. The release of histone H1 from DNA is suggested to be an important step in the repair of DSBs by non-homologous end-joining [38]. Additionally, the association of the *S.cerevisiae* linker histone with DNA inhibits HRR [39]. Clearly, covalently trapping of particular histones on the DNA would affect these repair processes. It would be of interest to examine the correlation of increased crosslinking of a given protein with the activity of other repair processes. The role of the non-homologous end-joining pathway itself in DPC repair is unknown, and should be studied using available mutant cell lines. As was noted in section 6.2-a, the study of synchronized cell populations will be particularly important in this regard because NER is believed to operate efficiently throughout the cell cycle; in contrast, HRR operates much more efficiently in G2 phase where the newly-replicated sister chromatids act as donors for homologous recombination; non-homologous end-joining is believed to operate throughout the cell cycle but to be a particularly important alternative to HRR in G1-phase cells.

6.7. DPCs induced by other agents

Many of the assays discussed here could also be used to examine the DPCs induced by other agents. This may be informative as to the biological consequences of DPCs, or of particular DPCs, if the same protein(s) are found to be crosslinked to DNA by many (every?) DPC-inducing agent. An interesting

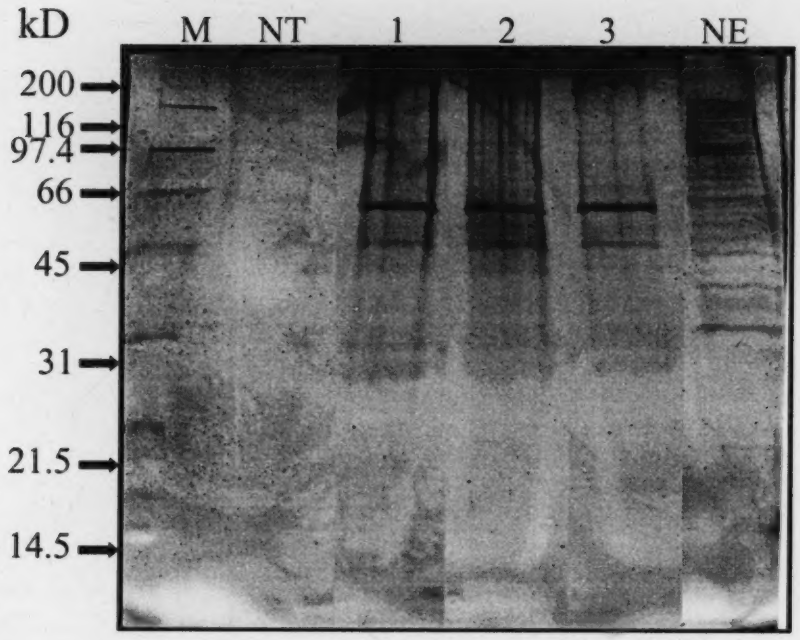

Figure 6-2: DPCs induced by DMSO

The figure is a composite of gels examining background DPC isolation from CHO cells that received no treatment "NT" or 10 µL of DMSO (1, 2, and 3; from 3 separate suppliers) and were incubated for 1 h at 37°C. DPCs were isolated using the DNAzol-Silica method and analyzed by SDS-PAGE and SYPRO-Tangerine staining. The "NE" lane is a total CHO cell nuclear extract.

finding that we came across in our work that warrants further investigation is the induction of DPCs by the solvent, DMSO (Figure 6-2). DMSO is used to administer many drugs and has even been used in the study of DPCs induced by topoisomerase poisons. Crosslinking of proteins by DMSO may be due to the production of aldehydes *in vivo* by this compound [40] although the dose we used is quite low, or it may be due to the crosslinking activity of a break-down product/contaminant of DMSO. The first step to validating this effect is to test a sample of DMSO of greater purity.

It would be informative to measure the extent of DPC induction caused by agents of interest in environmental pollution, such as arsenic, or due to their use in chemotherapy, such as melphalan (LPAM). Preliminary work indicates that LPAM induces DPCs (Figure 6-3), and these experiments should be repeated to isolate and identify the crosslinked proteins.

6.8. Isolation of proteins potentially involved in recombinational repair of DPCs and DNA interstrand crosslinks

Many bifunctional agents induce more than one type of damage and are capable of inducing DPCs and DNA interstrand crosslinks (ICLs). Both ICLs and DPCs may be repaired by recombinational repair pathways due to the size of these lesions and/or the steric challenges potentially faced by the repair machinery. Earlier work by the author was focused on determining the proteins that bind to ICLs, although it should be apparent from the earlier chapters that

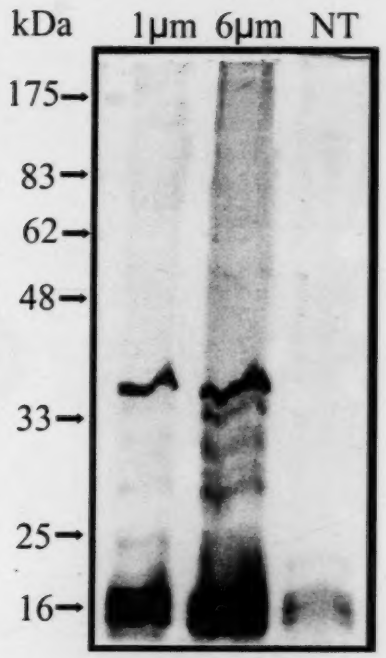

Figure 6-3: LPAM-induced DPCs in CHO cells

CHO cells received no treatment "NT", or 1 µm or 6 µm LPAM for 1 hour at 37°C. DPCs were isolated using the DNAzol-Strip method and analyzed by SDS-PAGE and silver staining. The "M" lane is the MW markers with the sizes indicated in kDa.

this information may also be critical to understanding the cellular mechanisms of DPC repair.

To identify proteins that recognize an ICL it was necessary to construct a synthetic DNA substrate. We designed the substrate to be of sufficient length toaccommodate binding of a repair complex and removal of a repair patch and to contain only a single, site-specific LPAM-induced ICL (Figure 6-4). LPAM was chosen as the crosslinking agent because it causes primarily ICLs as compared to other crosslinking agents (such as cisplatin) which cause primarily intrastrand crosslinks and/or monoadducts [41]. To limit the induction of damage, the substrate was constructed in stages using 3 sets of 2 complementary oligonucleotides. The central duplex contained an LPAM crosslinking site (5'-CNG-3') (Figure 6-5). Treating the substrate with drug while in duplex form rather than first treating it while single stranded and then annealing to the complement limits the induction of monoadducts [41]. The optimal LPAM treatment protocol was determined to be a combination of methods employed by Bauer and Povirk [41] and Osborne and Lawley [42]. The annealed duplex was incubated with 20 mM LPAM for a brief period, after which the substrate DNA was precipitated away from the drug and then incubated further to allow for reaction of the second side of the crosslink. An undamaged control duplex was also prepared. One strand of each duplex had been labeled prior to reaction. The crosslinked substrate duplex was subjected to digestion by HaeIII, because adduct formation will block digestion, and then purified by PAGE. The control

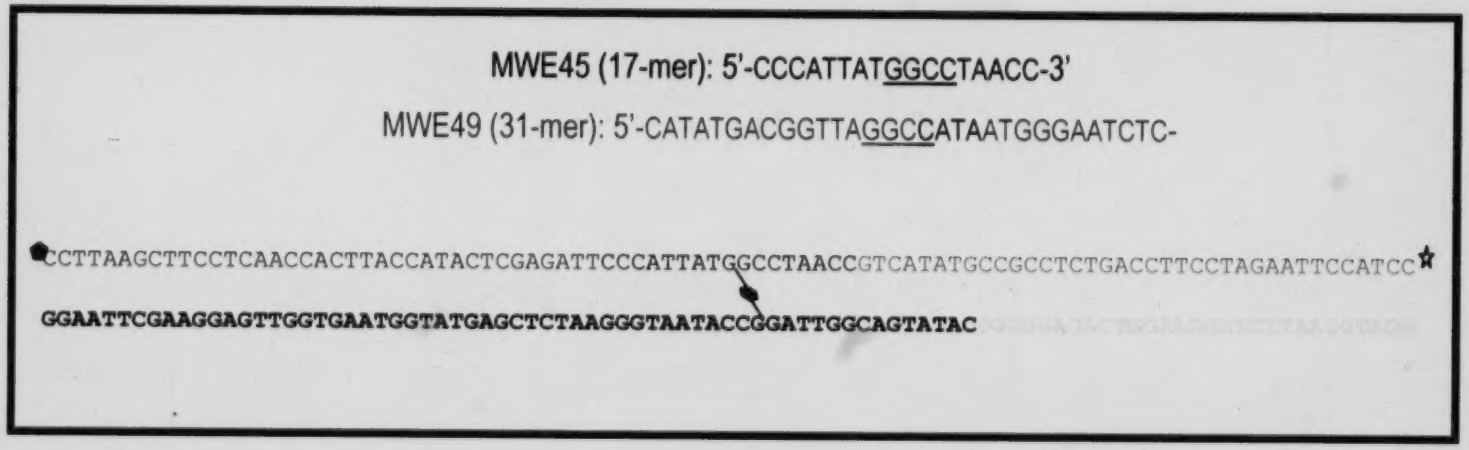
MWE45 (17-mer): 5'-CCCATTATGGCCTAACC-3'
MWE49 (31-mer): 5'-CATATGACGGTTAGGCCATAATGGGAATCTC-
CCTTAAGCTTCCTCAACCACTTACCATACTCGAGATTCCCATTATGGCCTAACCGTCATATGCCGCCTCTGACCTTCCTAGAATTCCATCC
GGAATTCGAAGGAGTTGGTGAATGGTATGAGCTCTAAGGGTAATACCGGATTGGCAGTATAC

Figure 6-4: Design of the interstrand crosslinked substrate

We designed a 17-mer and 31-mer duplex to contain an LPAM crosslink site. The full-length 91-bp oligonucleotide is composed of 6 shorter oligonculeotides and was labeled on each 5' terminus or was constructed using a 5' biotinylated (⬟) oligonucleotide at one terminus.

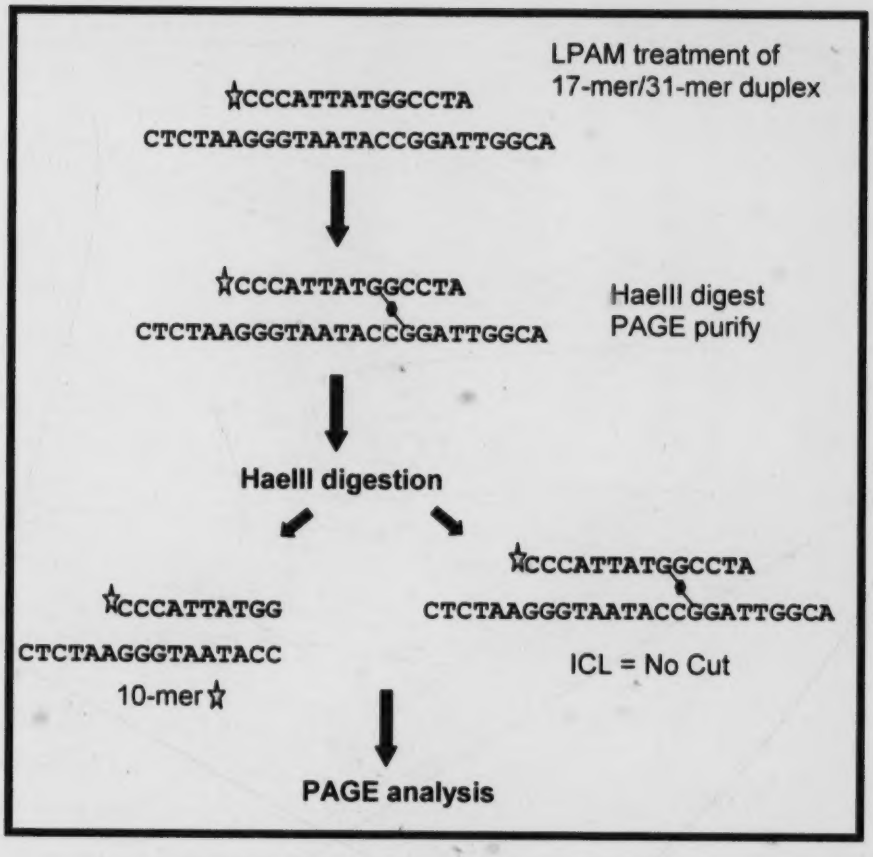

Figure 6-5: Construction of the interstrand crosslinked duplex

The 17-mer containing the two 5'-GNC sites was labeled with ^{32}P and the two central oligonucleotides were annealed and treated with LPAM for crosslink formation. The crosslinked DNA was subjected to HaeIII digestion and the uncut crosslinked duplex was purified by denaturing PAGE. The HaeIII digestion and PAGE analysis was performed again after purification to verify purity of the crosslinked duplex.

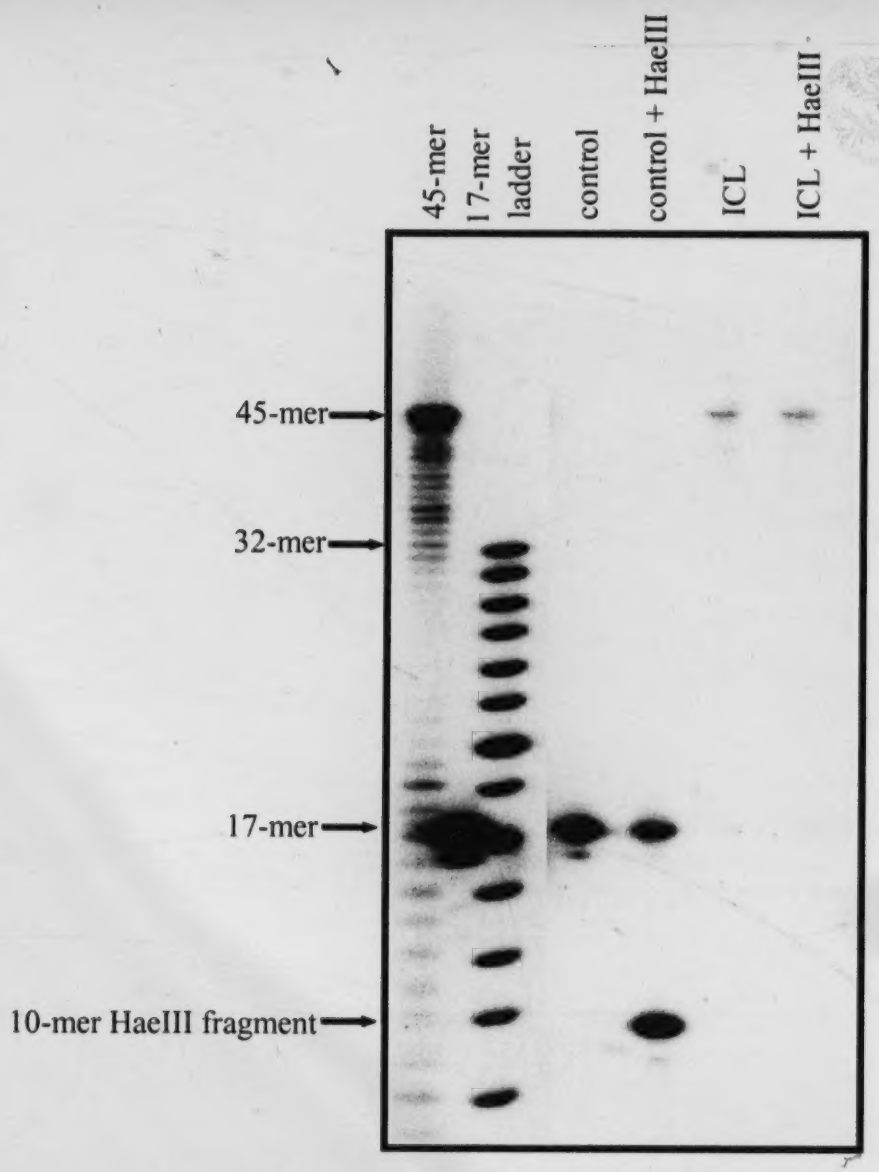

Figure 6-6: Restriction test of the interstrand crosslinked duplex

The undamaged and interstrand crosslinked duplex substrates were analyzed by HaeIII digestion and 20% denaturing PAGE. The first three lanes are various oligonucleotides used for size markers; an unpurified 45-mer, the purified 17-mer, and an 8-32-mer oligonucleotide ladder. Only the MWE45 (17-mer) oligonucleotide is labeled in each duplex assembled. The control duplex was run +/- HaeIII digestion and the purified interstrand crosslinked duplex was run +/- HaeIII digestion. The resulting, labeled 10-mer fragment is seen in the digested control sample. The crosslinked sample shows no digestion as there is no 10-mer fragment visible, even on extended exposure.

and purified ICL duplexes were each tested by HaeIII digestion to confirm the presence or absence of the adduct (Figure 6-6).

A portion of the crosslinked duplex was treated with alkali to yield the more stable formamidopyrimidine (FAPY) derivative of the LPAM ICL and this duplex was also purified, characterized, and made into full-length (91-bp)substrate. Each central duplex was then combined with the 4 remaining oligonucleotides (Figure 6-7), annealed and ligated. The full-length substrates were purified on a 20% denaturing polyacrylamide gel. We prepared two sets of control, ICL-containing, and FAPY-ICL-containing substrates; one set of substrates had one strand radio-labeled and one strand biotin-tagged and the second set of substrates had 5′ radiolabels on both strands.

To verify that the substrates were either undamaged or interstrand crosslinked, they were analyzed by restriction digestion and PAGE (Figures 6-7 and 6-8). The two labeled strands of the undamaged substrate were separable on PAGE but the strands of the ICL-containing substrate were not (Figure 6-8, lanes 3-5 and lanes 7, 9-11). The substrates were designed to contain 3 different restriction sites (Figure 6-7); XhoI, NdeI, and HaeIII. The HaeIII recognition site also contains the crosslink site. If a mono-adduct or crosslink is present at this site, the restriction enzyme will not be able to make the cut. The products of the digestion were of different sizes for the undamaged and ICL-containing substrates (Figure 6-8, lanes 3 and 9) because the ICL-containing substrate was not cut by HaeIII. The XhoI and NdeI restriction sites are outside of the crosslink site but the presence of the crosslink may prove distorting

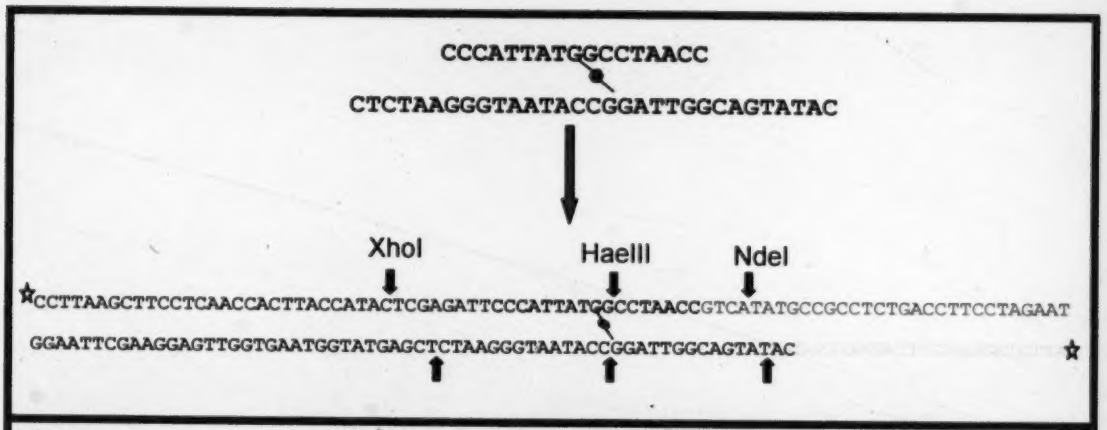

Substrate	XhoI	HaeIII	NdeI
Control	29-mer☆	44-mer ☆	31-mer☆
	59-mer☆	47-mer ☆	58-mer☆
ICL	29-mer☆	No cut	31-mer☆
	118-mer☆		118-mer☆

Figure 6-7: Restriction map of the interstrand crosslinked substrate

The full-length 91-bp oligonucleotide is composed of 6 shorter oligonucleotides and was labeled on each 5' terminus (☆). The full-length substrate was designed to contain 3 different restriction enzyme sites to be used to confirm the length, duplex nature, and damaged site. The fragments produced by digestion of each substrate are indicated in the bottom panel.

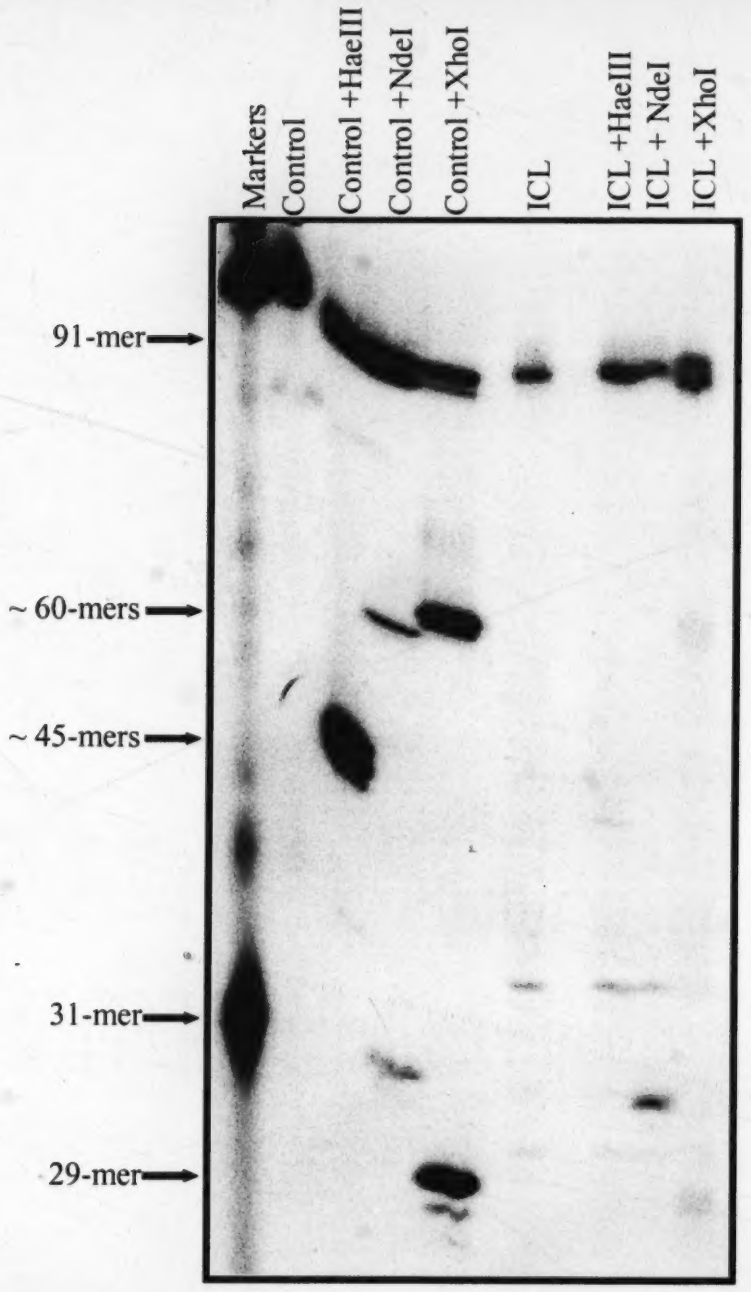

Figure 6-8: Restriction digest of the full-length interstrand crosslinked substrate

The undamaged and interstrand crosslinked full-length (91-mer) substrates were labeled at both termini and analyzed by digestion with HaeIII, NdeI, or XhoI and 20% denaturing PAGE. The first lane is oligonucleotides used for size markers; including a 100-bp marker.

enough to influence recognition, binding, and cutting by the enzyme. Digestion of the undamaged DNA substrate by XhoI or NdeI (Figure 6-8 lanes 4 and 5) yielded products of the expected sizes, whereas digestion of the crosslinked DNA substrate proceeded to a limited extent (Figure 6-8 lanes 10 and 11).

It was critical that we ensured that both sets of our substrates were indeed crosslinked. For the dual-labeled substrates, the PAGE analysis confirmed the size and the restriction digest results suggested that the crosslink was indeed present. We used separate methods to confirm the composition of our biotin-tagged substrates; we wanted to demonstrate the presence of both strands and the presence of the LPAM adduct. The undamaged, ICL-containing and FAPY-ICL-containing full-length substrates were bound to a positively charged nylon membrane (Figure 6-9). Part of the membrane (Figure 6-9, left-side) was autoradiographed to confirm the presence of the radiolabeled strand of each substrate. Part of the membrane was probed with antibodies to LPAM-FAPY adducts (Figure 6-9, centre, top panel) or LPAM adducts (Figure 6-9, centre, bottom panel) to confirm the presence (or absence, in control) of the LPAM adduct. Unfortunately there was no signal detected by the antibody to the underivatized LPAM adducts. These antibodies were generously given to us by Dr. Michael Tilby (University of Newcastle upon Tyne, UK). They are hybridoma tissue culture supernatants and the titers are low. We have limited quantities and therefore used only a very small volume per blot. The lack of signal is likely due to the low titer and not due to absence of a LPAM adduct given that the FAPY derivative antibody does recognize an adduct, and we have been able to detect a

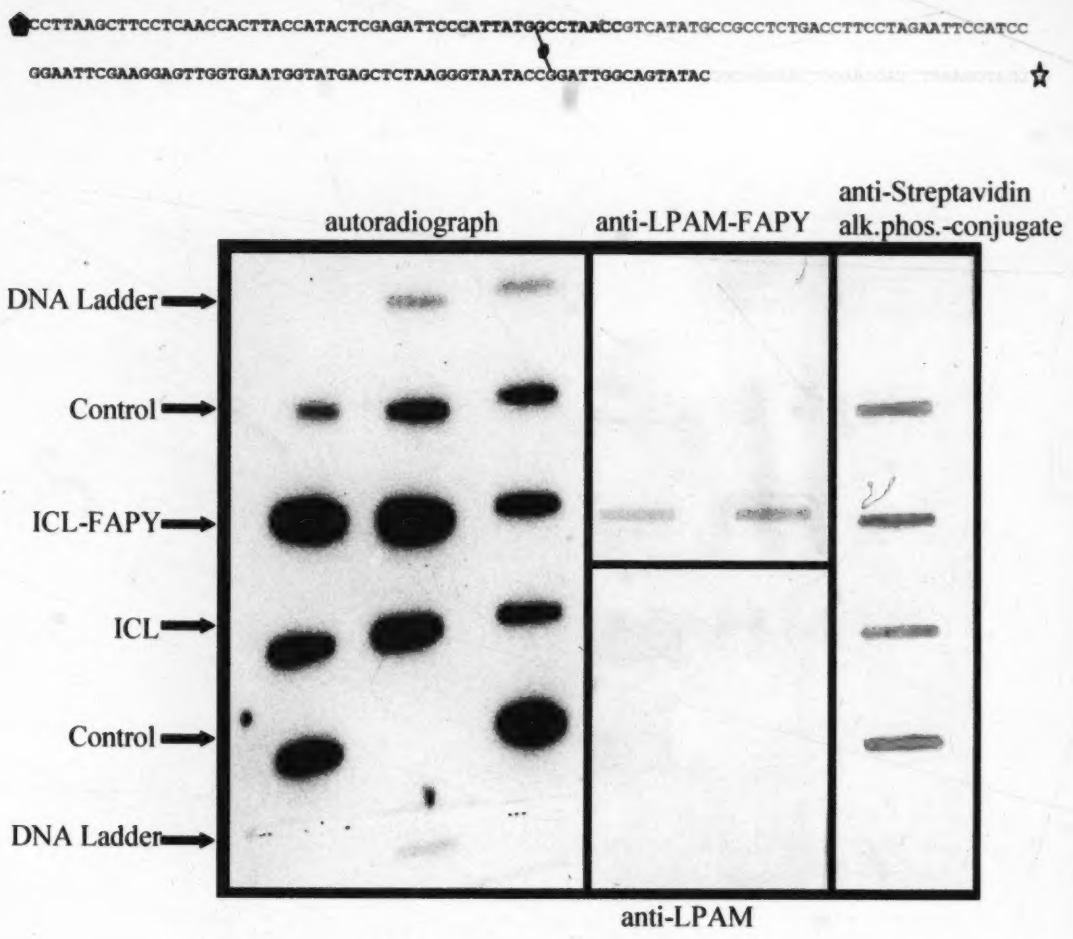

Figure 6-9: Characterization of the full-length biotin-tagged interstrand crosslinked substrate

The undamaged and interstrand crosslinked full-length (91-mer) substrates (containing either the LPAM crosslink or the more stable LPAM-FAPY crosslink) with a biotin tag (⬟) on one terminus and one terminus radio-labeled were immobilized on a nylon membrane in replicates. The left-hand panel was autoradiographed to demonstrate the presence of the radiolabeled strand of each substrate (N.B. not all slots contain samples). The centre panels were probed with antibodies to LPAM-FAPY adducts (centre, top panel) or LPAM adducts (centre, bottom panel) to demonstrate the presence (or absence, in control) of the adduct in each substrate. The right-hand panel was treated with streptavidin and then probed with an enzyme-conjugated anti-streptavidin antibody to demonstrate the presence of the biotin-labeled strand in each substrate.

signal with both antibodies in ELISA assays (data not shown). Part of the membrane (Figure 6-9, right-side) was treated with streptavidin and then probed with an enzyme-conjugated anti-streptavidin antibody to confirm the presence of the biotin labeled strand in each substrate. These results demonstrate the presence of both strands and the presence of an LPAM adduct. The size of the strands and the presence of the ICL were confirmed by restriction analysis (data not shown for the biotin-tagged substrates).

After preparation, purification, and characterization of the substrates, we proceeded to our second objective, which was to detect binding of proteins to the crosslinked substrate using electrophoretic mobility shift assays (EMSAs). This approach can identify proteins involved in binding, and therefore possibly repairing ICLs through comparison of shift patterns detected with various mammalian cell extracts, purified proteins, or reconstituted complexes. Figure 6-10 is a schematic view of how this technique works. The labeled damaged and undamaged substrates are run to show the position of the DNA in the gel. In separate reactions, the substrates are incubated with cell extract under conditions chosen to optimize protein binding, and these samples are also run on the native gel. The control substrate demonstrates shifts due to DNA-binding activities that are not ICL specific, such as proteins that bind free DNA ends. The crosslinked substrate will be shifted by these same non-ICL specific proteins as well as by proteins binding to the ICL, and we expect that there will be more than one such protein. Shifts seen with normal cell extracts will be compared to shifts

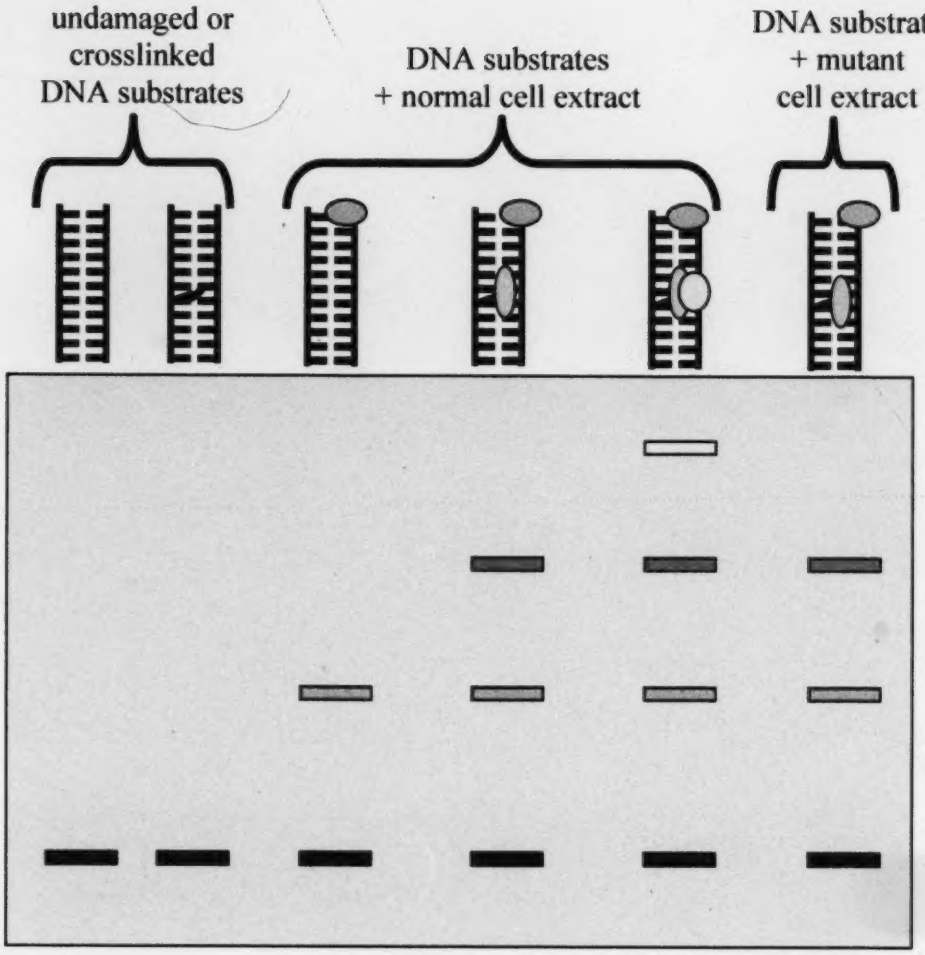

Figure 6-10: Schematic of the Electrophoretic Mobility Shift Assay (EMSA)

This figure depicts how the EMSA assay will provide information on the proteins that bind, and therefore potentially repair, ICLs. The binding of various proteins to the ICL will cause different degrees of retardation of migration of the substrates. The presence of the shifts seen with the undamaged substrate can be compared to those seen with the ICL-containing substrate to determine which shifts (and therefore proteins) are involved in recognizing ICLs.

seen using extracts deficient in putative ICL repair proteins. The loss of a particular shift in the mutant cell line suggests that that protein is an ICL binding activity. The true test of whether or not the shifts seen with the ICL substrate are actually due to ICL-specific binding proteins is to attempt to compete them off of the ICL substrate with cold, undamaged control. We have obtained some preliminary EMSA data (Figure 6-11). The control and crosslinked substrates were run alone (Figure 6-11, lanes 8 and 7, respectively) or were incubated with extracts of AA8 CHO cells and then run on the gel (Figure 6-11, lanes 6 and 5, respectively), or the ICL-containing substrate was incubated with AA8 extract and with varying amounts of undamaged substrate (Figure 6-11, lanes 1-4). We detected shifts due to non-ICL specific DNA binding activities present with both the control and ICL substrates (Figure 6-11, lanes 1 thru 6, bands A-C and F). We also detected an increased binding of particular proteins when the crosslinked and undamaged substrates were co-incubated with AA8 extract (Figure 6-11, lanes, 2-4, bands A-C). This increased binding in the presence of undamaged substrate is unexpected because the undamaged control should compete binding proteins off of the damaged substrate; however, we propose that these additional shifts may represent the binding of proteins involved in HRR as this repair pathway would be active when homologous sequence was available. We detected shifts that were presumably due to ICL binding activities because these shifts were not seen with the control sample (Figure 6-11, lanes 1-4, bands D and E) and persisted in the presence of competing undamaged control substrate.

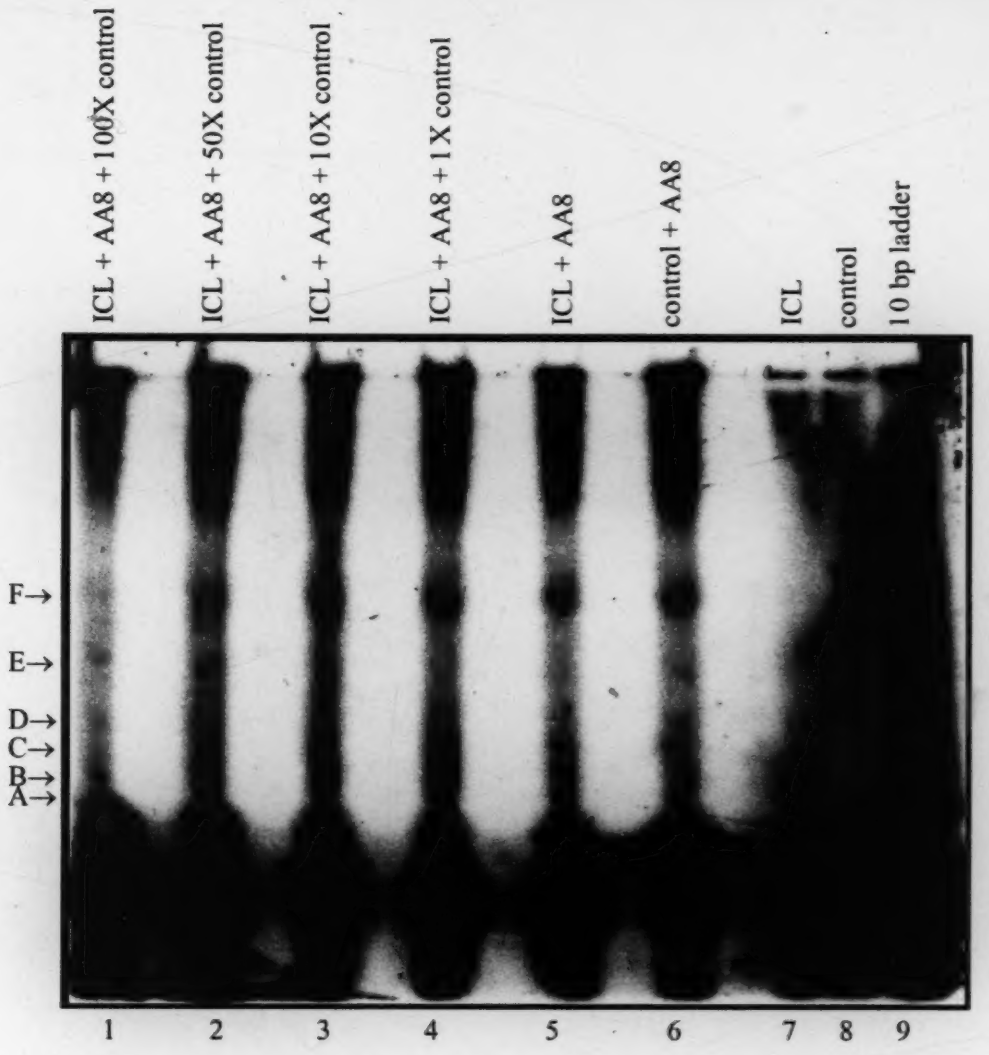

Figure 6-11: Detection of formation of protein complexes by EMSA

AA8 cell extract was incubated with undamaged control substrate, with ICL-containing substrate, or with ICL-containing substrate and varying amounts of competing, undamaged substrate. Samples were analyzed by 4% non-denaturing PAGE.

The EMSA technique demonstrates proteins binding to the ICL substrate, although our ultimate objective is to isolate and identify these proteins using a protein capture technique (Figure 6-12). To capture the ICL binding proteins, the biotinylated full-length control and crosslinked substrates will be incubated separately with normal cell extracts and the substrates with proteins bound will be isolated on streptavidin beads. Unbound proteins will be washed away and the bound proteins will be eluted. The eluted proteins will be separated by PAGE and further characterized by MS. In the time since this project was proposed, MS technology has improved and it is possible that these proteins could by analyzed and identified by LC-MS/MS without the need for electrophoretic separation. As well, the identity of some proteins involved in ICL repair may be determined using immunological methods for known proteins to which there are antibodies available. The unbiotinylated homologous sequence can be co-incubated with the damaged substrate to potentially examine recombinational repair proteins that would bind only in the presence of undamaged homologous sequence.

We have obtained preliminary data for this protein isolation work (Figure 6-13). The control and crosslinked biotinylated substrates were incubated with nuclear extracts of AA8 CHO cells. Substrates with bound proteins were captured on streptavidin beads. Proteins were eluted and analyzed using 1-D SDS-PAGE. There are a few proteins that bind to the control substrate and, as expected, these proteins were also bound by the crosslinked substrate. Additional proteins were eluted from the ICL substrate that were not eluted from

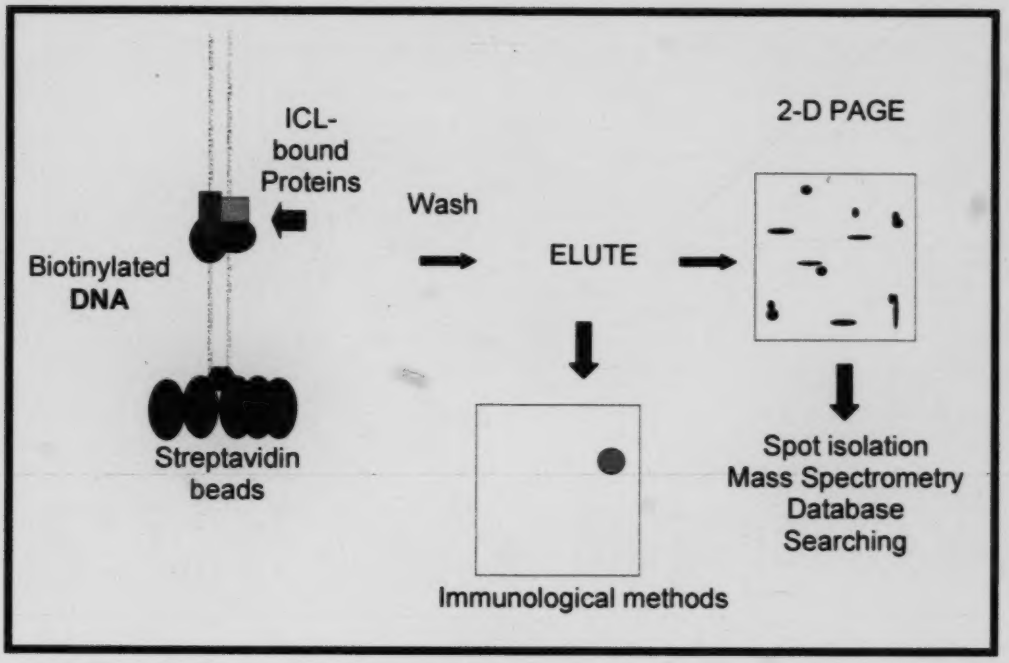

Figure 6-12: Schematic of the protein capture assay

The biotinylated control or ICL-containing substrate, or both, will be incubated with AA8 nuclear extract. Substrates with bound proteins will be isolated using streptavidin beads. Unbound proteins will be gently washed away and bound proteins will be eluted and analyzed by SDS-PAGE. Proteins can be excised and identified by MS or the gels can be used for transfer and protein identification/confirmation by Western blotting.

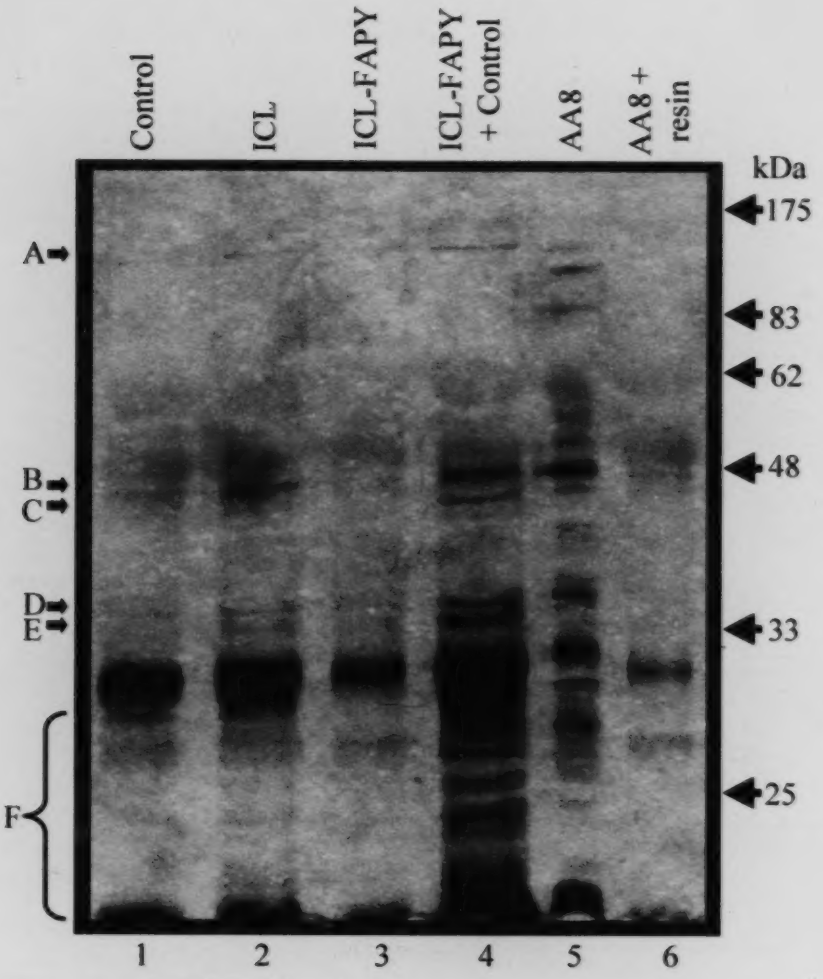

Figure 6-13: Proteins isolated by protein capture assay

The biotinylated control, ICL-containing substrate, ICL-FAPY-containing substrate, or ICL-FAPY-containing + non-biotinylated control substrates were incubated with AA8 nuclear extract. Substrates with bound proteins were isolated using streptavidin beads. Unbound proteins were washed away and bound proteins were eluted and analyzed by 1-D SDS-PAGE and silver staining.

the control substrate (Figure 6-13, lane 2, bands A-E). Although these same proteins were not eluted from the ICL-FAPY substrate alone (Figure 6-13, lane 3), they were eluted when the ICL-FAPY substrate was incubated with the cell extract and with 25-fold molar excess of unbiotinylated, undamaged homologous sequence (control substrate) (Figure 6-13, lane 4). Additional protein bands were also isolated only from the co-incubation reaction (Figure 6-13, lane 4, bands in region F). Before we can progress to 2D gel analysis we do have some work to do to optimize both the protein-DNA binding conditions and the washing steps.

To summarize, thus far we have constructed, purified, and confirmed our 91-bp crosslinked and control substrates. Preliminary EMSA experiments have demonstrated ICL-specific binding activities present in normal CHO cell extracts. These experiments should be repeated and expanded to include analysis of EMSA shifts from various repair-deficient cell lines and to include human cell extracts. Interestingly, there are shifts that start to appear only in the presence of competitor (undamaged substrate); whether or not these shifts are due to recombination related proteins could be determined by isolation of these complexes from the non-denaturing gels and MS identification of the proteins. The preliminary protein capture assays have resulted in the isolation of a few ICL–specific binding proteins and this approach should be optimized so that MS on these proteins can be done to identify proteins involved in ICL repair.

Our work on this project stalled when we could no longer obtain fresh LPAM from the chemical supply company. Alternatives to this approach would

be to use newer ICL synthesis methods being developed in the laboratory of Dr. O. Scharer [43], or to obtain active LPAM directly from a drug manufacturer or to use a different ICL-inducer such as the FR900482 class of antitumour drugs, [44]. Additionally, the FR900482 drugs are newer chemotherapy options and they appear to induce a much greater percentage of crosslinks compared to LPAM (where only 2-5% of total damage is ICLs)[43].

While the protein capture assay and analysis should identify proteins that bind interstrand crosslinked DNA and should allow us to propose steps in ICL repair, we appreciate that this is an *in vitro* assay and while the homologous sequence can be provided, the results may still not truly represent what occurs *in vivo*. A future phase of the project will be to perform *in vivo* assays using transfections of a shuttle vector with a single site-specific LPAM induced ICL and a reporter gene, similar to that done using a psoralen-induced ICL [45]. Plasmid replication (and therefore reporter gene expression) will be completely blocked until the ICL is repaired. The plasmid assay can also be modified to contain partial undamaged homologous sequence to allow intra-or inter-molecular recombinational repair.

Additionally, because of the potential involvement of HRR in DPC repair, a similar substrate could be constructed to contain a single DPC. The analyses described in section 6.8 could then be performed using the synthetic DPC substrate to isolate proteins binding to this type of lesion.

References for Chapter 6

[1] S.M. Chiu, L.R. Friedman and N.L. Oleinick The fate of DNA-protein crosslinks formed in gamma-irradiated metaphase cells, Int. J. Radiat. Biol. 58 (1990) 235-247.

[2] M.C. Elia and M.O. Bradley Influence of chromatin structure on the induction of DNA double strand breaks by ionizing radiation, Cancer Res. 52 (1992) 1580-1586.

[3] L.Y. Xue, L.R. Friedman, N.L. Oleinick and S.M. Chiu Induction of DNA damage in gamma-irradiated nuclei stripped of nuclear protein classes: differential modulation of double-strand break and DNA-protein crosslink formation, Int. J. Radiat. Biol. 66 (1994) 11-21.

[4] N. Oleinick, S. Chiu, L.R. Friedman and N. Ramakrishnan DNA-protein cross-links: New insightrs into their formation and repair in irradiated mammalian cells, in: Mechanisms of DNA Damage and Repair, Plenum Press, New York, 1996, pp. 181-192.

[5] R. Gantt A cell cycle-associated pathway for repair of DNA-protein crosslinks in mammalian cells, Mutat. Res. 183 (1987) 75-87.

[6] M. Kohli and T.J. Jorgensen The influence of SV40 immortalization of human fibroblasts on p53-dependent radiation responses, Biochem Biophys Res Commun 257 (1999) 168-176.

[7] T. Godard, E. Deslandes, F. Sichel, J.M. Poul and P. Gauduchon Detection of topoisomerase inhibitor-induced DNA strand breaks and apoptosis by the alkaline comet assay, Mutat Res 520 (2002) 47-56.

[8] P. Fiorani and M.A. Bjornsti Mechanisms of DNA topoisomerase I-induced cell killing in the yeast Saccharomyces cerevisiae, Ann N Y Acad Sci 922 (2000) 65-75.

[9] R.H. Mathijssen, W.J. Loos, J. Verweij and A. Sparreboom Pharmacology of topoisomerase I inhibitors irinotecan (CPT-11) and topotecan, Curr Cancer Drug Targets 2 (2002) 103-123.

[10] X.C. Le, J.Z. Xing, J. Lee, S.A. Leadon and M. Weinfeld Inducible repair of thymine glycol detected by an ultrasensitive assay for DNA damage, Science 280 (1998) 1066-1069.

[11] C. Ji, L. Li, M. Gebre, M. Pasdar and L. Li Identification and quantification of differentially expressed proteins in E-cadherin deficient SCC9 cells and SCC9 transfectants expressing E-cadherin by dimethyl isotope labeling, LC-MALDI MS and MS/MS, J. Prot. Res. In press (2005).

[12] Z. Nackerdien, G. Rao, M.A. Cacciuttolo, E. Gajewski and M. Dizdaroglu Chemical nature of DNA-protein cross-links produced in mammalian chromatin by hydrogen peroxide in the presence of iron or copper ions, Biochemistry 30 (1991) 4873-4879.

[13] M. Dizdaroglu, E. Gajewski, P. Reddy and S.A. Margolis Structure of a hydroxyl radical induced DNA-protein cross-link involving thymine and tyrosine in nucleohistone, Biochemistry 28 (1989) 3625-3628.

[14] E. Gajewski, A.F. Fuciarelli and M. Dizdaroglu Structure of hydroxyl radical-induced DNA-protein crosslinks in calf thymus nucleohistone in vitro, Int. J. Radiat. Biol. 54 (1988) 445-459.

[15] M.S. Weir Lipton, A.F. Fuciarelli, D.L. Springer and C.G. Edmonds Characterization of radiation-induced thymine-tyrosine crosslinks by electrospray ionization mass spectrometry, Radiat. Res. 145 (1996) 681-686.

[16] E. Gajewski, G. Rao, Z. Nackerdien and M. Dizdaroglu Modification of DNA bases in mammalian chromatin by radiation-generated free radicals, Biochemistry 29 (1990) 7876-7882.

[17] A.E. Cress and G.T. Bowden Covalent DNA-protein crosslinking occurs after hyperthermia and radiation, Radiat Res 95 (1983) 610-619.

[18] S.N. Mattagajasingh and H.P. Misra Analysis of EDTA-chelatable proteins from DNA-protein crosslinks induced by a carcinogenic chromium (VI) in cultured intact human cells, Mol. Cell. Biochem. 199 (1999) 149-162.

[19] S.K. Samuel, V.A. Spencer, L. Bajno, J.M. Sun, L.T. Holth, S. Oesterreich and J.R. Davie In situ cross-linking by cisplatin of nuclear matrix-bound transcription factors to nuclear DNA of human breast cancer cells, Cancer Res. 58 (1998) 3004-3008.

[20] S.N. Mattagajasingh and H.P. Misra Mechanisms of the carcinogenic chromium(VI)-induced DNA-protein cross-linking and their characterization in cultured intact human cells, J. Biol. Chem. 271 (1996) 33550-33560.

[21] C. Gerner, U. Frohwein, J. Gotzmann, E. Bayer, D. Gelbmann, W. Bursch and R. Schulte-Hermann The Fas-induced apoptosis analyzed by high throughput proteome analysis, J Biol Chem 275 (2000) 39018-39026.

[22] M.B. Goshe, T.P. Conrads, E.A. Panisko, N.H. Angell, T.D. Veenstra and R.D. Smith Phosphoprotein isotope-coded affinity tag approach for isolating and quantitating phosphopeptides in proteome-wide analyses, Anal Chem 73 (2001) 2578-2586.

[23] F.G. Hanisch, M. Jovanovic and J. Peter-Katalinic Glycoprotein identification and localization of O-glycosylation sites by mass spectrometric analysis of deglycosylated/alkylaminylated peptide fragments, Anal Biochem 290 (2001) 47-59.

[24] S. Henikoff, T. Furuyama and K. Ahmad Histone variants, nucleosome assembly and epigenetic inheritance, Trends Genet 20 (2004) 320-326.

[25] C.L. Peterson and M.A. Laniel Histones and histone modifications, Curr Biol 14 (2004) R546-551.

[26] H. Masumoto, D. Hawke, R. Kobayashi and A. Verreault A role for cell-cycle-regulated histone H3 lysine 56 acetylation in the DNA damage response, Nature 436 (2005) 294-298.

[27] E.R. Foster and J.A. Downs Histone H2A phosphorylation in DNA double-strand break repair, Febs J 272 (2005) 3231-3240.

[28] N.F. Lowndes and G.W. Toh DNA repair: the importance of phosphorylating histone H2AX, Curr Biol 15 (2005) R99-R102.

[29] A.E. Cress, K.M. Kurath, M.J. Hendrix and G.T. Bowden Nuclear protein organization and the repair of radiation damage, Carcinogenesis 10 (1989) 939-943.

[30] D.G. Maranon, A.O. Laudicina and M. Muhlmann In situ DNAse I sensitivity assay indicates DNA conformation differences between CHO cells and the radiation-sensitive CHO mutant IRS-20, Cytogenet Genome Res 104 (2004) 100-103.

[31] R.S. Malyapa, W.D. Wright and J.L. Roti Roti DNA supercoiling changes and nucleoid protein composition in a group of L5178Y cells of varying radiosensitivity, Radiat. Res. 145 (1996) 239-242.

[32] H.H. Kampinga, W.D. Wright, A.W. Konings and J.L. Roti Roti Changes in the structure of nucleoids isolated from heat-shocked HeLa cells, Int. J. Radiat. Biol. 56 (1989) 369-382.

[33] R.P. VanderWaal, D.R. Spitz, C.L. Griffith, R. Higashikubo and J.L. Roti Roti Evidence that protein disulfide isomerase (PDI) is involved in DNA-nuclear matrix anchoring, J. Cell. Biochem. 85 (2002) 689-702.

[34] D. Murray, L. Vallee-Lucic, E. Rosenberg and B. Andersson Sensitivity of nucleotide excision repair-deficient human cells to ionizing radiation and cyclophosphamide, Anticancer Res. 22 (2002) 21-26.

[35] J.C. Connelly and D.R. Leach Repair of DNA covalently linked to protein, Mol. Cell 13 (2004) 307-316.

[36] S.D. Desai, H. Zhang, A. Rodriguez-Bauman, J.M. Yang, X. Wu, M.K. Gounder, E.H. Rubin and L.F. Liu Transcription-dependent degradation of topoisomerase I-DNA covalent complexes, Mol Cell Biol 23 (2003) 2341-2350.

[37] A.C. Harvey and J.A. Downs What functions do linker histones provide? Mol Microbiol 53 (2004) 771-775.

[38] B. Kysela, M. Chovanec and P.A. Jeggo Phosphorylation of linker histones by DNA-dependent protein kinase is required for DNA ligase IV-dependent ligation in the presence of histone H1, Proc Natl Acad Sci U S A 102 (2005) 1877-1882.

[39] J.A. Downs, E. Kosmidou, A. Morgan and S.P. Jackson Suppression of homologous recombination by the Saccharomyces cerevisiae linker histone, Mol Cell 11 (2003) 1685-1692.

[40] J. March Advanced Organic Chemistry: Reactions, Mechanisms, and Structure, John Wiley and Sons, New York, 1991.

[41] G.B. Bauer and L.F. Povirk Specificity and kinetics of interstrand and intrastrand bifunctional alkylation by nitrogen mustards at a G-G-C sequence, Nucleic Acids Res 25 (1997) 1211-1218.

[42] M.R. Osborne and P.D. Lawley Alkylation of DNA by melphalan with special reference to adenine derivatives and adenine-guanine cross-linking, Chem Biol Interact 89 (1993) 49-60.

[43] O.D. Scharer DNA interstrand crosslinks: natural and drug-induced DNA adducts that induce unique cellular responses, Chembiochem 6 (2005) 27-32.

[44] L. Beckerbauer, J.J. Tepe, J. Cullison, R. Reeves and R.M. Williams FR900482 class of anti-tumor drugs cross-links oncoprotein HMG I/Y to DNA in vivo, Chem Biol 7 (2000) 805-812.

[45] L. Li, C.A. Peterson, X. Zhang and R.J. Legerski Requirement for PCNA and RPA in interstrand crosslink-induced DNA synthesis, Nucleic Acids Res 28 (2000) 1424-1427.